



THE HONG KONG
POLYTECHNIC UNIVERSITY

香港理工大學

Pao Yue-kong Library

包玉剛圖書館

Copyright Undertaking

This thesis is protected by copyright, with all rights reserved.

By reading and using the thesis, the reader understands and agrees to the following terms:

1. The reader will abide by the rules and legal ordinances governing copyright regarding the use of the thesis.
2. The reader will use the thesis for the purpose of research or private study only and not for distribution or further reproduction or any other purpose.
3. The reader agrees to indemnify and hold the University harmless from and against any loss, damage, cost, liability or expenses arising from copyright infringement or unauthorized usage.

IMPORTANT

If you have reasons to believe that any materials in this thesis are deemed not suitable to be distributed in this form, or a copyright owner having difficulty with the material being included in our database, please contact lbsys@polyu.edu.hk providing details. The Library will look into your claim and consider taking remedial action upon receipt of the written requests.

INTERACTIONS OF *LEGIONELLA PNEUMOPHILA* WITH
AMOEBAS AND HUMAN HOSTS: CELLULAR AND
MOLECULAR MECHANISMS

MOU QIANQIAN

PhD

The Hong Kong Polytechnic University

2019

The Hong Kong Polytechnic University
Department of Health Technology and Informatics

**Interactions of *Legionella pneumophila* with amoeba and
human hosts: cellular and molecular mechanisms**

MOU Qianqian

A thesis submitted in partial fulfillment of the requirements
for the degree of Doctor of Philosophy

September 2018

CERTIFICATE OF ORIGINALITY

I hereby declare that this thesis is my own work and that, to the best of my knowledge and belief, it reproduces no material previously published or written, nor material that has been accepted for the award of any other degree or diploma, except where due acknowledgement has been made in the text.

_____ (Signed)

MOU QIANQIAN _____ (Name of student)

Abstract

Background: *Legionella pneumophila* is a gram-negative bacterial species that has a wide distribution in both natural and artificial fresh water systems. Amoebas in biofilm in the water environment play a crucial role in the survival of *L. pneumophila*. Once ingested by an amoeba, *Legionella* multiply inside the amoeba instead of dying. Hence, the amoeba host facilitates the intracellular replication and spread of *L. pneumophila*. The organism is then released when the amoeba host ruptures. Inhalation by humans of aerosols contaminated with *L. pneumophila* causes Legionnaires' disease, a community-acquired pneumonia that has been reported worldwide in association with immunocompromised individuals. The virulence of the pathogen in humans is mainly due to its resistance to macrophages.

The survival of *L. pneumophila* within various hosts hinges on its successful evasion of the hosts' conserved phagocytic killing pathways. The organism possesses a repertoire of effector proteins that manipulate the host cell signaling and metabolic pathways. However, whether similar *L. pneumophila* virulence factors are expressed during intracellular replication in amoebas and macrophages remains unknown. The underlying mechanisms that lead to the outcomes of the two host types after *L. pneumophila* infection are also poorly understood.

Evidence has shown that *L. pneumophila* grown in the environmental host *Acanthamoeba castellanii* were more virulent and more readily infected human monocytes and macrophages. To understand the interactions between *L. pneumophila* and amoebas, a detailed analysis of gene expression must be performed in both the organism and the host.

Aims: The main studies involved in this thesis include a detailed comparison of the intracellular bacterial replication and the virulence gene expression levels of *L. pneumophila* and host cell death during intracellular growth in *A. castellanii* and monocyte THP-1. To determine precisely the interaction between *L. pneumophila* and its natural host *Acanthamoeba*, gfp-transfected *L. pneumophila* was used to infect *A. castellanii*, fluorescence-activated cell sorting was used to isolate the *L. pneumophila*-infected *Acanthamoeba*, and dual transcriptome profiling was performed for both the bacterial pathogen and the amoeba host.

Key findings: For intracellular growth of *L. pneumophila* in different hosts, the findings show that the growth of *L. pneumophila* in THP-1 cells caused no apparent increase in the bacterial count during the first 24 h after infection and an increase in bacterial cells of less than 10-fold from T36 to T48. In contrast, the growth of *L. pneumophila* in *A. castellanii* led to a 10-fold increase in the *L. pneumophila* count during the first 24 h after

infection, and the bacterial count remained stable from T24 to T48. The results show that *L. pneumophila* replicated more rapidly in *Acanthamoeba* than in THP-1 cells.

The two hosts showed different expression patterns of *L. pneumophila* virulence genes during intracellular growth. When *L. pneumophila* was grown in THP-1, *flaA* involved in the induction of pyroptosis was downregulated, whereas *sdhA* involved indirectly in the inhibition of host cell death was upregulated during the infection. The *vipD* and *sidF* genes involved in the induction and suppression of apoptosis showed no obvious change. In contrast, when *L. pneumophila* was grown in *Acanthamoeba*, *flaA* and *vipD* were upregulated during the late phases of infection, whereas *sdhA* and *sidF* were downregulated during the late phases. The gene expression patterns of *L. pneumophila* suggest that, during intracellular growth, cell death was suppressed in THP-1 but induced in *Acanthamoeba*.

In our investigation of host cell death, *L. pneumophila* induced the expression of caspase-1 but not caspase-3 or cell death in THP-1 at T48. The findings show that active caspase-1-associated pyroptosis could be more involved in THP-1 death than caspase-3-associated apoptosis. Notably, very small differences in active caspase production and cell death percentages between *L. pneumophila*-infected and uninfected THP-1 were seen, which suggests that *L. pneumophila* infection had little effect on THP-1 death. In contrast, *L. pneumophila* caused a high rate of cell death in *A. castellanii* from T12 to T48. Microscopic studies showed that the infected *A. castellanii* generated large numbers of rounded-up cells and cysts during the late stages. Furthermore, the metacaspase-1

responsible for encystation was upregulated in *Acanthamoeba* during the later stages of *Legionella* infection; this finding differs from the reports of other research groups. This study showed that *A. castellanii* cell death-mediated lytic release and *A. castellanii* encystment-mediated nonlytic release could co-occur in *L. pneumophila*-infected *A. castellanii*.

To elucidate the interactions between *L. pneumophila* and *Acanthamoeba*, *A. castellanii* infected with gfp-transfected *L. pneumophila* for 48 h was enriched by fluorescence-activated cell sorting for dual transcriptome analysis. The results show that the transcriptome of *L. pneumophila* genes was dominated by the upregulation of genes involved in flagellar activity, bacterial protein synthesis, and amino acid metabolism. However, the transcriptome of *L. pneumophila*-infected *A. castellanii* was dominated by the downregulation of genes involved in protein synthesis and amino acid metabolism. In addition, it was observed that the *pvc* genes in *L. pneumophila* were significantly upregulated during intracellular growth. The putative functions of the *pvc* genes were involved in the amino acid metabolism. The *pvcA*-knockout and *pvcB*-knockout *L. pneumophila* released from *A. castellanii* showed lower replication in THP-1 when compared with wild-type *L. pneumophila*. Replication in *Acanthamoeba* triggered the expression of *L. pneumophila pvc* genes, which could regulate the *L. pneumophila* virulence that further affects bacterial pathogenesis in human macrophages.

Conclusions: The studies performed as part of this thesis demonstrated that *Legionella pneumophila* better adapted to and more readily induced cell death to facilitate bacterial release in *Acanthamoeba castellanii*. In contrast, THP-1 preferentially induced pyroptosis during *Legionella* infection, which led to host cell death and limited bacterial growth. Dual transcriptomes of both the pathogen and amoeba host indicated that during the late stages of intracellular growth, flagellar assembly and energy metabolism were activated in *L. pneumophila*, whereas metabolic activities were inhibited in the *Acanthamoeba* host.

List of Publications

Scientific Journal Paper

MOU, Qianqian; LEUNG, Polly HM. Differential expression of virulence genes in *Legionella pneumophila* growing in *Acanthamoeba* and human monocytes. *Virulence*, 2018, 9.1: 185-196.

Acknowledgements

I thank my parents for their great love and support during my PhD study.

I express my deep appreciation to my chief supervisor, Dr. Polly Leung, for providing me with a valuable chance to receive PhD research training. Her patient guidance was of great assistance in overcoming all of the challenges and problems I met during my research work.

I thank Dr. Helen Law for her kind help in training me to perform flow cytometry and cell sorting.

I thank Dr. Lawrence Chan and Dr. Gilman Siu for their professional lessons and suggestions during my guided study.

I thank my best friend, Wang Xiaojun, for her help and for sharing in my life.

Table of Contents

Abstract	III
List of Publications	VIII
Acknowledgements	IX
Table of Contents	X
List of Figures and Tables	XV
List of Abbreviations and Symbols	XX
1. Introduction	2
1.1 General properties of <i>Legionella pneumophila</i>	2
1.2 Diseases caused by <i>L. pneumophila</i>	4
1.2.1 <i>L. pneumophila</i> is the major pathogen in Legionnaires' disease	4
1.2.2 Macrophages: accidental human hosts of <i>L. pneumophila</i>	6
1.3 Diagnosis and treatment	7
1.4 Epidemiology of LD	8
1.5 Roles of biofilm and amoebas in <i>L. pneumophila</i> survival	12
1.5.1 Biofilm mediates the environmental spread of <i>L. pneumophila</i>	12
1.5.2 <i>Acanthamoeba castellanii</i>: environmental host	13
1.5.3 Biphasic life cycle of <i>L. pneumophila</i>	16
1.6 <i>L. pneumophila</i> virulence factor and effector proteins	19
1.6.1 <i>L. pneumophila</i> T4SS: built by Dot/Icm proteins	22
1.6.2 Effector proteins	25
1.7 <i>L. pneumophila</i> intracellular interaction with hosts during intracellular growth	31
1.7.1 <i>L. pneumophila</i> entry into host cells	32
1.7.2 Intracellular <i>L. pneumophila</i> replicated inside LCV	33
1.7.3 <i>L. pneumophila</i> egress from host cell	34

1.8 Host cell death pathway induced by <i>L. pneumophila</i> infection	37
1.8.1 <i>L. pneumophila</i> induces cell death in macrophages.....	37
1.8.2 <i>L. pneumophila</i> infection and <i>Acanthamoeba</i> cell survival	41
2. Aims and Objectives.....	43
2.1 Research gaps	43
2.2 Aims	45
2.3 Objectives	45
3. Materials and Methods	47
3.1 Overview of workflow	47
3.2 Bacterial strain, <i>Acanthamoeba</i> , and THP-1 cell lines used	49
3.2.1 Standard ATCC <i>Legionella</i> strain	49
3.2.2 <i>Acanthamoeba castellanii</i> strain	49
3.2.3 THP-1 cell line	49
3.3 Extracellular growth of <i>L. pneumophila</i> in BYE broth.....	50
3.4 Intracellular growth of <i>L. pneumophila</i> in <i>A. castellanii</i> and THP-1	50
3.4.1 <i>L. pneumophila</i> intracellular growth in <i>A. castellanii</i>	50
3.4.2 <i>L. pneumophila</i> intracellular growth in THP-1.....	51
3.5 RNA isolation and two-step RT-quantitative PCR	52
3.5.1 RNA isolation.....	52
3.5.2 DNA removal of RNA samples and reverse transcription (RT).....	53
3.5.3 Quantitative real-time PCR for gene expression studies	53
3.6 Transformation of <i>L. pneumophila</i> with plasmid pBC(gfp)Pmip	57
3.6.1 Electroporation of <i>L. pneumophila</i>	57
3.6.2 Extracellular growth of gfp-transfected <i>L. pneumophila</i>	63
3.6.3 Intracellular growth of gfp-transfected <i>L. pneumophila</i>	63

3.7 Flow cytometry for host cell death staining measurement and for FACS enrichment of gfp-transfected <i>L. pneumophila</i>–infected <i>A. castellanii</i>	66
3.7.1 Flow cytometry startup operation	66
3.7.2 Propidium iodide (PI) staining	67
3.7.3 Active caspase-1 staining	68
3.7.4 Active caspase-3 staining	69
3.7.5 FACS enrichment of gfp-transfected <i>L. pneumophila</i>–infected <i>A. castellanii</i>	70
3.8 Microscopic observation of <i>A. castellanii</i> and THP-1 infected with gfp-transfected <i>L. pneumophila</i>	73
3.8.1 Co-culture preparation and microscopy settings	73
3.8.2 Live-image of host cells infected with gfp-transfected <i>L. pneumophila</i>	74
3.9 Transcriptome analysis of gfp-transfected <i>L. pneumophila</i> grown in <i>A. castellanii</i> at transmissive phase	76
3.9.1 RNA Preparation for RNA-sequencing	76
3.9.2 Library generation and RNA-sequencing	77
3.9.3 Verification of gene expression result using two-step quantitative RT-PCR	81
3.10 Knockout study in <i>L. pneumophila</i>	86
3.10.1 Knockout of <i>pvcA</i> and <i>pvcB</i> in <i>L. pneumophila</i> by allelic exchange	86
3.10.2 Verification of <i>pvcA</i>-knockout and <i>pvcB</i>-knockout <i>L. pneumophila</i>	88
3.10.3 Growth assay of <i>pvcA</i>-knockout and <i>pvcB</i>-knockout <i>L. pneumophila</i>	92
3.11 Statistical analysis	95
4. Results	96
4.1 Intracellular growth of <i>L. pneumophila</i> in <i>A. castellanii</i> and THP-1	96
4.1.1 Extracellular growth of <i>L. pneumophila</i> in BYE broth	96
4.1.2 Intracellular growth of <i>L. pneumophila</i> in <i>A. castellanii</i> and THP-1 by plate counts	98

4.1.3 Microscopic observation of gfp-transfected <i>L. pneumophila</i> –infected <i>A. castellanii</i> and THP-1	100
4.2 Differential virulence expression of <i>Legionella pneumophila</i> grown in amoebas and monocytes	107
4.2.1 Expression of <i>L. pneumophila</i> virulence genes in different hosts	107
4.2.2 Expression of <i>CASP</i> genes in the THP-1 host cells	111
4.2.3 <i>Metacaspase-1 (MCASP-1)</i> expression of infected and uninfected <i>A. castellanii</i>	113
4.3 Investigation of cell death in <i>L. pneumophila</i> –infected THP-1 and <i>Acanthamoeba castellanii</i>	115
4.3.1 Production of active caspase-1 in <i>L. pneumophila</i> –infected and uninfected THP-1 cells.....	115
4.3.2 Production of active caspase-3 in <i>L. pneumophila</i> –infected and uninfected THP-1 cells.....	119
4.3.3 Cell death assay in THP-1 cells	122
4.3.4 Cell death assay in <i>A. castellanii</i> cells	126
4.3.5 Microscopic observation of THP-1 and <i>A. castellanii</i> cell death when infected with gfp-transfected <i>L. pneumophila</i>	129
4.4 Transcriptome of FACS-enriched <i>A. castellanii</i> infected with gfp-transfected <i>L. pneumophila</i>	131
4.4.1 Extracellular and intracellular growth of gfp-transfected <i>L. pneumophila</i>	131
4.4.2 RNA sequencing information and alignment to reference genomes.....	137
4.4.3 Upregulated metabolism of <i>L. pneumophila</i> correlated with downregulated amino acid metabolism in <i>A. castellanii</i>	139
4.4.4 Enriched KEGG pathway in gfp-transfected <i>L. pneumophila</i> –infected <i>A. castellanii</i>	147
4.4.5 DEG annotation of gfp-transfected <i>L. pneumophila</i> –infected <i>A. castellanii</i>	158
4.4.6 Quantitative RT-qPCR verification of DEGs in FACS-enriched gfp-transfected <i>L. pneumophila</i> –infected <i>A. castellanii</i>	165

4.4.7 <i>L. pneumophila</i> and mutant strains grown in L-cysteine–limited and supplied BYE broths.....	172
4.4.8 Intracellular growth of <i>pvcA</i> -knockout and <i>pvcB</i> -knockout <i>L. pneumophila</i> strains	175
5. Discussion	181
5.1 Intracellular growth of <i>L. pneumophila</i> and virulence gene expression.....	181
5.1.2 <i>L. pneumophila</i> virulence genes involved in host cell death showed differences in expression in <i>A. castellanii</i> and THP-1	186
5.2 Host cell death after infection by <i>L. pneumophila</i>	191
5.2.1 Cell death responses of THP-1 after infection by <i>L. pneumophila</i>	191
5.2.2 Cell death responses in <i>A. castellanii</i> after <i>L. pneumophila</i> infection	194
5.2.3 Difference between THP-1 and <i>A. castellanii</i> cell death.....	196
5.3 Dual transcriptome analysis of FACS-enriched gfp-transfected <i>L. pneumophila</i> – infected <i>A. castellanii</i>	197
5.3.1 <i>L. pneumophila</i> protein synthesis, amino acid metabolism, and flagellar assembly were activated when grown in <i>A. castellanii</i>	198
5.3.2 <i>A. castellanii</i> protein synthesis and amino acid metabolism were repressed when infected with <i>L. pneumophila</i>	201
5.3.3 Verification of both <i>L. pneumophila</i> and <i>A. castellanii</i> gene expression in FACS- enriched gfp-transfected <i>L. pneumophila</i> –infected <i>A. castellanii</i>	203
5.3.4 Growth assay of <i>pvcA</i> -knockout and <i>pvcB</i> -knockout <i>L. pneumophila</i> in different conditions	206
5.3.5 Advantages and limitations of this dual transcriptome study	208
5.4 Conclusions	209
5.5 Suggestions for future works	211
Appendices	214
References	223

List of Figures and Tables

Figure 1.1 <i>Legionella</i> life cycle from environmental reservoir to human infection.	3
Figure 1.2 Documentation of identified <i>Legionella</i> spp. from different clinical cases during 1995–2005.	5
Figure 1.3 Rate of Legionnaires’ disease per million people in different regions.	10
Figure 1.4 Summary of reported cases of Legionnaires’ disease from 1994 to 2017 in Hong Kong.	11
Figure 1.5.1 Life cycle of <i>A. castellanii</i> in environment.	15
Figure 1.5.2 <i>L. pneumophila</i> life cycle from biofilm and amoeba to human macrophage.	18
Table 1.1 <i>L. pneumophila</i> virulence factors are involved in intracellular growth and pathogenesis.	20
Figure 1.6 The Dot/Icm T4SS of <i>L. pneumophila</i>	24
Table 1.2 <i>L. pneumophila</i> effector proteins that manipulate diverse host cell pathways during intracellular growth.	28
Figure 1.7 Intracellular growth pathway of <i>L. pneumophila</i>	36
Figure 1.8 Pathway involved in <i>L. pneumophila</i> –induced host cell death.	39
Figure 3.1 Overview of project workflow.	48
Table 3.1 Primers and TaqMan probes used in gene expression study.	55
Figure 3.2 Map of plasmid pBC(gfp)Pmip.	59

Figure 3.3.1 Identification of <i>L. pneumophila</i> colonies with green fluorescence.	61
Figure 3.3.2 Gel electrophoresis identification of the plasmid pBC(Pmip)gfp.	62
Figure 3.4 Key operations for FACS.	72
Figure 3.5 Facilities for co-culture visualization.	75
Figure 3.6 Workflow of RNA preparation for Illumina sequencing (Groken Bioscience, Hong Kong).	79
Figure 3.7 Standard Groken Bioinformatics workflow.	80
Table 3.2 Primers and probes used in RT-qPCR verification of gene expression.	83
Figure 3.8 Instruction of plasmids pJS5 and pJS6 facilitated site-directed mutagenesis in <i>L. pneumophila</i>.	87
Figure 3.9 Gel electrophoresis identification of the <i>aph(3')</i>-I insertion in <i>L. pneumophila pvcA</i> and <i>pvcB</i>.	90
Figure 3.10 Verification of <i>pvcA</i>-knockout and <i>pvcB</i>-knockout <i>L. pneumophila</i> strains.	91
Figure 4.1.1 Extracellular growth curve of <i>L. pneumophila</i>.	97
Figure 4.1.2 Intracellular growth curve of <i>L. pneumophila</i> in <i>A. castellanii</i> and THP-1.	99
Figure 4.1.3.1 Images of gfp-transfected <i>L. pneumophila</i>-infected <i>A. castellanii</i>.	102
Figure 4.1.3.2 Images of gfp-transfected <i>L. pneumophila</i>-infected THP-1-differentiated macrophages.	105

Figure 4.2.1.1 Expression of <i>L. pneumophila</i> virulence genes during intracellular growth in THP-1.	109
Figure 4.2.1.2 Expression of <i>L. pneumophila</i> virulence genes during intracellular growth in <i>A. castellanii</i>	110
Figure 4.2.2 Expression of <i>CASP</i> genes during <i>L. pneumophila</i> infection in THP-1.	112
Figure 4.2.3 Expression of <i>MCASP-1</i> during <i>L. pneumophila</i> grown in <i>A. castellanii</i> that changed from trophozoites to cysts.	114
Figure 4.3.1.1 Active caspase-1 production in <i>L. pneumophila</i> -infected and uninfected THP-1 cells.	117
Figure 4.3.1.2 Microscopic examination of active caspase-1 production in THP-1 cells.	118
Figure 4.3.2.1 Active caspase-3 production in <i>L. pneumophila</i> -infected and uninfected THP-1 cells.	120
Figure 4.3.2.2 Microscopic examination of active caspase-3 production in THP-1 cells.	121
Figure 4.3.3.1 Comparison of PI-positive percent between <i>L. pneumophila</i> -infected and uninfected THP-1 cells.	123
Figure 4.3.3.2 Microscopic examination of PI-stained THP-1 cells.	124
Table 4.3.1. Summary of flow cytometry data of active caspase-1 staining, active caspase-3 staining, and PI staining in THP-1 cells.	125
Figure 4.3.4.1 Comparison of PI-positive percent in <i>A. castellanii</i> cells between <i>L. pneumophila</i> -infected and uninfected groups.	127
Figure 4.3.4.2 Microscopic examination of PI-stained <i>A. castellanii</i> cells.	128

Figure 4.3.5 Microscopic examination of gfp-transfected <i>L. pneumophila</i> –infected <i>A. castellanii</i> and THP-1 at T48 that were stained with PI.....	130
Figure 4.4.1.1 Extracellular growth of <i>L. pneumophila</i> and gfp-transfected <i>L. pneumophila</i> in BYE broth.	132
Figure 4.4.1.2 Intracellular growth curve of <i>L. pneumophila</i> and gfp-transfected <i>L. pneumophila</i> in <i>A. castellanii</i>	134
Figure 4.4.1.3 Non-enriched and FACS-enriched <i>A. castellanii</i> infected with gfp-transfected <i>L. pneumophila</i> at T48.	136
Figure 4.4.3.1 Enriched GO terms by comparing <i>L. pneumophila</i> –infected <i>A. castellanii</i> with extracellular <i>L. pneumophila</i>	140
Figure 4.4.3.2 Enriched GO terms by comparing <i>L. pneumophila</i> -infected <i>A. castellanii</i> with uninfected <i>A. castellanii</i>	141
Figure 4.4.3.3 Enriched cysteine and methionine metabolism revealed upregulated <i>L. pneumophila</i> genes.	144
Figure 4.4.3.4 Downregulated genes of infected <i>A. castellanii</i> in cysteine and methionine metabolism.	145
Figure 4.4.3.5 Summary of metabolism deduced from dual transcriptome profiling in both intracellular <i>L. pneumophila</i> and infected <i>A. castellanii</i>	146
Table 4.4.1: Top 10 enriched KEGG pathways by comparing FACS-enriched gfp-transfected <i>L. pneumophila</i> –infected <i>A. castellanii</i> with extracellular <i>L. pneumophila</i> at T48.	149
Table 4.4.2: Top 10 enriched KEGG pathways by comparing FACS-enriched gfp-transfected <i>L. pneumophila</i> –infected <i>A. castellanii</i> with uninfected <i>A. castellanii</i> at T48.	150
Figure 4.4.4.1 Ribosomal protein biosynthesis pathway enriched in intracellular <i>L. pneumophila</i> transcriptome analysis.	152

Figure 4.4.4.2 Ribosomal protein biosynthesis pathway of infected <i>A. castellanii</i> from transcriptome analysis.	153
Figure 4.4.4.3 <i>L. pneumophila</i> flagellar assembly was highly induced in gfp-transfected <i>L. pneumophila</i>–infected <i>A. castellanii</i>.	155
Figure 4.4.4.4 DEGs annotation in citrate cycle pathway from infected <i>A. castellanii</i> transcriptome analysis.	157
Table 4.4.3: Top 10 upregulated genes of intracellular <i>L. pneumophila</i> from transcriptome analysis.	160
Table 4.4.4: Top 10 downregulated genes of intracellular <i>L. pneumophila</i> from transcriptome analysis.	161
Table 4.4.5: Top 10 upregulated and downregulated genes of <i>A. castellanii</i> infected with gfp-transfected <i>L. pneumophila</i> compared with uninfected <i>A. castellanii</i> at T48.	163
Figure 4.4.5 Virulence genes expression of FACS-enriched gfp-transfected <i>L. pneumophila</i>–infected <i>A. castellanii</i>.	168
Figure 4.4.6 Two-step RT-qPCR verification of <i>A. castellanii</i> genes expression.	171
Figure 4.4.7 <i>L. pneumophila</i> and mutant strains grown in BYE broths.	174
Figure 4.4.8.1 Intracellular growth of wild-type, <i>pvcA</i>-knockout and <i>pvcB</i>-knockout <i>L. pneumophila</i> in <i>A. castellanii</i>.	177
Figure 4.4.8.2 Intracellular growth of wild-type, <i>pvcA</i>-knockout and <i>pvcB</i>-knockout <i>L. pneumophila</i> in THP-1.	178
Figure 4.4.8.3 <i>L. pneumophila</i> strains released from <i>A. castellanii</i> grown in THP-1.	180
Table 5.1 Summary of <i>Legionella</i> growth in different hosts reported by different research groups.	184

List of Abbreviations and Symbols

ATCC	American type culture collection
ATP	Adenosine triphosphate
BCYE	Buffered charcoal yeast extract
BP	Biological process
bp	Base pair
BSA	Bovine serum albumin
BYE	Buffered yeast extract
CASP	Caspase
CC	Cellular component
cDNA	Complementary deoxyribonucleic acid
CFU	Colony-forming unit
CO ₂	Carbon dioxide
°C	Degrees Celsius
Ct	Threshold cycle
ddH ₂ O	Double deionized water
DEG	Differentially expressed gene
dNTPs	Deoxyribonucleotide triphosphates

(A, Adenosine; G, guanosine; C, Cytidine; and T, thymine)

Dot	Defect in organelle trafficking
<i>E. coli</i>	<i>Escherichia coli</i>
EDTA	Ethylenediaminetetraacetic acid
EWGLI	European Working Group for Legionella Infections
ER	Endoplasmic reticulum
FACS	Fluorescence-activated cell sorting
FITC	Fluorescein isothiocyanate
FLA	Free-living amoeba
g	Gram
$\times g$	Gravitational force
GAPDH	Glyceraldehyde-3-phosphate dehydrogenase
GFP	Green fluorescence protein
GO	Gene ontology
h	Hour
Icm	Intracellular multiplication
kb	Kilo-base
KEGG	Kyoto encyclopedia of genes and genomes
L	Liter
Log	Logarithm
LCA	<i>Legionella</i> -containing aerosol

LCV	<i>Legionella</i> -containing vacuole
LD	Legionnaires' disease
LPS	Lipopolysaccharide
LUT	Look-up table
M	Molar
MALDI-TOF	Matrix-assisted laser desorption/ionization-time of flight
MCASP	Metacaspase
MF	Molecular function
min	Minute
mL	Milliliter
mM	Millimolar
MOI	Multiplicity of infection
MW	Molecular weight
NAMC	Nikon advanced modulation contrast
ND	Numeric dimension
NF κ B	Nuclear factor- κ B
ng	Nanogram
NGS	Next-generation sequencing
nm	Nanometer
OD	Optical density
p	Probability

PAS	Page's amoeba saline
PBS	Phosphate-buffered saline solution
PC	Phosphocholine
PCR	Polymerase chain reaction
PE	Phosphatidylethanolamine
PI	Propidium iodide
PMA	Phorbol-12-myristate 13-acetate
PRPP	Phosphoribosyl pyrophosphate
PYG	Peptone yeast glucose
RIN	RNA integrity number
RNA	Ribonucleic acid
RPKM	Reads per kb bases per million reads
RT	Reverse transcription
s	Second
SEM	Standard error of mean
SNARE	Soluble NSF (N-ethylmaleimide-sensitive factor) Attachment protein receptor
T _m	Melting temperature
T4SS	Type IV secretion system

U	Unit
UV	Ultraviolet
V	Voltage
μg	Microgram
μL	Microliter
μM	Micromolar
%	Percent

1. Introduction

1.1 General properties of *Legionella pneumophila*

Legionella is an aerobic gram-negative bacillus of the γ -proteobacterial lineage (Hubber and Roy 2010). More than 55 *Legionella* species with 70 serogroups were isolated from various environmental water sources (Hilbi et al. 2011, Hubber and Roy 2010), and 30 of them were identified as pathogenic and as causing respiratory tract infections in humans (Cunha et al. 2016). Most infections were caused by *Legionella pneumophila* serogroup 1 strain (Diederer 2008, Phin et al. 2014). *Legionella* infection can be caused by the inhalation of pathogen-containing aerosols (Figure 1.1). *Legionella* can survive in a temperature range between 5°C and 63°C and a pH range of 5.0 to 9.0 in various environmental habitats, including soil and water supplies (Fields 1996, Jules and Buchrieser 2007). *Legionella* is nutritionally fastidious organism whose growth requires the presence of L-cysteine and iron (Feeley et al. 1979, Pine et al. 1979). However, fastidious *Legionella* are ubiquitous in artificial water systems such as cooling towers, evaporative condensers, whirlpools, and water outlets; and environmental protozoa support *Legionella* growth (Declerck 2010, Fields 1996). *Legionella* are motile, rod-shaped bacteria with monopolar flagella (Diederer 2008). The average size of the *Legionella* cell has been given as 2 μm long and 0.75 μm wide (Hilbi et al. 2001, Segal et al. 1999).

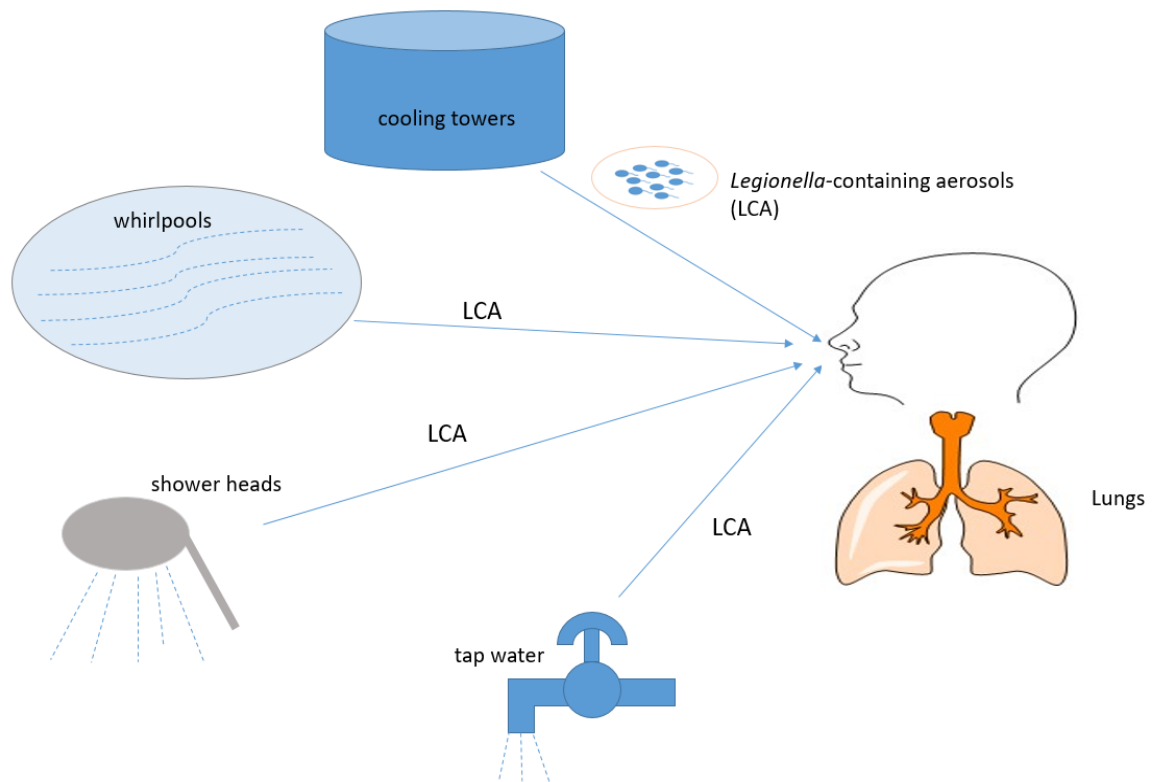


Figure 1.1 Legionella life cycle from environmental reservoir to human infection. *Legionella* is frequently distributed in artificial water system, and amoeba species are their environmental hosts. *Legionella* can then replicate with amoeba support, and aerosols that contain the bacteria can be inhaled by humans to cause infections (Richards et al. 2013).

1.2 Diseases caused by *L. pneumophila*

1.2.1 *L. pneumophila* is the major pathogen in Legionnaires' disease

Artificial water systems are common reservoirs of *Legionella spp.*, so humans have a great likelihood of exposure to this environmental pathogen. Among the various *Legionella* species (Figure 1.2), *L. pneumophila* is the most well known to cause the respiratory tract infection known as Legionellosis, which takes two forms: Legionnaires' disease (LD), a severe type of pneumonia, and Pontiac fever, a milder illness with fever-like symptoms (Lau and Ashbolt 2009). It has been reported that the *L. pneumophila* serogroup 1 accounts for more than 90% of all clinical cases of *Legionella* infection, but only 28% of environmental isolates belong to this strain (Doleans et al. 2004, Yu et al. 2002), which suggests that the *L. pneumophila* serogroup 1 is more pathogenic (Newton et al. 2010) than the other *Legionella* strains. As a result, *L. pneumophila* is also the main research focus for determination of its virulence pathway.

The fatality rate of LD has been reported at around 10%, and this rate is even higher among immunocompromised populations (Fields et al. 2002, Lam et al. 2011). *L. pneumophila* infection in sensitive human populations such as the elderly, smokers, and hospitalized individuals can develop from Pontiac fever into LD because of a lack of awareness (Demirjian et al. 2015). The unspecific symptoms of LD, including cough, fever, muscle aches, and malaise, are easily ignored or underestimated (Cunha et al. 2016).

Isolates number of different *Legionella* species from infection cases during ten years

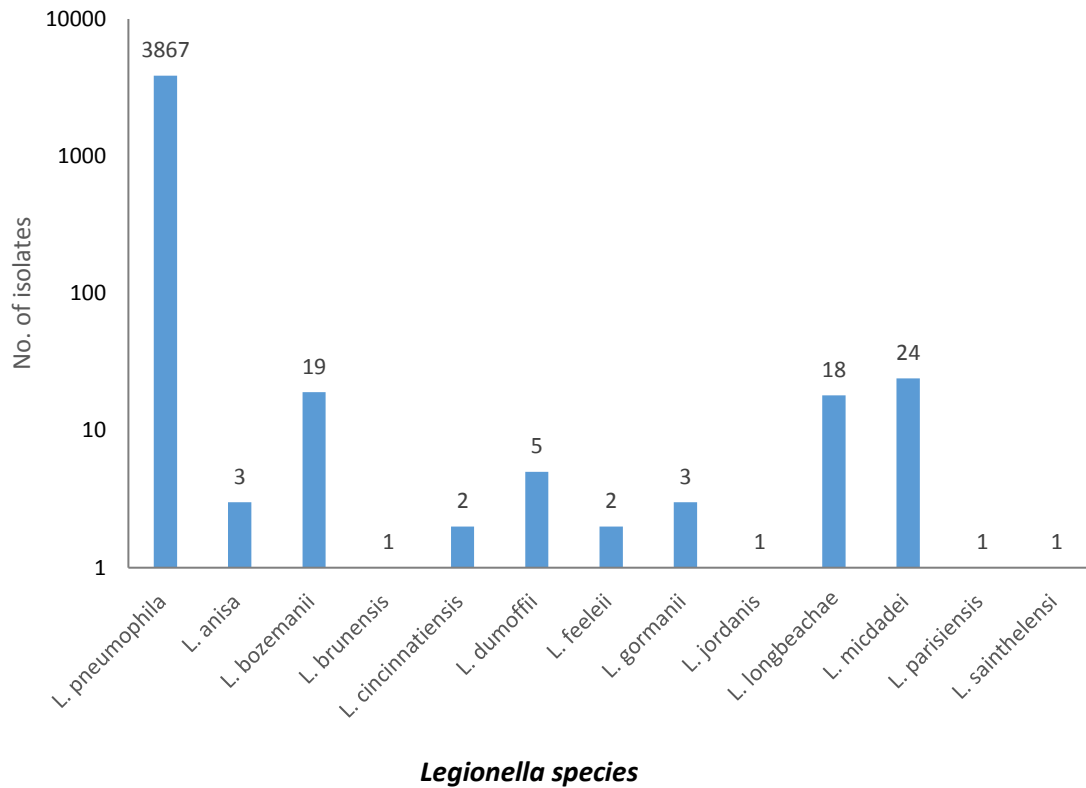


Figure 1.2 Documentation of identified *Legionella* spp. from different clinical cases during 1995–2005. This chart is based on data provided from the European Working Group for Legionella infections (EWGLI) (Diederer 2008).

1.2.2 Macrophages: accidental human hosts of *L. pneumophila*

L. pneumophila can accidentally infect alveolar macrophages and cause LD (Diederer 2008), which implies that macrophages can support *L. pneumophila* multiplication and development. The presence of antimicrobial mechanisms inside the macrophage compromises the intracellular replication of *L. pneumophila* (Copenhaver et al. 2014). *L. pneumophila* derived from environmental amoebas is frequently associated with human infections, but person-to-person transmission of *L. pneumophila* infection has never been reported (Khodr et al. 2016), which suggests that *L. pneumophila* may not be well adapted to macrophages. It remains unknown whether *L. pneumophila* derived from macrophages lack specific virulence traits or whether macrophages cannot fully equip *L. pneumophila* to cause transmission between humans.

Because primary macrophages possess heterogeneity between people (Qin 2012), the use of primary macrophages to study the *L. pneumophila* life cycle and virulence may cause variations between experiments (Daigneault et al. 2010). The human monocytic leukemia cell line THP-1 bears a genetic resemblance to primary monocytes and macrophages. THP-1 cells can differentiate into macrophages upon induction by phorbol-myristate-acetate (Geissmann et al. 2010). Due to its ease of manipulation, THP-1 is widely used to

investigate *L. pneumophila* infection (Dreskin et al. 2001, Qin 2012). Monocytic THP-1 was used to investigate *L. pneumophila* infection in this study.

1.3 Diagnosis and treatment

Accurate diagnosis of LD relies upon the isolation of *L. pneumophila*. The isolation and identification of *Legionella spp.* from clinical specimens is based on the culture method. The *Legionella* culture method is time-consuming with the use of a specific *Legionella*-selective culture medium. Nonculture methods include PCR-based identification (Mentasti et al. 2012) and urinary antigen testing. The latter method can be applied directly to urine specimens and has been reported to be specific and accurate for serogroup 1 strain (Pierre et al. 2017). A combination of both culture and nonculture methods has been suggested to obtain a diagnosis with a high degree of accuracy.

There is currently no useful vaccine to prevent infection from *L. pneumophila*. The effective treatment of *L. pneumophila* infection or LD has been explored. Because *L. pneumophila* is an intracellular pathogen, the antimicrobial agents should be bioactive in infected cells, and therapy with most macrolides and quinolones, but not β -lactams, is effective (Cunha et al. 2016). Erythromycin is a macrolide antibiotic that is used to treat both community-acquired and nosocomial pneumonia (Roig et al. 1993).

Fluoroquinolones are also used to treat LD because its effectiveness is similar to that of erythromycin (Sabria et al. 2005).

1.4 Epidemiology of LD

Since the first identified case of LD in Philadelphia in 1976, many outbreaks of LD caused by *L. pneumophila* infection in humans have been documented around the world (Figure 1.3). One large documented outbreak of LD occurred in Murcia, Spain, in 2001 that involved more than 800 reported cases (Garcia-Fulgueiras et al. 2003, Joseph 2004). The sporadic cases of pneumonia caused by *L. pneumophila* are deserving of greater research attention. The average mortality rate of LD was reported to be 15-20% in hospitalized cases (Gacouin et al. 2002, Roig and Rei 2003). A recent report from the United States of cases caused by a hospital's potable water system demonstrated that nosocomial-associated LD had a 30% fatality rate (Demirjian et al. 2015). In contrast, the fatality rate of the Murcia outbreak was only 1%. This discrepancy could be a result of the clinicians' awareness of the risk of LD when outbreaks occur (Fields et al. 2002, Joseph 2004). The first reported case of travel-associated LD occurred in 2010 in Mexico; it was then suggested to make LD reportable in Mexico (Hampton et al. 2016). In New York City, 213 LD cases with 18 deaths were reported from 2005 to 2015, of which the 2015 outbreak included 138 infected patients and 16 deaths (Fitzhenry et al. 2017). The LD outbreaks were often associated with cooling towers, which highlighted the necessity of appropriate maintenance of cooling tower systems (Weiss et al. 2017). It has been suggested that LD has a high incidence in tropical and temperate areas (Garrison et al. 2016, Hampton et al. 2016); however, its reported incidence (rate per million people) in

Singapore is lower than in European countries, the United States, and Australia (Phin et al. 2014).

In Hong Kong, 460 cases of LD were reported between 1994 and 2017 (Figure 1.4). The number of reported LD cases increased sharply from 2004 to 2015 in Hong Kong, possibly as a result of increased awareness and improved diagnostic methods. In addition, some mild cases of Legionellosis could be under-reported (Chan-Yeung and Yu 2003). From an environmental survey in Hong Kong, the frequently reported identifications in both household and public water systems indicates a potential threat to public health (Chan-Yeung and Yu 2003, Chen et al. 2014). The incidence of LD in Hong Kong is close to 10 per million people based on the reported cases in 2016 and 2017. The incidence in Hong Kong was higher than those in Canada, Japan, and Singapore (Figures 1.3 and 1.4). The variation in the incidence of LD could be due to the differences in reporting and surveillance systems in various countries and strategies adopted for the prevention of LD (Kruse et al. 2016).

Distribution of reported Legionnaires' disease cases per million people in different regions

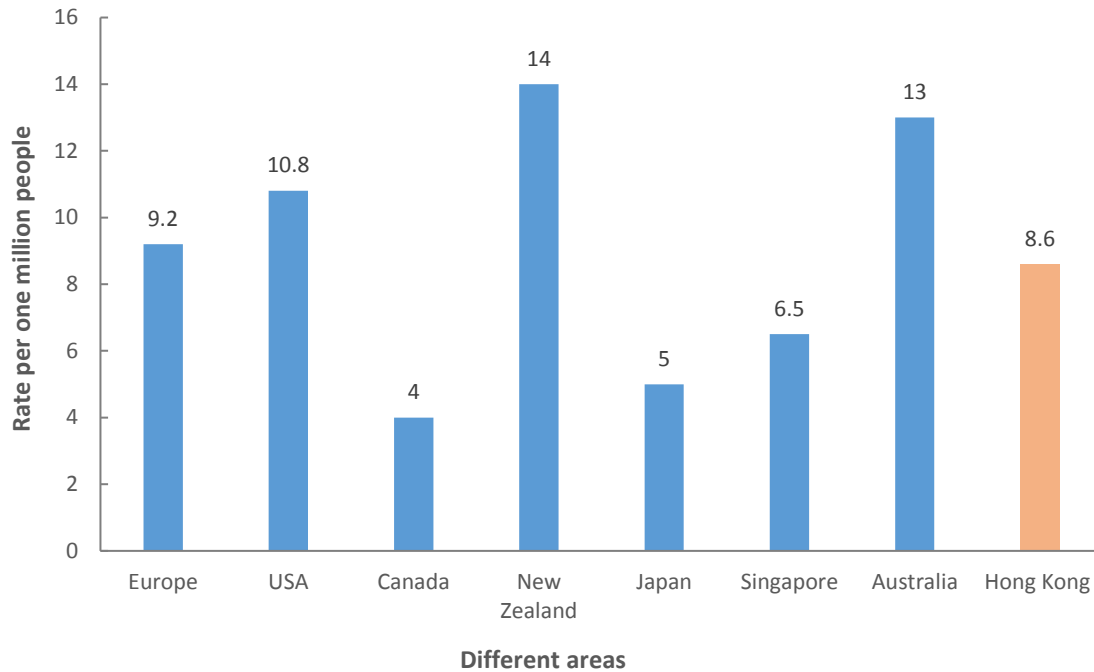


Figure 1.3 Rate of Legionnaires' disease per million people in different regions. Data are based on reported cases divided by the total population (Phin et al. 2014), as compared with the average incidence in Hong Kong between 2014 and 2017.

Annual reported Legionnaires' disease cases from 1994 to 2017 in Hong Kong

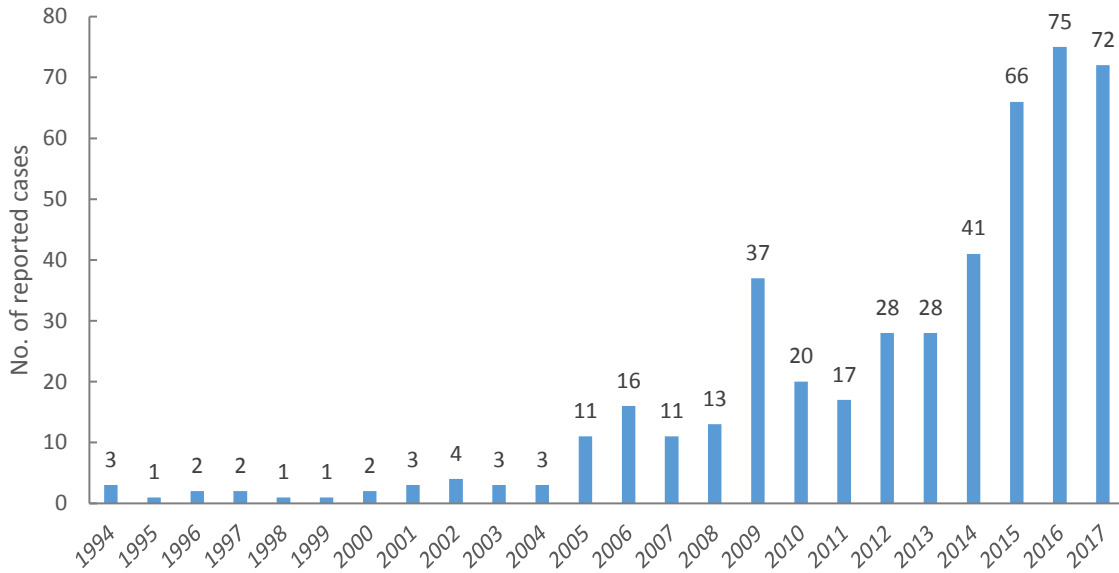


Figure 1.4 Summary of reported cases of Legionnaires' disease from 1994 to 2017 in Hong

Kong. Data were collected based on the reported cases shown on the website

(<https://www.chp.gov.hk/en/static/24012.html>) of the Centre for Health Protection, Department of Health, Hong Kong.

1.5 Roles of biofilm and amoebas in *L. pneumophila* survival

1.5.1 Biofilm mediates the environmental spread of *L. pneumophila*

Biofilms include densely packed microorganisms growing on a solid surface in contact with water. *Legionella* that grows inside biofilm obtains nutrients and protection from an adverse environment (Declerck 2010, Guerrieri et al. 2008). Biofilms have been reported to provide replicative support for environmental microbes, including *L. pneumophila*, which displays complicated microbe-microbe interactions (Abdel-Nour et al. 2013, Bitar et al. 2004). *L. pneumophila* exists in the anthropogenic water biofilm, which also includes other opportunistic waterborne pathogens, including *Pseudomonas*, *Sphingomonas*, and *Mycobacterium* species (Falkinham et al. 2015). *Sphingomonas* species have been revealed as antagonistic to *L. pneumophila*, but *Mycobacterium* has been reported to enhance *L. pneumophila* cultivability (Giao et al. 2011). *Pseudomonas aeruginosa* is frequently identified in association with *L. pneumophila* (Abdel-Nour et al. 2013), and *P. aeruginosa* has the antagonistic effect to inhibit *L. pneumophila* colonization in biofilm; however, *Klebsiella pneumonia* was reported to alleviate this antagonistic effect (Stewart et al. 2012). The molecular mechanisms involved in *L. pneumophila* interaction with other microbial species remain unclear. In addition to prokaryotic microbes, eukaryotic amoebae were reported to correlate with the *L. pneumophila* biomass in plumbing biofilm (Liu et al. 2012b). Amoebas such as *Hartmannella vermiformis* and *Acanthamoeba castellanii* are widely distributed in biofilm and support the survival of *L. pneumophila* (Hilbi et al. 2007, Lam et al. 2011) (Figures 1.5.1 and 1.5.2). Knowledge of the potential interactions of *L. pneumophila* with

other species in the biofilm facilitates the formation of strategies to prevent infection with this pathogen.

1.5.2 *Acanthamoeba castellanii*: environmental host

Free-living amoebas (FLAs) play important roles in the dissemination of *L. pneumophila* in water (Scheid 2014). *Acanthamoeba* and *Hartmannella* are the two most frequently identified FLAs in water (Valster et al. 2010). Like biofilm-associated amoeba, FLAs feed on bacteria (Delafont et al. 2013). However, certain bacteria can survive inside FLAs, including *L. pneumophila*. It has been reported that FLAs are able to resuscitate starved viable but noncultivable *L. pneumophila* from environmental water (Garcia et al. 2007). FLAs have been found to support *L. pneumophila* survival in heat-treated water, especially *Acanthamoeba* (Dobrowsky et al. 2016).

Acanthamoeba spp. have been reported as the most-identified *L. pneumophila* environmental host (Shoff et al. 2008), possibly because the optimal growth temperature of *Acanthamoeba* species is close to room or environmental temperature (25°C to 29°C) (Buse and Ashbolt 2011). It has also been reported that the persistence of *Acanthamoeba* in the water system enhances the spread of *L. pneumophila* and may account for LD (Magnet et al. 2015).

A. castellanii is a major environmental host of *L. pneumophila* and an opportunistic pathogen that causes keratitis in humans (Lorenzo-Morales et al. 2015). *A. castellanii* can act as a reservoir of pathogens in the environment that subsequently cause human infection (Khan 2006, Magnet et al. 2015). *A. castellanii* exists in two forms: trophozoite and cyst (Figure 1.5.1). The *A. castellanii* trophozoite is mobile and replicative, which engulfs bacteria. The formation of cysts in *A. castellanii* is induced when the growth conditions become unfavorable; the cysts enable the *Acanthamoeba* to survive (Siddiqui and Khan 2012). *Acanthamoeba* cysts are also resistant to biocides and chemicals (Khan 2006, Khunkitti et al. 1998); hence, the cysts protect the intracellular *L. pneumophila* from disinfectant treatment in water (Shanmuganathan and Khan 2009).

In addition to protecting intracellular *L. pneumophila* from environmental challenges, *A. castellanii* enhances the ability of *L. pneumophila* to invade macrophages (Cirillo et al. 1994b). *Acanthamoeba* play important roles in the adaptation to intracellular life and propagation of *L. pneumophila* (Escoll et al. 2013). The successful intracellular replication of *L. pneumophila* in *A. castellanii* is a prerequisite for the dissemination of *L. pneumophila* in the aquatic environment and transmission of the pathogen to humans (Al-Quadani et al. 2012).

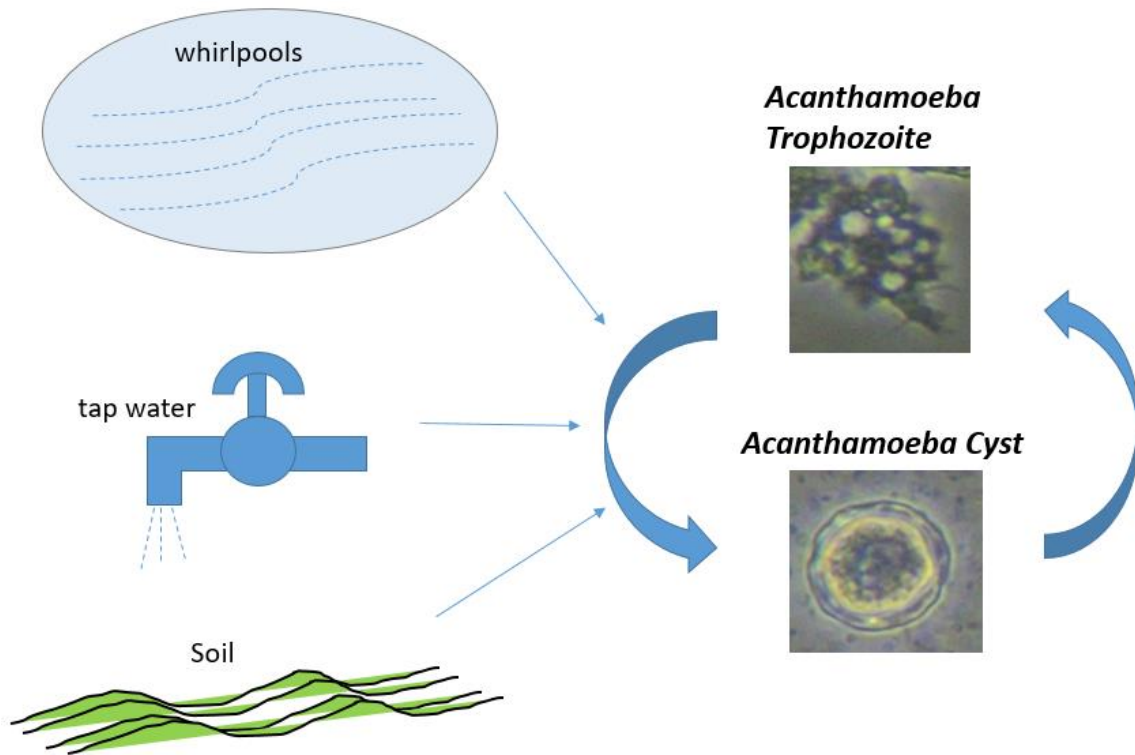


Figure 1.5.1 Life cycle of *A. castellanii* in environment. *Acanthamoeba* are widely distributed in the environment, including swimming pools, tap water, and soil. There are two forms of *Acanthamoeba*: cyst and trophozoite. The morphology of feeding and dividing trophozoite was reported as acanthopoda around 20 to 50 μm that have a rough exterior with several spine-like projections (Siddiqui and Khan 2012). The cyst is spherical, around 15 μm in diameter, and double-walled with pores (Trabelsi et al. 2012).

1.5.3 Biphasic life cycle of *L. pneumophila*

Extracellular and intracellular *L. pneumophila* both have biphasic life cycles that consist of replicative and transmissive phases. During extracellular growth, *L. pneumophila* undergoes exponential growth when nutrients and conditions are optimal, which is the replicative phase (Declerck 2010, Newton et al. 2010). When nutrients become limited, *L. pneumophila* enters a transmissive phase during which it expresses virulence factors (post-exponential growth phase) (Manske and Hilbi 2014).

During intracellular growth, *L. pneumophila* also has both replicative and transmissive phases (Al-Bana et al. 2014). During the replicative phase, *L. pneumophila* grows exponentially. At the late stage of intracellular growth, *L. pneumophila* enters a transmissive phase and expresses virulence strongly related to transmission (Schunder et al. 2014). *L. pneumophila* is also known as the mature infection form at this stage, during which it has been reported to have a greater capacity to infect phagocytes and survive in environmental biofilms (Molofsky and Swanson 2004) (Figure 1.5.2). Studies have demonstrated that *L. pneumophila* shows different virulence traits between the replicative and transmissive phases. *L. pneumophila* becomes more motile and resistant during the transmissive phase (Molofsky and Swanson 2003). Bacterial regulators such as LetA and sigma factors such as RpoS are induced during the late stage of *L. pneumophila* intracellular growth to activate the expression of flagellin (Molmeret et al. 2010). The differentiation of replicative *L. pneumophila* to transmissive *L. pneumophila* can trigger the development of virulent traits (Robertson et al. 2014). Bacteria in the two growth

phases have also exhibited different protein expression profiles (Garduño 2008), and *L. pneumophila* in the transmissive phase has been considered as more virulent via expression of abundant virulent or effector proteins (Hayashi et al. 2010). Due to this characteristic, *L. pneumophila* in the transmissive phase is generally used to investigate the virulence expression of the pathogen.

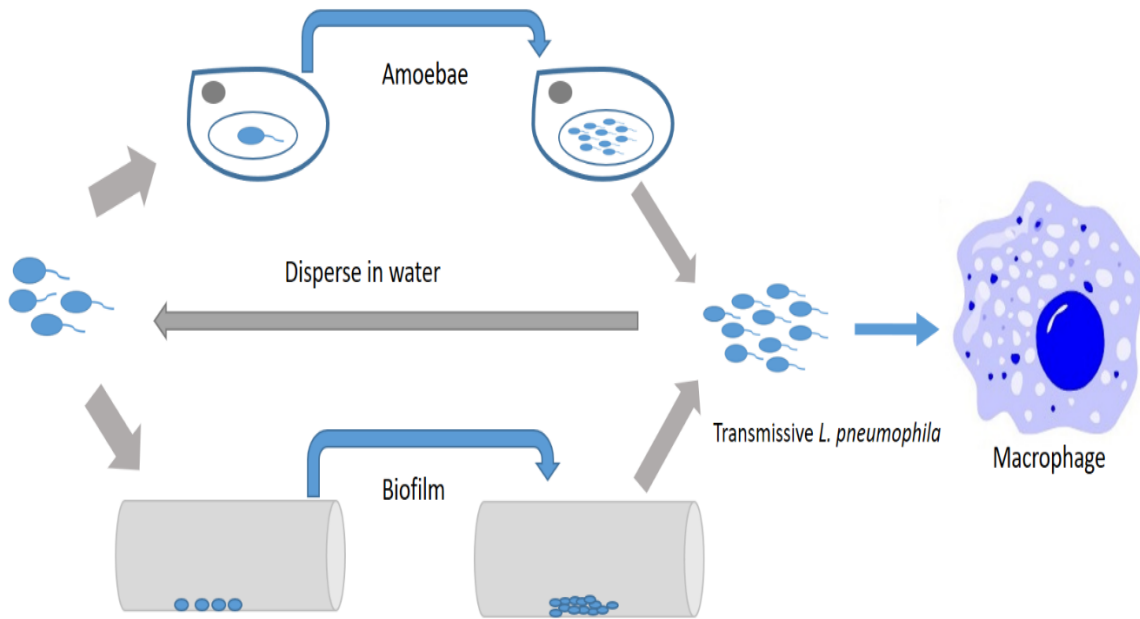


Figure 1.5.2 *L. pneumophila* life cycle from biofilm and amoeba to human macrophage. *L. pneumophila* is widely distributed in biofilm of artificial water systems, and amoeba as predator of bacteria are often located on surface of biofilm. The amoebas and biofilms are the major survival environment of *L. pneumophila* (Hilbi et al. 2010). After *L. pneumophila* underwent either intracellular replication in amoeba or extracellular replication in biofilm, the bacteria entered the transmissive phase. At this stage, *L. pneumophila* was more virulent and ready to infect macrophages (Garduño 2008). The transmissive *L. pneumophila* with greater survival ability can also be dispersed in water and begin another environmental life cycle.

1.6 *L. pneumophila* virulence factor and effector proteins

L. pneumophila virulence factors are widely defined as bacterial proteins that can affect the intracellular survival and growth of *L. pneumophila* (Cianciotto 2001, Zhu 2015). *L. pneumophila* virulence factors that can be translocated via a type IV secretion system (T4SS) have been defined as effector proteins. As a result, the virulence factor but not effector was defined as the T4SS-independent bacterial protein that played a virulent role in the survival and growth of *L. pneumophila* (Bruggemann et al. 2006). *L. pneumophila* virulence factors were found throughout the intracellular life, and Table 1.1 exhibits virulence factors but not effector proteins that work in different ways to affect bacterial survival. The T4SS-independent virulence factors are often related to bacterial surface and structural proteins that affected bacterial attachment to the host cell and intracellular survival (Zhu 2015).

T4SS-independent virulence factors have been less reported than effector proteins. Most interestingly, *L. pneumophila* secreted more than 300 effector proteins. The quantity of effectors was reported to be remarkable relative to other well-known bacteria, including *Salmonella enterica* and *Escherichia coli* (Ensminger 2016). The *L. pneumophila* T4SS and effectors are introduced as follows.

Table 1.1 *L. pneumophila* virulence factors are involved in intracellular growth and pathogenesis

Gene	Virulence proteins	Proposed function	Pathways and Interactions	References
lpg2515	RtxA	Structural toxin protein	Adherence and entry into cell	(Cirillo et al. 2001, Cirillo et al. 2002)
lpg2639	EnhC	Enhanced entry protein	Bacterial cell wall maintenance	(Liu et al. 2008, Liu et al. 2012a)
lpg0791	Mip	Peptidyl-prolyl isomerase	Pathogenesis, amoeba/macrophage infectivity potentiator	(Cianciotto and Fields 1992, Fischer et al. 1992)
lpg1284	RpoS	Sigma factor	Trigger virulence expression at transmissive phase	(Abu-Zant et al. 2006, Bachman and Swanson 2004)
lpg1782	FliA	Sigma factor that triggers flagellum expression	Flagella biosynthesis and motility	(Heuner et al. 2002, Schulz et al. 2012)

Table 1.1 Continued

Gene	Virulence proteins	Proposed function	Pathways and Interactions	References
lpg0748	LPS	Lipopolysaccharide protein	Bacterial surface antigen that can trigger proinflammatory response	(Case et al. 2013, Helbig et al. 1997, Zhu 2015)
lpg2657	FeoB	Ferrous iron transport protein	Iron acquisition	(Cianciotto 2007, Robey and Cianciotto 2002)

1.6.1 *L. pneumophila* T4SS: built by Dot/Icm proteins

1.6.1.1 Introduction of *L. pneumophila* T4SS

The translocation of *L. pneumophila* effector proteins depended mainly on the T4SS (type IV secretion system), which is the core transporter system (Luo and Isberg 2004). Gram-negative bacteria including *Coxiella burnetii* and *L. pneumophila* use a type IVB secretion system (T4BSS) to inject effectors into the host cell to ensure bacterial safety and reproduction inside the cell during pathogenesis (Nagai and Kubori 2011). The T4SS is also called the Dot/Icm (defect in organelle trafficking/intracellular multiplication) secretion system because the *dot/icm* loci genes encode the constructs of this core secretion complex. The *dot/icm* mutants are unable to multiply in both macrophages and *Acanthamoeba* (Al-Khodor et al. 2008).

1.6.1.2 Dot/Icm secretion system

There were 26 identified *dot/icm* genes in the Dot/Icm T4SS core system (Seshadri et al. 2003) (Figure 1.6). DotC, DotD, DotF, DotG, and DotH formed the core transmembrane complexes (Vincent et al. 2006). Components located in the bacterial cytoplasm included IcmS and IcmW, which adapted with bacterial effector proteins (Coers et al. 2000). The cytoplasmic DotB was regarded as the ATPase of this secretion system (Nagai and

Kubori 2011). IcmQ was reported to insert pores into the lipid membrane via regulation of the chaperone protein IcmR (Dumenil et al. 2004). DotU and IcmF were reported to be conserved among diverse species, and both were involved in maintaining the stability of the Dot/Icm system (Sexton et al. 2004). Transmembrane protein IcmT was also reported to be essential for bacteria-mediated pore formation during infection (Molmeret et al. 2002), which is important for bacterial egress. The transmembrane protein DotK was reported to facilitate the stabilization of the Dot/Icm apparatus (Nagai and Kubori 2011). Despite the essential role of the core Dot/Icm secretion system, the secreted effector proteins also contributed to *L. pneumophila* pathogenesis in various ways. The key process involved in the intracellular growth of *L. pneumophila*, including bacterial attachment and entry, modulation of vesicle trafficking, lysosome avoidance, and host cell death manipulation were reported as Dot/Icm-dependent (Ensminger and Isberg 2009).

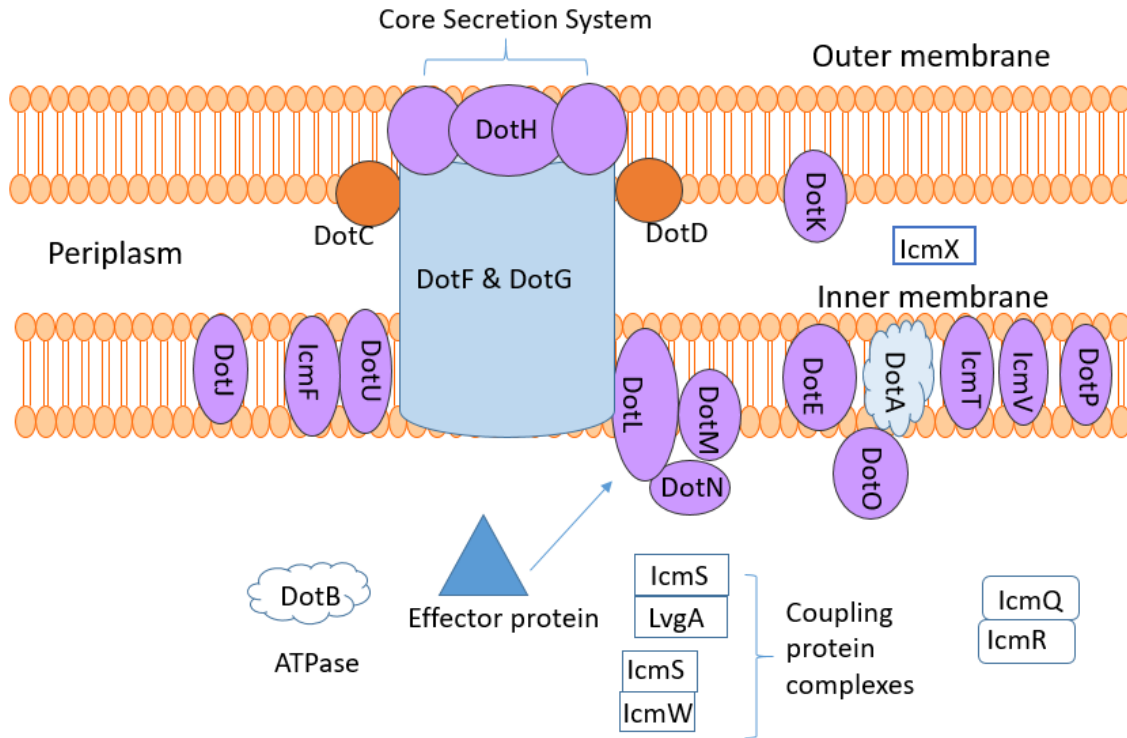


Figure 1.6 The Dot/Icm T4SS of *L. pneumophila*. Twenty-six Dot/Icm substrates facilitate the T4SS to deliver various effector proteins. The key Dot/Icm substrates have multiple roles, it can function as core transmembrane proteins, translocators, and signal transduction mediators (Nagai and Kubori 2011, van Schaik et al. 2013).

1.6.2 Effector proteins

More than 300 effector proteins were translocated throughout *L. pneumophila* T4SS to manipulate the host cell functions and support the pathogenesis of *L. pneumophila*, and the family of T4SS-dependent effectors continued to grow during past years (Isaac and Isberg 2014). *L. pneumophila* effector proteins were involved in the entire intracellular life from entry to release, and Table 1.2 exhibits some well-studied effector proteins.

L. pneumophila effector SdeA (LaiA) has been reported to contribute to bacterial adhesion and entry into the host cell (Bruggemann et al. 2006). After being uptaken, *L. pneumophila* LidA can cooperate with SidM (DrrA) to recruit host cell Rab1 (GTPase-activating protein) to the *Legionella*-containing vacuole (LCV) where *L. pneumophila* resides and replicates (Hubber and Roy 2010, Murata et al. 2006). Eukaryotic Rab1 and Arf1 (ADP-ribosylation factor 1) are involved in trafficking endoplasmic reticulum (ER) and Golgi vesicles, respectively (Isberg et al. 2009). The RalF can recruit Arf1 to the LCV (Nagai et al. 2002). Most interestingly, the bacterial LepA and LepB effectors were reported to be similar to the eukaryotic SNAREs, which are often involved in vesicle fusion. *L. pneumophila* LepA and LepB were both proposed to be involved in vesicle fusion to the LCV, and both were involved in bacterial nonlytic release (Chen et al. 2004, Chen et al. 2007).

This pathogen has many other effector proteins that have homology with eukaryotic proteins, and the redundancy of *L. pneumophila* effectors also enhance the difficulty of

exploring one effector's role. One example is LegK1, which is similar to eukaryotic serine/threonine protein kinase that may be involved in vesicle trafficking and NFκB pathway disruption (Haenssler and Isberg 2011). Another example is the effector AnkX, which contains ankyrin repeats domain, and AnkX was found to be the phosphocholine transferase involved in vesicle trafficking to LCV and in lysosome avoidance (Allgood et al. 2017, Hubber and Roy 2010). *L. pneumophila* SidK is another effector that avoids lysosomal digestion by targeting host cell v-ATPase to repress LCV acidification (Xu et al. 2010).

L. pneumophila can also disrupt host cell transcription and translation (Rolando and Buchrieser 2014). RomA was found to methylate host chromatin histone to inhibit host cell gene transcription (Rolando et al. 2013). *L. pneumophila* Lgt1/2/3 belongs to glucosyltransferase that can inhibit host cell elongation factor (eEF1A) (Belyi et al. 2006, Belyi et al. 2008), and SidI is another effector that targets eEF1A (Shen et al. 2009). Both SidI and Lgt1/2/3 can activate the NFκB pathway by disrupting the NFκB inhibitory factor IκB. Moreover, *L. pneumophila* had different effector proteins to modulate the host cell death pathway (Table 1.2), which is introduced later.

L. pneumophila produces large numbers of effectors, and this pathogen can also grow in wide range of hosts. Ensminger (2016) suggested an interesting concept that *L. pneumophila* could use different patterns of effector proteins when grown in different host cells (Ensminger 2016). Amoebic species played an important role in *L.*

pneumophila evolution, and *L. pneumophila* grown in wide ranges of host cells could be one trigger to equip this pathogen with so many eukaryote-like effector proteins (Cazalet et al. 2004, Escoll et al. 2013, Isaac and Isberg 2014). Amoebas may have selective pressure for *L. pneumophila* virulence expression, which makes this pathogen further transmissible to macrophages; as a result, the interaction of *L. pneumophila* and amoebas may be a valuable treasure to reveal the pathogen-host interaction. This further indicates that a comparison of *L. pneumophila* gene expression patterns when grown in amoebas and in macrophages may help to reveal how *L. pneumophila* interacts differentially with two evolutionarily distant hosts.

Table 1.2 *L. pneumophila* effector proteins that manipulate diverse host cell pathways during intracellular growth

Gene	Effector proteins	Proposed function	Pathways and Interactions	References
lpg2157	SdeA (LaiA)	Adhesion protein	Promote bacterial internalization	(Bruggemann et al. 2006)
lpg1950	RalF	Guanine nucleotide exchange protein	Recruit and activate Arf1 (ADP ribosylation factor) on the LCV	(Amor et al. 2005, Nagai et al. 2002)
lpg0940	LidA	Located on the surface of LCV to cooperate with Rab1 GEF	Promote the recruitment of Rab1 to LCV	(Conover et al. 2003, Machner and Isberg 2006)
lpg2464	SidM (DrrA)	Rab1 guanine nucleotide-exchange factor	Rab1 recruitment to LCV	(Machner and Isberg 2006, Murata et al. 2006)
lpg0695	AnkX	Ankyrin repeat containing protein, phosphocholine transferase	Prevent LCV fusion with lysosome	(Allgood et al. 2017)
lpg1483	LegK1	Ser/Thr kinase	ER recruitment, and activation of NF-κB signaling	(Ge et al. 2009, Hervet et al. 2011)
lpg2556	LegK3	Ser/Thr Kinase	Modulates <i>saccharomyces</i> vesicle trafficking	(Wang et al. 2014)

Table 1.2 Continued

Gene	Effector proteins	Proposed function	Pathways and Interactions	References
lpg2793	LepA	GTP-binding protein, homology to SNAREs	Promote exocytic (nonlytic) release from protozoan	(Chen et al. 2004)
lpg2490	LepB	Homology to SNAREs that mediate vesicle fusion	Regulate Rab1 cycling, and related to nonlytic release	(Chen et al. 2007)
lpg0968	SidK	Inhibit ATP hydrolysis	Blocking vacuolar acidification through targeting host v-ATPase	(Xu et al. 2010)
lpg2504	SidI	Inhibition of elongation factor (eEF1A and eEF1BY)	Induction of host stress response	(Shen et al. 2009)
lpg1368	Lgt1	glucosyltransferase	Inhibit host elongation factor 1A	(Belyi et al. 2006, Belyi et al. 2008)
lpg2815	MavN (IroT)	Intravacuolar associated protein responsible for iron acquisition	Iron acquisition during intracellular growth	(Isaac et al. 2015, Portier et al. 2015)
lpg1683	RavZ	Autophagy related protein Atg8 deconjugation	Inhibition of host cell autophagy	(Choy et al. 2012)

Table 1.2 Continued

Gene	Effector proteins	Proposed function	Pathway and Interactions	References
lpg1184	RomA	Methyltransferase that involved in histone posttranslational modification	Control host cell gene expression	(Rolando et al. 2013)
lpg0376	SdhA	Work with phospholipase <i>plaA</i> to maintain the LCV integrity	Inhibit pyroptosis and LCV maintenance	(Creasey and Isberg 2012, Laguna et al. 2006)
lpg2584	SidF	phosphoinositide phosphatase	Inhibit apoptosis by targeting Bcl2 proteins	(Banga et al. 2007, Hsu et al. 2012)
lpg2831	VipD	phospholipase	Modulation of phospholipids	(Gaspar and Machner 2014, Zhu et al. 2013)
lpg1340	FliC (FlaA)	flagellin protein induced pyroptosis	Induced the inflammatory pyroptosis and promote bacterial egress	(Ren et al. 2006, Silveira and Zamboni 2010)

1.7 *L. pneumophila* intracellular interaction with hosts during intracellular growth

L. pneumophila can grow in a wide range of host cells, from environmental protozoa to mammalian cells. The intracellular growth ability of *L. pneumophila* could differ when grow in different hosts (Ensminger 2016, Xiong et al. 2017). It has been reported that *L. pneumophila* cannot grow in monocyte culture medium supplied with lysed monocytic cells, but the bacteria can infect and replicate inside live human monocytes (Horwitz and Silverstein 1980). The multiplication of intracellular *L. pneumophila* involves not only the bacterial acquisition of nutrients from host cells, the complex pathogen and host interaction could also be dominant which is poorly understood (Shin and Roy 2008).

Although *L. pneumophila* has been reported to use similar strategies to avoid host cell defenses in both mammalian cells and protozoa (Gao et al. 1997), differences remain between macrophages and *Acanthamoeba*. The phagocytic cell-like macrophages have pathogen-recognition receptors and can thus induce a signaling cascade for immune defense. *Acanthamoeba* was not found to have pathogen-recognition receptors to induce immune response cascades. Still, numerous studies have used *Acanthamoeba* as the infection model of *L. pneumophila* (Garrison et al. 2016, Hilbi et al. 2007) because *Acanthamoeba* played an important role in the evolution of the virulence of *L. pneumophila*. Comparison of *L. pneumophila* grown in environmental host *A. castellanii* and human monocyte THP-1 may help to reveal the underlying differences in permissiveness and pathogenesis.

1.7.1 *L. pneumophila* entry into host cells

The replication of *L. pneumophila* inside host cells involves a conserved intracellular life cycle in protozoa and in human macrophages (Figure 1.6). However, there were different observations on the entry of *L. pneumophila* into host cells (Newton et al. 2010). The uptake of *L. pneumophila* by coiling phagocytosis has been documented in both *Acanthamoeba* and macrophages (Haenssler and Isberg 2011). Macrophages also have various pattern-recognition receptors to internalize pathogens, and Nod-like receptor was reported to internalize *L. pneumophila* and activate an inflammasome-associated signaling cascade (Wen et al. 2013). Despite the host cell's active uptake of *L. pneumophila*, a flagella-mediated motility and Dot/Icm secretion system was reported that induces *L. pneumophila* to invade the hosts (Hubber and Roy 2010). In addition, *L. pneumophila* has different virulence factors, including RtxA and EnhC (Table 1.1), that enhance bacterial adherence to the host cell, which facilitates bacterial entry. The entry of *L. pneumophila* into the host cell is believed to be a two-way interaction, which may lead to differences in the number of *L. pneumophila* that are internalized by various hosts (Xiong et al. 2017). Although macrophages possess various mechanisms for the uptake of *L. pneumophila*, no study has shown that macrophages can internalize more *L. pneumophila* than *Acanthamoeba* when challenged with same dosage of bacteria.

1.7.2 Intracellular *L. pneumophila* replicated inside LCV

After entry into the host cell, *L. pneumophila* resides and replicates in an LCV. The LCV has a connection with the host cell ER and Golgi complex, which can secrete and recycle vesicles that can be recruited by *L. pneumophila* effectors to the LCV. After entering the host cell, *L. pneumophila* inside the LCV were found to be surrounded by mitochondria and vesicles (Figure 1.7). The vesicles were derived from ER-Golgi trafficking by subverting the host cell Rab1 (cell membrane organizer) and Arf1 (vesicle trafficking-related protein), as introduced in Section 1.6.2 (Derre and Isberg 2004, Ensminger and Isberg 2009, Kagan et al. 2004).

The LCV was then reported to be surrounded by ribosomes instead of vesicles and mitochondria (Ge and Shao 2011, Xu and Luo 2013), and *L. pneumophila* inside the LCV were found to begin replication at this stage (Hubber and Roy 2010). *L. pneumophila* effector proteins, including SidD and LepB, can inactivate Rab1 for removal and recycling of vesicles (Neunuebel et al. 2011). The development and maturation of the LCV remains under discussion. One can be sure that LCV development is strongly connected with the host cell rough endoplasmic reticulum and that *L. pneumophila* has various effectors to subvert host cell vesicle trafficking (Garrison et al. 2016).

L. pneumophila inside LCV were protected from host cell defenses, including lysosomal digestion and the macrophage inflammatory response (Creasey and Isberg 2012). It was reported that the LCV fused with the lysosomal compartment during the final stage of *L.*

pneumophila intracellular life (Isaac and Isberg 2014, Shin and Roy 2008), as it was found that *L. pneumophila* was resistant to acid when it reached the end of the replicative phase (Hubber and Roy 2010, Newton et al. 2010). When the bacteria completed replication inside the LCV, it sought to escape or egress from the host cells and infect the neighboring cells.

1.7.3 *L. pneumophila* egress from host cell

Observations have differed about how *L. pneumophila* escaped the host cell after intracellular replication. One argument regards whether *L. pneumophila* was released from the LCV into the host cell cytoplasm before its egress or whether *L. pneumophila* inside the whole LCV escaped from the host cell without first releasing into the cytoplasm (Appelt and Heuner 2017). There were two forms of *L. pneumophila* egress, lytic and nonlytic release, which have both been observed in *L. pneumophila*-infected *Acanthamoeba* cells. The involvement of *L. pneumophila* LepA and LepB were reported in bacterial nonlytic release via exocytosis (Chen et al. 2004, Chen et al. 2007), and it has been observed that multiple LCVs contained with *L. pneumophila* are released from the *Acanthamoeba* cell (Berk et al. 1998). Another form lytic release observed in *L. pneumophila*-infected *Acanthamoeba* was mediated via rapid necrosis (Gao and Kwaik 2000).

Gao and Kwaik also reported that the escape of *L. pneumophila* from macrophages was mediated mainly via apoptosis (Gao and Abu Kwaik 1999a), which cannot be used by *L. pneumophila* inside *Acanthamoeba* to release bacteria (Gao and Abu Kwaik 1999b, Hagele et al. 1998). Despite host cell death-mediated pore formation or membrane destruction, *L. pneumophila* was reported to have a potential pore-forming toxin to trigger cytolysis (Molmeret and Kwaik 2002). The *L. pneumophila* mutant of *icmT* caused dysfunction of cytolysis, and bacteria could not be released at the end of intracellular replication (Molmeret et al. 2002, Zink et al. 2002).

It was later revealed that exposure of *L. pneumophila* flagellin FlaA (FliC) during the late stage of intracellular life could trigger host cell pyroptosis-mediated pore formation and bacterial rupture in macrophages (Alli et al. 2000, Silveira and Zamboni 2010). *L. pneumophila* is a potential pathogen that can trigger various forms of host cell death, including apoptosis, necrosis, and pyroptosis, all of which have been reported (Speir et al. 2014). The egress of *L. pneumophila* is strongly associated with host cell death.

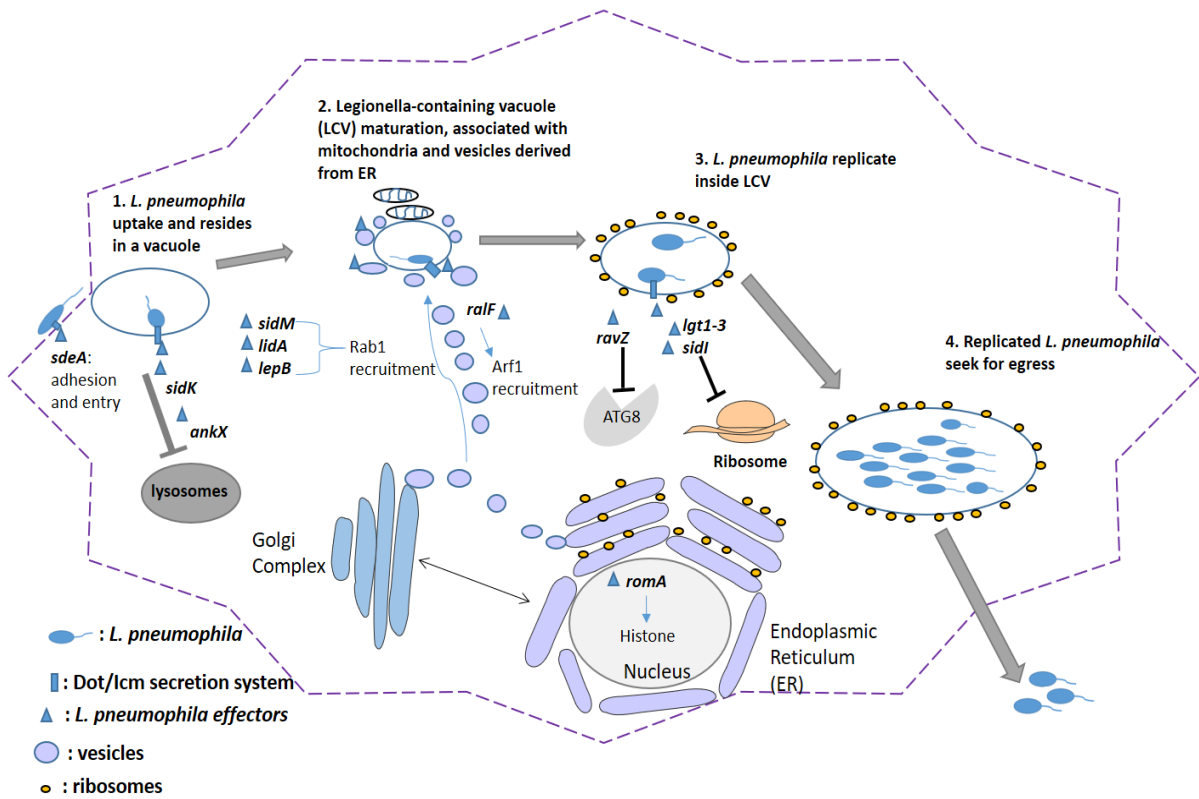


Figure 1.7 Intracellular growth pathway of *L. pneumophila*. After *L. pneumophila* entered host cells, the bacteria could facilitate the formation and maturation of LCV by secreting various effector proteins to subvert the host cell's ER-Golgi trafficking. The bacteria Dot/Icm type IV secretion system (T4SS) can translocate multiple effector proteins to facilitate bacterial intracellular survival and growth with modulation of the host cell's normal functions (Isberg et al. 2009).

1.8 Host cell death pathway induced by *L. pneumophila* infection

1.8.1 *L. pneumophila* induces cell death in macrophages

Key *L. pneumophila* virulence factors, including FlaA, VipD, SdhA, and SidF, contribute to regulate macrophage cell death (Creasey and Isberg 2012, Lamkanfi and Dixit 2010). Of these, *flaA* encodes *L. pneumophila* flagellin, a flagellar component produced during the post-exponential growth phase of *L. pneumophila* (Molofsky et al. 2005). In addition to its role as a structural protein, flagellin exhibits effector functions. For example, the injection of flagellin into the host cytoplasm from the LCV leads to activation of the inflammasome and caspase-1 and thus to pyroptosis (Silveira and Zamboni 2010). Biofilm-derived *L. pneumophila* has been reported to be more pathogenic than planktonic *L. pneumophila* in murine macrophages by inhibiting flagellin expression to limit the induction of host cell death (Abu Khweek et al. 2013).

Several researchers have studied the role of VipD, a phospholipase. Gaspar et al. demonstrated that VipD could inhibit endosomal fusion with the LCV in COS-1 and CHO cell models, and they observed rounding and death in cells that produce VipD (Gaspar and Machner 2014). In addition, Zhu et al. described VipD-induced apoptosis in *L. pneumophila*-infected macrophages and observed that this phospholipase hydrolyzed both phosphatidylethanolamine (PE) and phosphocholine to destabilize the mitochondrial membrane, and that the consequent release of cytochrome c led to caspase-3 activation and apoptosis (Zhu et al. 2013).

In contrast to *flaA* and *vipD*, which trigger death in *L. pneumophila*-infected host cells, *sdhA* and *sidF* have been shown to inhibit host cell death (Figure 1.8). The gene *sdhA* encodes a Dot/Icm-translocated effector protein that prevents pyroptosis by blocking the activation of AIM2 inflammasome and caspase-1 and is therefore required for multiplication of *L. pneumophila* within macrophages (Ge et al. 2012). *L. pneumophila* SdhA may also be involved in the maintenance of LCV integrity (Creasey and Isberg 2012). In the absence of *sdhA*, *L. pneumophila* infection causes nuclear degradation, mitochondrial disruption, and significant cell death in infected macrophages (Laguna et al. 2006). In addition, an infection study reported an association of *sdhA*-deficient *L. pneumophila* with an increase in dendritic cell death (Nogueira et al. 2009). The SidF effector inhibits macrophage apoptosis by interacting with the endogenous proapoptotic Bcl-2 family proteins to facilitate the intracellular multiplication of *L. pneumophila* (Banga et al. 2007). However, the *L. pneumophila* virulence genes (*flaA*, *vipD*, *sdhA*, and *sidF*) have been less explored in *Acanthamoeba*.

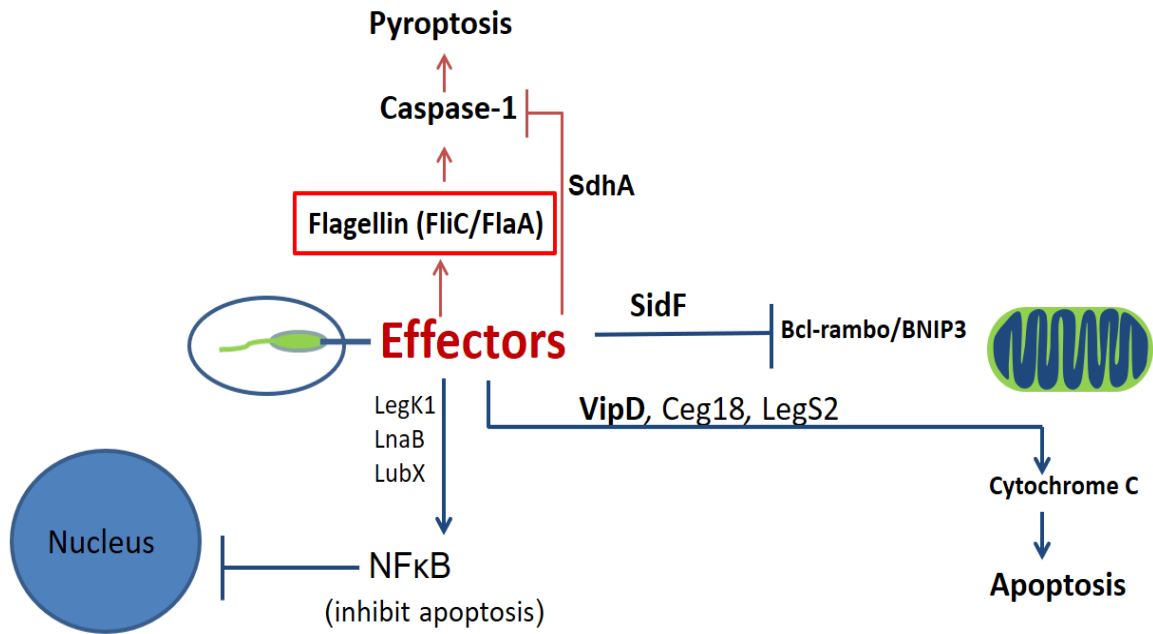


Figure 1.8 Pathway involved in *L. pneumophila*–induced host cell death. Two major types of cell death were identified during *L. pneumophila* infection: apoptosis and pyroptosis. The bacterial effector FlaA could activate caspase-1–dependent pyroptosis, but SdhA functions in the opposite way. The *L. pneumophila* effector SidF inhibits apoptosis by blocking death proteins, but VipD could work in the opposite way (Speir et al. 2014).

The *L. pneumophila* flagellin effector FlaA and the surface protein LPS can both directly induce the caspase-1–associated inflammasome activation and then cause pyroptosis in human macrophages (Lamkanfi et al. 2007); the inflammation leads to cell death and eventually clears the bacterial infection. This may be one reason why macrophages are only accidental hosts of the pathogen *L. pneumophila*. In contrast to caspase-1-associated pyroptosis caspase-3-associated apoptosis belongs to non-inflammatory cell death, caspase-3 activation was also detected during the early stage of *L. pneumophila* intracellular replication, which was found to have importance in the protection of the LCV from the endosomal pathway (Molmeret et al. 2004). The regulation of the host cell death pathway by *L. pneumophila* is believed to depend upon the bacterial dose and growth phase (Molmeret et al. 2004).

Once *L. pneumophila* completed intracellular replication, the bacteria activated the host cell death program to escape from the human host. Programmed cell death, including both pyroptosis and apoptosis, can lead to cell membrane destruction, which finally promotes the release of bacteria from the host cells (Speir et al. 2014). The difference between apoptosis and pyroptosis is that pyroptosis can directly cause lysis of the cell membrane and release inflammatory cytokines, but late apoptosis can cause cell membrane destruction without releasing cytokines. Both pyroptosis and apoptosis have been observed in *L. pneumophila*–infected macrophages, but it remains unknown whether *L. pneumophila* uses both to release the bacteria or whether *L. pneumophila* selectively induces different programmed cell deaths in different circumstances.

1.8.2 *L. pneumophila* infection and *Acanthamoeba* cell survival

Acanthamoeba can live with bacteria with symbiotic status, but *Legionella* was found to have the ability to trigger necrosis of *Acanthamoeba* after intracellular replication (Gao and Abu Kwaik 2000). It has also been shown that after *L. pneumophila* replication, LCV were released from *Acanthamoeba* before encystation (Ohno et al. 2008). The encystation process was mediated by metacaspase-1, which could be a marker of *Acanthamoeba* differentiation from trophozoite to cyst. Encystation is often used by *Acanthamoeba* to avoid cell death. A recent study reported that *L. pneumophila* infection reduced the production of cell cycle protein and impaired the cell proliferation of *Acanthamoeba* (Mengue et al. 2016) in the co-culture. It remains unclear whether *Legionella* infection caused the death of *Acanthamoeba* cells after intracellular growth.

Neither apoptosis nor pyroptosis were found in *L. pneumophila*-infected *Acanthamoeba* cells. The exploration of the killing mechanism initiated by *L. pneumophila* when grown in *A. polyphaga* inspired researchers to determine whether the bacteria could activate the host cell death pathway and further facilitate bacterial rupture after intracellular replication (Gao and Kwaik 2000). It is a sophisticated regulation, because the bacteria could choose to either activate or inhibit host cell death based on differences in the growth phase. As the *L. pneumophila* environmental host and virulence developing field,

Acanthamoeba is a key element to explore the evolution or development in *L. pneumophila* of the ability to regulate the host cell death pathway in mammalian cells.

2. Aims and Objectives

2.1 Research gaps

The pathogenesis of *L. pneumophila* depends on its successful replication and release from the host cells. *L. pneumophila* can grow in both *Acanthamoeba* and macrophages, which are two evolutionarily distant hosts. There are still a lot of questions remained to be addressed regarding the intracellular life of *L. pneumophila*. Can *L. pneumophila* replicate in macrophage to the same extend as it does in *Acanthamoeba*? Because macrophages have a pattern recognition receptor, can the macrophage internalize more *L. pneumophila* when challenged with the same dose of bacteria as *Acanthamoeba*? Can *L. pneumophila* infection cause the same extend of host cell death in either macrophage or *Acanthamoeba*?

After intracellular replication of *L. pneumophila*, bacteria must be released from the host cell. Previous observations of the release of *L. pneumophila* from *Acanthamoeba* and macrophages are very diverse. Both lytic (necrosis) and nonlytic (exocytosis) release have been reported in *L. pneumophila*-infected *Acanthamoeba*, but it remains unclear whether both lytic and nonlytic *L. pneumophila* release can occur simultaneously in the *Acanthamoeba* population in the presence of *L. pneumophila* infection. Both apoptosis and pyroptosis were reported in *L. pneumophila*-infected macrophages, but it is unknown whether apoptosis or pyroptosis predominates in *L. pneumophila*-infected macrophages. Although studies have evaluated the roles of *L. pneumophila* genes *flaA*, *vipD*, *sdhA*, and

sidF in host death after *L. pneumophila* infection, no study has examined their expression patterns when grown in *Acanthamoeba* and when grown in macrophages. A detailed investigation about the expression patterns of these genes in various hosts during different stages of *L. pneumophila* intracellular growth would enable a better understanding of the interaction between *L. pneumophila* and its hosts.

L. pneumophila can replicate in a wide range of hosts, from protozoa to mammalian cells. One obvious and mysterious property of *L. pneumophila* is that the human infections it causes are often associated with environmental protozoa; however, human-to-human transmission has never been reported. *L. pneumophila* is a model organism to explore host and pathogen interaction, as this pathogen encodes a large number of effectors to adapt to intracellular life, including many homologues of eukaryotic proteins. It has been discussed that protozoa including *Acanthamoeba* play an important role in the evolution of *L. pneumophila* virulence, but the underlying mechanism remains less explored. The transcriptome comparison between extracellularly grown *L. pneumophila* during the transmissive phase and *L. pneumophila* grown in *Acanthamoeba* during the transmissive phase could help to determine why *L. pneumophila* derived from *Acanthamoeba* is more virulent and transmissive. Dual transcriptome analysis of both *L. pneumophila* and *Acanthamoeba* could further enrich our understanding of host and pathogen interaction.

2.2 Aims

This project aimed to explore the interaction between *L. pneumophila* and its two hosts (*A. castellanii* and human monocyte THP-1) by investigating bacterial virulence gene expression patterns and their association with bacterial intracellular growth and host cell death. Because *L. pneumophila* from *A. castellanii* were found to be more virulent and transmissible, the dual-transcriptome analysis of *L. pneumophila* grown in *A. castellanii* could help to describe the pathogen and host interactions.

2.3 Objectives

Objective 1: To investigate and compare the intracellular growth of *L. pneumophila* in *Acanthamoeba* and THP-1. Both plate counts and microscopic observation of gfp (green fluorescence protein)–transfected *L. pneumophila* grown in two hosts were used to evaluate whether *A. castellanii* or THP-1 could support greater replication of intracellular *L. pneumophila*.

Objective 2: To compare the bacterial expression of *flaA*, *vipD*, *sdhA*, and *sidF* in intracellular *L. pneumophila* during different growth phases in *A. castellanii* and THP-1 monocyte hosts. The correlated host cell genes *metacaspase-1* (*A. castellanii*), *caspase-1* (THP-1), and *caspase-3* (THP-1) were also investigated and compared with the uninfected host cells after various durations of growth.

Objective 3: To investigate host cell death after infection with *L. pneumophila* based on propidium iodide (PI) staining and active caspase-1 and caspase-3 staining (only for THP-1).

Objective 4: To analyze the transcriptomic profiles of the intracellular *L. pneumophila* and the *A. castellanii* hosts. To achieve this objective, RNA sequencing was done in *L. pneumophila*-infected *A. castellanii* after FACS (fluorescence-activated cell sorting) enrichment.

3. Materials and Methods

3.1 Overview of workflow

L. pneumophila and gfp-transfected *L. pneumophila* were used in this study. Both were subjected to co-culture with two host cells: THP-1 and *A. castellanii*. The co-cultures were collected for different experiments, as shown in Figure 3.1.

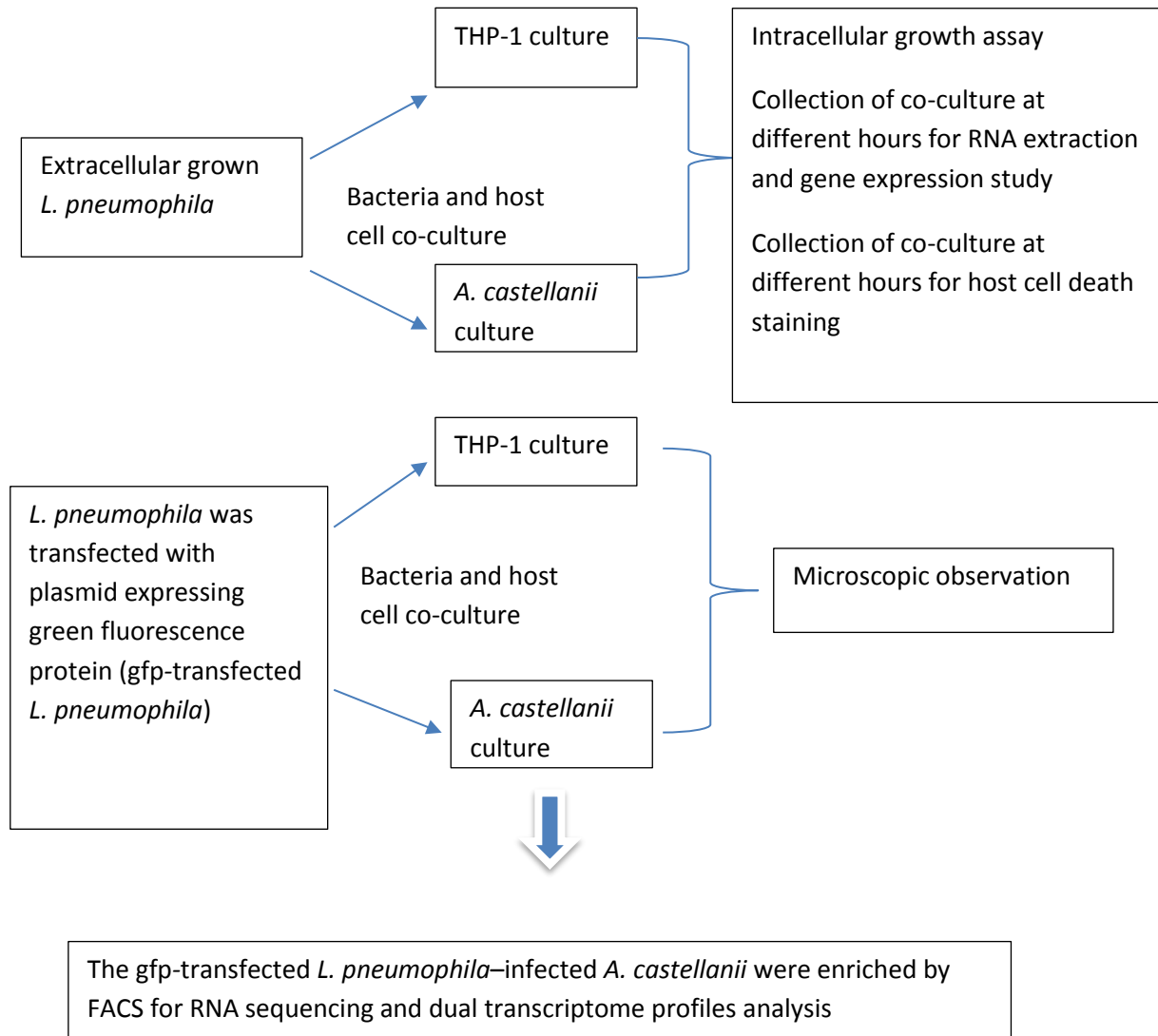


Figure 3.1 Overview of project workflow.

3.2 Bacterial strain, *Acanthamoeba*, and THP-1 cell lines used

3.2.1 Standard ATCC *Legionella* strain

L. pneumophila Philadelphia strain (ATCC 33152) was used in this study. *L. pneumophila* was cultured on α BCYE agar plates supplemented with α BCYE growth supplement (Oxoid, Appendix 2) and GVPC selective reagents (Oxoid). The cultures were incubated at 37°C with 5% CO₂ for 3 to 5 days. For the liquid culture, *L. pneumophila* was grown in the liquid BYE broth (Appendix 1).

3.2.2 *Acanthamoeba castellanii* strain

Standard *Acanthamoeba castellanii* (ATCC 30234) was cultured in peptone yeast glucose (PYG) medium (Appendix 1) at 25°C for 1 to 2 weeks to obtain confluent growth of *A. castellanii* trophozoites before use.

3.2.3 THP-1 cell line

Human monocyte THP-1 (ATCC TIB-202) was used in this study; the cells were grown in RPMI 1640 growth medium (Gibco) supplemented with 10% fetal bovine serum (Gibco) and 1% penicillin-streptomycin (Gibco) at 37°C with 5% CO₂ for 3 to 5 days before use.

3.3 Extracellular growth of *L. pneumophila* in BYE broth

To determine the duration required for *L. pneumophila* to reach the post-exponential phase, a liquid culture was set up, and viable *L. pneumophila* were counted every 12 h from 0 to 48 h. One hundred microliters of *L. pneumophila* at a concentration of 10^9 colony-forming units (CFU)/mL was inoculated in 10 mL of BYE broth (Appendix 1) and incubated at 37°C with agitation at 250 rpm. The bacterial density was enumerated by plate counting.

3.4 Intracellular growth of *L. pneumophila* in *A. castellanii* and THP-1

3.4.1 *L. pneumophila* intracellular growth in *A. castellanii*

The co-culture of *L. pneumophila* and *A. castellanii* was performed by challenging *A. castellanii* culture in PYG with bacteria at a multiplicity of infection (MOI) of 10. Two milliliters of *A. castellanii* culture at a concentration of 10^6 cells per mL was inoculated in each well of a six-well plate (Corning), followed by the addition of 20 μ L of *L. pneumophila* suspension (10^9 CFU/mL) grown during the post-exponential phase. After centrifugation at $900 \times g$ for 5 min, the plate was incubated at 37°C in 5% CO₂ for 3 h. After washing in Page's amoeba saline (PAS) buffer (Appendix 1), the co-culture medium in each well was replaced with 2 mL of gentamicin (100 μ g/mL in PYG). After incubation for 2 h, the co-culture was washed twice with PAS and replaced with 2 mL of fresh PYG in each well. This time point was denoted as T0. For plate counting of intracellular bacteria, the co-culture in each well was added to 2 mL of sterile distilled water and incubated for 10 min, followed by lysis via 5-10 forced passage through a

syringe (5 mL; Terumo) with a 23-gauge needle (Dietersdorfer et al. 2016). The *L. pneumophila* released from the lysed co-culture were enumerated by plate counts. The plate counts were performed every 12 h from 0 to 48 h. Co-cultures were also performed and collected at each time point for RNA isolation. All experiments were repeated in triplicate.

3.4.2 *L. pneumophila* intracellular growth in THP-1

L. pneumophila was co-cultured with THP-1 cells at an MOI of 10. Briefly, 2 mL of THP-1 (10^6 cells/mL) in RPMI 1640 medium (without 10% fetal bovine serum and 1% penicillin/streptomycin) were mixed with 20 μ L of *L. pneumophila* (10^9 CFU/mL) during the post-exponential phase in every 5-mL centrifuge tube (SPL). The mixture was centrifuged at $900 \times g$ for 5 min, followed by incubation at 37°C in 5% CO₂ for 3 h. After incubation, the pellet was washed once with PBS (Gibco) buffer and replaced with 2 mL of RPMI 1640 medium containing gentamicin (100 μ g/mL) for another 2 h of incubation at 37°C in 5% CO₂ to kill extracellular *L. pneumophila*. The co-culture was then washed twice with PBS and resuspended in 2 mL of fresh RPMI 1640 medium. This point was regarded as “time zero” (T0). At T0 and at every 12-h interval up to 48 h (T12 to T48), the THP-1 cells were incubated with 2 mL of sterilized distilled water at room temperature for 10 min. The THP-1 cells were then lysed by forcing through a 23-gauge syringe needle (5 mL; Terumo) five to ten times. The *L. pneumophila* released from the lysed co-culture were enumerated by plate counting. The co-culture was also collected at every 12 h from 0 to 48 h for isolations, and all experiments were repeated in triplicate.

3.5 RNA isolation and two-step RT-quantitative PCR

3.5.1 RNA isolation

The *L. pneumophila* co-cultures collected above at each time point were centrifuged at $8000 \times g$ for 5 min, and the pellets could be stored at -80°C before RNA isolation. One hundred microliters of lysozyme (10 mg/mL, Sigma) was added into each pellet followed by passing through a 21-gauge syringe (1 mL, Terumo) to homogenize the sample in 5 min. One milliliter of Trizol reagent (Invitrogen) was then added to the homogenized pellet, followed by incubation at room temperature for 30 to 60 min. Two hundred microliters of chloroform (Sigma) was then added to the previous 1-mL Trizol suspension, and the tube was shaken vigorously for 15 s and then incubated for another 2 or 3 min. The sample was then centrifuged at $12,000 \times g$ for 15 min at 4°C , and the upper aqueous portion was transferred carefully into a new tube for the following RNA wash and elution.

The above aqueous phase was added to an equal volume (approximately 500 μL) of 75% ethanol, followed by vortexing to mix it well. The sample was then transferred to a Spin Cartridge (PureLink RNA Mini Kit, Invitrogen) according to the manufacturer's instructions. After centrifugation at $12,000 \times g$ for 15 s, the flow-through was discarded, followed by washing with Wash Buffer I and Wash Buffer II (PureLink). Finally, the RNA in the Spin Cartridge was eluted in 50 μL of RNase-free water (stored at -80°C before use).

3.5.2 DNA removal of RNA samples and reverse transcription (RT)

The concentrations of the isolated RNA samples were measured via the NanoDrop spectrophotometer (Thermo Fisher Scientific) reading to evaluate purity (A260/280 in the range of 1.8 to 2.1 was considered pure) and quantity. A consistent quantity of RNA (<800 ng RNA per DNase I reaction) was then digested using the DNase I kit (Sigma) at 37°C for 30 min to remove any DNA contamination in the RNA sample. Digested RNA (10 µl) was reverse-transcribed into cDNA using a RevertAid First Strand cDNA Synthesis kit (Fermentas). To monitor the presence of DNA contamination in the digested RNA sample, a second reverse transcription without reverse transcriptase (no-reverse transcriptase control) was set up simultaneously. The no-reverse transcriptase control was tested by quantitative real-time PCR, and a Ct (threshold cycle) value larger than 35 represented clean removal of DNA in RNA samples.

3.5.3 Quantitative real-time PCR for gene expression studies

Quantitative real-time PCR was performed in 20-µL PCR mixtures consisting of 1 µL of cDNA, 1×SYBR Green Mastermix (Roche), and 500 µM of each forward and reverse primer (Life Technologies). For TaqMan probe assay, the 20-µL PCR mix comprised 1 µL of cDNA, 1× TaqMan Universal PCR Mastermix (ABI), and 1 µL of 20× TaqMan probes (containing the 4-µM probe, and 10 µM of each forward and reverse primer). The primers and probes used in this study are shown in Table 3.1. PCRs were run on an ABI7500 system (Applied Biosystems). The thermal cycling conditions comprised an initial denaturation step at 95°C for 10 min, followed by 40 cycles of 95°C for 30 s and

60°C for 1 min. (For the primers and Roche SYBR Green Mastermix used, a melting curve stage was added in the thermal cycling to ensure the specific PCR product produced.) The threshold cycle (CT) values of the target genes were normalized to those of the reference genes. The fold changes in the expression of various target genes at T12 to T48 were compared with the expression at T0.

Threshold cycles of target genes were normalized to the housekeeping gene:

$$\Delta Ct = Ct_{\text{target}} - Ct_{\text{housekeeping}}$$

The differences in the normalized threshold cycle from T12 to T48 were compared with T0:

$$\Delta\Delta Ct = \Delta Ct_{\text{T12-T48}} - \Delta Ct_{\text{T0}}$$

Fold change of genes expression was calculated as: $2^{-\Delta\Delta Ct}$

Table 3.1 Primers and TaqMan probes used in gene expression study. All primers and probes were designed using online Primer-BLAST program of NCBI (National Centre for Biotechnology Information).

Gene	Primer/probe Sequence (5'-3')	Amplicon size (bp)
Primers and probes for <i>L. pneumophila</i> -specific genes		
<i>gyrB</i> (reference gene)	Forward: AGCGATGAATCAATTACCGT Reverse: ATCAAATTTACCTCCGGCAT	123
<i>flaA</i>	Forward: GTTGCTGCTCCTCCTCCAAT Reverse: ATGGTTCTTTCTCTGGCGCA	178
<i>sdhA</i>	Forward: ATCCAGAGCTTCTTGCGCTT Reverse: TACGCATCCAAACCCGTCAA	159
<i>sidF</i>	Forward: GTTACAGGGCAGCCTGATGT Reverse: CCGCTTTTGCTTTGTCGGAA	190
<i>vipD</i>	Forward: CAGCGCATGCACAAGCTATT Reverse: GAGGGCAAAGGCCTTCTCTT	161
Primers and probes for THP-1-specific genes		
<i>GAPDH</i> (reference gene)	Forward: GACTCATGGTATGAGAGCTGG Reverse: TGGTCTGCAAAAGGAGTGAG	205
<i>CASP-1</i>	Forward: CCTCCTCACAGTTGGGTAAT Reverse: GCAGCAGTGGTTCCTAAATG	225
<i>CASP-3</i>	Forward: GATTATCCTGAGATGGGT Reverse: TTGCTGCATCGACATCTG Probe: FAM-GGAATGACATCTCGGT-MGB	100

Table 3.1 Continued

Gene	Primer/probe Sequence (5'-3')	Amplicon size (bp)
Primers and probes for <i>A. castellanii</i> -specific genes		
<i>18S rDNA gene</i>	Forward: CTGCGAAAGCATCTGCCAAG	106
	Reverse: TGGTCGGCATCGTTTATGGT	
<i>MCASP-1</i>	Forward: CGTACACTCGATTTAGAAGC	100
	Reverse: CCCTGCTGGTATGGATCAGG	
	Probe: FAM-ATGGCATACCCCTACG-MGB	

3.6 Transformation of *L. pneumophila* with plasmid pBC(gfp)Pmip

3.6.1 Electroporation of *L. pneumophila*

L. pneumophila was transformed with the plasmid pBC(gfp)Pmip via electroporation. pBC(gfp)Pmip is a 4600-base pair (bp) plasmid that harbors the gene encoding gfp (Figure 3.2). The plasmid was a generous gift from Prof. Lu of the Sun Yat-Sen University, Guangzhou.

3.6.1.1 Competent bacterial cell preparation

L. pneumophila colonies freshly grown on α BCYE plates were harvested and suspended in sterilized double-distilled water (ddH₂O). The *L. pneumophila* suspension was adjusted to an OD_{600nm} of 1, and 4 mL of the suspension was centrifuged at 5000 $\times g$ for 10 min at 2°C. The pellet was washed twice with 4 mL of ice-cold ddH₂O and then with 4 mL of ice-cold 10% (v/v) glycerol solution (Sigma). The centrifuged pellet was then resuspended in 40 μ L ($\sim 10^{10}$ cells) of 10% glycerol solution (Appendix 1).

3.6.1.2 Electroporation

An aliquot of 0.2 μ g of pBC(gfp)Pmip was mixed with the 40 μ L suspension of *L. pneumophila*. The mixture was transferred aseptically to a prechilled electroporation cuvette (0.2-cm electrode gap, Bio-Rad). Electroporation was carried out with Bio-Rad Gene Pulser apparatus under 25 μ F capacitance, 0.5 to 2.4 kV voltage, and 100 to 1000 Ω

resistance. The pulsed suspension in the cuvette was immediately suspended in 3 mL of BYE broth without antibiotics and incubated at 37°C for 4 h with agitation at 150 rpm. The suspension was serially diluted and evenly spread onto the selective α BCYE agar supplemented with 5 μ g/mL chloramphenicol (Sigma).

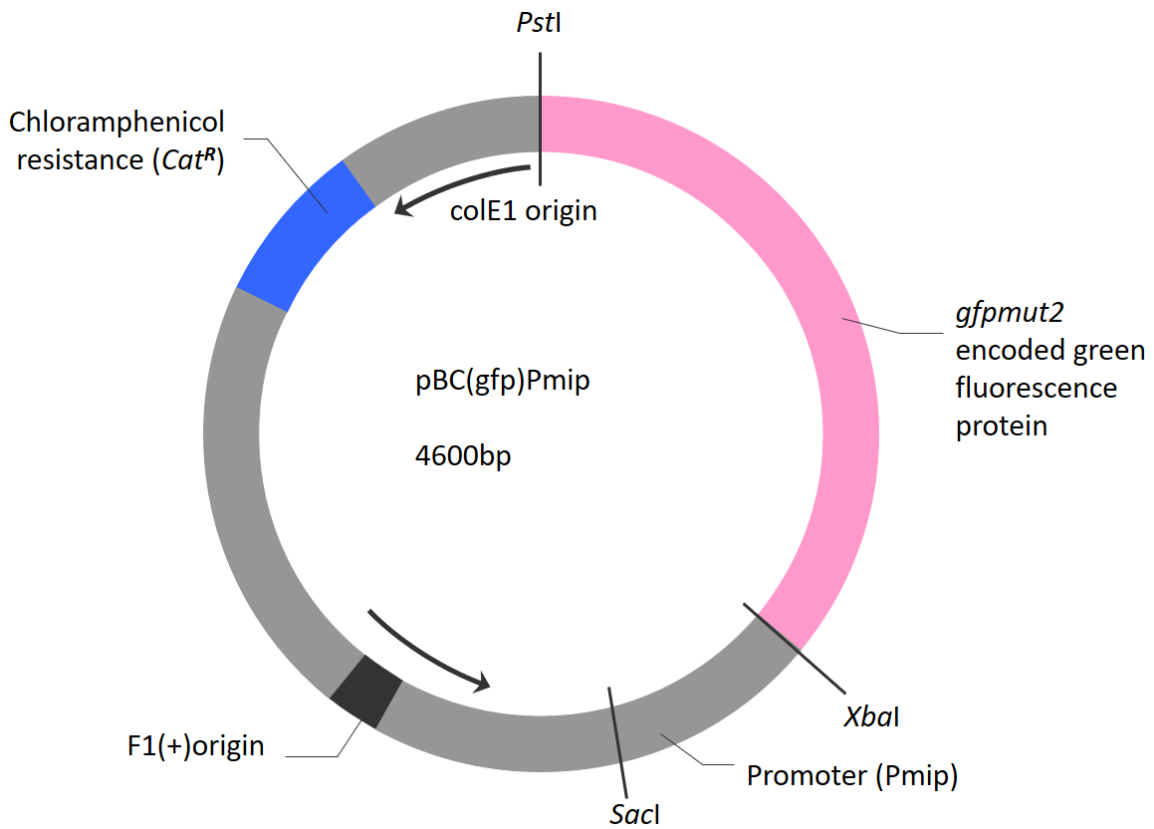


Figure 3.2 Map of plasmid pBC(gfp)Pmip. The plasmid was constructed by inserting the *L. pneumophila mip* promoter and *gfp* gene from the vector pKEN into the pBC KS+ plasmid. It has been shown that the constructed pBC(gfp)Pmip can be kept and stably expressed in *L. pneumophila* (Chen et al. 2006, Kohler et al. 2000).

3.6.1.3 Identification of *L. pneumophila* carried with pBC(gfp)Pmip (gfp-transfected *L. pneumophila*)

The identities of the colonies grown on the selective agar plates were confirmed using the Biotyper matrix-assisted laser desorption/ionization–time of flight (MALDI-TOF) mass spectrometry system (Bruker). After confirmation of the bacterial identity, the plate was examined under an ultraviolet (UV) box (Chromato-Vue) at a λ of 302 nm to observe for the presence of colonies with green fluorescence (Figure 3.3.1).

A *L. pneumophila* colony with green fluorescence was further sub-cultured onto α BCYE plate supplemented with 15 μ g/mL chloramphenicol. The grown colonies on chloramphenicol supplemented α BCYE plate were used for plasmid isolation by using QIAprep kit (Qiagen). Isolated plasmid was also used for digestion with KpnI (Fermentas; 37°C for 2 h) followed by gel electrophoresis. The plasmid with the 4600-bp band in gel electrophoresis (arrow indicates in Figure 3.3.2) indicated that *L. pneumophila* was successfully transformed with pBC(gfp)Pmip (gfp-transfected *L. pneumophila*).

The gfp-transfected *L. pneumophila* colonies was stored in 20% glycerol (Appendix 1) at –80°C for long-term use and was used for following co-cultures with *A. castellanii* and THP-1.

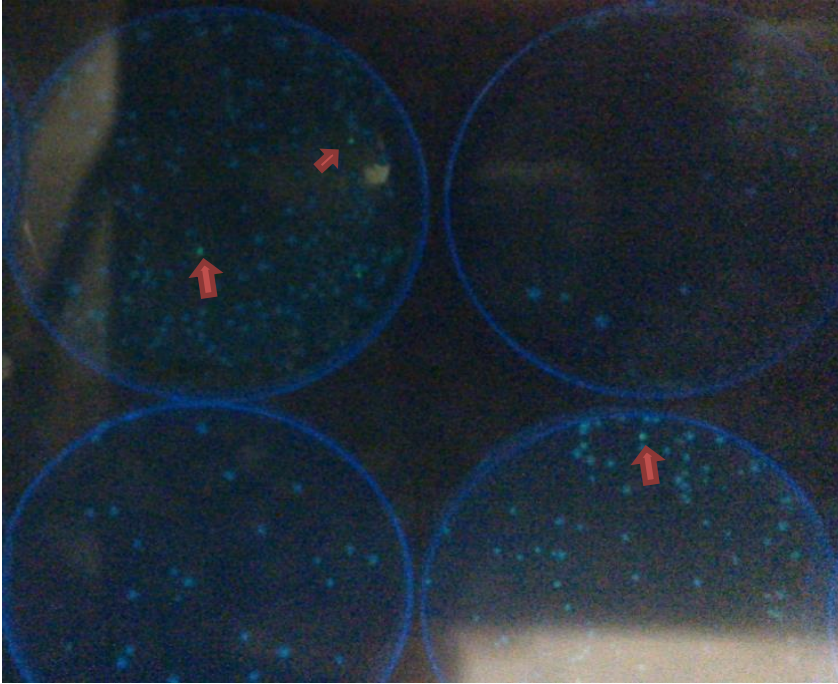


Figure 3.3.1 Identification of *L. pneumophila* colonies with green fluorescence. After electroporation, bacteria were grown on an α BCYE plate supplemented with chloramphenicol. The plates were examined under a UV lamp at λ of 302 nm, and the image was taken under a UV box (Chromato-Vue). The transformed *L. pneumophila* colonies with green fluorescence are indicated by red arrows.

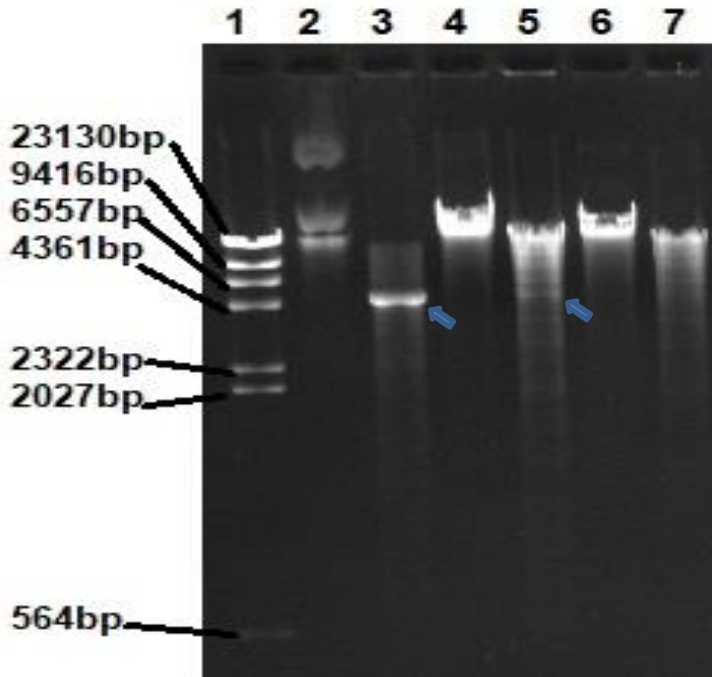


Figure 3.3.2 Gel electrophoresis identification of the plasmid pBC(Pmip)gfp. 1, Lambda DNA/HindIII Marker (Fermentas); 2, Plasmid pBC(gfp)Pmip isolated from DH5 α ; 3, KpnI-digested pBC(gfp)Pmip isolated from DH5 α ; 4, plasmid DNA from transformed *L. pneumophila*; 5, KpnI-digested plasmid DNA from transformed *L. pneumophila*; 6, plasmid DNA from untransformed *L. pneumophila*; 7, KpnI-digested plasmid DNA from untransformed *L. pneumophila*. The plasmid pBC(gfp)Pmip had more than 2 bands in lane 2, which could contain relaxed circular plasmid forms (higher than 4600 bp), and the genomic DNA of bacteria that has not been completely removed could also be mixed with the plasmid DNA. After KpnI digestion, the relaxed circular plasmid forms were linearized, and a band at 4600 bp was obtained (lane 3, arrow indicates). The transformed *L. pneumophila* colonies (lane 5) also showed a narrow 4600 bp band (arrow indicates).

3.6.2 Extracellular growth of gfp-transfected *L. pneumophila*

The gfp-transfected *L. pneumophila* was grown in BYE broth containing 15 µg/mL chloramphenicol. The number of bacteria grown was plate counted every 12 h from 0 to 48 h. Fresh bacterial colonies grown on an αBCYE plate supplemented with chloramphenicol (15 µg/mL) were suspended in PBS buffer, and the OD_{600nm} was adjusted to 1; 0.1 mL of the suspension was then added to 15-mL BYE broth (this time point was denoted as 0 h, T0). At every time point (T0, T12, T24, T36, and T48), 100 µL of bacterial broth culture was collected and serially diluted in PBS buffer. One hundred microliters of the diluted bacterial suspension were used for plate enumeration. The grown colonies were counted, and the bacterial concentration in broth was calculated as the number of colonies × dilution factor × 100 CFU per mL. The experiments were repeated three times.

3.6.3 Intracellular growth of gfp-transfected *L. pneumophila*

The gfp-transfected *L. pneumophila* was co-cultured with THP-1 and *A. castellanii*. The co-cultures were used for live image microscopy studies to examine the intracellular growth of gfp-transfected *L. pneumophila*. The intracellular growth of gfp-transfected *L. pneumophila* in *A. castellanii* was also measured via standard plate counts.

3.6.3.1 Co-culture with THP-1

Co-culture of gfp-transfected *L. pneumophila* with THP-1 was performed by adding 4 mL of 48-h BYE broth culture of gfp-transfected *L. pneumophila* ($\sim 10^8$ bacteria) into the 10 mL of THP-1 (10^6 per mL) in RPMI 1640 medium supplemented with 15 $\mu\text{g/mL}$ chloramphenicol. After initial centrifugation ($900 \times g$; 5 min), the co-culture was incubated at 37°C in 5% CO_2 for 3 h. The co-culture was then washed with PBS buffer and replaced with 10 mL of RPMI 1640 medium supplemented with 100 $\mu\text{g/mL}$ gentamicin and 15 $\mu\text{g/mL}$ chloramphenicol for incubation at 37°C in 5% CO_2 for 2 h. After incubation, the co-culture was washed twice with PBS buffer and replaced with 10 mL of 15- $\mu\text{g/mL}$ chloramphenicol-supplemented RPMI 1640 medium, and this time point was denoted as T0. The co-culture of THP-1 and gfp-transfected *L. pneumophila* were collected for microscopic observation.

3.6.3.2 Co-culture with *A. castellanii*

The co-culture of *A. castellanii* and gfp-transfected *L. pneumophila* was performed by challenging *A. castellanii* with bacteria at MOI of 10. Every 800 μL of bacterial broth culture at T48 ($\sim 2 \times 10^7$ bacteria) was added to 2 mL of *A. castellanii* culture (10^6 cells per mL) in a six-well plate, and the plate was centrifuged at $900 \times g$ for 5 min. The plate was incubated at 37°C in 5% CO_2 for 3 h and replaced with PYG broth containing 100 $\mu\text{g}/\text{mL}$ gentamicin and 15 $\mu\text{g}/\text{mL}$ chloramphenicol. The plate was further incubated at 37°C in 5% CO_2 for 2 h, and the co-culture was then washed three times with PAS. The co-culture was finally replaced with fresh PYG medium containing 15 $\mu\text{g}/\text{mL}$ chloramphenicol, and this time point was denoted as 0 h (T0).

For plate counting of intracellular bacteria, the co-culture in each well was added to 2 mL of sterile distilled water and incubated for 10 min, followed by lysis via five to ten forced passages through a syringe with a 23-gauge needle. The gfp-transfected *L. pneumophila* released from the lysed co-culture were enumerated by plate counting. The plate counts were performed every 12 h from 0 to 48 h. Co-cultures were also performed and collected at each time point for cell sorting.

3.7 Flow cytometry for host cell death staining measurement and for FACS enrichment of gfp-transfected *L. pneumophila*–infected *A. castellanii*

3.7.1 Flow cytometry startup operation

FACSAriaIII (Becton-Dickinson [BD]) was used for host cell death staining measurement, and AriaIII (BD) was used to sort gfp-transfected *L. pneumophila*–infected *A. castellanii* cells based on the manufacturer’s instructions. The FACSDiva software (BD) was used to control the flow cytometry and cell sorting.

A 100- μm nozzle was selected for detection of both THP-1 (9 to 18 μm diameter) (Wang et al. 1992) and *A. castellanii* cells (trophozoite length, 25 to 40 μm ; cyst diameter, 13 to 20 μm) (Marciano-Cabral and Cabral 2003). Lasers with wavelengths of 488, 633, and 375 nm were used to detect green, red, and blue fluorescence, respectively. The stream shown on the breakoff window was automatically adjusted before turning on the sweet spot, which maintained a stable flow stream during sample collection and cell sorting (Figure 3.4).

Before flow cytometry and cell sorting, the cytometer setup and tracking performance was calibrated using cytometer setup and tracking standard beads (BD) to check the cytometer-collected fluorescence signals run in normal spectrums. Once the cytometer setup and tracking check was successfully reported, flow cytometer was continued to follow the detection of fluorescence signal measurement and sorting.

3.7.2 Propidium iodide (PI) staining

Propidium iodide was used to stain the *L. pneumophila*-infected THP-1 and *A. castellanii* cells every 12 h from 0 to 48 h. THP-1 and *A. castellanii* cells without challenging bacteria were used to perform the same operation as co-culture for collection of uninfected host cells. At each time point, 1 mL of both uninfected and infected host cells (*A. castellanii* and THP-1) at a concentration of 10^6 /mL were collected and washed twice with 1 mL of PBS buffer. The washed cells were resuspended in 500 μ L of wash buffer with 1 μ L of PI solution (500 \times concentrated, Abcam) and then incubated in 37 $^{\circ}$ C incubator with 5% CO₂ for 1 h. The PI-stained cells were then washed twice with 500 μ L of wash buffer (Abcam) and resuspended in 500 μ L of wash buffer. The PI-stained cells were loaded into AriaIII, and phycoerythrin fluorochromes (excitation/emission = 566/576 nm) were selected for fluorescence measurement. Before PI-stained cell loading, 50,000 unstained cells were subjected to flow cytometry, and the unstained cells were used for target cell gating and to set the baseline for the fluorescence signals. The PI-stained cells were analyzed with the flow cytometer, and fluorescence values greater than baseline were interpreted as positive. The data are shown as the percentage of cells with positive fluorescence signals. The PI-stained cells were also seeded into 48-well plates (Corning) for visualization using an Eclipse Ti Inverted Microscope (Nikon) within 1 h. All experiments were repeated three times.

3.7.3 Active caspase-1 staining

Active caspase-1 staining (ab219935, green fluorescence) kit (Abcam) was used to stain both the *L. pneumophila*-infected and uninfected THP-1 cells. This assay kit was based on the fluorescence inhibitor of caspase-1, FAM-YVAD-FMK (Broz et al. 2010), which is permeable inside THP-1 cells to specifically bind with active caspase-1, and the fluorescence intensity reflected the amount of active caspase-1. *L. pneumophila*-infected THP-1 co-cultures ($\sim 10^6$ cells at each time point) were collected every 12 h from 0 to 48 h. At the same time, the uninfected THP-1 cells ($\sim 10^6$ cells) were also collected every 12 h. The collected cells were washed twice with PBS buffer and resuspended in 900 μ L of wash buffer (supplied in ab219935 kit, Abcam), and 6 μ L of FAM-YVAD-FMK solution (150 \times concentrated) was added to the wash buffer. The above cells were incubated in a 37 $^{\circ}$ C incubator in 5% CO₂ for 1 h in the dark. The stained THP-1 cells were then centrifuged at 200 $\times g$ for 5 min and washed twice with 1 mL of wash buffer. After washing, the cells were suspended in 500 μ L washing buffer.

Before examining active caspase-1-stained cells, unstained THP-1 cells were loaded in the flow cytometer for target cell gating and to set the fluorescence reading baseline by selecting fluorescein isothiocyanate (FITC) fluorochromes channel (excitation/emission = 495/519 nm). The positive caspase-1-stained cells (over baseline) were presented as a percentage. The caspase-1-stained cells were also seeded in 48-well plates at every time point for microscopic examination using an Eclipse Ti inverted microscope (Nikon) within 1 h. All experiments were performed three times.

3.7.4 Active caspase-3 staining

An active caspase-3 staining kit (ab65617, red fluorescence; Abcam), based on the red fluorescence-labeled caspase-3 inhibitor DEVD-FMK (Springer et al. 1999) as the fluorescent in situ marker to stain both *L. pneumophila*-infected and uninfected THP-1 cells at each time point (T0 to T48). For active caspase-3 staining, 1 μL of Red-DEVD-FMK (Abcam) was added to each of the collected and washed cells ($\sim 5 \times 10^5$ cells suspended in 300- μL supplied wash buffer) based on manufacturer's instructions. The caspase-3 staining suspensions were incubated at 37°C in 5% CO₂ for 1 h, and the cells were then washed twice with 500 μL of wash buffer (Abcam). The stained THP-1 cells were finally resuspended in 500 μL of wash buffer for flow cytometry and microscopy.

Unstained THP-1 cells were first loaded into the flow cytometer for target gate and baseline setting under PE fluorochromes (excitation/emission = 566/576 nm) selection. Fifty thousand caspase-3-stained positive cells were detected and expressed as percentages in all gated cells. The stained cells were also seeded in 48-well plates for microscopic visualization using an Eclipse Ti inverted microscope (Nikon) within 1 h. All experiments were repeated three times.

3.7.5 FACS enrichment of gfp-transfected *L. pneumophila*–infected *A. castellanii*

At each time point, the *A. castellanii* infected with gfp-transfected *L. pneumophila* were collected and loaded onto the AriaIII (BD) to sort the host cells with green fluorescence. The FITC fluorochrome channel was used. Before cell sorting, the *A. castellanii* cells infected with *L. pneumophila* were loaded into the flow cytometer for gating target cells and to set the fluorescence measurement baseline under the FITC channel. *A. castellanii* infected with gfp-transfected *L. pneumophila* within the gate with a fluorescence signal higher than the baseline was selected for sorting.

3.7.5.1 Drop delay value setting

Before cell sorting, the drop delay value was set by running the Accudrop beads (FACS, BD), and the “Auto Delay” mode was used to automatically run and select the most appropriate drop delay value to achieve sorted beads with more than 90% purity. The drop delay value determined which drop needed to be deflected and sorted from the flowed sample during the sorting process (Figure 3.4).

3.7.5.2 Sample loading and sorting

After the drop delay setting, $\sim 10^6$ per mL of *A. castellanii* infected with gfp-transfected *L. pneumophila* at various time points were loaded into the flow cytometer, and cell sorting began (Figure 3.4, sample loading and sorting). The positive population (*A. castellanii* containing gfp-transfected *L. pneumophila*) was selected for sorting according to the set-

up protocol. The sorting was performed continuously until the loaded samples were exhausted. The positive population contained drops in the left sorting tube in the sorting chamber (Figure 3.4).

Sorting was stopped by unloading the samples or automatically when the loaded samples were exhausted, and the number of sorted cells was shown on the “Sort Layout” window. The number of sorted positive gfp-transfected *L. pneumophila*–infected *A. castellanii* cells shown on the “Sort Layout” window fell between 10^4 and 10^5 each time. As a result, the sorted cells were pelleted and stored at -80°C until enough cells were collected for RNA extraction.

3.8 Microscopic observation of *A. castellanii* and THP-1 infected with gfp-transfected *L. pneumophila*

3.8.1 Co-culture preparation and microscopy settings

An Eclipse Ti inverted microscope (Nikon) was used for visualization of the gfp-transfected *L. pneumophila*–infected *A. castellanii* and THP-1. Because THP-1 cells are difficult to focus under a microscope, THP-1 was differentiated to adherent macrophage-like cells using 100-nM phorbol-12-myristate 13-acetate (PMA, Sigma) supplement medium for 48 h before co-culture. Before microscopic examination of *A. castellanii* and THP-1 differentiated macrophage-like cells that were infected with gfp-transfected *L. pneumophila*, co-culture operations were set up as described in Sections 3.7.2 and 3.7.3.

The *NIS Element* software was operated to control the settings of live-image visualization from T0 to T48. The phase contrast objective (40×, Nikon Advanced Modulation Contrast) was selected to focus on the *A. castellanii* and THP-1 differentiated macrophage-like cells. An appropriate laser pathway (GFP for green fluorescence) was selected to visualize the gfp-transfected *L. pneumophila* fluorescence (Figure 3.5, 4) and was then merged with the phase contrast images. The LUTs (look-up table) control panel (NIS-Elements Viewer, Nikon) was used to make appropriate adjustments to the light intensity to decrease the background intensity by comparison with the unstained cell control.

3.8.2 Live-image of host cells infected with gfp-transfected *L. pneumophila*

Co-cultures of gfp-transfected *L. pneumophila* with host cells at T0 in a six-well plate (Corning) were placed in the box incubator on the inverted microscope (Figure 3.5, 2).

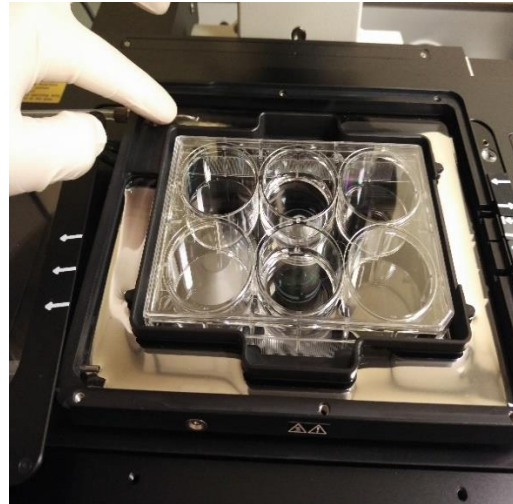
The surrounded groove of the box incubator was filled with deionized water to maintain a humidified environment. The temperature and gas controller (Figure 3.5, 1) was operated to monitor the box incubator temperature. The lens heater was set at 37°C, the bath heater was set at 41°C, and the stage heater was set at 35.5°C, with all tested to ensure that the temperature of the box incubator remained at around 37°C. The controller also indicated the input of 5% CO₂ by showing the pumped-up beads (gas pressure), which was connected to the box incubator (Figure 3.5, 3) to maintain the co-culture incubation in humidified conditions at 37°C in 5% CO₂ for 48 h.

After plate incubation setting, the *NIS-Element* software (Nikon) was connected to the microscope. *A. castellanii* cells and THP-1 differentiated macrophage-like cells were examined in different co-cultures under 40× NAMC phase contrast objective. After this procedure, the appropriate visualization settings were selected from the ND Acquisition menu of the *NIS-Element* software (Figure 3.5, 4). Images were taken each hour during the 48-h incubation, and the settings was fixed throughout 48 hours, which facilitated continuous observation of the targeted host cells infected with gfp-transfected *L. pneumophila*.

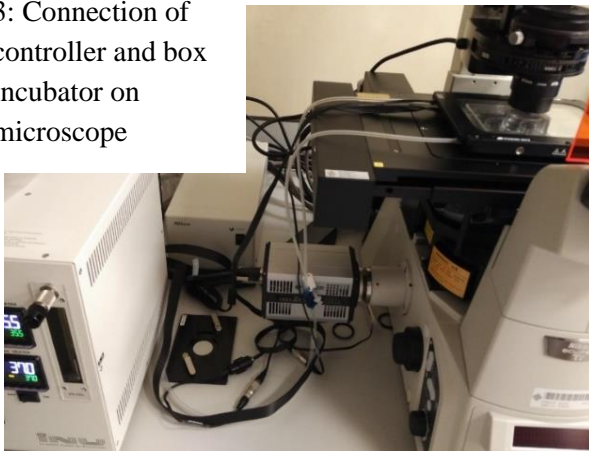
1: Temperature and gas controller



2: Box Incubator



3: Connection of controller and box incubator on microscope



4: NIS-Elements software (Nikon) operation for visualization

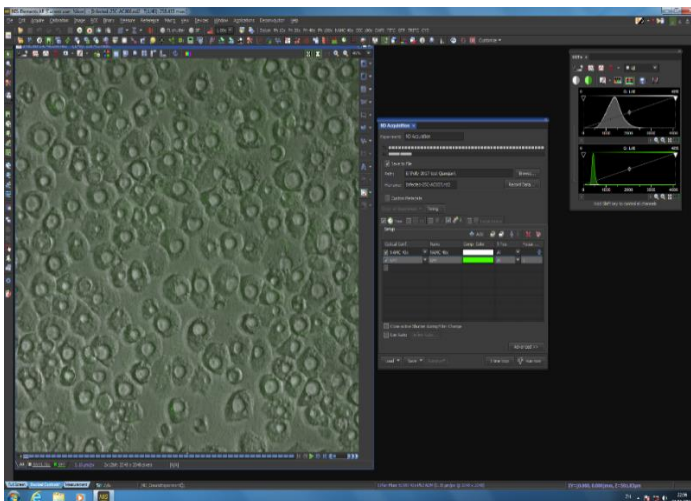


Figure 3.5 Facilities for co-culture visualization. 1, Temperature and gas controller that controlled and indicated the temperatures surrounding the box incubator, and the 5% CO₂ input shown on the pump indicator (red circle). 2, Box incubator was filled with deionized water in the surrounding groove. 3, Box incubator connected to temperature and gas controller, which maintained incubation around 37°C in 5% CO₂. 4, NIS-Elements software (Nikon) controlled the visualization settings.

3.9 Transcriptome analysis of gfp-transfected *L. pneumophila* grown in *A. castellanii* at transmissive phase

3.9.1 RNA Preparation for RNA-sequencing

A 48-h co-culture of *A. castellanii* and gfp-transfected *L. pneumophila* with a volume of 36 mL was collected and flowed through the Aria III (BD). The sorted population (*A. castellanii* containing gfp-transfected *L. pneumophila*) was collected to 10^6 cells (stored under -80°C before RNA isolation). Extracellular grown gfp-transfected *L. pneumophila* in BYE broth at T48 (10 mL), *A. castellanii* co-culture without challenging bacteria at T48 (10 mL), and 10^6 FACS-enriched gfp-transfected *L. pneumophila*-infected *A. castellanii* were collected for RNA isolation using a Purelink RNA mini kit (Invitrogen) according to the manufacturer's instructions.

The isolated RNA was digested with DNaseI (Sigma), and the Purelink RNA mini kit was used to further purify the RNA. The RNA purity was measured using a NanoDrop 2000 spectrophotometer (Thermo Fisher Scientific) to ensure an $\text{OD}_{260}/\text{OD}_{280} > 2.0$. The RNA concentration was measured with a Qubit 3.0 fluorometer (Invitrogen) to ensure that the concentration exceeded $50 \mu\text{g/mL}$. The RIN (RNA integrity number) was measured with an Agilent 2100 Bioanalyzer (Centre of Genomic Science, the University of Hong Kong), and when the RIN exceeded 6.0, $3 \mu\text{g}$ of each RNA sample was sent for Illumina Sequencing (Groken Bioscience, Hong Kong).

3.9.2 Library generation and RNA-sequencing

The total RNA was fragmented (100 to 500 nt), and the RNA fragments were ligated to barcoded adaptors with a 5' phosphate and a 3' blocking group. The barcoded RNAs were pooled and depleted of rRNA using an rRNA depletion kit (Ribo-Zero rRNA Removal kit, Illumina). Primers adapted to the barcoded adaptor were used for first-strand cDNA synthesis, and a second adaptor was ligated to the first-strand cDNA. Primers targeting the constant region of the 3' and 5' ligated adaptors were used in PCR amplification for cDNA library generation (NEBNext UltraII Directional RNA Library Prep Kit for Illumina).

The synthesized cDNAs were then used for Illumina HiSeq 2500 sequencing (Figure 3.6). Quality control ensured that Q20 (i.e., the probability of incorrect base calling of 1 in 100) exceeded 98% for sequencing reads. Sequencing readings were mapped to the *L. pneumophila Philadelphia* genome (NC_002942.5) and to the *A. castellanii* Neff genome (NW_004457442.1).

The computational analysis of RNA-seq data was performed by standard workflow (Figure 3.7) (Groken Bioscience, Hong Kong). Raw reads were filtered and aligned with reference genomes (*A. castellanii* strain *Neff*, 42 Mb genome; *L. pneumophila* strain *Philadelphia 1*, 3.4 Mb genome). The values in reads per million were calculated for unigene (Mortazavi et al. 2008) and compared with different transcripts. The expression difference was measured using log₂ ratio. An analysis of differential expressed genes (DEGs) in *L. pneumophila*-infected *A. castellanii* was performed by comparing the gene expression levels of intracellular *L. pneumophila* with extracellular *L. pneumophila*,

using *gyrB* (lpg0004) as the reference gene. The DEGs of infected *A. castellanii* were compared with uninfected *A. castellanii*, and *18S rRNA* (ACA1_053610) was used as the reference gene. Hypergeometric analysis was performed to calculate the false discovery rate (Benjamini and Yekutieli 2001); if the false discovery rate was less than 0.001 and the \log_2 ratio of the target gene expression under different conditions exceeded 2, the gene was considered to be significantly expressed. GO (gene ontology) functional analysis and KEGG (Kyoto Encyclopedia of Genes and Genomes) pathway analysis were then conducted from the DEGs.

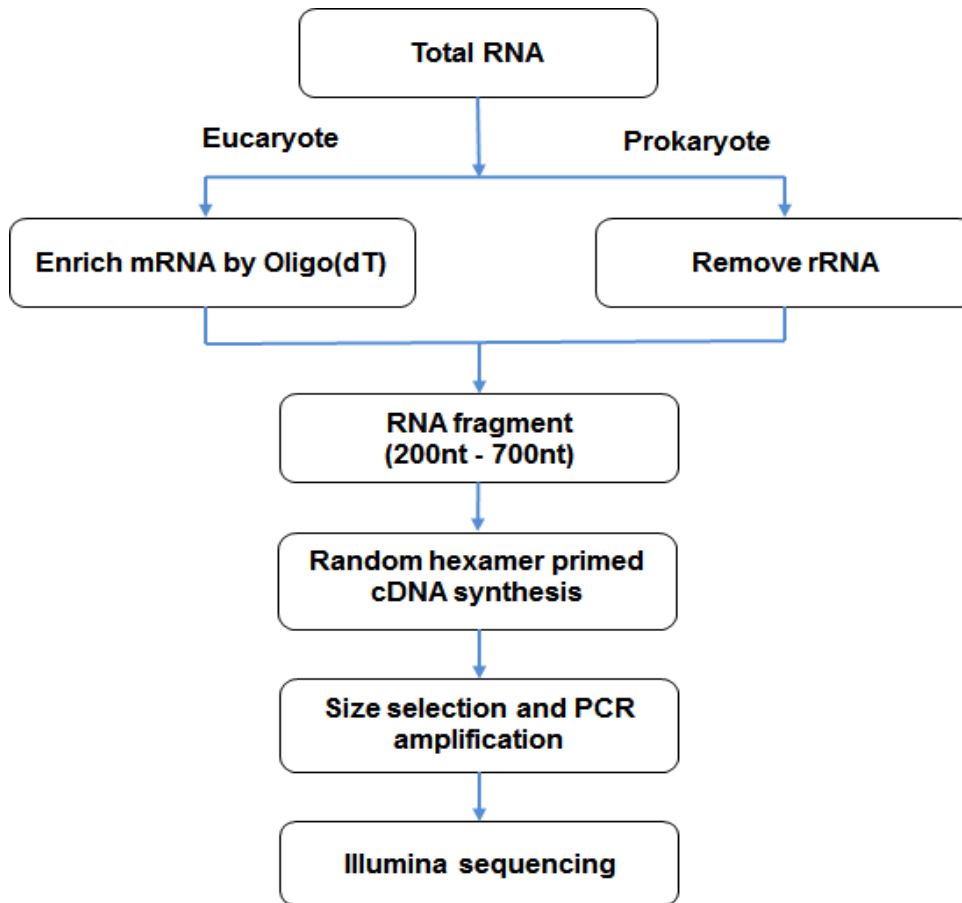


Figure 3.6 Workflow of RNA preparation for Illumina sequencing (Groken Bioscience, Hong Kong).

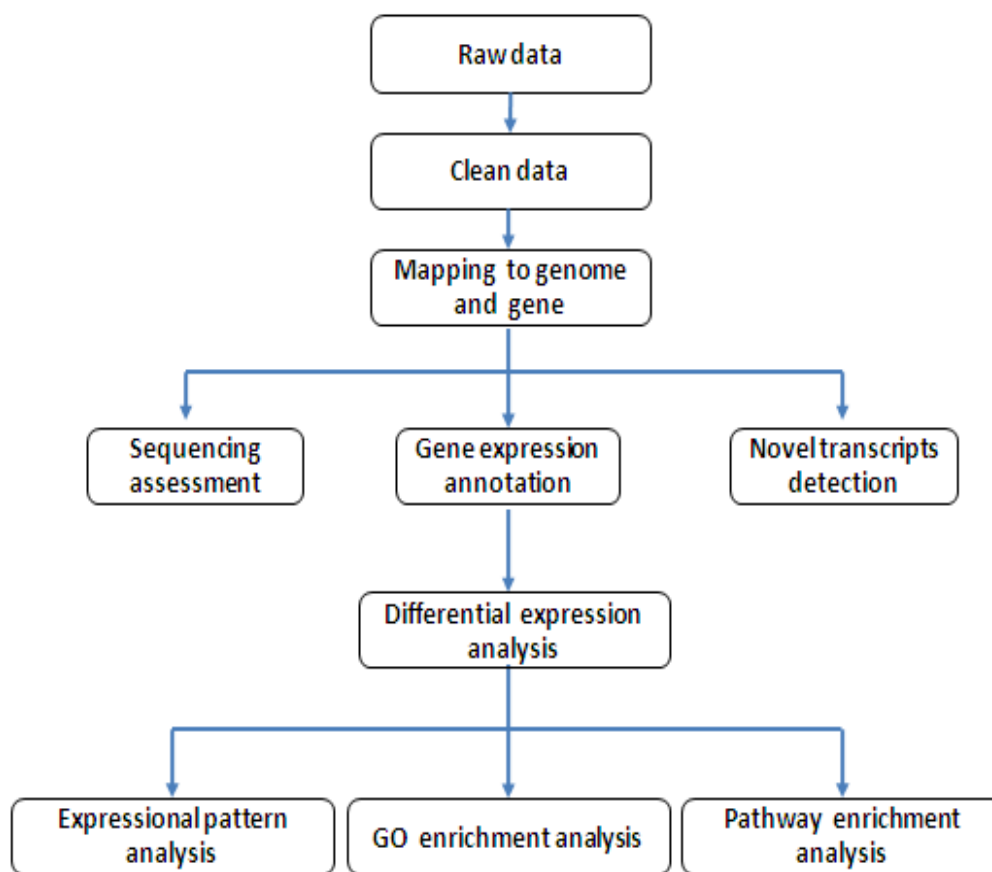


Figure 3.7 Standard Groken Bioinformatics workflow. Enriched pathways and gene ontology were generated through differential expressed genes allocation from RNA-sequencing reads (Groken Bioscience, Hong Kong).

3.9.3 Verification of gene expression result using two-step quantitative RT-PCR

3.9.3.1 RNA preparation and DNA removal of FACS-enriched *A. castellanii* infected with gfp-transfected *L. pneumophila*

Co-cultures of gfp-transfected *L. pneumophila* with *A. castellanii* were collected at T24 and T48 for FACS enrichment, as introduced in Section 3.7.5. The FACS-enriched cells were accumulated to 10^6 at each time point for RNA isolation (Section 3.5). A consistent quantity of RNA (<800 ng RNA per DNase I reaction) was then digested using DNase I at 37°C for 30 min to remove any DNA contamination in the RNA sample. Digested RNA (10 μ L) was then reverse transcribed into cDNA using a RevertAid first-strand cDNA synthesis kit. A second reverse transcription without reverse transcriptase (no-reverse transcriptase control) was set up simultaneously to monitor for the effective removal of DNA. The no-reverse transcriptase control was tested by quantitative real-time PCR, and a Ct (threshold cycle) value larger than 35 represented clean removal of the DNA in RNA samples. Extracellular grown gfp-transfected *L. pneumophila* at T48 and *A. castellanii* co-culture without challenging *L. pneumophila* at T48 were also collected for RNA isolation, DNA removal, and reverse transcription to cDNA.

3.9.3.2 Quantitative real-time PCR of synthesized cDNA

Quantitative real-time PCR was performed in 20- μ L PCR mixtures consisting of 4 μ L of cDNA, 1 \times SYBR Green Mastermix (Roche), and 500 μ M of each forward and reverse primer (Life Technologies). For probe assay, the 20- μ L PCR mix comprised 4 μ L of

cDNA, 1× PrimeTime Gene Expression Mastermix (IDT), and 1 μL of 20× Probe assay mix (containing the 4-μM probe and 10 μM of each forward and reverse primer). The primers and probes used in this study are shown in Table 3.2. PCR was run on a LightCycler480 real-time PCR system (Roche). The thermal cycling conditions comprised an initial denaturation step at 95°C for 10 min, followed by 40 cycles at 95°C for 30 s and 60°C for 1 min. For the primers and Roche SYBR Green Mastermix used, a melting curve stage was added after thermal cycling to ensure the specific PCR product produced. The threshold cycle (CT) values of the target genes were normalized to those of the reference genes. The fold changes of the intracellular *L. pneumophila* target genes at T24 and T48 were compared with those of extracellular grown *L. pneumophila* at T48. The expression of *A. castellanii* genes in FACS-enriched *A. castellanii* infected with *L. pneumophila* at T24 and T48 were compared with the uninfected *A. castellanii* at T48. The formula for the calculation of fold change was the same as described in Section 3.5.3.

Table 3.2 Primers and probes used in RT-qPCR verification of gene expression. The primers and probes were designed using the IDT (Integrated DNA Technology) Primer Quest Tool.

Gene	Primer/probe Sequence (5'-3')	Amplicon size (bp)
Primers and probes for <i>L. pneumophila</i>-specific genes		
<i>gyrB</i> (reference gene)	Forward: CGTGGAAGCAGGAGCAATA Reverse: GAACCTCTTTGGCGGGATAAA Probe: FAM-TCTAACTCAGTGCGCGTTGGATGG-IBFQ	103
<i>flaA</i>	Forward: GCAACGGCATTAAACCAACTC Reverse: AGCAGCAGTGAGTGTCATATT Probe: FAM-TGGCGTCAGCCAAACTGGAGT-IBFQ	108
<i>vipD</i>	Forward: CCTTACAAGAGCGCGGAAA Reverse: TCCATGCCAACGGCTAATATAC Probe: FAM-AATCTGACCCATGTTAGCGGAGCA-IBFQ	94
<i>fliA</i>	Forward: AAAGGATGCCCTTGGATG Reverse: TCATCTGCTCGGGCGATTAC	115
<i>sidI</i>	Forward: GCAAAAACAGGTGATGGGCA Reverse: CCTGTTGGGAATGGGATGCT	125
<i>legK1</i>	Forward: CCTTAGTGAGACGCCCAAGA Reverse: ACACAATACCGTACGCTCCC	102
<i>legK3</i>	Forward: TGCAGGCGAAGACGATAACC Reverse: AGCACTTTCGCCCCATAAGA	139
<i>tnpA</i>	Forward: GACGCCTGGTGGTTCTCTTT Reverse: GGAGAGCGTGGTTGTGTCTT	187

Table 3.2 Continued

Gene	Primer/probe Sequence (5'-3')	Amplicon size (bp)
<i>pvcA</i>	Forward: GTGTCCCGGAAACCATTAGT Reverse: CGGGAAGGCAGGCAATATAA Probe: FAM-AAAGTGCGCTTCACCTCATTTGCC-IBFQ	125
<i>pvcB</i>	Forward: AGCGTTACAGTTTGCCTCTT Reverse: GGTGATACCGTCTTGCTGTTAT Probe: FAM-AGGTGAGTGGTACCTACCAAAGGA-IBFQ	102
<i>pvcC</i>	Forward: GCACATGGTCATGCATTTTCG Reverse: AGCTCACCGGAAGTCTCTAT Probe: FAM-TGAAGCTGAGCGTAAGCCAGTAGC-IBFQ	102
Primers and probes for <i>A. castellanii</i>-specific genes		
<i>Acanthamoeba</i>	Forward: CAAAGCAGGCAGATCCAATTT	99
<i>ribosomal 18S</i> (reference gene)	Reverse: CCTTAGTCCTCAAACCAACTGA Probe: FAM-TGCCACCGAATACATTAGCATGGGA-IBFQ	
<i>Acanthamoeba</i>	Forward: GCTGGTCTCACGCAGAAGAA	154
<i>ATPeV</i>	Reverse: GGACCAGAGACCAAACGAGG	
<i>Acanthamoeba</i>	Forward: AGCCGATCTCACCAATCGAC	117
<i>IRSp53</i>	Reverse: TGATTCGCTTCGGCCTTCTT	
<i>Acanthamoeba</i>	Forward: ATCCAACGAACGCGAACTCT	113
<i>ATG14</i>	Reverse: GGAGGGTTTGTGGGATCTGG	
<i>Acanthamoeba</i>	Forward: TCGAAGGTTCCGCTATGCTC	132
<i>ribosomal S4</i>	Reverse: TGAAGACCTGGGTCTGGAGG	

Table 3.2 Continued

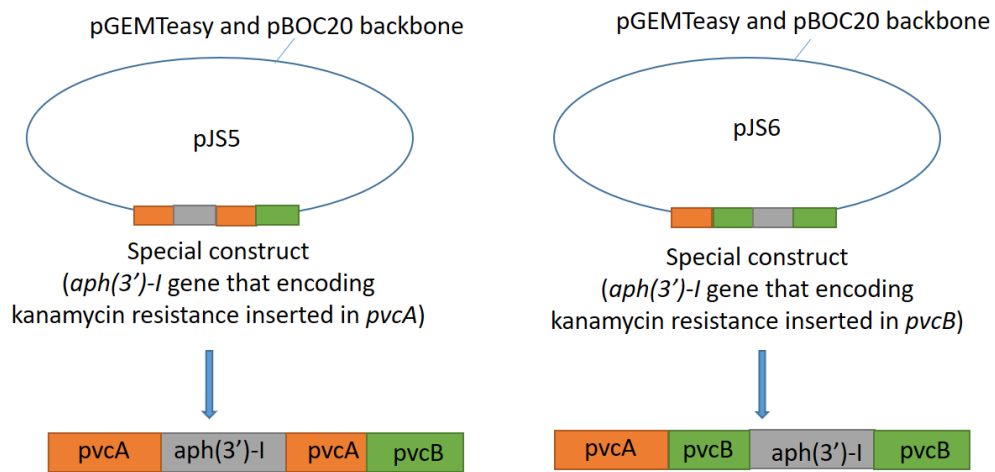
Gene	Primer/probe Sequence (5'-3')	Amplicon size (bp)
<i>Acanthamoeba</i>	Forward: GTGATCAGCCAGACCCAGAG	137
<i>ribosomal L35</i>	Reverse: ACGGTCTTGGCGTTCTTCTC	
<i>Acanthamoeba</i>	Forward: AGCACAGCAACGAAGACAGA	161
<i>CoA Kinase</i>	Reverse: GAGCGCATCAGCTTCCGATA	
<i>Acanthamoeba</i>	Forward: CGACCTATAGGCCCAAGCTG	134
<i>Ser/Thr</i> <i>phosphatase</i>	Reverse: CTCGTCTTCATGCGGTTCTCCT	
<i>Acanthamoeba</i>	Forward: TAACGGACGCCACTTCCTTC	193
<i>ATPase</i>	Reverse: CCGATGCTGCCATAGTCCAA	
<i>Acanthamoeba</i>	Forward: GAGCAACTCGGTCTTCACCA	129
<i>MCM8</i>	Reverse: GGTCCGCTTTTGAGGAGGAA	

3.10 Knockout study in *L. pneumophila*

3.10.1 Knockout of *pvcA* and *pvcB* in *L. pneumophila* by allelic exchange

The plasmids pJS5 and pJS6 (gifts from Prof. Cianciotto, Northwestern University, Chicago) were used to generate *pvcA*-knockout and *pvcB*-knockout *L. pneumophila* strains, respectively. The plasmids pJS5 and pJS6 were constructed by cloning pGEMTeasy plasmid cloned with gene *aph(3')-I* in *pvcA* and *pvcB* DNA fragments into the counter-selective plasmid pBOC20, respectively (Allard et al. 2006) (Figure 3.8, A). The *aph(3')-I* (aminoglycoside-O-phosphotransferase) gene encoding kanamycin resistance. The plasmid with the specific constructs can be transformed by *L. pneumophila* to facilitate allelic exchange, and transformed plasmids can finally be excreted by culturing the transformed bacteria in selective medium supplemented with sucrose (Allard et al. 2006, Cianciotto et al. 1988). The plasmids pJS5 and pJS6 were transfected in *L. pneumophila*. (The transfection operation is described in Section 3.6.1) (Figure 3.8, B). Transfected *L. pneumophila* were spread onto the selective α BCYE plate supplemented with 25 μ g/mL kanamycin (Sigma) and 10% sucrose (Sigma).

A. Constructs of plasmids pJS5 and pJS6



B. Workflow of pJS5 facilitated site-directed mutagenesis in *L. pneumophila*

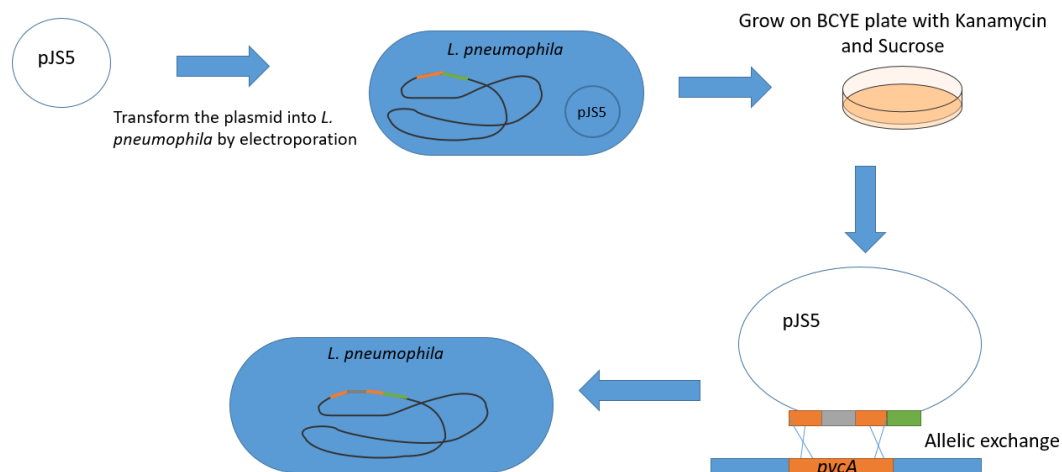


Figure 3.8 Instruction of plasmids pJS5 and pJS6 facilitated site-directed mutagenesis in *L. pneumophila*. **A.** Constructs of plasmids pJS5 and pJS6, which were used for knockout of gene *pvcA* and *pvcB*, respectively. **B.** Workflow of pJS5 facilitated site-directed mutagenesis in *L. pneumophila*; furthermore, the *pvcA* could be knocked out by inserting *aph(3')-I* in the *L. pneumophila* genome. The pJS6 was done in the same way for knockout of *pvcB* gene in *L. pneumophila* genome.

3.10.2 Verification of *pvcA*-knockout and *pvcB*-knockout *L. pneumophila*

The pJS5 and pJS6 facilitated allelic exchange in the *L. pneumophila* genome, which led to the insertion of a *aph(3')-I* gene that encoding kanamycin resistance in the *pvcA* and *pvcB* genes, respectively. The selective α BCYE plate supplemented with kanamycin and sucrose facilitated the selection of the successful *pvcA*-knockout and *pvcB*-knockout *L. pneumophila*. Colonies grown on the selective plates were further obtained and subcultured on the α BCYE plate supplemented with 25 μ g/mL kanamycin and 10% sucrose for five passages to obtain the *pvcA*-knockout and *pvcB*-knockout *L. pneumophila* strains with the excretion of plasmid pJS5 and pJS6, respectively. The grown colonies were further subjected to verification by PCR, gel electrophoresis, and Sanger sequencing (Figures 3.9 and 3.10).

For PCR verification of pJS5 and pJS6 transformed *L. pneumophila*, one colony grown on the selective plate was selected in the 50- μ L PCR mix that comprised 1 \times Phusion high-fidelity buffer (NEB), 200 μ M of dNTPs, 200 nM of forward and reverse primers, nuclease-free water, and 1 unit of Phusion DNA polymerase (NEB). Allard et al. (2006) used primers *pvcA9F* and *pvcB6* to confirm insertion in *L. pneumophila pvcAB* (Allard et al. 2006); furthermore, their study used primers aligned to the *aph(3')-I* fragment to confirm the junction of *pvcAB* with *aph(3')-I* by sequencing. The primer information is shown in Figure 3.10. PCRs were run on a Veriti 96-well thermal cycler (ABI). The thermal cycling conditions comprised an initial denaturation step at 98°C for 1 min, followed by 40 cycles of 98°C for 30 s, 56°C for 30 s, and 72°C for 1 min. The PCR

products were further loaded onto 1.2% agarose gel (Sigma) supplemented with 1× SYBR safe stain dye (Thermo Fisher) for electrophoresis at 120 V for 1 h. The DNA in the gel was further exposed under ChemiDoc MP system (Bio-Rad) with Image Lab software, and the result is shown in Figure 3.9. The specific PCR products of primers *pvcA9F* and *Kan1R* and of primers *pvcB1F* and *Kan2R* were respectively cut from the gel (indicated by red arrow in Figure 3.9) for purification with a PureLink Quick gel extraction kit (Invitrogen). The purified PCR products were further subjected to Sanger sequencing to confirm the insertion of *aph(3')-I* in *pvcA* and *pvcB*, respectively (Tech Dragon Sequencing, Hong Kong).

L. pneumophila with *aph(3')-I* insertion in *pvcA* and *pvcB* gene were confirmed as *pvcA*-knockout *L. pneumophila* and *pvcB*-knockout *L. pneumophila*, respectively (Figure 3.10). The *pvcA*-knockout *L. pneumophila* and *pvcB*-knockout *L. pneumophila* were further stored in 20% glycerol at -80°C , respectively.

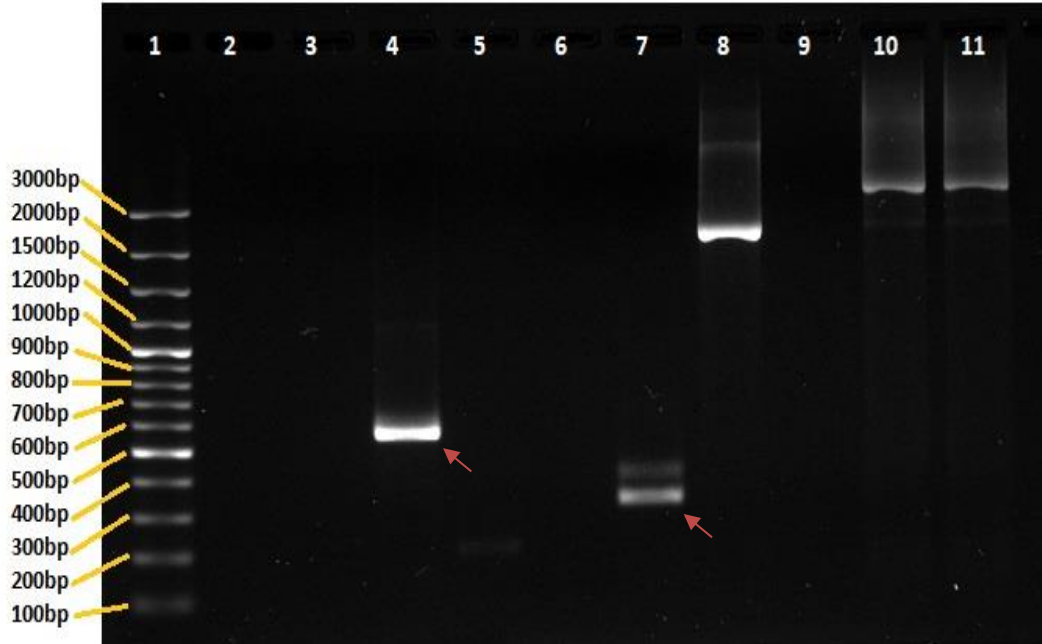


Figure 3.9 Gel electrophoresis identification of *aph(3')*-I insertion in *L. pneumophila pvcA* and *pvcB*. From left to right lanes: **1**, GeneRuler 100bp Plus DNA Ladder (Fermentas); **2**, wild-type *L. pneumophila* in PCR with pvcA9F and Kan1R primers; **3**, negative control of pvcA9F and Kan1R PCR; **4**, pJS5-transformed *L. pneumophila* in pvcA9F and Kan1R PCR; **5**, wild-type *L. pneumophila* in PCR with pvcB1F and Kan2R primers; **6**, negative control of pvcB1F and Kan2R PCR; **7**, pJS6-transformed *L. pneumophila* in pvcB1F and Kan2R PCR; **8**, wild-type *L. pneumophila* in PCR with pvcA9F and pvcB6R primers; **9**, negative control of pvcA9F and pvcB6R PCR; **10**, pJS5-transformed *L. pneumophila* in pvcA9F and pvcB6R PCR; **11**, pJS6-transformed *L. pneumophila* in pvcA9F and pvcB6R PCR.

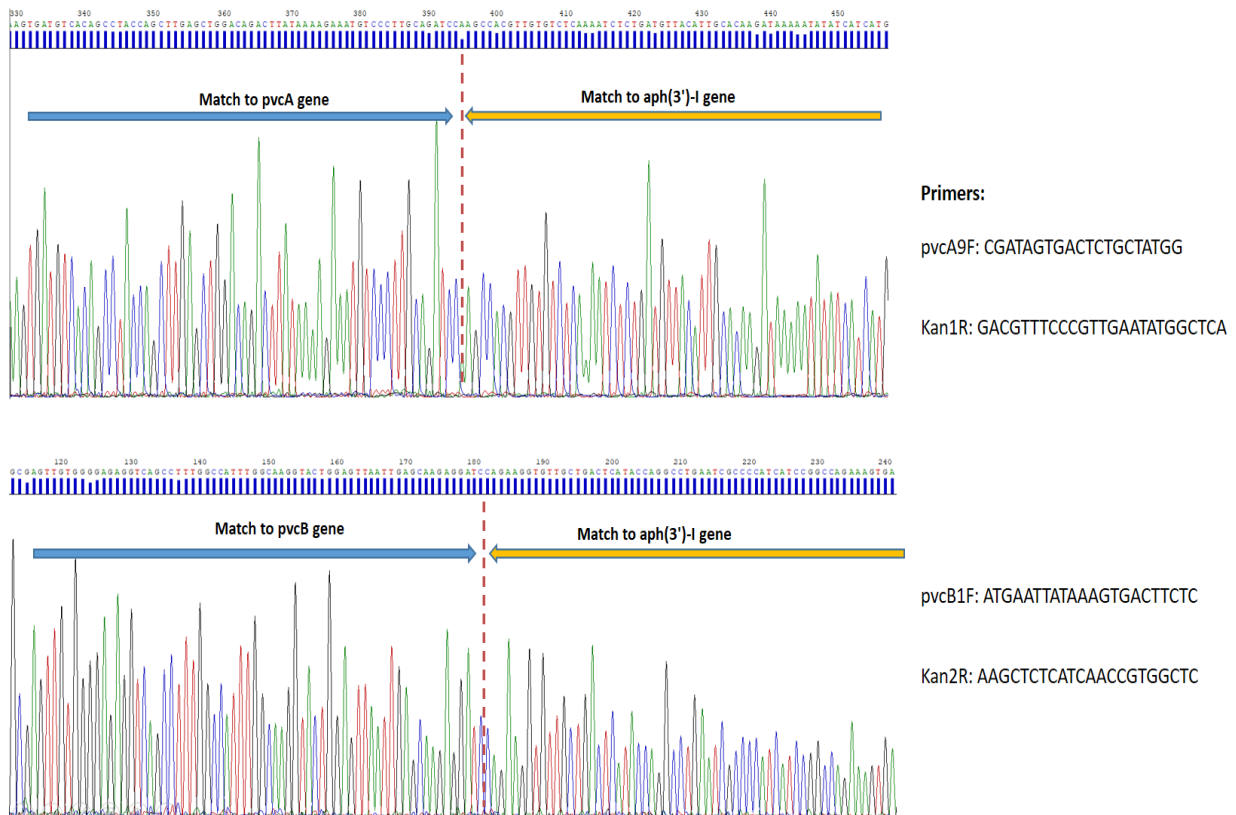


Figure 3.10 Verification of *pvcA*-knockout and *pvcB*-knockout *L. pneumophila* strains. *L. pneumophila* transformed with pJS5 and pJS6 were subjected to PCR with primers pvcA9F-Kan1R and PCR with primers pvcB1F-Kan2R, respectively. The two PCR products (indicated in Figure 3.9) were subjected to Sanger sequencing (Tech Dragon Sequencing, Hong Kong). The two pairs of primer sequences are shown on the right. The upper panel shows the PCR product's sequence of pJS5 transformed *L. pneumophila*, and the insertion of *aph(3')-I* in *pvcA* can be seen. The lower panel shows the PCR product's sequence of pJS6 transformed *L. pneumophila*, and the insertion of *aph(3')-I* in *pvcB* can be seen.

3.10.3 Growth assay of *pvcA*-knockout and *pvcB*-knockout *L. pneumophila*

3.10.3.1 *L. pneumophila* and mutant strains grown in BYE broth with and without L-cysteine supplement

L. pneumophila samples, including wild-type, *pvcA*-knockout, and *pvcB*-knockout strains, were grown in BYE broth. Two different groups of BYE broth were used, with and without supplementation with cysteine. (The recipes are listed in Appendix 1.) First, *L. pneumophila* grown on selective BCYE plates (4-day culture) were picked and suspended in 2 mL of PBS, and the OD_{600nm} was adjusted to 1. A 20- μ L *L. pneumophila* suspension was then added into every 20 mL of BYE broth in a 50-mL conical tube (Corning), and this time point was denoted as T0. The conical tube was incubated in a shaking incubator at 37°C with 200-rpm shaking. Every 12 h from T0 to T72, a 100- μ L suspension of each group of *L. pneumophila* grown in BYE broth was added to one well of a 48-well plate (Corning) to measure the OD_{600nm} with a DTX800 Multimode Microplate Reader (Beckman Coulter). The final optical density of *L. pneumophila* grown in BYE broth was normalized to BYE broth read under OD_{600nm}. The experiments were repeated three times, and the data are expressed as the percentage of each hour's optical density divided by that of T0.

3.10.3.2 Intracellular growth assay of *L. pneumophila* and mutant strains

L. pneumophila *pvcA*-knockout and *pvcB*-knockout strains were grown on α BCYE plates supplemented with 25 μ g/mL kanamycin, and wild-type *L. pneumophila* was grown on α BCYE plates. The fresh-grown colonies (4-day culture) were suspended in 2 mL of PBS, and the OD_{600nm} was adjusted to 1 ($\sim 10^9$ *L. pneumophila* per mL), and the *L. pneumophila* in PBS suspension with an OD_{600nm} of 1 were then used for co-cultures.

Each 20 μ L sample of *L. pneumophila* was added to 2 mL of *A. castellanii* (10^6 cell per mL) cultured in PYG, and the co-culture operation proceeded as described in Section 3.4.1. PYG was used as the co-culture medium for the wild-type *L. pneumophila*, and PYG supplemented with 25 μ g/mL kanamycin was used as the co-culture medium for both *pvcA*-knockout and *pvcB*-knockout *L. pneumophila*. The plate counts of *L. pneumophila* grown in *A. castellanii* were performed every 12 h from 0 to 48 h.

The *L. pneumophila* suspension in PBS with an OD_{600nm} of 1 was also used for co-culture with THP-1, and each 20- μ L sample of *L. pneumophila* was added to 2 mL of THP-1 cultured in RPMI 1640 medium (Gibco). The co-culture operation was as described in Section 3.4.2. RPMI 1640 was used as the co-culture medium for the wild-type *L. pneumophila*, and RPMI 1640 supplemented with 25 μ g/mL kanamycin was used as the co-culture medium for *pvcA*-knockout and *pvcB*-knockout *L. pneumophila*. The co-culture was collected every 12 h from 0 to 48 h for plate counts. The data were expressed

as percentages of each hour's plate count divided by the plate count at 0 h. Each experiment was performed three times.

3.10.3.3 Growth assay of *L. pneumophila* and mutant strains released from *A. castellanii* in THP-1

Based on the plate counts of *L. pneumophila* and mutant strains' intracellular growth in *A. castellanii* (Section 3.10.3.2), 10-mL samples of wild-type *L. pneumophila* co-culture with *A. castellanii*, 18-mL samples of *pvcA*-knockout *L. pneumophila* co-culture with *A. castellanii*, and 100-mL samples of *pvcB*-knockout *L. pneumophila* co-culture with *A. castellanii* were used to further release the bacteria to be challenged into 10-mL samples of THP-1 culture in RPMI 1640 at an MOI of 1.

The *L. pneumophila* co-cultured with *A. castellanii* (as introduced in Section 3.10.3.2) at T48 were collected and released by adding the same volume of sterile distilled water to the co-culture and incubating for 10 min, followed by five to ten passages through a syringe with a 23-gauge needle (10 mL; Terumo). The lysed *L. pneumophila* were further collected in 50-mL conical tubes and centrifuged at $150 \times g$ for 2 min to remove the *A. castellanii* debris. The bacterial pellets of *L. pneumophila* and the mutant strains were then suspended in 100- μ L PBS and inoculated into each 10-mL sample of THP-1 cells at a concentration of 10^6 per mL in co-culture medium. The co-culture operations were the

same as described above. Each 2-mL co-culture was collected for plate counts every 12 h from 0 to 48 h. The data are expressed as the percentage of each hour's plate count divided by the plate count at 0 h. All experiments were performed three times.

3.11 Statistical analysis

The data are presented as means \pm SEM (standard error of mean) and analyzed with SPSS software (v24.0; IBM). Curves and histograms were generated in Excel (Microsoft Office 2016). The normal distribution of data was verified by Shapiro-Wilk testing; a p value of greater than 0.05 on the Shapiro-Wilk test indicates that the data set has a normal distribution. Statistical comparisons among multiple groups regarding plate counts, fold changes, and flow cytometry percentages were performed by either paired *t*-test or Wilcoxon-signed test (if the data were not normally distributed). Differences were considered to be statistically significant if the p value was less than 0.05.

4. Results

4.1 Intracellular growth of *L. pneumophila* in *A. castellanii* and THP-1

4.1.1 Extracellular growth of *L. pneumophila* in BYE broth

Before *L. pneumophila* was used to infect the host cells, extracellular growth in broth was set up to investigate the extracellular grown bacterial number and to determine the post-exponential growth phase in BYE broth. The standard *L. pneumophila* strain (ATCC33152) grown on α BCYE plates (fresh *L. pneumophila* colonies were suspended in PBS and adjusted to an OD_{600nm} of 1, which represented $\sim 10^9$ bacteria per mL) was inoculated in the BYE broth for bacterial extracellular growth. A growth curve was generated with the standard plate count method every 12 h from 0 to 48 h.

During extracellular growth in the BYE broth, the number of *L. pneumophila* increased from 10^8 to 10^{10} CFU per mL during the first 24 h. From 24 to 48 h, the number of viable *L. pneumophila* remained near 10^{10} CFU per mL (Figure 4.1.1), which suggests that the *L. pneumophila* had reached the post-exponential growth phase that was reported to be more virulent and ready to infect host cells (Molofsky and Swanson 2004). The 48-h *L. pneumophila* broth culture was used to infect the host cells, including *A. castellanii* and THP-1 cells.

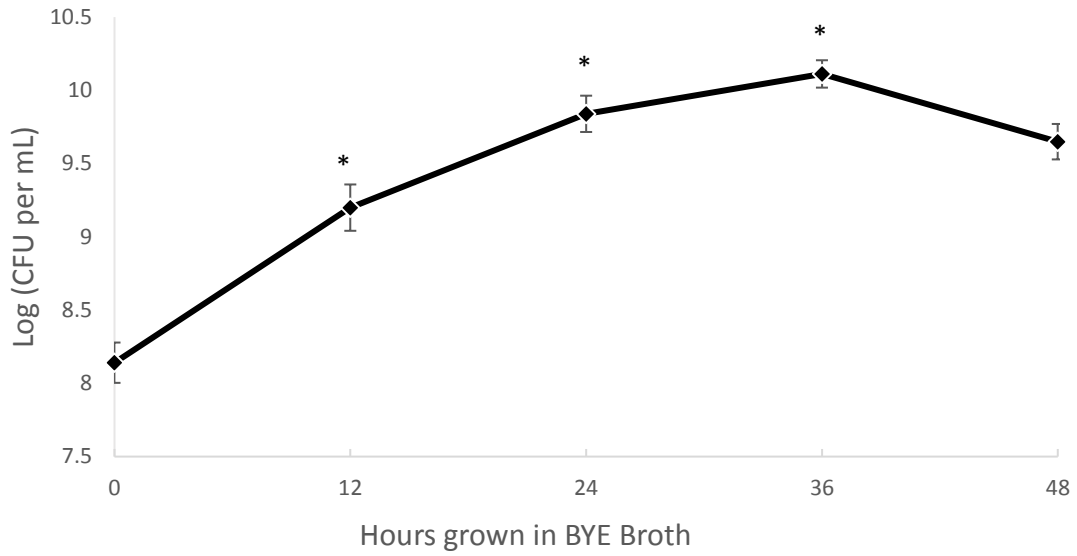


Figure 4.1.1 Extracellular growth curve of *L. pneumophila*. The number of viable and culturable *L. pneumophila* grown in BYE broth was enumerated every 12 h with the plate count method. BCYE agar plates were used for plate counts. Wilcoxon-signed rank test was used to compare the bacterial counts from 12 to 48 h to that of the previous time point, and p values less than 0.05 were considered to indicate statistical significance (*).

4.1.2 Intracellular growth of *L. pneumophila* in *A. castellanii* and THP-1 by plate counts

A standard plate count method was used to compare the number of viable *L. pneumophila* in *A. castellanii* and THP-1. After the *A. castellanii* and THP-1 were challenged with *L. pneumophila* for 3 h, the extracellular bacteria were removed by gentamicin treatment. *A. castellanii* and THP-1 from the co-culture were collected for plate counts at various time points. THP-1 and *A. castellanii* cells were both challenged with *L. pneumophila* at an MOI of 10. However, the initial intracellular *L. pneumophila* count at 0 h in THP-1 was 1-log less than that in *A. castellanii*, indicating a difference in the hosts' ability to uptake *L. pneumophila* (Figure 4.1.2).

Figure 4.1.2 illustrates the growth pattern of *L. pneumophila* in the two hosts. When grown in THP-1 cells, the intracellular *Legionella* number remained stable during the first 24 h after infection and exhibited a 0.4-log increase from 24 to 36 h after infection. Although the increase between 24 and 36 h after infection was small, the difference reached statistical significance ($p=0.043$). A 0.2-log increase was seen between 36 and 48 h after infection ($p=0.310$).

In contrast, the intracellular *L. pneumophila* in *A. castellanii* exhibited a 1-log increase in growth during the first 24 h ($p=0.043$) and no further increase up to 48 h ($p=0.068$). The results show that *L. pneumophila* replicated better in *A. castellanii*.

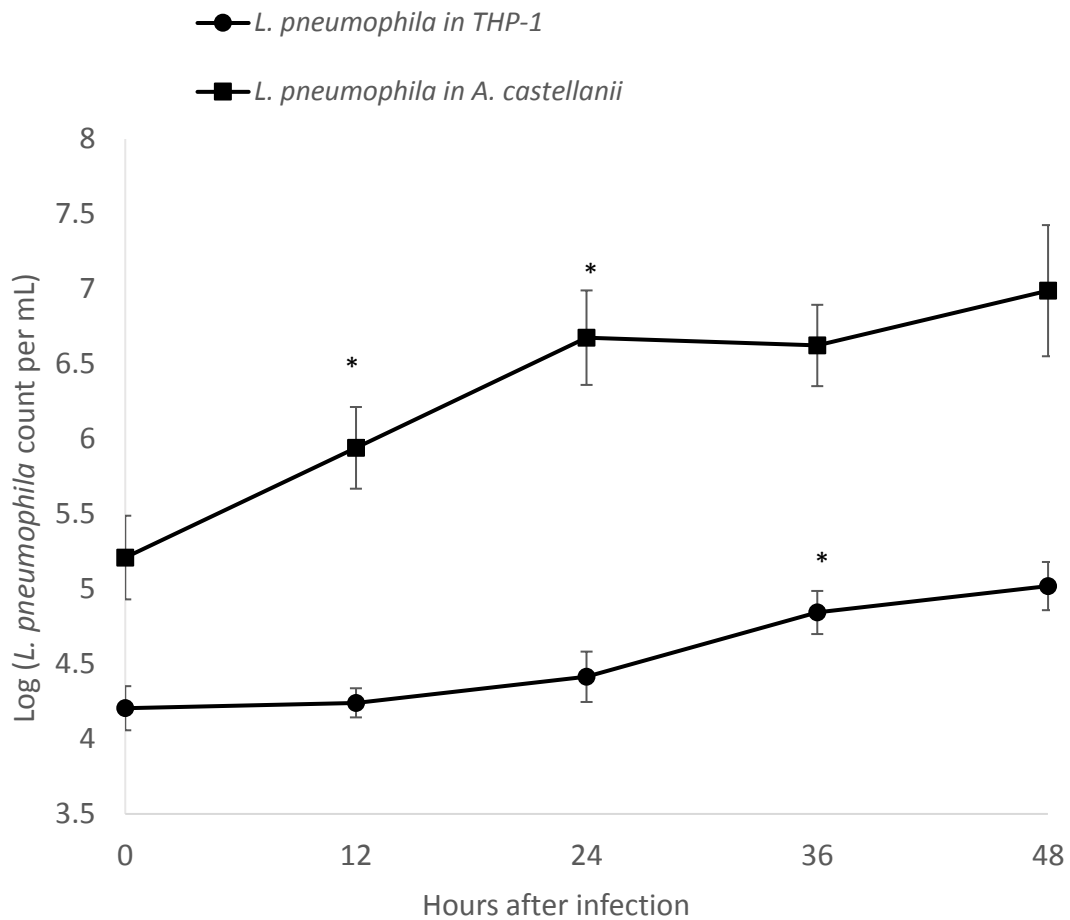


Figure 4.1.2 Intracellular growth curve of *L. pneumophila* in *A. castellanii* and THP-1.

Viable and culturable *L. pneumophila* grown in THP-1 and *A. castellanii* were released via lysis of the host cells at 12-h intervals up to 48 h. The released *L. pneumophila* cells were enumerated with the plate count method. BYE agar plates were used for plate counts. The Wilcoxon-signed rank test was used to compare the bacterial counts at 12 to 48 h with those at the previous time points (T0 and T12; T12 and T24; T24 and T36; T36 and T48). A p value of less than 0.05 was considered to indicate statistical significance (*).

4.1.3 Microscopic observation of gfp-transfected *L. pneumophila*–infected *A. castellanii* and THP-1

The *A. castellanii* and THP-1 were infected with gfp-transfected *L. pneumophila*; after the co-culture, live images of gfp-transfected *L. pneumophila*–infected host cells (from T0 to T48) were visualized with the inverted confocal microscope (Eclipse Ti, Nikon).

4.1.3.1 *A. castellanii* infected with gfp-transfected *L. pneumophila*

The microscopic images of gfp-transfected *L. pneumophila*–infected *A. castellanii* show an obvious increase in the number of *A. castellanii* cells rounded up together with the GFP signals (Figure 4.1.3.1). This indicates that the replication of *L. pneumophila* inside the *A. castellanii* increased gradually during the first 12 h and then more rapidly from T12 to T24 (Figure 4.1.3.1).

The GFP signals showed no obvious increase or propagation after T36, which could be due to the decreased viability of *A. castellanii* (Figure 4.1.3.1). The host *A. castellanii* also showed obvious morphological changes between T0 and T48. *A. castellanii* cells were confluent and adhesive during the early phase and were rounded up and floating in the late stage. The morphological changes of *A. castellanii* could have been caused by *L. pneumophila* infection or deprivation of nutrients in the co-culture.

Our microscopic study also showed that the GFP signals were both focal and dispersed from T16 to T28 (Figure 4.1.3.1). However, the GFP signals were dispersed in most of the infected *A. castellanii* cells from T32 to T48 (Figure 4.1.3.1). The focal GFP indicated that gfp-transfected *L. pneumophila* was encapsulated in the LCV, and the dispersal signals indicated the presence of motile gfp-transfected *L. pneumophila* inside the *A. castellanii* cell (Xiong et al. 2017), ready for rupture and release from the host.

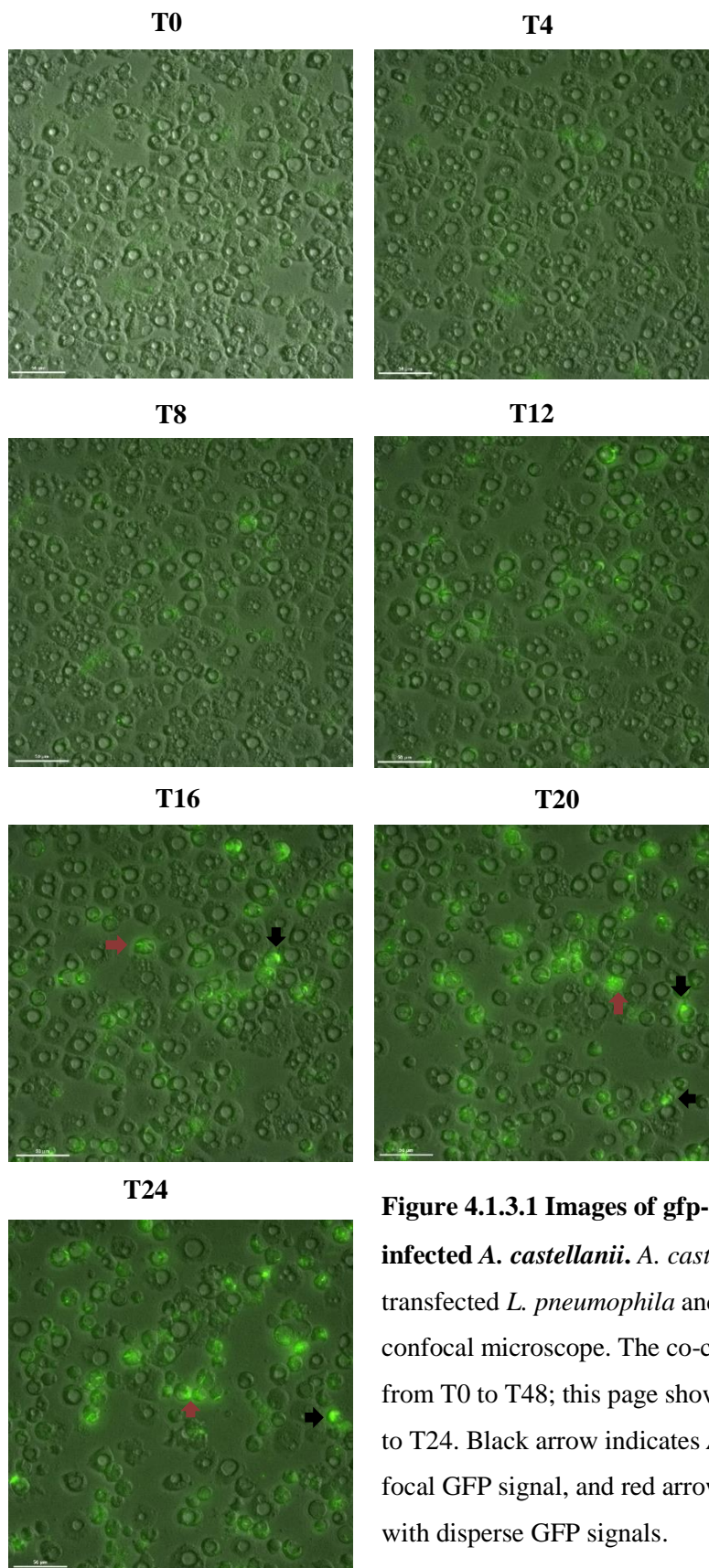


Figure 4.1.3.1 Images of gfp-transfected *L. pneumophila*-infected *A. castellanii*. *A. castellanii* were infected with gfp-transfected *L. pneumophila* and observed under an inverted confocal microscope. The co-culture was visualized every hour from T0 to T48; this page shows images of every 4 hours from T0 to T24. Black arrow indicates *A. castellanii* cells contained with focal GFP signal, and red arrow indicates *A. castellanii* contained with disperse GFP signals.

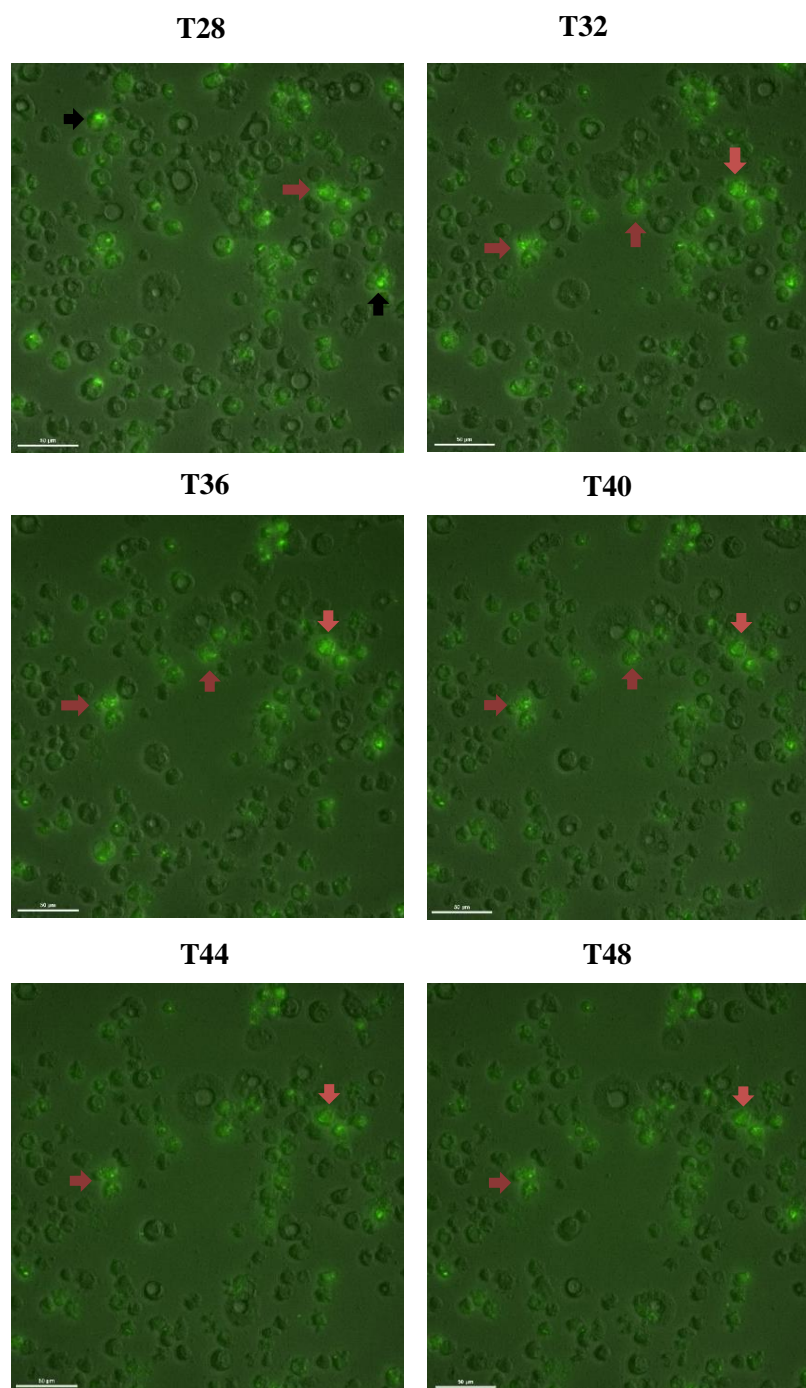


Figure 4.1.3.1 Continued. Images of gfp-transfected *L. pneumophila*-infected *A. castellanii*. *A. castellanii* were infected with gfp-transfected *L. pneumophila* and observed under an inverted confocal microscope. The co-culture was visualized every hour from T0 to T48; this page shows images of every 4 hours from T28 to T48. Black arrow indicates *A. castellanii* cells contained with focal GFP signal, and red arrow indicates *A. castellanii* contained with disperse GFP signals.

4.1.3.2 Gfp-transfected *L. pneumophila* grown in THP-1 for 48 h

When gfp-transfected *L. pneumophila* was grown in THP-1–differentiated macrophages, the green fluorescence signals were less obvious than that grown in *A. castellanii* (see Figure 4.1.3.2). Because THP-1 cells are nonadhesive, THP-1 cells were differentiated into adhesive macrophages using PMA (Phorbol-12-myristate 13-acetate) before challenge with gfp-transfected *L. pneumophila*. THP-1 at a concentration of 10^6 /mL was treated with 100-nM PMA in supplied RPMI medium for 2 days and used for co-culture (introduced in Section 3.6.3).

The images show fewer macrophages with green fluorescence. The microscopic observation agreed with the plate counts of intracellular *L. pneumophila* released from THP-1, which also demonstrated an increase of less than 1-log in *L. pneumophila* (from T0 to T36). Some THP-1 cells have internalized the gfp-transfected *L. pneumophila*, but no growth is visible inside the host. Some GFP signals internalized by THP-1 cells had disappeared in the next visualization (Figure 4.1.3.2; T0 and T4; arrows), possibly because of the antimicrobial activities of the THP-1 cells.

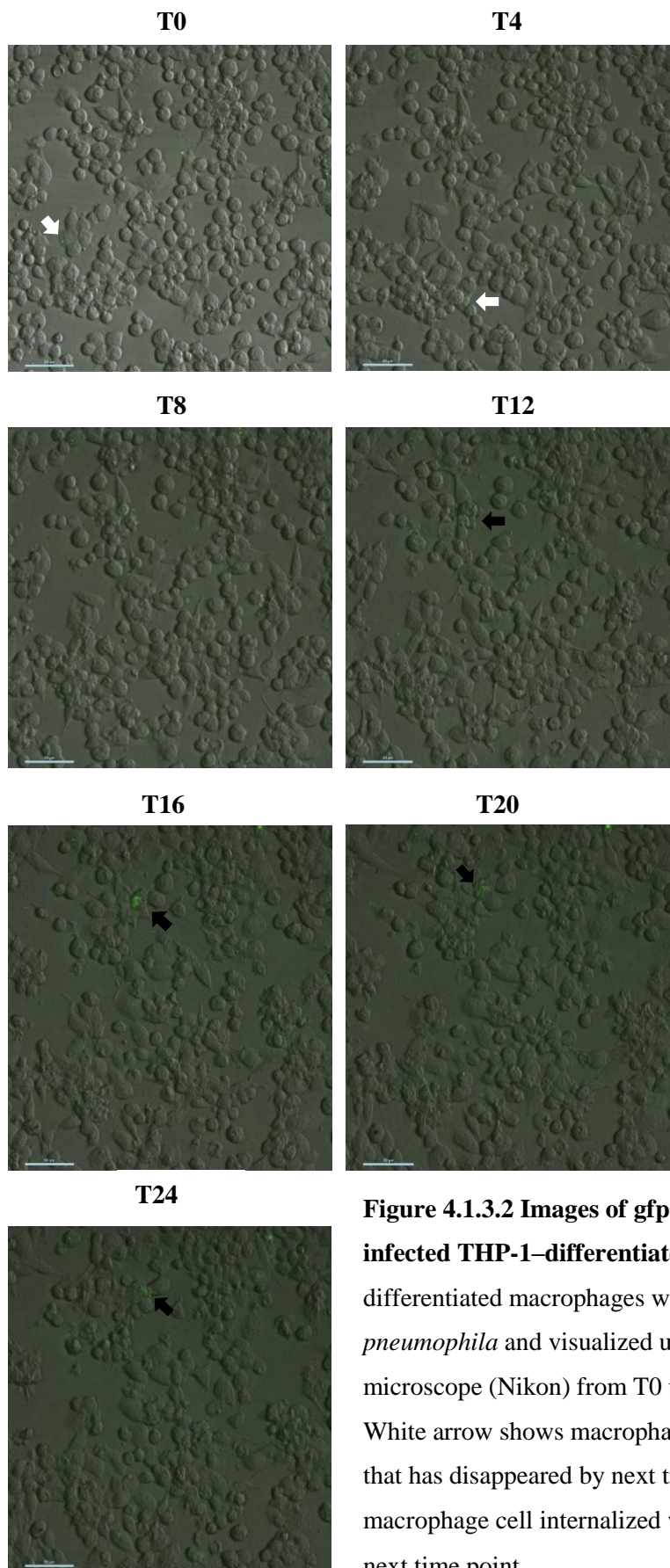


Figure 4.1.3.2 Images of gfp-transfected *L. pneumophila*-infected THP-1-differentiated macrophages. THP-1-differentiated macrophages were infected with gfp-transfected *L. pneumophila* and visualized under an inverted confocal microscope (Nikon) from T0 to T48 (this page shows T0 to T24). White arrow shows macrophage cell contained with GFP signal that has disappeared by next time point. Black arrow represents macrophage cell internalized with GFP signal that is sustained in next time point.

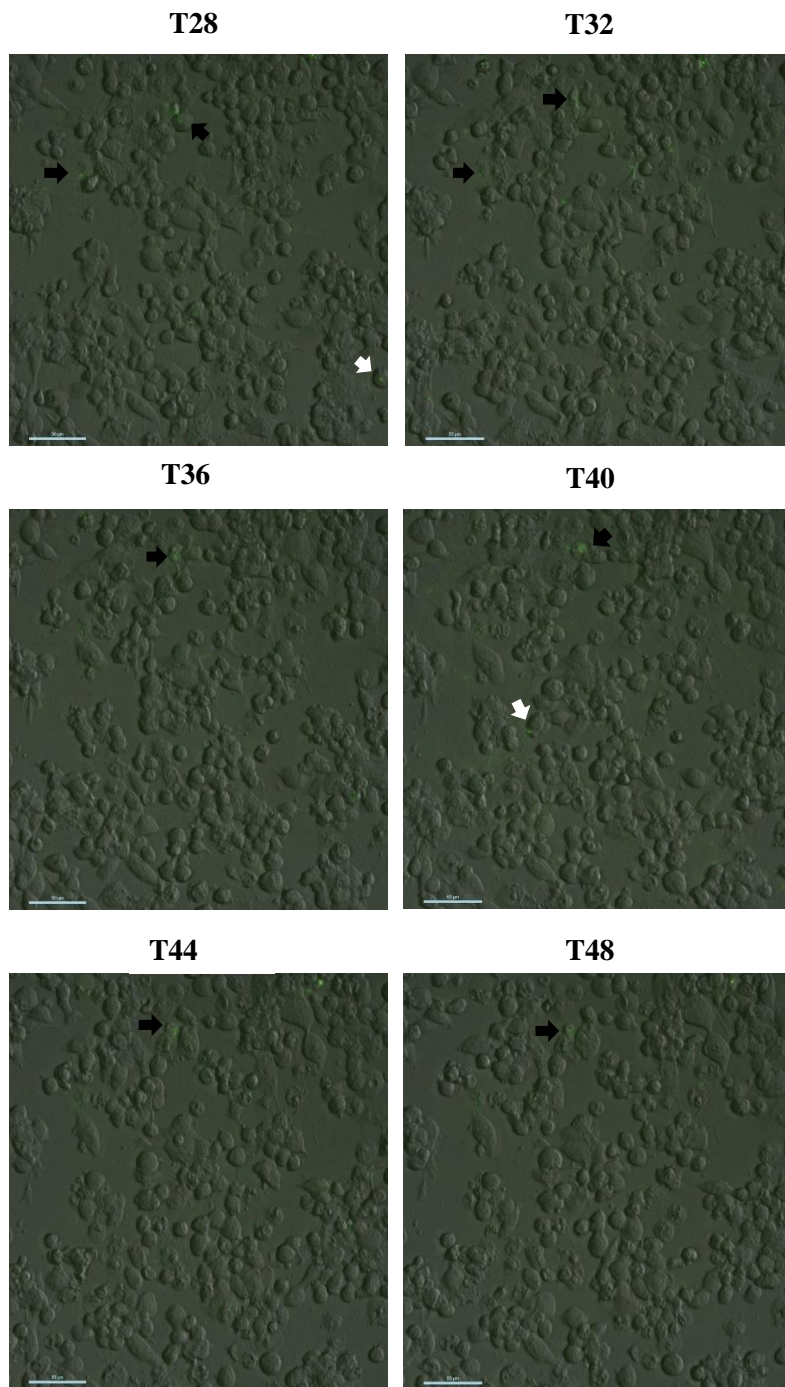


Figure 4.1.3.2 Continued. Images of gfp-transfected *L. pneumophila*-infected THP-1-differentiated macrophages. THP-1-differentiated macrophages were infected with gfp-transfected *L. pneumophila* and were visualized under an inverted confocal microscope (Nikon) from T0 to T48 (this page shows T28 to T48). White arrow shows macrophage cell contained with GFP signal that has disappeared by next time point. Black arrow represents macrophage cell internalized with GFP signal that is sustained in next time point.

4.2 Differential virulence expression of *Legionella pneumophila* grown in amoebas and monocytes

4.2.1 Expression of *L. pneumophila* virulence genes in different hosts

4.2.1.1 *L. pneumophila* expression patterns in THP-1

When grown in THP-1 cells, the expression of the pyroptosis-related genes *flaA* and *sdhA* varied dynamically over time. The expression of *flaA* decreased from –3.6-fold to –6.7-fold over time, whereas the expression of *sdhA* was upregulated at all time points (T0 to T48), increasing from 1.5-fold upregulation at 12 h to 8.1-fold at 48 h after infection. In contrast, the expression of the apoptosis-related genes *vipD* and *sidF* was more static, with slight decreases (<2-fold downregulation) over time (Figure 4.2.1.1).

4.2.1.2 *L. pneumophila* expression patterns in *A. castellanii*

The expression of both *flaA* and *vipD* was upregulated in *A. castellanii*. During the first infection cycle, the expression of *flaA* had not obviously changed (1.7-fold upregulation) at 12 h after infection, but it peaked (13.1-fold) at 24 h, followed by decreases during the second infection cycle to 8.6- and 7.4-fold upregulation at 36 and 48 h, respectively. Although *vipD* exhibited 1.8- and 1.3-fold downregulation at 12 and 24 h, respectively, the expression levels increased during the second infection cycle, with 1.8- and 4.6-fold upregulation at 36 and 48 h, respectively (Figure 4.2.1.2). In contrast, *sdhA* and *sidF* exhibited changes of less than 2-fold at most time points, except for 4.3-fold downregulation of *sdhA* at 48 h after infection (Figure 4.2.1.2).

In summary, these gene expression studies indicate that during growth in THP-1 cells, the *L. pneumophila* genes responsible for pyroptosis activation were downregulated, whereas those involved in the suppression of host pyroptosis were activated. In contrast, the *L. pneumophila* genes responsible for the initiation of host cell death were upregulated during growth in *A. castellanii*.

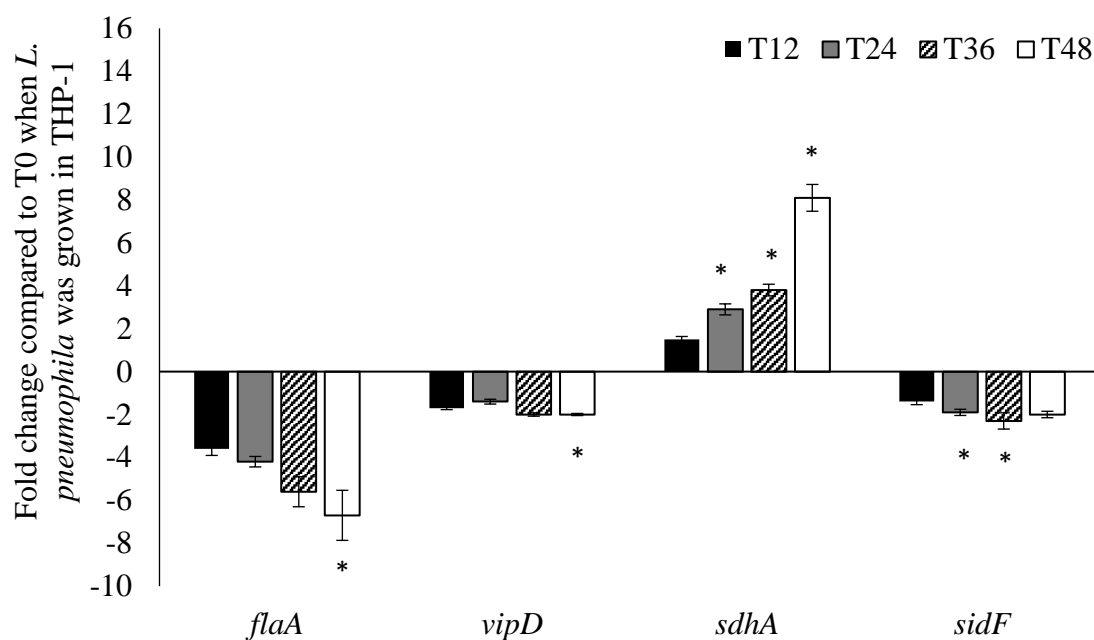


Figure 4.2.1.1 Expression of *L. pneumophila* virulence genes during intracellular growth in THP-1. *L. pneumophila* grown in THP-1 were collected for RNA isolation at various time points and used to run quantitative RT-PCR. All virulence genes had been normalized to the housekeeping gene *gyrB*. The data are expressed as the mean fold change ($2^{-\Delta\Delta CT}$) from T0. Error bars show the SEM (standard error of the mean). The fold changes at T24 and T48 were statistically compared with that at T12 with the Wilcoxon signed rank test; asterisks (*) represent significant differences ($p < 0.05$).

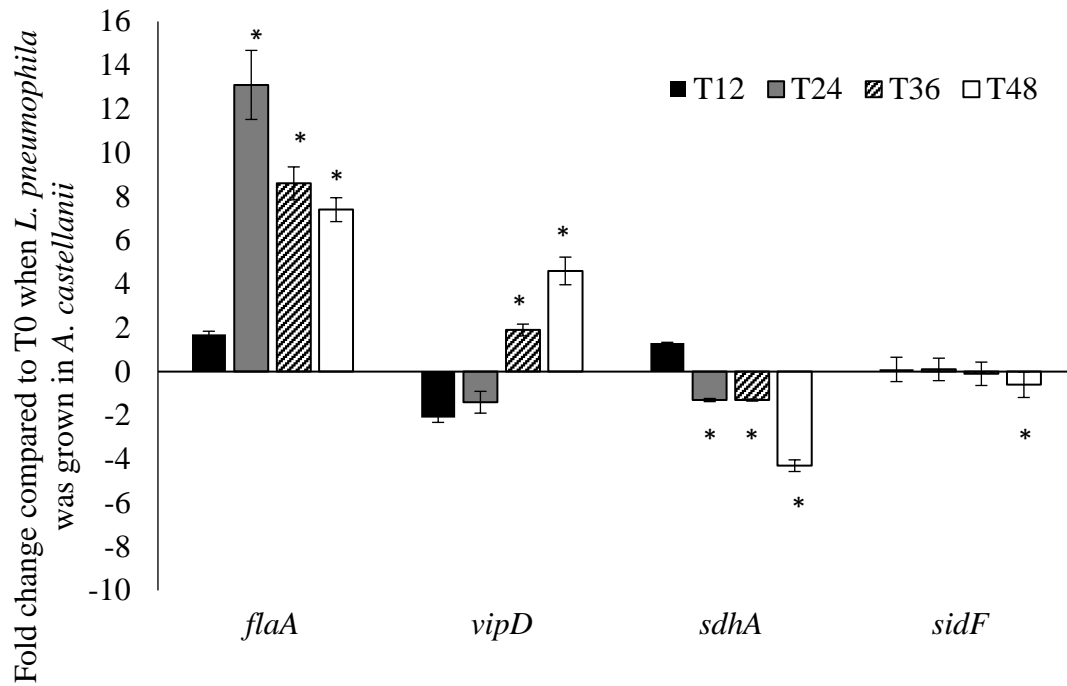


Figure 4.2.1.2 Expression of *L. pneumophila* virulence genes during intracellular growth in *A. castellanii*. *L. pneumophila* grown in *A. castellanii* were collected for RNA isolation at various time points and used to run quantitative RT-PCR. All virulence genes had been normalized to the housekeeping gene *gyrB*. The data are expressed as the mean fold change ($2^{-\Delta\Delta CT}$) from T0. Error bars show the SEM (standard error of the mean). The fold changes at T24 and T48 were statistically compared with that at T12 with the Wilcoxon signed rank test; asterisks (*) represent significant differences ($p < 0.05$).

4.2.2 Expression of *CASP* genes in the THP-1 host cells

To understand the host cell responses during *L. pneumophila* infection, we investigated the expression of *CASP-1* and *CASP-3* in THP-1 cells (Figure 4.2.2). In the uninfected THP-1 cells, the expression of *CASP-1*, which encodes caspase-1, showed strong upregulation, with increases ranging from 6.1- to 16.3-fold between 12 and 48 h. Despite the strong upregulation of *CASP-1* at 48 h, however, the number of viable cells was not remarkably reduced (Figure 4.3.3.1). In contrast, *CASP-1* was only modestly upregulated in *L. pneumophila*-infected THP-1 cells, with increases ranging from 2- to 3.2-fold between 12 and 48 h after infection. Overall, our results show that *CASP-1* expression was lower in the *L. pneumophila*-infected THP-1 cells than in the uninfected THP-1 cells.

The expression of *CASP-3*, which encodes the apoptotic protein caspase-3, was lower in the *L. pneumophila*-infected THP-1 cells than in the uninfected cells at all time points except for T36, when the pattern reversed slightly (Figure 4.2.2). The 8.6-fold downregulation of *CASP-3* expression seen at 48 h after infection may have been caused by a decrease in the number of viable THP-1 cells. In summary, our results demonstrate reduced activation of caspase genes in *Legionella*-infected cells relative to uninfected cells.

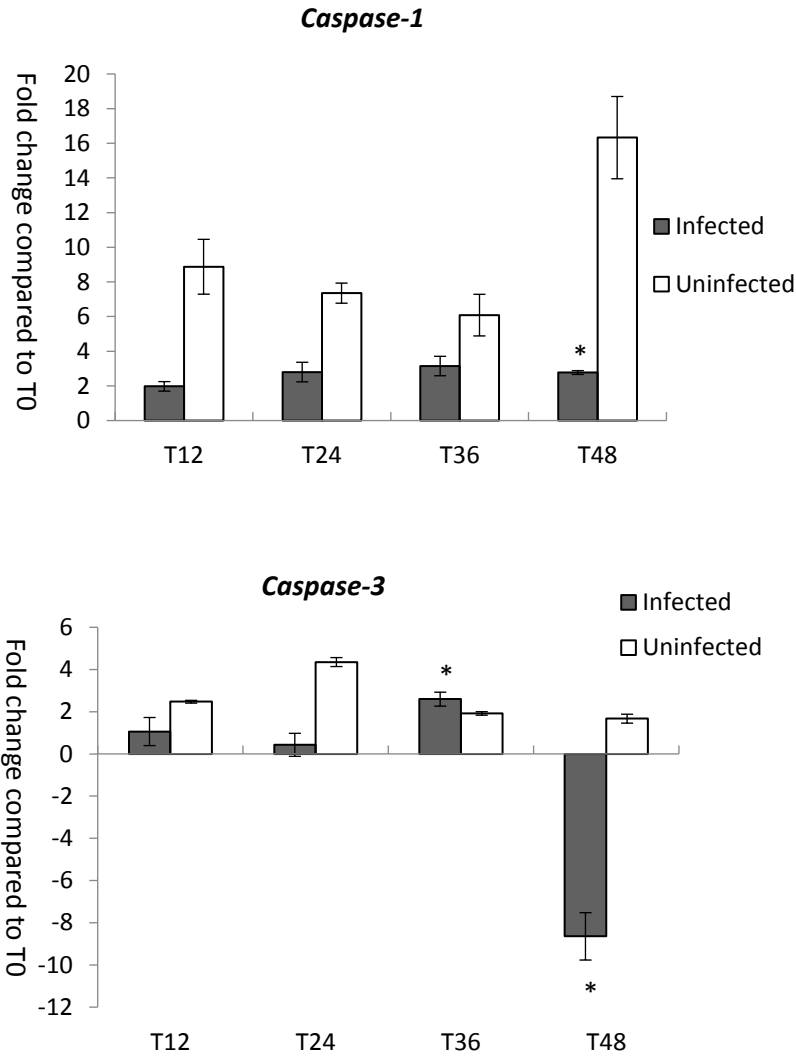


Figure 4.2.2 Expression of *CASP* genes during *L. pneumophila* infection in THP-1. Fold changes in the expression of *CASP-1* and *CASP-3* in THP-1 were detected with quantitative RT-PCR every 12 h from T0 to T48. The expression levels of the THP-1 genes were normalized to those of its housekeeping gene *GAPDH*. The data are expressed as the mean fold change. Error bars show the SEM (standard error of the mean). Fold changes at T24 and T48 were statistically compared with that at T12 with the Wilcoxon signed rank test; asterisks (*) represent significant differences ($p < 0.05$).

4.2.3 Metacaspase-1 (MCASP-1) expression of infected and uninfected *A. castellanii*

The expression of the *A. castellanii* metacaspase-1 gene (*MCASP-1*) was also investigated (Figure 4.2.3, left panel). In uninfected *A. castellanii*, a change in *MCASP-1* expression of less than 2-fold was observed between the 12- and 48-h time points. In *Legionella*-infected *A. castellanii*, however, *MCASP-1* expression kept increasing between 12 and 48 h after infection. The *MCASP-1* expression was downregulated by 4.5-fold at 12 h, downregulated by only 1.5-fold at 24 and 36 h, and upregulated by 3.5-fold at 48 h, indicating that *MCASP-1* activation occurred later after *L. pneumophila* infection. Because *MCASP-1* promotes amoeba encystment, we performed microscopic examinations of both uninfected and infected cells for the presence of amoeba cysts at various time points. At 48 h, amoeba cysts were present in 1% and 32% of the uninfected and infected *A. castellanii*, respectively, which demonstrates that *L. pneumophila* infection led to increased cyst formation (Figure 4.2.3, right panel).

From microscopic observation of the *A. castellanii* cells' morphology co-cultured with *L. pneumophila*, the *A. castellanii* cells exhibited an obvious blebbing appearance and/or encystment 24 h after infection. *MCASP-1* was reported to express the caspase-like protein metacaspase-1, which may be involved in *Acanthamoeba* encystment. The accumulated number of *L. pneumophila* in the late stage grown in *A. castellanii* is associated with the upregulation of *MCASP-1* at T48 in *A. castellanii*.

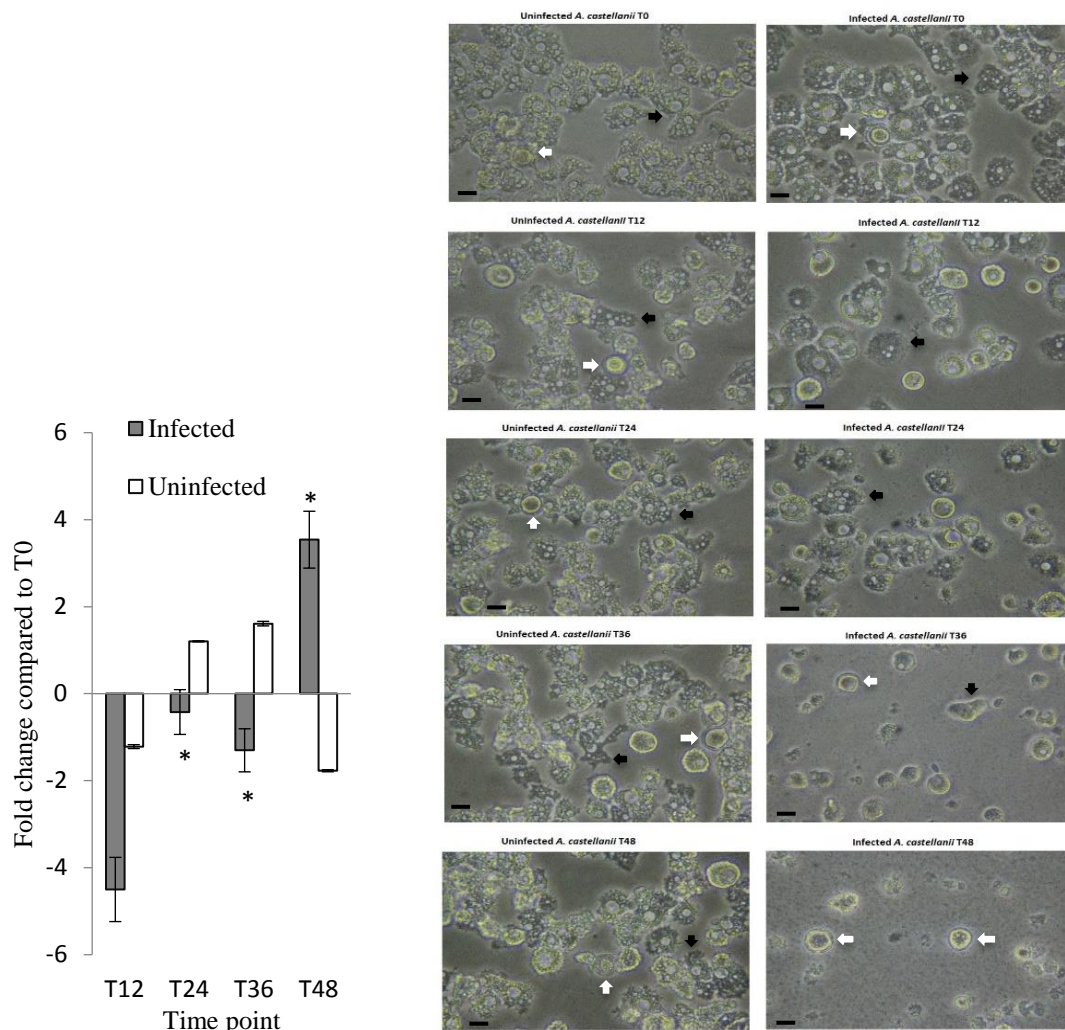


Figure 4.2.3 Expression of *MCASP-1* during *L. pneumophila* grown in *A. castellanii* that changed from trophozoites to cysts. Fold changes in the expression of *MCASP-1* in *A. castellanii* were detected with quantitative RT-PCR every 12 h from T0 to T48 (left). The expression level of *MCASP-1* was normalized to that of *A. castellanii 18S rRNA* gene. The data are expressed as the mean fold change. Error bars show the SEM (standard error of the mean). Fold changes at T24 to T48 were statistically compared with that at T12 with the Wilcoxon signed rank test; asterisks (*) represent a significant change ($p < 0.05$). Microscopic images (right) show the uninfected and infected *A. castellanii*. Black arrows indicate trophozoites, and white arrows indicate cyst forms with a two-layer cell wall (scale bar = 25 μm ; magnification 400 \times).

4.3 Investigation of cell death in *L. pneumophila*-infected THP-1 and *Acanthamoeba castellanii*

For accurate investigation of whether caspase-1-mediated pyroptosis or caspase-3-mediated apoptosis dominated in THP-1 cells' death when infected with *L. pneumophila*, active caspase-1 and active caspase-3 were stained in both infected and uninfected THP-1. Propidium iodide staining was used to compare cell death between *L. pneumophila*-infected and uninfected host cells, which helped us to evaluate the ability of cell death caused by *L. pneumophila*.

4.3.1 Production of active caspase-1 in *L. pneumophila*-infected and uninfected THP-1 cells

Figure 4.3.1.1 shows the results of flow cytometry of active caspase-1 protein. The percentage of caspase-1-positive cells was measured at each time point in both groups. The percentages of caspase-1-positive cells increased gradually from T0 to T48. The percentage of THP-1 cells that produced caspase-1 ranged from 1.9% to 14.9% in the *L. pneumophila*-infected group and from 1.5% to 13.6% in the uninfected group. From T0 to T12, the percentages of caspase-1-positive cells were similar in both groups. At T24, the percentage of caspase-1-positive cells was lower in the *L. pneumophila*-infected group than in the uninfected group, and a statistically significant difference was observed at T24 ($p=0.015$). In contrast, from T36 to T48, the percentages of caspase-1-positive cells were higher in the *L. pneumophila*-

infected group, and a statistically significant difference was observed at T48 (p=0.019).

Microscopic examination was performed on the THP-1 cells stained with FITC-labelled FAM-YVAD-FMK. When observed under a confocal microscope, a gradual increase was seen in the caspase-1-positive cells in both the *L. pneumophila*-infected and uninfected THP-1 cells between T0 and T48 (Figure 4.3.1.2). It was also observed that both uninfected and infected groups had cells with stronger green fluorescence than others obtained in the same image, representing the greater production of active caspase-1 in these cells (arrows indicate in Figure 4.3.1.2). It is well known that active caspase-1 can further induce pyroptosis, that is, inflammatory cell death (Miao et al. 2010). The increase in active caspase-1 production in both *L. pneumophila*-infected and uninfected THP-1 suggests that *L. pneumophila* infection was not the only reason that caspase-1 activation was triggered.

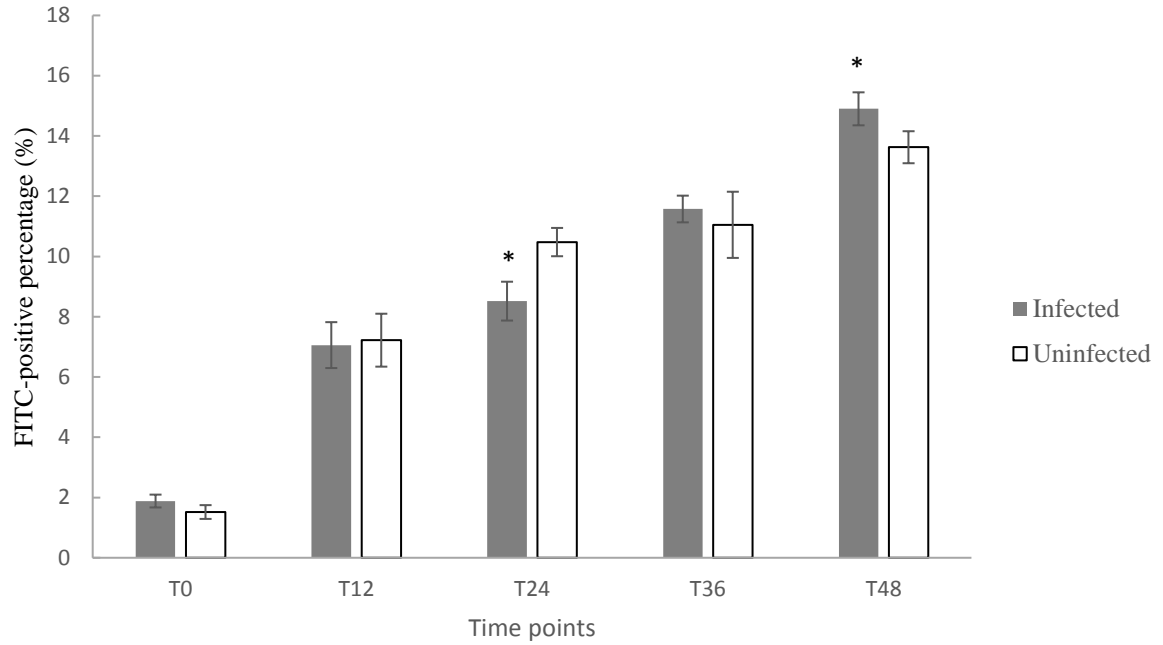


Figure 4.3.1.1 Active caspase-1 production in *L. pneumophila*-infected and uninfected

THP-1 cells. THP-1 cells obtained at various time points were stained with FITC-labeled

FAM-YVAD-FMK, and the signals were detected with a BD FACSAria III flow cytometer.

The data are presented as the percentage of cells that express caspase-1. The percentages in

the *L. pneumophila*-infected and uninfected groups were compared at each time point with a

paired *t*-test. A *p* value of less than 0.05 was considered to indicate statistical significance (*).

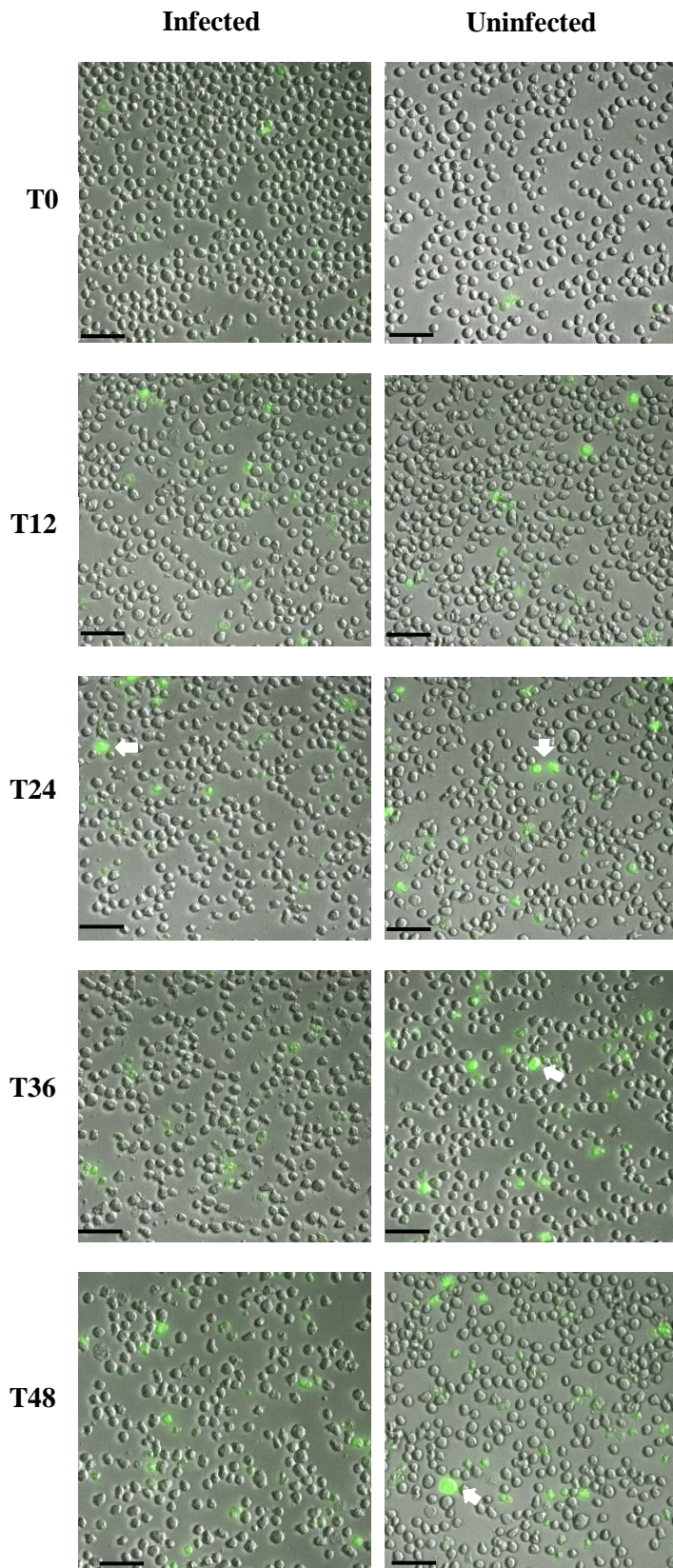


Figure 4.3.1.2 Microscopic examination of active caspase-1 production in THP-1 cells. A Nikon Eclipse Ti inverted microscope was used to visualize the THP-1 cells stained with FITC-labeled FAM-YVAD-FMK from T0 to T48. The left and right panels represent *L. pneumophila*-infected and uninfected THP-1 cells, respectively. Arrow indicates cell with stronger green fluorescence. Green fluorescence indicates cells that produced active caspase-1. Bar – 50 μm .

4.3.2 Production of active caspase-3 in *L. pneumophila*-infected and uninfected THP-1 cells

Flow cytometry measurements of the active caspase-3 in both *L. pneumophila*-infected and uninfected THP-1 cells were made every 12 h from T0 to T48. The percentages of THP-1 cells that produced active caspase-3 ranged from 0.6% to 1.1% in the *L. pneumophila*-infected group and from 0.7% to 1.3% in the uninfected group. Both groups had much lower percentages of cells that produced caspase-3 than those that produced caspase-1, and the percentage of caspase-3-positive cells was increased mildly from T0 to T24. During this period, the *L. pneumophila*-infected group had a lower percentage of caspase-3-positive cells than the uninfected group, but the difference was not statistically significant. At T36 and T48, the percentages of caspase-3-positive cells had decreased to a level similar to that seen at T12. The *L. pneumophila*-infected group had a higher percentage of caspase-3-positive cells than the uninfected group at T48, but the difference was not statistically significant (Figure 4.3.2.1).

The microscopic images of the *L. pneumophila*-infected and uninfected groups show that most cells were negative for active caspase-3 (Figure 4.3.2.2). Our data show that less than 2% of cells were caspase-3-positive at all time points, which suggests less involvement of active caspase-3 protein in both the *L. pneumophila*-infected and uninfected THP-1 cells.

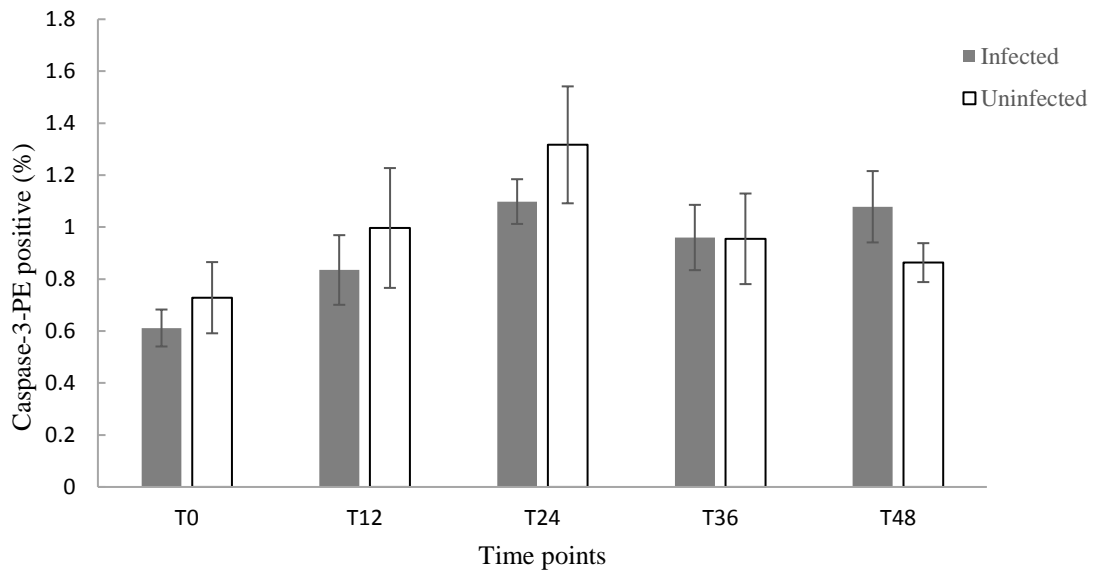


Figure 4.3.2.1 Active caspase-3 production in *L. pneumophila*-infected and uninfected THP-1 cells. THP-1 cells obtained at various time points were stained with PE-labeled DEVD-FMK, and signals were detected with a BD FACSAria III flow cytometer. The data are presented as the percentages (%) of cells that expressed caspase-1. The percentages in the *L. pneumophila*-infected and uninfected groups were compared at each time point with a paired *t*-test. A *p* value of greater than 0.05 was considered to indicate a lack of a significant difference.

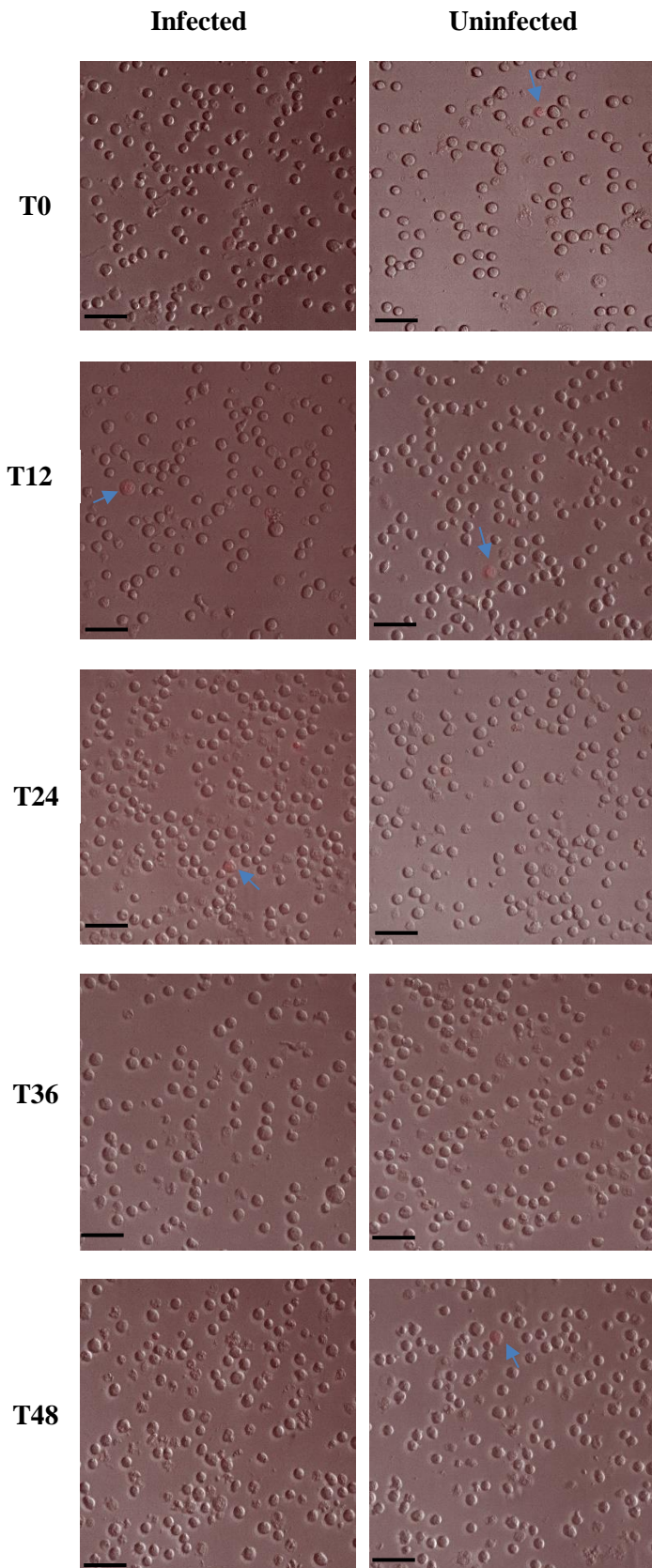


Figure 4.3.2.2 Microscopic examination of active caspase-3 production in THP-1 cells. A Nikon Eclipse Ti inverted microscope was used to visualize THP-1 cells stained with PE-labeled DEVD-FMK from T0 to T48. The left and right panels show *L. pneumophila*-infected and uninfected THP-1 cells, respectively. Arrow indicates THP-1 cell with the weak red fluorescence. Red fluorescence indicates cells that produced active caspase-1 protein. Bar – 50 μ m.

4.3.3 Cell death assay in THP-1 cells

PI can penetrate damaged cells and bind to nucleic acids. Hence, the percentage of PI-positive cells reflects the percentage of damaged cells as a result of cell death. Figure 4.3.3.1 shows the percentages of PI-positive cells in the *L. pneumophila*-infected and uninfected groups. Our results show that 1.4% of the *L. pneumophila*-infected THP-1 cells stained positive with PI at T0, and a sharp increase to 7.05% and 7.7% was seen at T12 and T24, respectively. The percentage of PI-positive cells continued to increase to 9.4% at T36 and 12.9% at T48. The pattern of the infected THP-1 cells was similar to that of the uninfected counterpart. In the uninfected group, the percentage of PI-positive cells increased sharply from 2.2% at T0 to 8.93% at T24. Little change was seen in the PI-positive percentage from T24 to T36, but the percentage increased from 9.05% at T36 to 11.2% at T48. The infected group had a significantly higher percentage of PI positive cells than the uninfected group at T48 ($p=0.031$).

The microscopic observation (Figure 4.3.3.2) of PI-stained THP-1 cells showed no obvious difference between the *L. pneumophila*-infected and uninfected THP-1 cells from T0 to T48. We observed that certain PI-positive cells were dilated (blue arrow in Figure 4.3.3.2) in both the *L. pneumophila*-infected and uninfected THP-1 cells, which suggests the possible involvement of necrosis or pyroptosis (Kroemer et al. 2009, Ziegler and Groscurth 2004).

From cell death staining (Table 4.3.1), including active caspase-1, active caspase-3, and PI staining, narrow gaps were seen between the *L. pneumophila*-infected and uninfected THP-1 cells at all time points. THP-1 cell death could be triggered by nutrient deprivation instead of bacterial infection.

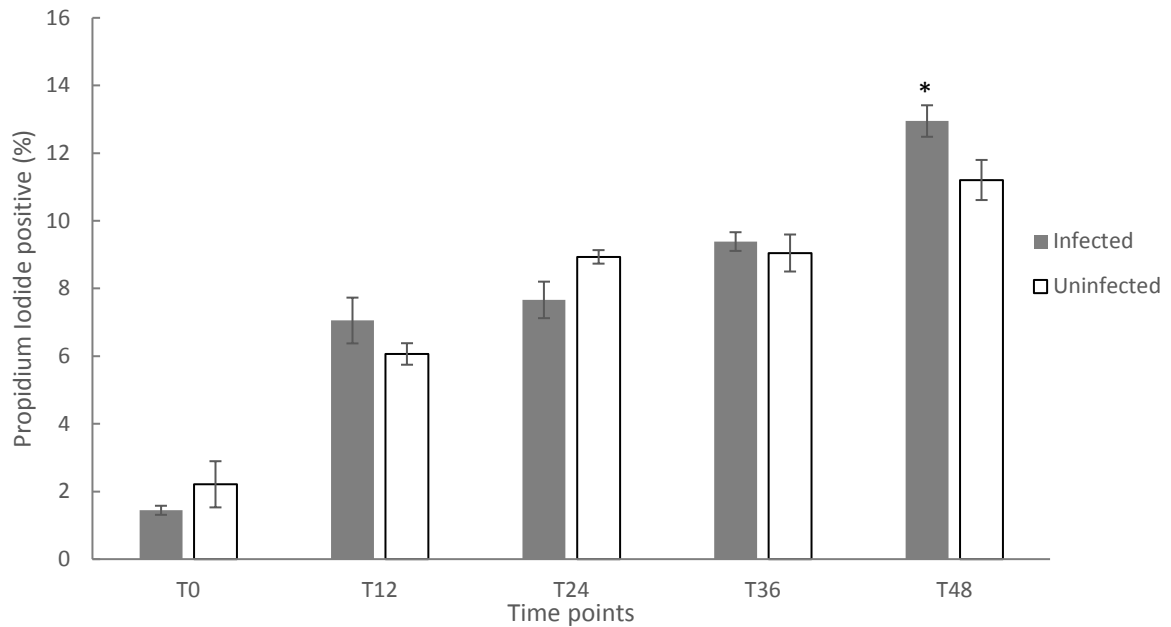


Figure 4.3.3.1 Comparison of PI-positive percent between *L. pneumophila*-infected and uninfected THP-1 cells. THP-1 cells obtained at various time points were stained with PI, and the signals were detected with a BD FACS Aria III flow cytometer. The data are presented as the percentage (%) of cells with PI-stained red fluorescence. The percentages in the *L. pneumophila*-infected and uninfected groups at each time point were compared with a paired *t*-test. A *p* value of less than 0.05 was considered to indicate statistical significance (*).

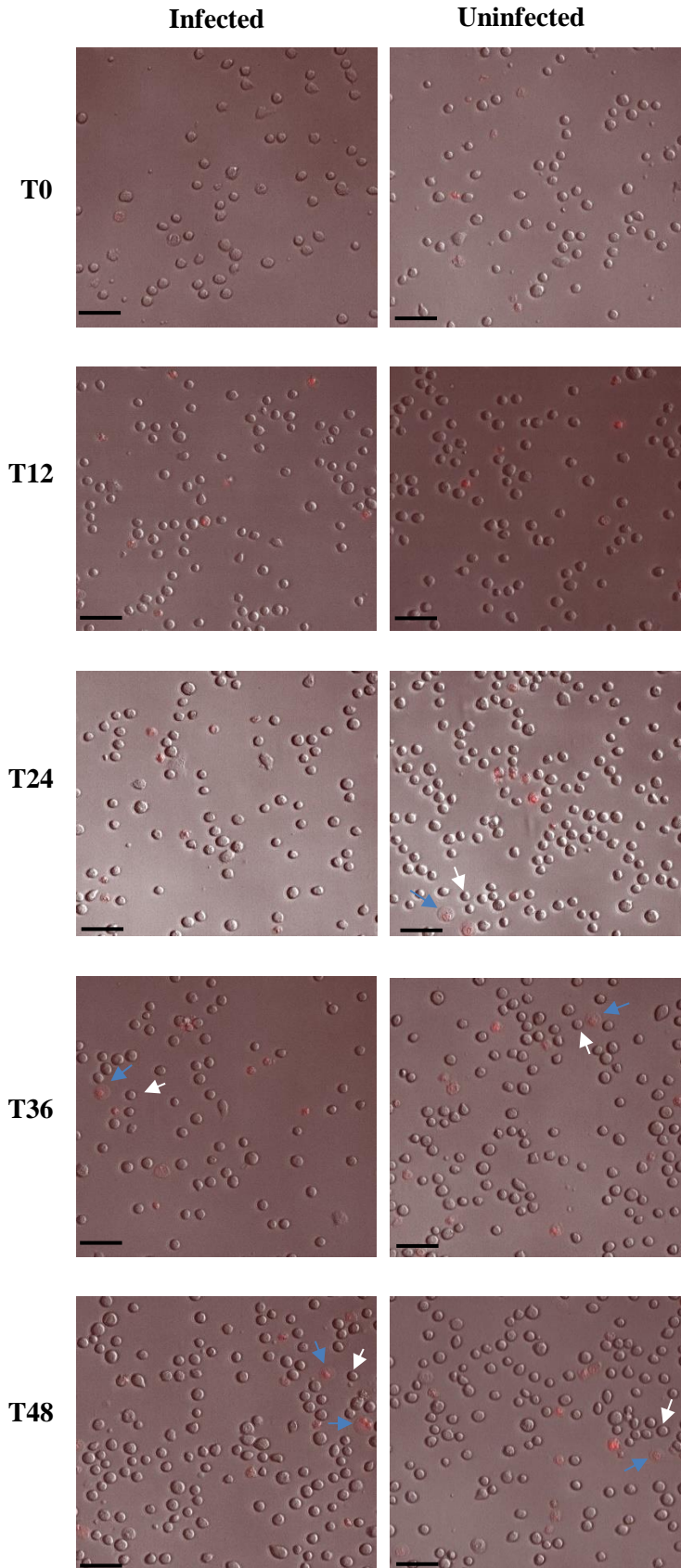


Figure 4.3.3.2 Microscopic examination of PI-stained THP-1 cells. A Nikon

Eclipse Ti inverted microscope was used to visualize the THP-1 cells stained with PI from T0 to T48. The left and right panels represent *L. pneumophila*-infected and uninfected THP-1 cells, respectively. Red fluorescence indicates PI-positive cells. Blue arrow indicates PI-positive cell with dilated morphology compared to some PI-negative cells (white arrows indicate). Bar – 50 μm .

Table 4.3.1. Summary of flow cytometry data of active caspase-1 staining, active caspase-3 staining, and PI staining in THP-1 cells. *L. pneumophila*-infected and uninfected THP-1 were compared at each time point with a paired *t*-test. A p value of less than 0.05 indicates a statistically significant (*) difference.

% of active caspase-1 stain positive				% of active caspase-3 stain positive			% of PI stain positive (cell death)		
Time point	Infected THP-1	Uninfected THP-1	p value	Infected THP-1	Uninfected THP-1	p value	Infected THP-1	Uninfected THP-1	p value
T0	1.88±0.21	1.52±0.23	0.149	0.6±0.21	0.7±0.4	0.371	1.4±0.4	2.2±2.05	0.250
T12	7.06±0.76	7.22±0.88	0.972	0.8±0.4	0.99±0.7	0.532	7.05±2.02	6.06±0.95	0.192
T24	8.52±0.64	10.5±0.47	0.015*	1.09±0.26	1.32±0.7	0.319	7.7±1.6	8.93±0.6	0.085
T36	11.6±0.44	11.05±1.1	0.491	0.96±0.38	0.96±0.5	0.977	9.4±0.8	9.05±1.6	0.489
T48	14.9±0.55	13.6±0.53	0.019*	1.07±0.4	0.86±0.2	0.088	12.9±1.4	11.2±1.78	0.031*

4.3.4 Cell death assay in *A. castellanii* cells

The results of PI staining in *A. castellanii* differed greatly from those in the THP-1 cells. The percentages of PI-positive *A. castellanii* were significantly higher in the *L. pneumophila*-infected groups than in the uninfected cells from T12 to T48 (Figure 4.3.4.1). The percentage of PI-positive *Acanthamoeba* increased rapidly from 1.53% at T0 to 10.9% at T12, 16.8% at T24, 22.6% at T36, and 39.3% at T48. In contrast to the uninfected group, the percentages of PI-positive *Acanthamoeba* varied from 1.1% to 4.65% from T0 to T48. The difference in the PI-positive percentages between the two groups was significant from T12 to T48 ($p = 0.017, 0.013, 0.003, \text{ and } 0.004$, respectively).

Figure 4.3.4.2 shows PI-positive *A. castellanii* cells with red fluorescence in both *L. pneumophila*-infected and uninfected groups. *L. pneumophila*-infected *A. castellanii* had more cells with red fluorescence than uninfected *A. castellanii* from T12 to T48. We also observed that PI-positive cells had reduced cell volume (white arrow indicates) compared with *A. castellanii* trophozoite cell (black arrow indicates) in both *L. pneumophila*-infected and uninfected groups. It was also shown that *A. castellanii* infected with *L. pneumophila* at T48 had cysts penetrated by PI (blue arrow indicates).

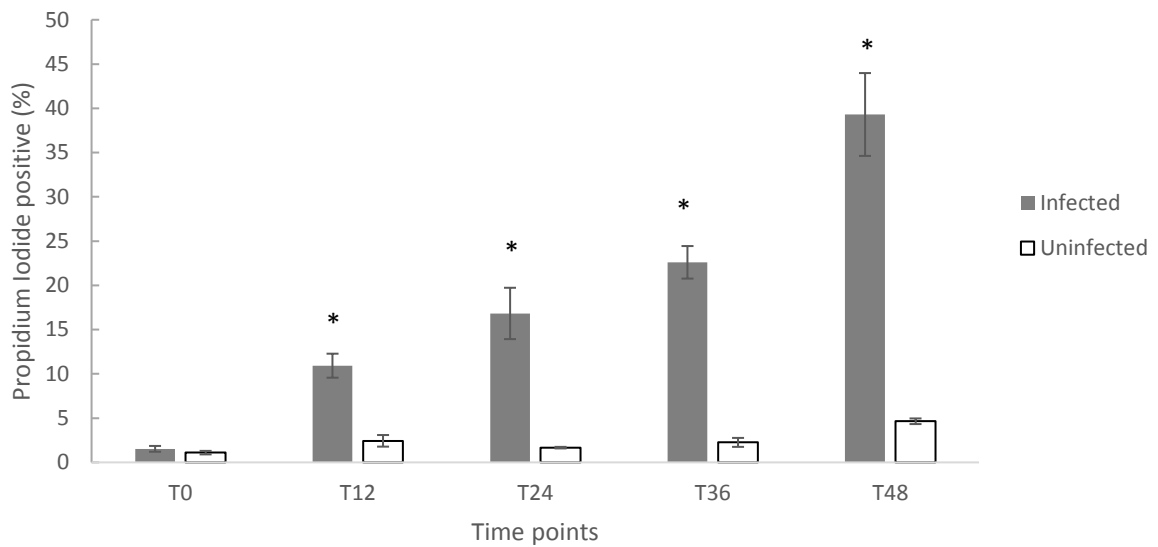


Figure 4.3.4.1 Comparison of PI-positive percent in *A. castellanii* cells between *L. pneumophila*-infected and uninfected groups. *A. castellanii* cells obtained at various time points were stained with PI, and the signals were detected with a BD FACS Aria III flow cytometer. The data are presented as the percentage (%) of PI-positive cells. The percentages in the *L. pneumophila*-infected and uninfected groups were compared at each time point with a paired *t*-test. A *p* value of less than 0.05 was considered to indicate statistical significance (*).

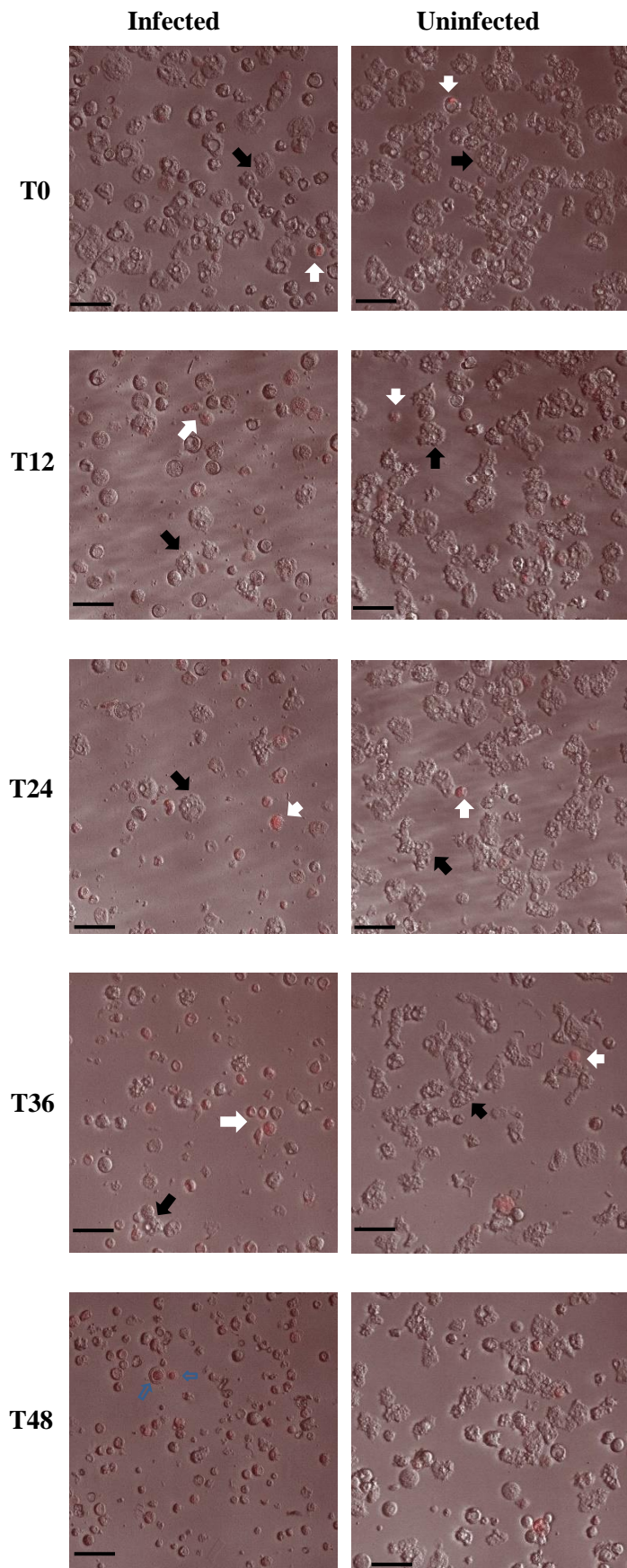


Figure 4.3.4.2 Microscopic examination of PI-stained *A. castellanii* cells. A Nikon Eclipse Ti inverted microscope was used to visualize the *A. castellanii* cells stained with PI from T0 to T48. The left and right panels represent *L. pneumophila*-infected and uninfected *A. castellanii*, respectively. Red fluorescence indicates PI-positive cells. White arrow indicates PI-positive cell, black arrow indicates trophozoite cell, and blue arrow indicates cyst stained with PI. Bar – 50 μm .

4.3.5 Microscopic observation of THP-1 and *A. castellanii* cell death when infected with gfp-transfected *L. pneumophila*

THP-1 and *A. castellanii* were challenged with gfp-transfected *L. pneumophila*, and the cells were then collected for PI staining. Figure 4.3.5 shows that THP-1 and *A. castellanii* cells infected with gfp-transfected *L. pneumophila* at T48 showed green fluorescence and simultaneously presented PI-positive cells that showed red fluorescence.

A. castellanii cells with both gfp-transfected *L. pneumophila* and PI penetration were observed (white arrow in upper panel of Figure 4.3.5), which suggests that *L. pneumophila* infection in *A. castellanii* could directly cause cell death. In contrast, THP-1 cells with gfp-transfected *L. pneumophila* cannot be penetrated by PI (yellow arrow in lower panel of Figure 4.3.5), which suggests that *L. pneumophila* infection could prevent membrane destruction in THP-1 cells. At the same time, THP-1 cells with red fluorescence showed no green fluorescence (blue arrow indicates), which suggests that THP-1 cell death was not caused by *L. pneumophila* infection.

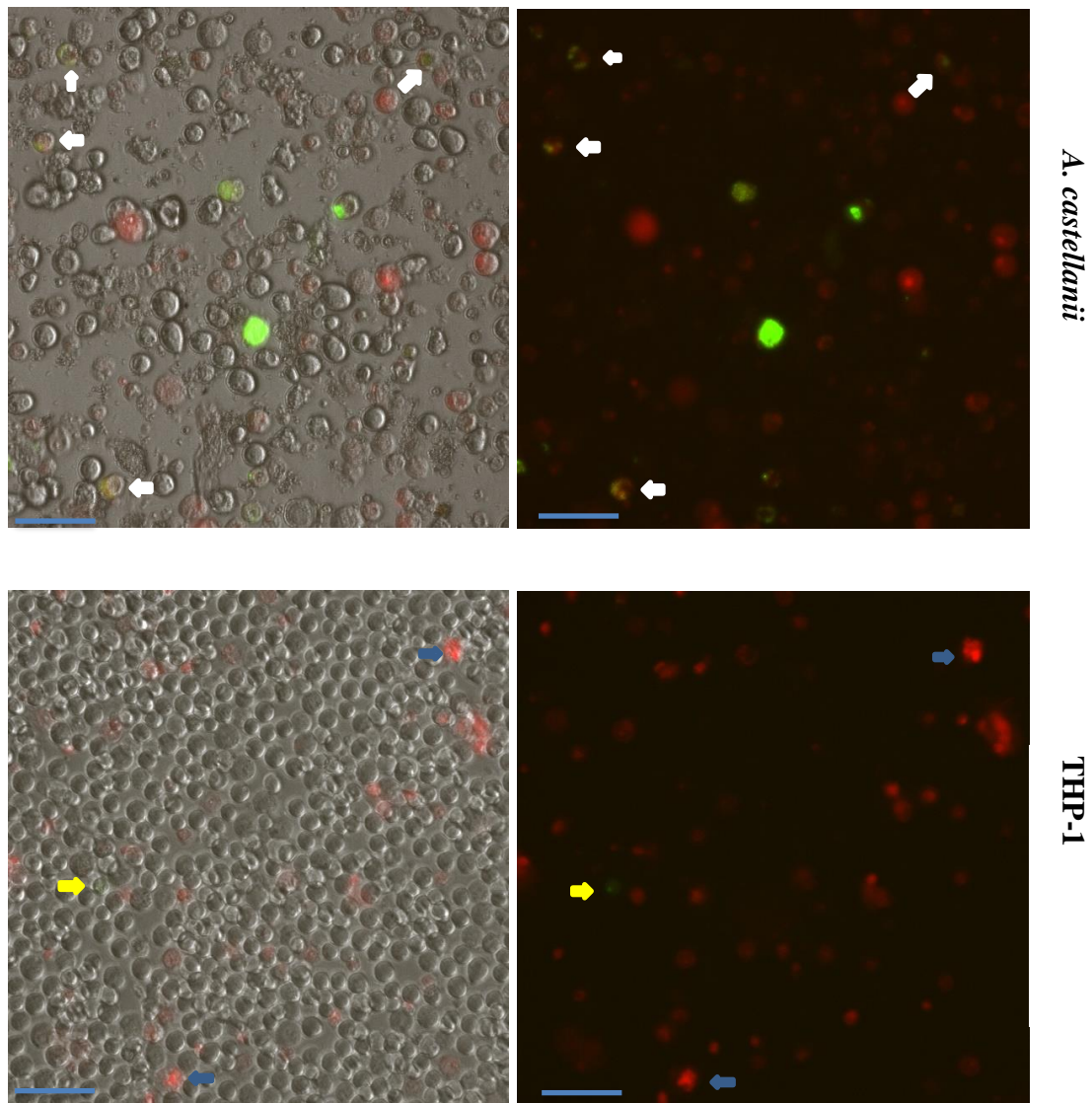


Figure 4.3.5 Microscopic examination of *gfp*-transfected *L. pneumophila*-infected *A. castellanii* and THP-1 at T48 that were stained with PI. An inverted confocal microscope (Nikon) was used to visualize *A. castellanii* and THP-1 infected with *gfp*-transfected *L. pneumophila* at T48 that were stained with PI. The upper and lower panels represent *gfp*-transfected *L. pneumophila*-challenged *A. castellanii* and THP-1, respectively. Green fluorescence indicates the presence of *gfp*-transfected *L. pneumophila*, and red fluorescence indicates PI-staining positive. Bar – 50 μ m.

4.4 Transcriptome of FACS-enriched *A. castellanii* infected with gfp-transfected *L. pneumophila*

4.4.1 Extracellular and intracellular growth of gfp-transfected *L. pneumophila*

4.4.1.1 Extracellular growth of gfp-transfected *L. pneumophila* in BYE broth

The gfp-transfected *L. pneumophila* grown in BYE broth showed a slight decline from T0 (7.01-log CFU per mL) to T12 (6.56-log CFU per mL) and then increased by more than 1-log from T12 to T24 (8-log CFU per mL). When grown in BYE broth, the number of gfp-transfected *L. pneumophila* peaked at T36 (8.1-log CFU per mL). No increase was seen in gfp-transfected *L. pneumophila* at T48 (7.55-log CFU per mL), and the bacteria from this phase were used to infect *A. castellanii*.

The *L. pneumophila* grown in BYE broth had a 2-log increase in the number of bacteria from T0 (8-log CFU per mL) to T36 (10-log CFU per mL) and then showed no further increase at T48 (9.6-log CFU per mL). When we compared growth in BYE broth between the wild-type *L. pneumophila* and gfp-transfected *L. pneumophila*, the duplication of gfp-transfected *L. pneumophila* showed about 2-log lower replication (Figure 4.4.1.1), but this could have been caused by a lower gfp-transfected *L. pneumophila* count at T0. Nevertheless, both bacterial strains entered the late stationary phase, which was considered to be more virulent and infectious, at T48.

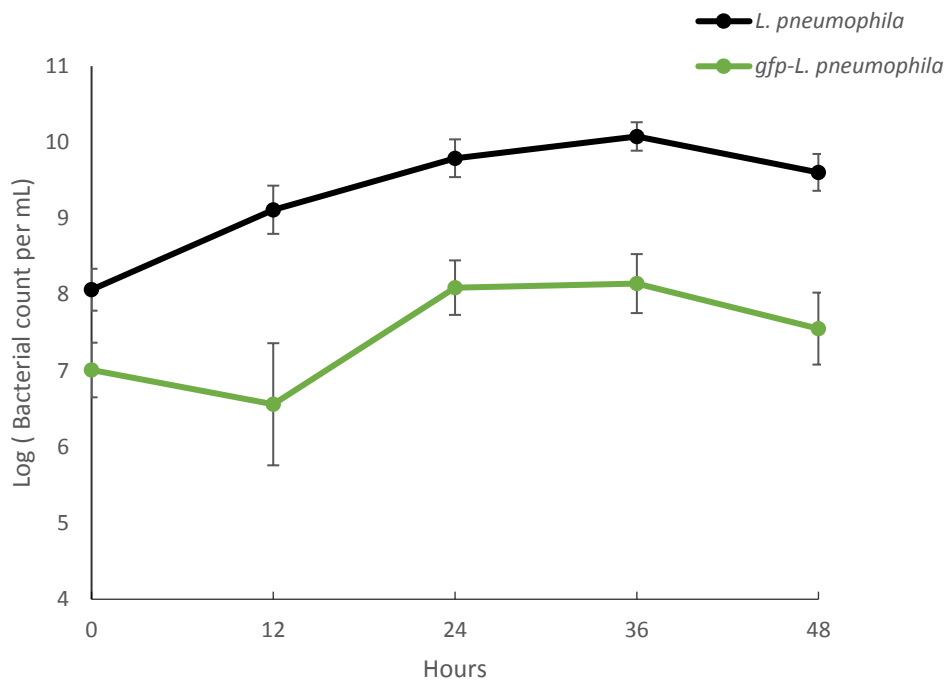


Figure 4.4.1.1 Extracellular growth of *L. pneumophila* and *gfp*-transfected *L.*

***pneumophila* in BYE broth.** *L. pneumophila* and *gfp*-transfected *L. pneumophila* were grown on α BCYE and α BCYE with chloramphenicol, respectively. The two bacterial strains were then inoculated in BYE broth and in BYE broth with chloramphenicol, respectively. The number of bacteria grown in broth was counted every 12 h from 0 to 48 h with a standard bacterial enumeration method.

4.4.1.2 Intracellular growth of gfp-transfected *L. pneumophila* in *A. castellanii*

L. pneumophila grown in *A. castellanii* underwent two cycles of intracellular growth: from T0 (5.2-log CFU per mL) to T24 (6.67-log CFU per mL) and from T24 to T48 (6.99-log CFU per mL) (Figure 4.1.2). Few *A. castellanii* cells were available at T48 to support further bacterial infection and growth (Figure 4.2.3) in the co-culture.

When gfp-transfected *L. pneumophila* was grown in *A. castellanii* co-culture, the number of bacteria peaked at T36 and reached the intracellular transmissive phase at T48 (Figure 4.4.1.2). The gfp-transfected *L. pneumophila* grown in *A. castellanii* showed less than 1-log growth from T0 (4.91-log CFU per mL) to T24 (5.58-log CFU per mL), and the number of bacteria increased further to 5.87-log CFU per mL at T36. The bacterial number showed no further increase at T48 (5.86-log CFU per mL). The *L. pneumophila* grown in *A. castellanii* in the late phase was considered to be more virulent and transmissive (Hammer et al. 2002). As a result, the gfp-transfected *L. pneumophila* grown in *A. castellanii* at T48 was collected for FACS enrichment and RNA sequencing.

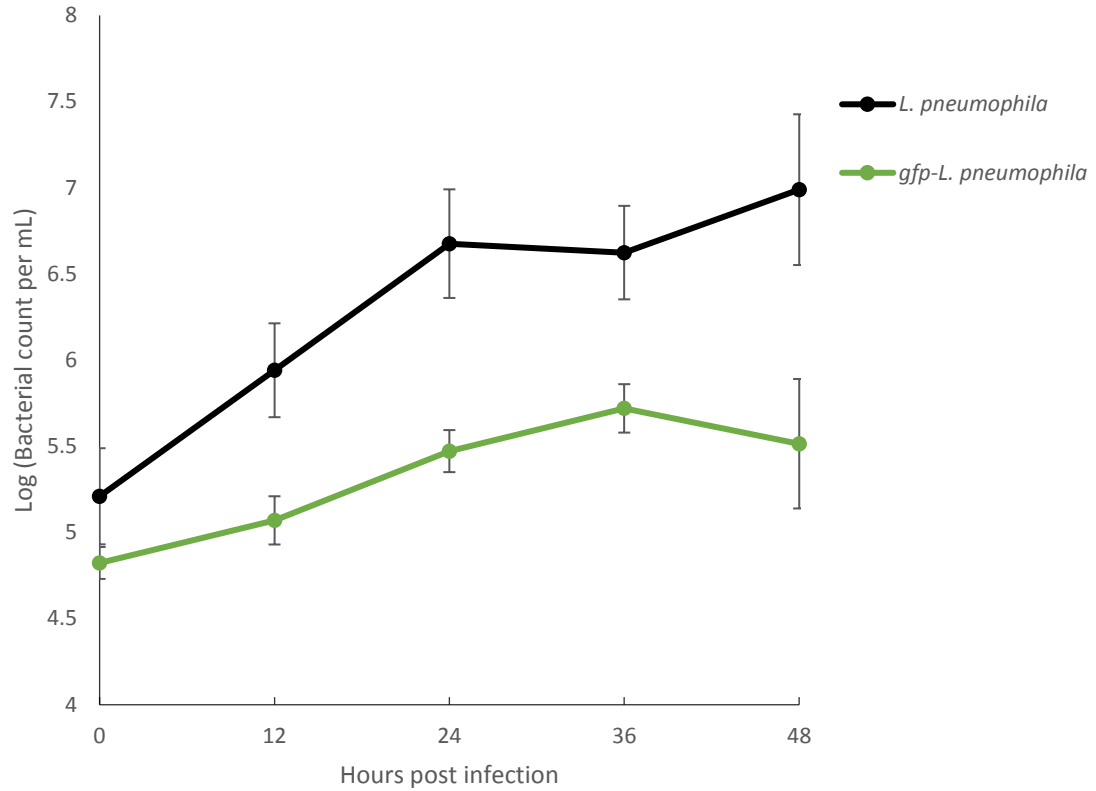


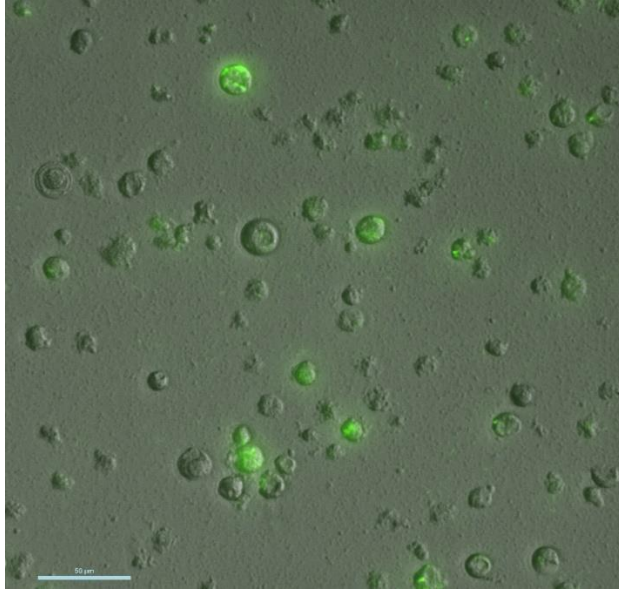
Figure 4.4.1.2 Intracellular growth curve of *L. pneumophila* and *gfp*-transfected *L. pneumophila* in *A. castellanii*. Co-culture of *A. castellanii* with *L. pneumophila* and *gfp*-transfected *L. pneumophila* was done at each time point. Bacteria grown in *A. castellanii* were released from the host cells every 12 h from 0 to 48 h and enumerated onto α BCYE with a standard plate count method.

4.4.1.3 Gfp-transfected *L. pneumophila*–infected *A. castellanii* in the transmissive phase was used for transcriptome analysis

L. pneumophila is widely known to have a biphasic life cycle (Hammer and Swanson 1999). When *L. pneumophila* reached the exponential growth phase, their major task was to duplicate themselves. They acquired nutrients from the living surroundings, but bacteria obtained in the post–exponential growth phase would be more virulent and transmissive (Byrne and Swanson 1998). Previous studies elucidated that *L. pneumophila* in the transmissive phase expressed many virulent traits (Bachman and Swanson 2004). As a result, the use of gfp-transfected *L. pneumophila* in the transmissive phase would be valuable to uncover the virulence and pathogenesis of this bacteria. The following bacterial transcriptome analysis was based on the comparison of *L. pneumophila*–infected *A. castellanii* with extracellular *L. pneumophila*. The *A. castellanii* transcriptome analysis was based on the contrast between *L. pneumophila*–infected *A. castellanii* and uninfected *A. castellanii*.

Figure 4.4.1.3 shows that the FACS-enriched *A. castellanii* co-culture (approximately 90% gfp-positive *A. castellanii*) had a higher proportion of *A. castellanii* infected with gfp-transfected *L. pneumophila* than the non-enriched infected *A. castellanii* (approximately 40% gfp-positive *A. castellanii*). FACS helped to eliminate the interference of extracellular bacteria and uninfected *A. castellanii* in co-culture.

Non-enriched gfp-transfected *L. pneumophila*-infected *A. castellanii* at T48



FACS-enriched gfp-transfected *L. pneumophila*-infected *A. castellanii* at T48

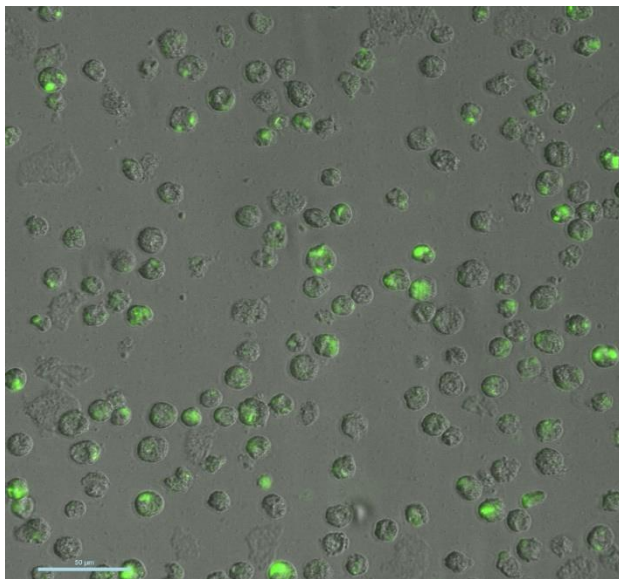


Figure 4.4.1.3 Non-enriched and FACS-enriched *A. castellanii* infected with gfp-transfected *L. pneumophila* at T48. *A. castellanii* co-culture with gfp-transfected *L. pneumophila* at T48 was collected for FACS by BD FACSAria III. Non-enriched and FACS-enriched co-culture were visualized with an inverted confocal microscope (Nikon). The upper and lower panels represent the non-enriched *L. pneumophila*-infected *A. castellanii* at T48 and the FACS-enriched *L. pneumophila*-infected *A. castellanii* at T48, respectively.

4.4.2 RNA sequencing information and alignment to reference genomes

When the reads were mapped to the *L. pneumophila Philadelphia* genome (NC_002942.5), 44,796,251 of 79,038,670 reads (56.7%) from the extracellular-grown gfp-transfected *L. pneumophila* and 6,803,944 of 86,120,934 reads (8%) from the FACS-enriched *L. pneumophila*-infected *A. castellanii* were respectively matched to the unique genomic locations of the bacterial reference genome. The reads of *L. pneumophila*-infected *A. castellanii* were matched to *L. pneumophila* and *A. castellanii* genomes, respectively.

When the readings were mapped to the *A. castellanii* Neff genome (NW_004457442.1), 7,282,551 of 111,144,916 reads (6.6%) from the FACS-enriched *L. pneumophila*-infected *A. castellanii* and 5,997,422 of 108,562,376 reads (5.5%) from the uninfected *A. castellanii* matched the unique genomic locations of the reference genome. Because this is the first transcriptome study of *A. castellanii* infected with gfp-transfected *L. pneumophila* with the use of RNA-sequencing, no reference exists to determine whether the low percent of mapping is normal. However, one transcriptome analysis between *A. castellanii* cysts and trophozoites presented 12.4% DEGs allocations (Moon et al. 2011b). *A. castellanii* activated only a small part of the genes from the genome to facilitate its differentiation activity from trophozoites to cysts. In this study, the *A. castellanii* cells could also activate a small part of the genome against *L. pneumophila* infection.

It was recommended that the optimal sequencing depth for Illumina RNA-sequencing for differential expression study ensure 5 million reads for bacterial genomes and 10 million reads for intermediate genomes like *Drosophila* (Encyclopedia of DNA Elements, ENCODE 2011 RNA-Seq Standards). The current dual RNA-sequencing profiles provided at least 20 million reads for sufficient sequencing depth (Westermann et al. 2017). According to the results, the sequencing depth for *L. pneumophila* and *A. castellanii* transcriptomes study reached the required standard.

After the read sequences were mapped to the reference genomes, the gene expression levels were calculated based on the RPKM (reads per kb bases per million reads) method (Mortazavi et al. 2008). *L. pneumophila gyrB* was used as reference gene, and *A. castellanii 18S rDNA* was used as reference gene. The FDR (false discovery rate) less than 0.001 was used to exclude those low-quality readings. The results showed that 729 genes were differentially expressed in *L. pneumophila*-infected *A. castellanii* compared with the extracellular *L. pneumophila* and that 1941 genes were differentially expressed in the *L. pneumophila*-infected *A. castellanii* compared with the uninfected *A. castellanii*.

4.4.3 Upregulated metabolism of *L. pneumophila* correlated with downregulated amino acid metabolism in *A. castellanii*

4.4.3.1 Gene ontology enrichment analysis of DEGs in the intracellular *L. pneumophila* and infected *A. castellanii* host

GO classified the DEGs into three categories: molecular function (MF), cellular component (CC), and biological process (BP). To determine the functions of DEGs, all DEGs were mapped to the terms in the GO database. There were 502 DEGs that mapped to *L. pneumophila* GO identity, and 1264 DEGs mapped to *A. castellanii* GO identity. Our GO enrichment analysis showed that most genes were upregulated in the intracellular *L. pneumophila* as compared with the extracellular *L. pneumophila*. In the GO enrichment analysis of DEGs of the intracellular *L. pneumophila*, the most enriched terms under MF, CC, and BP were “catalytic activity,” “cell,” and “metabolic process,” respectively (Figure 4.4.3.1). Among the three GO terms, “metabolic process” was dominant in the intracellular *L. pneumophila* (Figure 4.4.3.1).

For the *A. castellanii* host, most genes in the infected *A. castellanii* were downregulated as compared with the uninfected *A. castellanii*. In the GO enrichment analysis of DEGs of the infected *A. castellanii*, the most enriched terms under MF, CC, and BP were “ATP binding,” “cytoplasm,” and “translation,” respectively (Figure 4.4.3.2). The GO term “ATP binding” was the most enriched term in the infected *A. castellanii* (Figure 4.4.3.2).

Enriched GO of *L. pneumophila*-infected *A. castellanii* vs. extracellular *L. pneumophila*

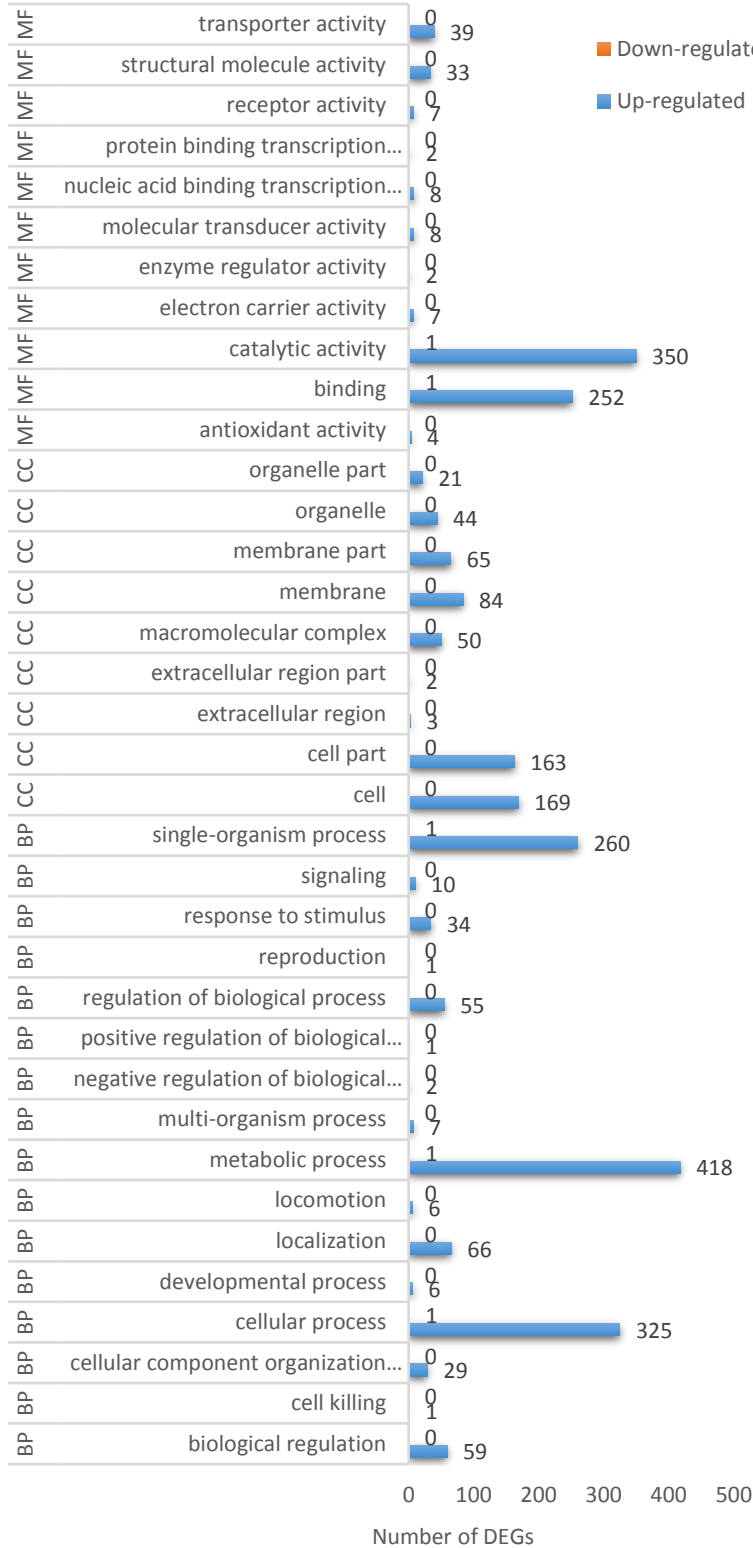


Figure 4.4.3.1 Enriched GO terms by comparing *L. pneumophila*-infected *A. castellanii* with extracellular *L. pneumophila*. Molecular function (MF), cellular component (CC), and biological process (BP) were the three major GOs. The enriched GO terms were generated by comparing gfp-transfected *L. pneumophila*-infected *A. castellanii* at T48 with extracellular-grown gfp-transfected *L. pneumophila* at T48. The number of upregulated and downregulated genes of intracellular *L. pneumophila* is also presented on the bar chart.

Enriched GO of *L. pneumophila*-infected *A. castellanii* vs. uninfected *A. castellanii*

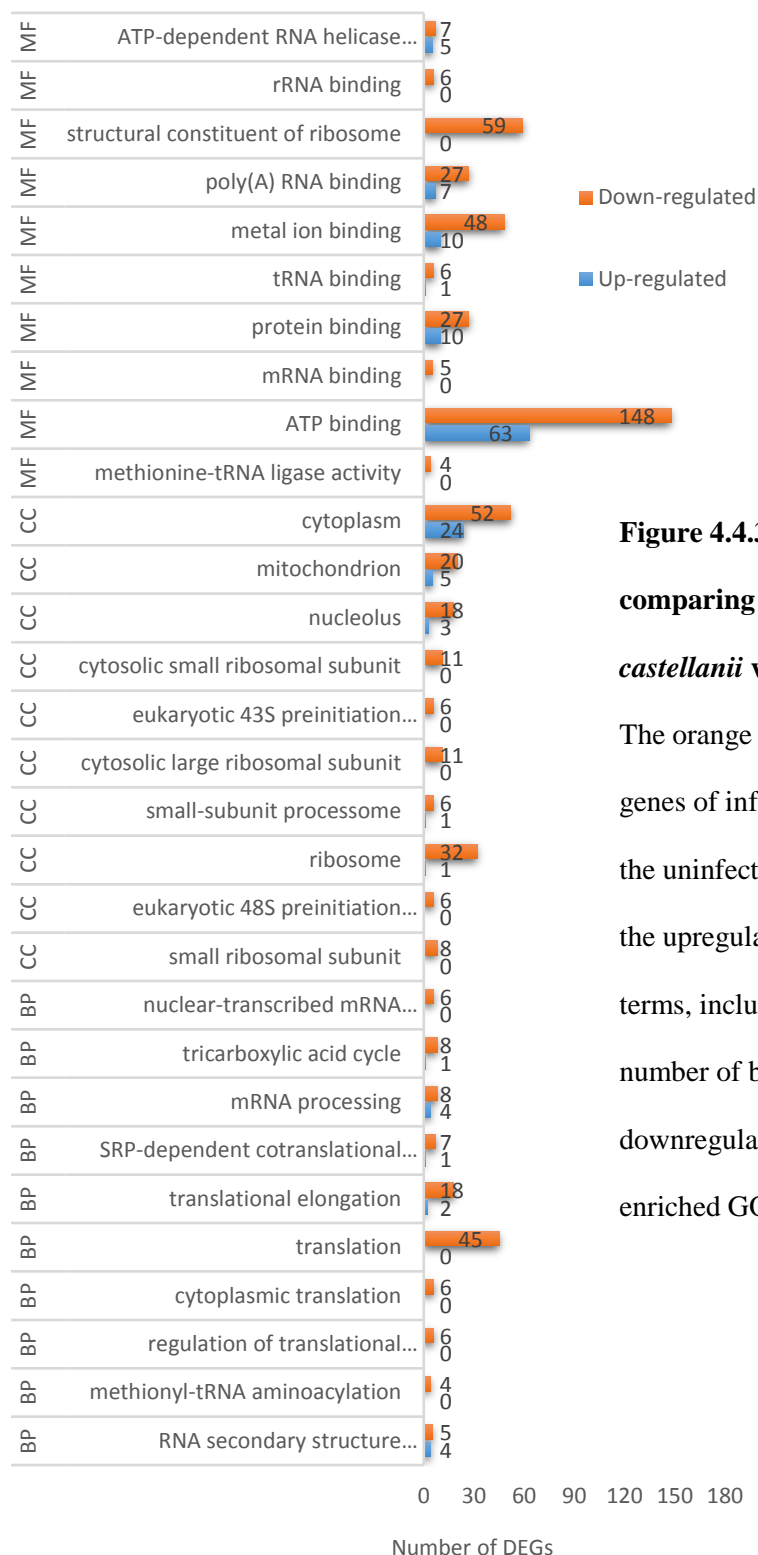


Figure 4.4.3.2 Enriched GO terms by comparing *L. pneumophila*-infected *A. castellanii* with uninfected *A. castellanii*.

The orange bar represents the downregulated genes of infected *A. castellanii* compared to the uninfected ones, and the blue bar represent the upregulated genes in the enriched GO terms, including MF, CC, and BP. The number of both upregulated and downregulated genes are presented on each enriched GO term.

4.4.3.2 Differentially regulated pathways in the intracellular *L. pneumophila* and *A. castellanii* host

Mapping of the DEGs to KEGG pathways (Nakao et al. 1999, Ogata et al. 1999) provides an idea about the functional relationship of a set of genes. There were 541 DEGs from the intracellular *L. pneumophila* and 894 from the infected *A. castellanii* that mapped to the terms in the KEGG database. The KEGG pathway enrichment analysis showed that the cysteine metabolism (ko00270) was differentially regulated in both intracellular *L. pneumophila* and infected *A. castellanii* (Figures 4.4.3.3 and 4.4.3.4). Figure 4.4.3.3 shows that the biosynthesis of serine and transformation from L-serine to L-cysteine were highly up-regulated in intracellular *L. pneumophila*. However, in infected *A. castellanii* the degradation of L-cysteine and L-methionine was down-regulated as shown in figure 4.4.3.4. The pathways were deduced from RNA sequencing reads aligned to KEGG allocation, this inspires further works to prove whether those marked genes function in the same way.

The figure 4.4.3.5 summarizes the key metabolism pathways that related to glycolysis, biosynthesis and degradation of amino acids in both infected *A. castellanii* and intracellular *L. pneumophila*. In infected *A. castellanii*, the production of glycine, citrate and phosphoribosyl pyrophosphate (PRPP) were up-regulated. However, the citrate cycle was inhibited in infected *A. castellanii*. The biosynthesis of amino acid threonine, both degradation and biosynthesis of lysine were up-regulated in infected *A. castellanii*. However, the degradation of serine and cysteine were inhibited in infected *A. castellanii*. In the intracellular *L. pneumophila*, phenylalanine biosynthesis was inhibited. However, the biosynthesis of alanine, histidine, lysine and tryptophan were

up-regulated in intracellular *L. pneumophila*. Furthermore, the glycolysis in intracellular *L. pneumophila* was highly activated from the dual RNA sequencing alignments (Figure 4.4.3.5).

L-cysteine is known to be an essential amino acid for the support of *L. pneumophila* growth (Pine et al. 1979). It has been demonstrated that intracellular *L. pneumophila* uses host cell amino acids during infection (Wieland et al. 2005). Both *L. pneumophila* and *A. castellanii* were reported to be auxotrophic to arginine, isoleucine, leucine, methionine and valine; and furthermore *L. pneumophila* was reported to be auxotrophic for cysteine and threonine (Best and Kwaik, 2018). Infected *A. castellanii* produced more threonine that could also be used by intracellular *L. pneumophila* (Figure 4.4.3.5). Serine has also been reported as the major amino acid consumed by intracellular *L. pneumophila* (Oliva et al. 2018). Intracellular *L. pneumophila* also had activated production of serine synthesized from glycine, which could be derived from the infected *A. castellanii* which limited self's catabolism of glycine (Figure 4.4.3.5).

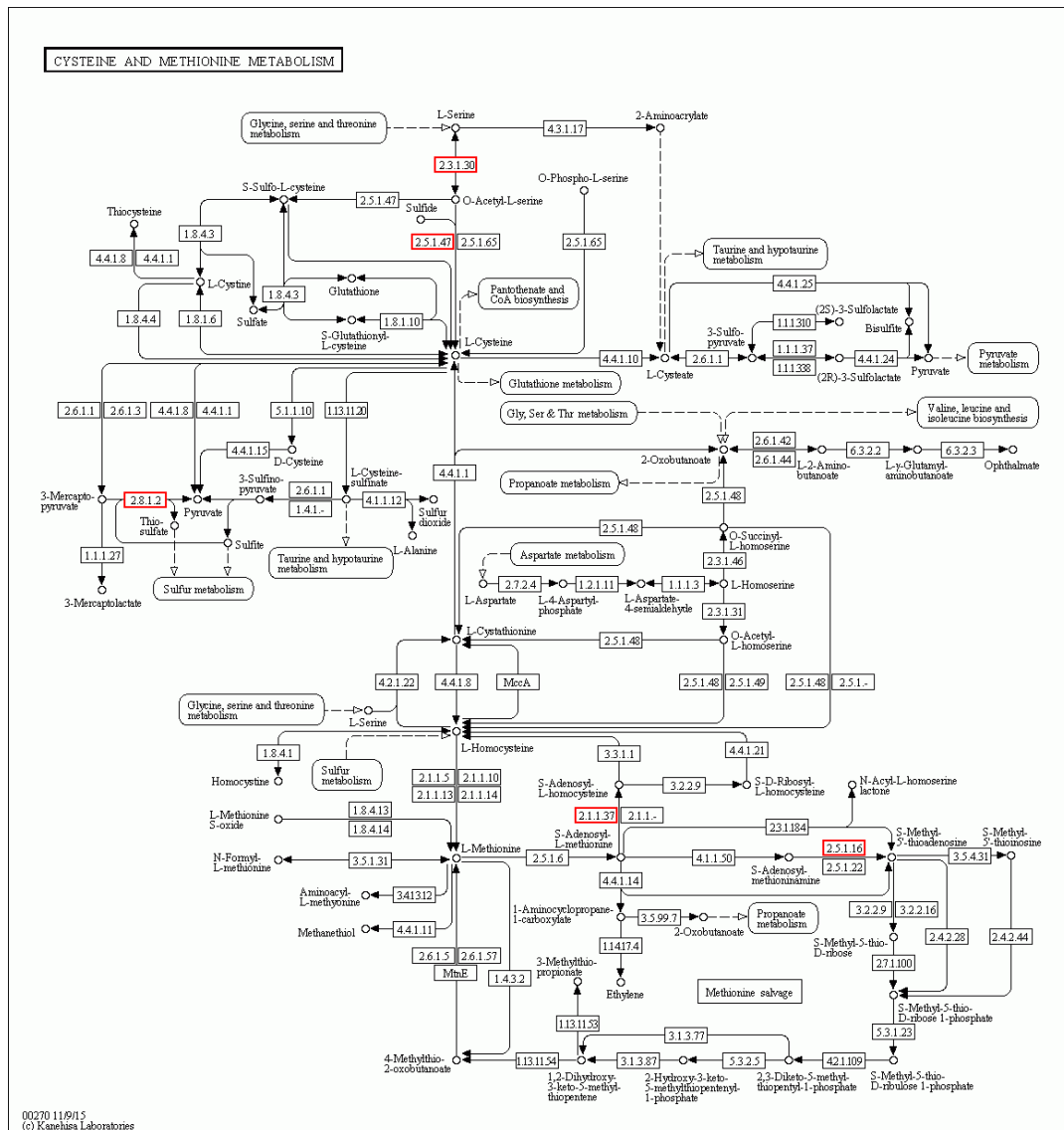


Figure 4.4.3.3 Enriched cysteine and methionine metabolism revealed upregulated *L. pneumophila* genes. The upregulated intracellular gfp-transfected *L. pneumophila* genes involved in cysteine and methionine metabolisms are labeled in red. Five bacterial genes (with KEGG enzyme alignments) were upregulated: *lpg0606* (EC 2.3.1.30 for serine acetyltransferase, 4.1- \log_2 ratio), *lpg0178* (EC 2.5.1.47 for acetylserine sulfhydrylase, 3.4- \log_2 ratio), *lpg2306* (EC 2.8.1.2 for β -mercapto pyruvate sulfur transferase, 2.9- \log_2 ratio), *lpg1236* (EC 2.1.1.37 for methyltransferase, 1.4- \log_2 ratio), and *lpg0690* (EC 2.5.1.16 for spermidine synthase, 1.3- \log_2 ratio).

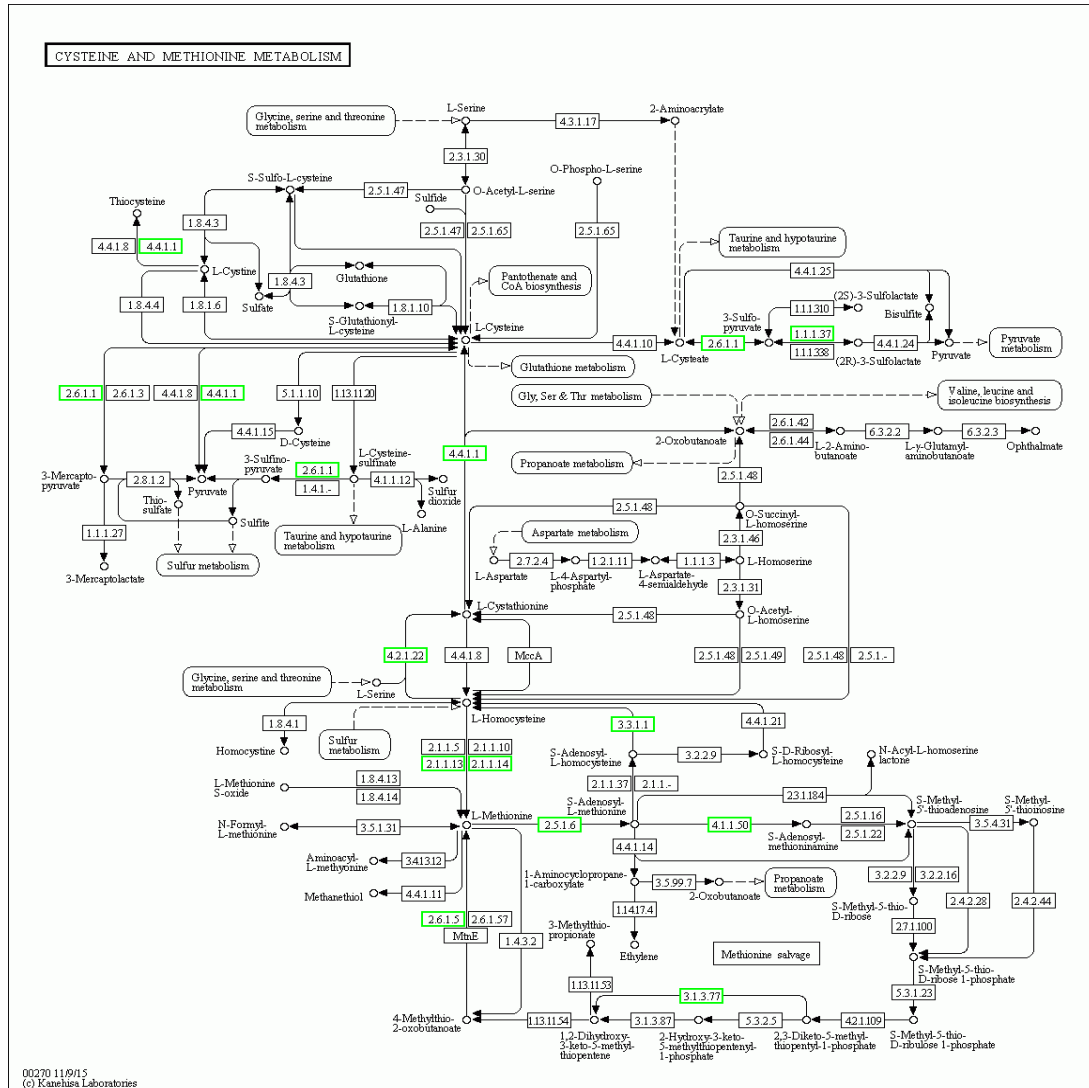


Figure 4.4.3.4 Downregulated genes of infected *A. castellanii* in cysteine and methionine metabolism. The downregulated genes in infected *A. castellanii* are labeled in green, and the log₂ ratio of genes (with KEGG enzyme alignments) are presented: *14920058* (EC 4.4.1.1 for cysteine desulfhydrase): -5.58; *14926712* (EC 2.6.1.1 for transaminase): -2.65; *14925099* (EC 1.1.1.37 for malate dehydrogenase): -4.28; *14911994* (EC 4.2.1.22 for serine sulfhydrylase): -3.02; *14921544* (EC 3.3.1.1 for adenosylhomocysteine hydrolase): -8.26; *14918298* (EC 2.1.1.13 for methyltransferase): -2.43; *14915670* (EC 2.1.1.14 for homocysteine transmethylase): -6.48; *14913646* (EC 2.5.1.6 for methionine adenosyltransferase): -2.57; *14916546* (EC 4.1.1.50 for adenosylmethionine decarboxylase): -4.02; *14921984* (EC 2.6.1.5 for tyrosine transaminase): -4.02; and *14914823* (EC 3.1.3.77 for acireductone synthase): -4.02.

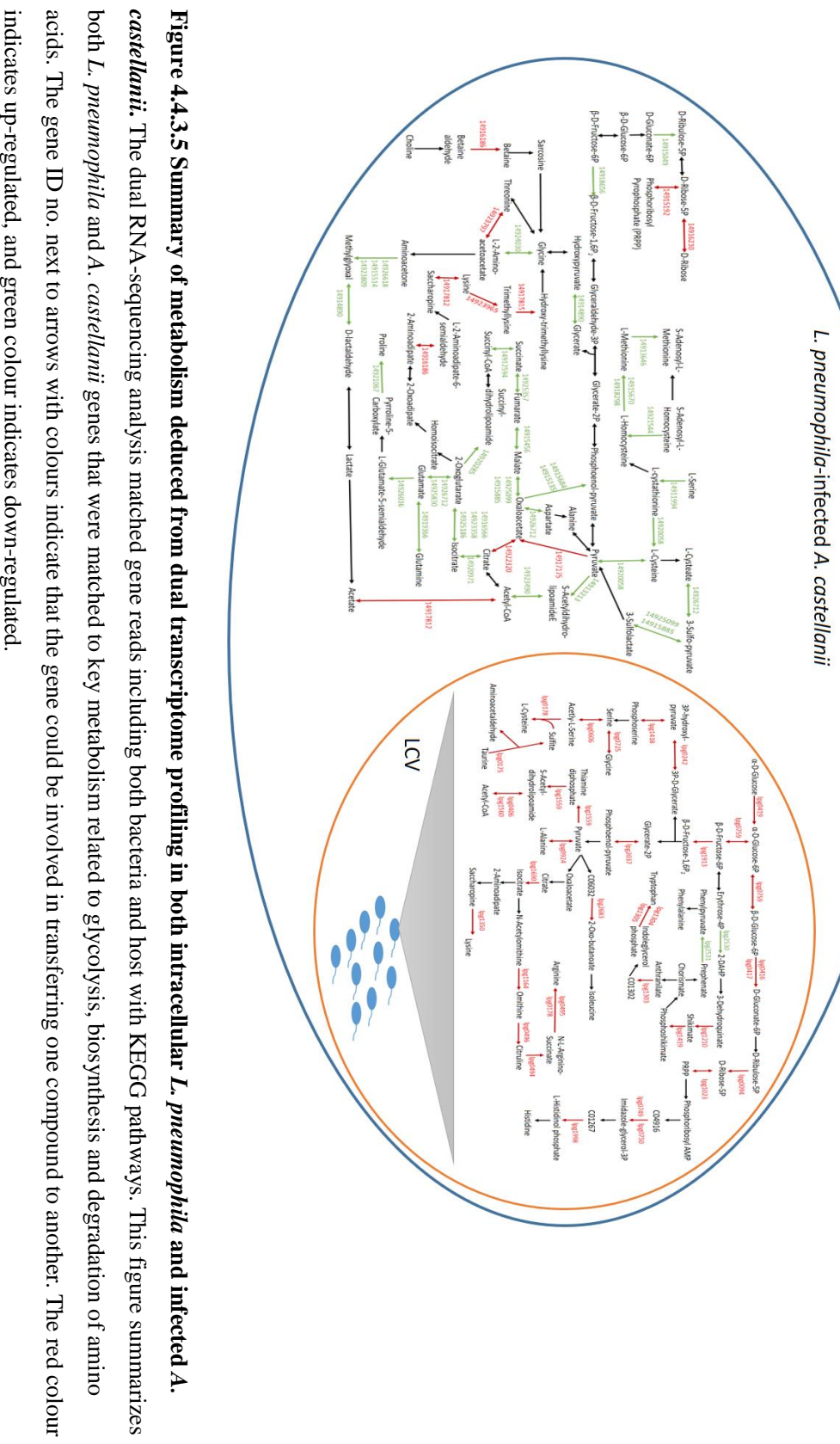


Figure 4.4.3.5 Summary of metabolism deduced from dual transcriptome profiling in both intracellular *L. pneumophila* and infected *A. castellanii*. The dual RNA-sequencing analysis matched gene reads including both bacteria and host with KEGG pathways. This figure summarizes both *L. pneumophila* and *A. castellanii* genes that were matched to key metabolism related to glycolysis, biosynthesis and degradation of amino acids. The gene ID no. next to arrows with colours indicate that the gene could be involved in transferring one compound to another. The red colour indicates up-regulated, and green colour indicates down-regulated.

4.4.4 Enriched KEGG pathway in gfp-transfected *L. pneumophila*-infected *A. castellanii*

The DEGs were subjected to GO functional classification and KEGG pathway analysis. The KEGG pathways were analyzed based on the allocation of DEGs in the pathogen and in the host. The p value was generated with a hypergeometric test, and a p value of less than 0.05 was considered to indicate statistical significance. Tables 4.4.1 and 4.4.2 present the most enriched pathways in intracellular *L. pneumophila* and in infected *A. castellanii*, respectively.

In the KEGG analysis, the most enriched pathway of *L. pneumophila* was ribosome, followed by flagella biosynthesis, which was associated with *L. pneumophila* virulence and differentiation (Heuner et al. 1997, Ren et al. 2006). In both the bacteria and the host cell, the most-enriched pathways were involved in ribosomal protein synthesis.

In addition to ribosome biosynthesis and flagella assembly, metabolism-related pathways were involved in nucleic acid synthesis (RNA polymerase, pyrimidine, and purine metabolism) and carbohydrate metabolism (glycolysis, pentose phosphate pathway, and ascorbate metabolism), which were highly enriched in the intracellular *L. pneumophila* (Table 4.4.1). Pentose phosphate pathway can transfer ribose-5-phosphate into phosphoribosyl pyrophosphate that can further be used in purine,

pyrimidine and histidine metabolisms. Those metabolisms were also considered to extract carbon and energy sources for intracellular *L. pneumophila* (Oliva et al. 2018).

The metabolism pathways within *L. pneumophila*-infected *A. castellanii*, including citrate cycle, pyruvate metabolism, and amino acid metabolisms, were significantly enriched. The enriched pathways involved in ribosome activity and metabolisms were anticipated in the infected *A. castellanii* and could be induced by intracellular bacterial growth. The enriched pathway of cardiac muscle contraction also showed significance (Table 4.4.2), and this pathway was involved in actin and myosin rearrangement. The involvement of cellular filament protein contraction in bacterial intracellular growth remains a mystery. It has been revealed that the host cell actin rearrangement can promote bacterial internalization (Zhou et al. 2001). The amoeba (*Dictyostelium*) actin was reported to contribute to *L. pneumophila* uptake and bacterial delivery (Lu and Clarke 2005).

Table 4.4.1 Top 10 enriched KEGG pathways by comparing FACS-enriched gfp-transfected *L. pneumophila*-infected *A. castellanii* with extracellular *L. pneumophila* at T48

Pathway	DEGs with pathway annotation (541)	All genes with pathway annotation (1037)	P-value	Q-value	Pathway ID
Ribosome	44 (8.13%)	59 (5.69%)	2.47E-04	3.17E-02	ko03010
Flagellar assembly	14 (2.59%)	17 (1.64%)	9.80E-03	4.06E-01	ko02040
Metabolic pathways	203 (37.52%)	355 (34.23%)	1.16E-02	4.06E-01	ko01100
Glycolysis / Gluconeogenesis	15 (2.77%)	19 (1.83%)	1.49E-02	4.06E-01	ko00010
Pentose phosphate pathway	13 (2.4%)	16 (1.54%)	1.59E-02	4.06E-01	ko00030
Pyrimidine metabolism	31 (5.73%)	46 (4.44%)	2.39E-02	5.10E-01	ko00240
Purine metabolism	38 (7.02%)	59 (5.69%)	3.49E-02	5.45E-01	ko00230
Ascorbate and aldarate metabolism	5 (0.92%)	5 (0.48%)	3.83E-02	5.45E-01	ko00053
RNA polymerase	5 (0.92%)	5 (0.48%)	3.83E-02	5.45E-01	ko03020
Pentose and glucuronate interconversions	7 (1.29%)	8 (0.77%)	4.51E-02	5.78E-01	ko00040

Table 4.4.2 Top 10 enriched KEGG pathways by comparing FACS-enriched gfp-transfected *L. pneumophila*-infected *A. castellanii* with uninfected *A. castellanii* at T48

Pathway	DEGs in term (1251)	All gene in term (7525)	P-value	Q-value	Pathway ID
Ribosome	62 (4.96%)	101 (1.34%)	2.52E-24	7.12E-22	ko03010
Citrate cycle (TCA cycle)	22 (1.76%)	39 (0.52%)	1.74E-08	2.46E-06	ko00020
Aminoacyl- tRNA biosynthesis	21 (1.68%)	56 (0.74%)	1.36E-04	1.19E-02	ko00970
Pyruvate metabolism	19 (1.52%)	49 (0.65%)	1.68E-04	1.19E-02	ko00620
Carbon metabolism	36 (2.88%)	130 (1.73%)	9.49E-04	5.22E-02	ko01200
Biosynthesis of amino acids	29 (2.32%)	99 (1.32%)	1.11E-03	5.22E-02	ko01230
Arginine and proline metabolism	15 (1.2%)	45 (0.6%)	4.58E-03	1.84E-01	ko00330
beta-Alanine metabolism	12 (0.96%)	34 (0.45%)	6.48E-03	2.28E-01	ko00410
Ribosome biogenesis in eukaryotes	31 (2.48%)	122 (1.62%)	8.35E-03	2.62E-01	ko03008
Cardiac muscle contraction	7 (0.56%)	16 (0.21%)	9.85E-03	2.78E-01	ko04260

4.4.4.1 Pathway of ribosomal protein biosynthesis in gfp-transfected *L. pneumophila*–infected *A. castellanii*

Figures 4.4.4.1 and 4.4.4.2 present the most enriched ribosome biosynthesis pathways in intracellular *L. pneumophila* and infected *A. castellanii*, respectively. In *L. pneumophila*, most genes involved in the biosynthesis of large and small ribosomal subunits were upregulated (Figure 4.4.4.1), which suggests that intracellular *L. pneumophila* translation activity could be activated.

However, most genes involved in ribosome biosynthesis in the infected *A. castellanii* were downregulated (Table 4.4.5), including the large and small ribosomal subunits (Figure 4.4.4.2). This indicates inhibited translation in *L. pneumophila*–infected *Acanthamoeba*. The inhibition of ribosomal biosynthesis indicates that the *L. pneumophila*–infected *A. castellanii* could be in a repressed state.

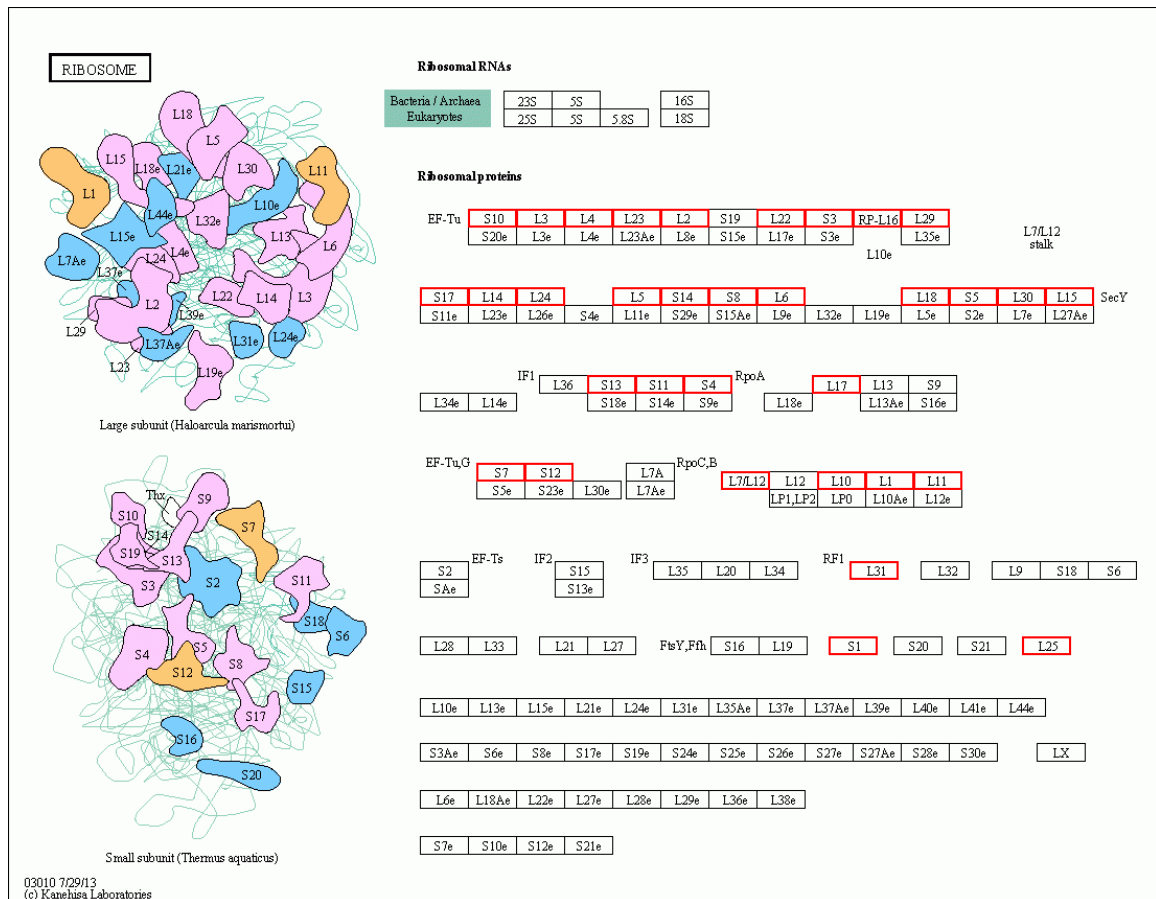


Figure 4.4.4.1 Ribosomal protein biosynthesis pathway enriched in intracellular *L. pneumophila* transcriptome analysis. DEGs were annotated to the KEGG pathway analysis. *L. pneumophila* ribosome biosynthesis was the most enriched, and the genes involved were upregulated (labeled in red). The eight most upregulated genes were *rplK* encoding 50S ribosomal protein L11 (lpg0318, 4.6- \log_2 ratio), *rpsJ* encoding 30S ribosomal protein S10 (lpg0328, 4.2- \log_2 ratio), *rplJ* encoding 50S protein L10 (lpg0320, 4- \log_2 ratio), *rplW* encoding 50S protein L23 (lpg0331, 3.8- \log_2 ratio), *rpsN* encoding 30S protein S14 (lpg0342, 3.7- \log_2 ratio), *rplL* encoding 50S protein L7/L12 (lpg0321, 3.6- \log_2 ratio), *rplD* encoding 50S protein L4 (lpg0330, 3.5- \log_2 ratio), and *rplA* encoding 50S protein L1 (lpg0319, 3.4- \log_2 ratio).



Figure 4.4.2 Ribosomal protein biosynthesis pathway of infected *A. castellanii* from transcriptome analysis. From the DEG annotation in infected *Acanthamoeba*, the most-enriched pathway is ribosome biosynthesis. Most genes involved were downregulated (labeled in green), except the putative *Rpl7A* encoding ribosomal protein (14915188, 1.2- \log_2 ratio). The ten most downregulated genes related to ribosomal protein were 14924264 encoding L35 (-9- \log_2 ratio), 14914629 encoding S4 (-8.1- \log_2 ratio), 14926214 encoding S8e (-8- \log_2 ratio), 14923544 encoding S10p/S20e (-7.3- \log_2 ratio), 14913021 encoding S27 (-7.2- \log_2 ratio), 14926158 encoding L4/L1 family protein (-6.8- \log_2 ratio), 14926793 encoding eukaryotic L18 (-6.6- \log_2 ratio), 14925005 encoding 60S acidic ribosomal protein (-6.6- \log_2 ratio), 14917001 encoding 60S protein L23 (-6.3- \log_2 ratio), and 14915869 encoding 40S ribosomal protein S3a (-6.2- \log_2 ratio).

4.4.4.2 *L. pneumophila* flagellar assembly

The intracellular *L. pneumophila* flagellar assembly was the second most-enriched pathway. From the KEGG pathway, eight bacterial virulence genes were upregulated (Figure 4.4.4.3), of which seven (*flgB*, *C*, *D*, *E*, *G*, *H* and *I*) were known to be involved in the construction of bacterial flagellar hooks. This finding indicates the activated biosynthesis of *L. pneumophila* flagella when grown in *A. castellanii* in the late phase. *L. pneumophila motAB* were reported to be ion channels that could generate the power to rotate, and the second encoding operon of *motAB* (*motA2B2*) has also been reported (Appelt and Heuner 2017); the roles of *motAB* are still under discussion.

The biosynthesis of *L. pneumophila* flagella occurs in a highly regulated order (Schulz et al. 2008), The *flgBCDEGHI* construct the class II of the flagellum, and the *motAB* belong to class III of *L. pneumophila* flagella, whose construction is followed by that of the class II structures. All class II flagellum genes were upregulated, which implies that the pathway of *L. pneumophila* flagellum biosynthesis was triggered during the transmissive phase.

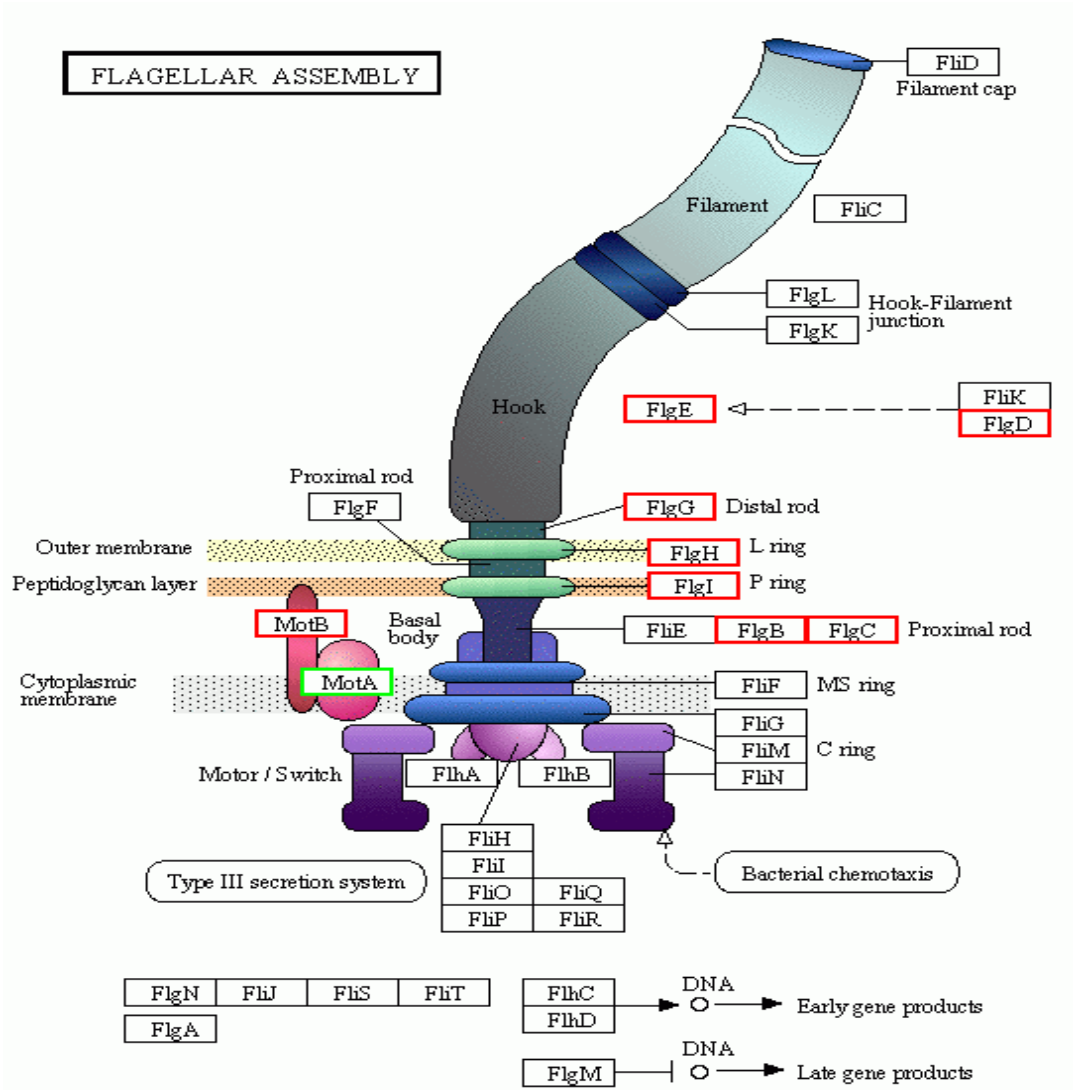


Figure 4.4.4.3 *L. pneumophila* flagellar assembly was highly induced in *gfp*-transfected *L. pneumophila*-infected *A. castellanii*. Eight virulence factors (labeled in red) were upregulated, and only *motA* (labeled in green) was downregulated (-2.5- \log_2 ratio). The upregulated genes are *flgB* (1.8- \log_2 ratio), *flgC* (2.3- \log_2 ratio), *flgD* (3.6- \log_2 ratio), *flgE* (1- \log_2 ratio), *flgG* (1.7- \log_2 ratio), *flgH* (2.1- \log_2 ratio), *flgI* (1.9- \log_2 ratio), and *motB* (1.4- \log_2 ratio).

4.4.4.3 Citrate cycle in infected *A. castellanii*

Figure 4.4.4.4 shows the DEGs involved in the enriched citrate cycle (also known as the tricarboxylic acid cycle) pathway from the *L. pneumophila*-infected *A. castellanii* transcriptome. Of the 22 DEGs involved in the citrate cycle, 16 were downregulated. Of the six upregulated genes, the most upregulated gene (*I4917823*, 3.17- \log_2 ratio) was encoding the putative aconitase involved in reversible isomerization of citrate. The most downregulated *A. castellanii* genes were encoding putative isocitrate dehydrogenase (KEGG enzyme EC1.1.1.42; *I4923358*, -6.3- \log_2 ratio; *I4925186*, -6- \log_2 ratio; and *I4916566*, -4.6- \log_2 ratio). Isocitrate dehydrogenase is known for its simultaneous involvement in the oxidation of isocitrate and the generation of reduced nicotinamide adenine dinucleotide, which can further be used for mitochondrial ATP production. The inhibited energy generation seen in the infected *A. castellanii* could be the response against bacterial infection.

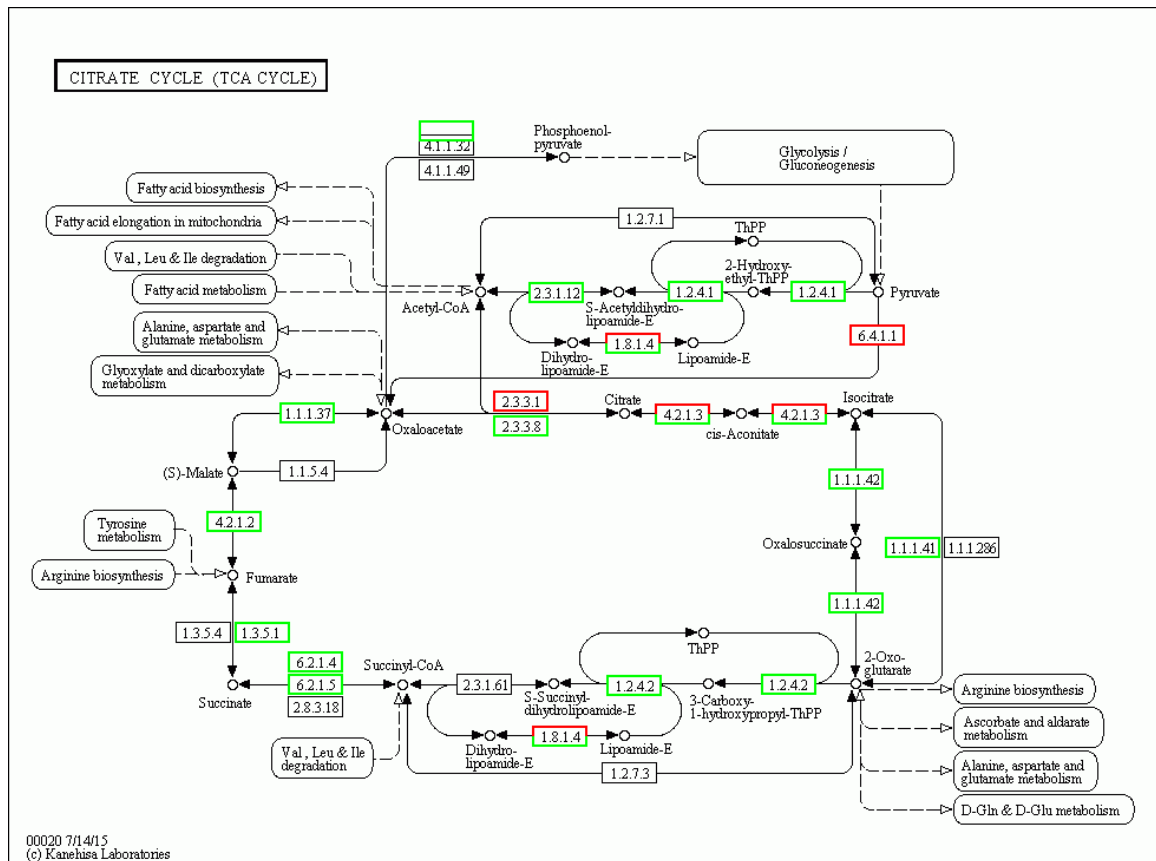


Figure 4.4.4.4 DEG annotation in citrate cycle pathway from infected *A. castellanii* transcriptome analysis. Most genes were downregulated during the citrate cycle (also called the tricarboxylic acid cycle). KEGG enzyme classification numbers are shown in the pathway. Upregulated genes are labeled in red, and downregulated genes are labeled in green.

4.4.5 DEG annotation of gfp-transfected *L. pneumophila*–infected *A. castellanii*

4.4.5.1 *L. pneumophila* DEGs grown in *A. castellanii* during transmissive phase

From the DEG annotation (Tables 4.4.3 and 4.4.4) calculated with the RPKM (reads per kb per million) method, bacterial *pvcA* (*lpg0174*, 6.98- \log_2 ratio), *pvcB* (*lpg0175*, 8.2- \log_2 ratio), and putative *pvcC* (*lpg0176*, 7.37- \log_2 ratio) genes were highly upregulated in intracellular *L. pneumophila*. A transcriptome analysis by Faucher et al. (2011) also uncovered the upregulation of *pvcA* and *pvcB* genes in *L. pneumophila* grown in macrophages (Faucher et al. 2011). The role of *pvc* genes of *L. pneumophila* in macrophages is unknown. No study has yet revealed the functional role of the *pvc* genes of *L. pneumophila* when grown in amoebas and macrophages.

From the DEG allocation in the KEGG pathways analysis, *L. pneumophila* enzyme encoded by *pvcA* (acted as monooxygenase, EC1.14.14.1) was shown to be involved in fatty acid degradation, tryptophan metabolism, and aminobenzoate degradation for microbial metabolism in diverse environments. These pathways of *L. pneumophila* could explain their ability to persist and survive in different environments by using various carbon and energy sources (Ehrhardt and Rehm 1985, Shinoda et al. 2004). *pvcB* encoding enzyme that was involved in lysine degradation and sulfur metabolism (Figure 4.4.5). Taurine can be catalyzed to sulfite with the *L. pneumophila pvcB* encoded enzyme (acted as taurine dioxygenase, EC 1.14.11.17), and sulfite can then be used to synthesize L-cysteine. *pvcC* encoded 3-propionate hydroxylase (EC 1.14.13.127, family of oxidoreductases) that was involved in phenylalanine metabolism. The DEG allocation in the KEGG pathway analysis revealed that the *pvc*

gene clusters (*pvcA*, *pvcB*, and *pvcC*) were related to microbial amino acid metabolism, which also suggests that *L. pneumophila* can survive in different host cells, including *A. castellanii*.

In addition to *pvc* genes, the most downregulated gene *tnpA* (*lpg1086*, -12.48- \log_2 ratio) in *L. pneumophila* grown in *A. castellanii* has been poorly explored. No study has yet examined the role of *L. pneumophila tnpA* in host cells, but it has been revealed that *tnpA* encoded transposase that may be involved in homologous recombination and gene repair in bacteria (De Palmenaer et al. 2008). The inhibition of *L. pneumophila tnpA* may be due to its survival in *A. castellanii*, which may trigger genetic modification of *L. pneumophila*.

L. pneumophila legK3 (*lpg2556*, -3.89- \log_2 ratio) was also highly downregulated, and *legK3* encoded the eukaryote-like serine/threonine protein kinase that could be involved in the activation of host cell transcriptional factor (Haenssler and Isberg 2011). The inhibition of *L. pneumophila legK3* indicates the repressed modification of *A. castellanii* host transcriptional activity during the late stage.

Table 4.4.3 Top 10 upregulated genes of intracellular *L. pneumophila* from transcriptome analysis. The RNA-sequencing DEGs analysis was based on comparing FACS-enriched gfp-transfected *L. pneumophila*-infected *A. castellanii* (Intra-Lp) with extracellular grown *L. pneumophila* (Extra-Lp). Both p value and FDR (False discovery rate) were less than 0.001 for the 10 DEGs.

Gene	Intra-Lp coverage	Extra-Lp coverage	Intra-Lp RPKM	Extra-Lp RPKM	Log ₂ ratio	Gene Product/KEGG
lpg0175	98.33%	48.63%	425.71	1.45	8.20	pyoverdine biosynthesis protein PvcB K00471//gamma-butyrobetaine dioxygenase [EC:1.14.11.1];K03119//taurine dioxygenase
lpg0563	93.84%	99.16%	56329.91	247.42	7.83	hypothetical phasin protein
lpg0176	97.92%	54.75%	223.39	1.35	7.37	hypothetical PvcC K05712//3-(3-hydroxy-phenyl)propionate hydroxylase [EC:1.14.13.127];K03380//phenol 2-monooxygenase
lpg1968	99.74%	98.56%	1763.42	11.43	7.27	Hypothetical monooxygenase protein
lpg0174	98.15%	94.35%	625.83	4.95	6.98	pyoverdine biosynthesis protein PvcA K00493//unspecific monooxygenase [EC:1.14.14.1]
lpg1565	99.58%	97.37%	987.72	8.56	6.85	thiamine biosynthesis protein NMT-1 K15598//putative hydroxymethylpyrimidine transport system substrate-binding protein
lpg0810	91.19%	98.43%	566.79	10.32	5.78	hypothetical protein K02237//competence protein ComEA
lpg2231	99.20%	86.32%	144.54	3.07	5.56	3-oxoacyl-ACP reductase K00059//3-oxoacyl-[acyl-carrier protein] reductase [EC:1.1.1.100]
lpg0894	99.78%	98.10%	1316.17	30.22	5.44	cytokinin oxidase K00279//cytokinin dehydrogenase [EC:1.5.99.12];K00104//glycolate oxidase [EC:1.3.1.5]
lpg2889	99.95%	99.36%	1504.76	40.56	5.21	tRNA uridine 5-carboxymethylaminomethyl modification protein GidA K03495//tRNA uridine 5-carboxymethylaminomethyl modification enzyme

Table 4.4.4 Top 10 downregulated genes of intracellular *L. pneumophila* from transcriptome analysis. The RNA-sequencing DEG analysis was based on comparing FACS-enriched gfp-transfected *L. pneumophila*-infected *A. castellanii* (Intra-Lp) with extracellular grown *L. pneumophila* (Extra-Lp). Both the p value and the FDR (False discovery rate) were lower than 0.001 for the 10 DEGs.

Gene	Intra-Lp coverage	Extra-Lp coverage	Intra-Lp RPKM	Extra-Lp RPKM	Log ₂ ratio	Gene Product/KEGG
lpg1086	0	25.67%	0.00	5.70	-12.48	IS4 family transposase TnpA
lpg2556	99.06%	100.07%	285.97	4243.35	-3.89	protein kinase (legK3)/ K15486//Serine/threonine-protein kinase
lpg2997	97%	99.83%	152.07	2189.53	-3.85	alkane-1 monooxygenase
lpg2048	98.59%	99.65%	448.32	5681.50	-3.66	hypothetical zinc finger protein
lpg1742	98.66%	99.55%	2389.84	18530.97	-2.95	Hypothetical ribonuclease P RNA (mpB) protein
lpg0537	99.73%	99.73%	11980.50	92467.82	-2.95	transmission trait enhancer LetE
lpg1773	94.43%	99.79%	67.06	495.31	-2.88	small stress protein PASS1
lpg2545	99.31%	99.66%	1660.41	11598.05	-2.80	hypothetical transporter protein
lpg0443	99.72%	99.72%	5421.67	35399.14	-2.71	IcmR/ K12220//Intracellular multiplication protein IcmR
lpg1976	98.49%	99.42%	93.40	607.48	-2.70	UVB-resistance protein UVR8 (legG1)

4.4.5.2 *A. castellanii* DEGs when infected with gfp-transfected *L. pneumophila*

In the gfp-transfected *L. pneumophila*-infected *A. castellanii*, the most upregulated *A. castellanii* gene (14917946, 8.85- \log_2 ratio) encoded Ser/Thr phosphatase that might have been involved in cell differentiation during the transmissive phase, and the gene that encoded ATPase (14920057, 8.12- \log_2 ratio) could have supplied the energy for *A. castellanii* cell differentiation. Most interesting, the *A. castellanii* genes encoding MCM8 (14918687, 7.7- \log_2 ratio) and transposase (14918687, 7.5- \log_2 ratio) that were involved in homologous recombination repair were highly upregulated in *L. pneumophila*-infected *A. castellanii* during the transmissive phase (Table 4.4.5). The activated homologous recombination repair in *A. castellanii* could be triggered by intracellular *L. pneumophila*.

The most downregulated genes in the infected *L. pneumophila*-*A. castellanii* encoded the ribosomal protein L35 (14924264, -9.0- \log_2 ratio) and ribosomal S4 (14914629, -8.1- \log_2 ratio), indicating the inhibition of ribosomal biosynthesis and transcriptional activity in *L. pneumophila*-infected *A. castellanii* hosts (Table 4.4.5). The gene that encoded the dephosphoCoA kinase (14921988, -8.539- \log_2 ratio) was also highly downregulated, which implied downregulation of the amino acid metabolism in the *L. pneumophila*-infected *A. castellanii* host.

Table 4.4.5 Top 10 upregulated and downregulated genes of *A. castellanii* infected with gfp-transfected *L. pneumophila* compared with uninfected *A. castellanii* at T48.

Upregulated			Downregulated		
Gene ID	Gene product	log ₂ ratio	Gene ID	Gene product	log ₂ ratio
14917946	Ser/Thr phosphatase, putative	8.849	14924264	ribosomal protein L35, putative	-8.999
14920057	ATPase, AAA domain containing protein	8.115	14921988	dephosphoCoA kinase	-8.539
14918687	MCM8 protein	7.741	14921544	Sadenosyl-L-homocysteine hydrolase, putative	-8.264
14920053	hypothetical transposase protein	7.536	14914629	ribosomal protein S4, putative	-8.103
14918289	WD40 repeat protein, COMPASS complex protein	7.485	14920060	SAM domain (Sterile alpha motif) domain containing protein	-8.034
14920054	zinc finger, c2h2 type domain containing protein	7.483	14926214	ribosomal protein S8e, putative	-8.016
14913122	inosineuridine nucleoside N-ribohydrolase	7.419	14917963	hypothetical mRNA splicing factor protein	-7.855
14918461	hypothetical nucleotidyltransferase protein	7.174	14911452	hydroxymethylglutarylCoA synthase	-7.584
14922083	regulator of chromosome condensation (RCC1) repeat domain containing protein	7.141	14918945	ankyrin 2,3/unc44, putative	-7.584
14925472	serine/threonine protein kinase, putative	7.102	14920148	Golgi family protein, putative	-7.584

Table 4.4.5 Continued.

Upregulated			Downregulated		
Gene ID	Gene product	log ₂ ratio	Gene ID	Gene product	log ₂ ratio
14917430	hypothetical transporter protein	7.001	14911825	PHD-finger domain containing protein	-7.518
14917431	CBS domain containing protein	6.920	14913532	hypothetical cell surface protein	-7.475
14921606	tetratricopeptide repeat domain containing protein	6.885	14920276	SAM domain (Sterile alpha motif) domain containing protein	-7.475
14924039	IQ calmodulin-binding motif domain containing protein	6.881	14917906	short chain dehydrogenase/reductase family oxidoreductase	-7.458
14913653	uncharacterized protein	6.812	14924759	PWWP domain containing protein	-7.458
14919893	protein kinase domain containing protein	6.605	14912867	Hypothetical signal transduction protein	-7.338
14923730	hypothetical cytoplasmic tRNA-thiolation protein	6.560	14921969	Leucine rich repeat domain containing protein	-7.338
14920462	Sestrin-like protein	6.556	14923544	ribosomal protein S10p/S20e, putative	-7.264
14920129	RFX DNA-binding domain containing protein	6.529	14912475	F-box domain containing protein	-7.169
14917912	Rho-GEF domain containing protein	6.314	14913021	ribosomal protein s27, putative	-7.169

4.4.6 Quantitative RT-qPCR verification of DEGs in FACS-enriched gfp-transfected *L. pneumophila*-infected *A. castellanii*

4.4.6.1 Virulence genes expression of intracellular *L. pneumophila*

L. pneumophila grown in *A. castellanii* had upregulated *pvcA*, *pvcB*, and *pvcC* at both T24 and T48 as compared with the extracellular-grown *L. pneumophila* during the transmissive phase (Figure 4.4.5). *pvcA*, *pvcB*, and *pvcC* were upregulated by 5.4-, 14.6-, and 14.7-fold, respectively, at T24; and *pvcA*, *pvcB*, and *pvcC* were upregulated by 4.2-, 3.8-, and 4.5-, respectively, at T48. The lower level of upregulation of *pvcABC* in *L. pneumophila* when grown in *A. castellanii* at T48 could be due to the faded growth during the transmissive phase.

L. pneumophila *fliA* and *flaA* involved in flagellar biosynthesis were both highly upregulated (Figure 4.4.5) at intracellular T24 and T48, indicating that the activation of the flagellar biosynthesis pathway when *L. pneumophila* are grown in *A. castellanii*. *fliA* was upregulated by 10- and 21.3-fold at T24 and T48, respectively, and *flaA* was upregulated by 8.6- and 23-fold at T24 and T48, respectively. *L. pneumophila* flagellin proteins were often activated after the exponential growth phase (Schulz et al. 2012). The increase in the upregulation of flagellin proteins at the end of the second round of intracellular replication (T48) indicates that more flagellated *L. pneumophila* had been generated after replication in *A. castellanii*.

In addition to flagellar biosynthesis, *flaA* is widely known to activate pyroptosis (Silveira and Zamboni 2010). *vipD* encoded a phospholipase, and its intracellular role has been revealed to promote the release of cytochrome c (Zhu et al. 2013) to induce apoptosis. *vipD* was downregulated by 2.19-fold at T24, but *vipD* was mildly upregulated (1.9-fold) at T48 when compared with the extracellular-grown *L. pneumophila* at T48. Both *flaA* and *vipD* involved in the activation of programmed cell death were upregulated during the intracellular transmissive phase (T48) (Figure 4.4.5).

tnpA was downregulated by 7.2- and 8.4-fold at T24 and T48, respectively. Intracellular *L. pneumophila tnpA* was highly downregulated at both T24 and T48 as compared with extracellular-grown *L. pneumophila*, which implies that the transposase activity was repressed when *L. pneumophila* was grown in *A. castellanii*. *legK3* was downregulated by 4.1- and 5.5-fold at T24 and T48, respectively. *legK1* was downregulated by 2- and 3.4-fold at T24 and T48, respectively. Both *L. pneumophila legK1* and *legK3* belong to the family that encodes serine/threonine protein kinase (Haenssler and Isberg 2011), furthermore both LegK1 and LegK3 effectors have the potential to phosphorylate host cell proteins for modulation of signal transduction.

legK3 was identified to activate the host cell NFκB pathway via cooperation with *sidI*. Intracellular *L. pneumophila sidI* was also highly downregulated at T24 (-6.4-fold change) and T48 (-5.3-fold change). *sidI* and *legK1* can work together to suppress host death, in which *sidI* sustainably blocks host cell IκB (kinase) binding to NFκB

and *legK1* activates NFκB to further delay cell death and promote cytokine release (Ge and Shao 2011, Ge et al. 2009, Shen et al. 2009). The upregulation of *flaA* and *vipD* and the downregulation of *sidI* and *legK1* at intracellular T48 suggest that intracellular *L. pneumophila* during the late phase can trigger cell death that in turn facilitates its release from the host.

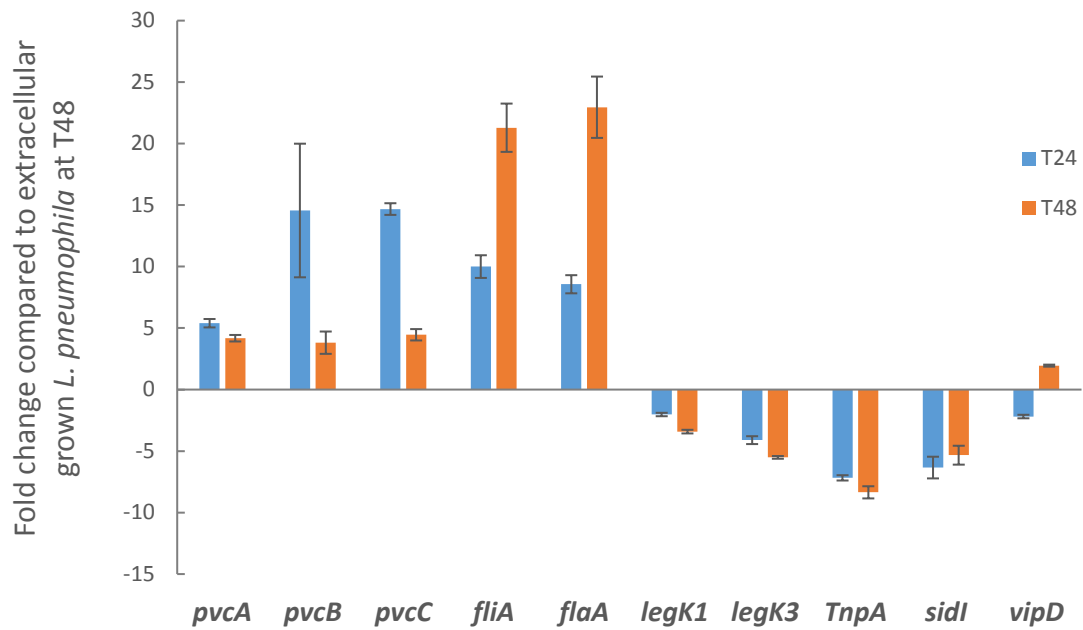


Figure 4.4.5 Virulence gene expression of FACS-enriched gfp-transfected *L.*

pneumophila–infected *A. castellanii*. *L. pneumophila* virulence gene expression was studied in FACS-enriched gfp-transfected *L. pneumophila*–infected *A. castellanii* at T24 and T48.

Two-step quantitative RT-qPCR was used to quantify the gene expression normalized with housekeeping gene *gyrB*, and gene expression levels were calculated based on a comparison with extracellular-grown gfp-transfected *L. pneumophila* at T48. The Wilcoxon-signed test was used to compare the data ($2^{-\Delta\Delta C_t}$) between T24 and T48. A p value of greater than 0.05 indicates a lack of a significant difference.

4.4.6.2 Expression of genes in infected *A. castellanii*

The *A. castellanii* gene encoding serine/threonine (Ser/Thr) phosphatase was mildly upregulated at T24 (1.78-fold change), followed by a great increase in upregulation at T48 (8-fold change), which agrees with the transcriptome DEGs allocation. However, the *A. castellanii* gene encoding ATPase showed no change at T24 and was upregulated by 1.28-fold at T48, possibly the gene encoding ATPase has low copy numbers that can lead to the RNA-seq quantification different from the RT-qPCR quantification. When *A. castellanii* was infected with *L. pneumophila*, the gene encoding MCM8 (minichromosome maintenance protein) showed no change at T24 (0.96-fold change), followed by a great increase in upregulation at T48 (7.95-fold change) when compared with uninfected *A. castellanii* at T48. The activated MCM8 involved in DNA repair in *L. pneumophila*-infected *A. castellanii* during the late stage could be caused by *L. pneumophila* infection led to more cell damage. The activated activity of DNA repair in *L. pneumophila*-infected *A. castellanii* at T48 could also be a signal of *A. castellanii* cell differentiation into cyst before the release of *L. pneumophila*.

In comparison, *A. castellanii* IRSp53 was found to be involved in eukaryotic cell actin rearrangement (Ridley 2006), and ATG14 is an autophagy-related protein that seemed to be less involved in *L. pneumophila*-infected *A. castellanii*. The gene encoding IRSp53 had no change at T24 and was 1.5-fold upregulated at T48; the gene encoding ATG14 was downregulated by 1.9-fold at T24 and upregulated by 1.15-fold at T48. The *A. castellanii* gene encoding ATPeV was downregulated by 3.5- and 1.2-fold at

T24 and T48, respectively. This finding implies that the lysosomal pathway of *A. castellanii* was repressed when *L. pneumophila* was grown in *A. castellanii*.

The *A. castellanii* gene encoding ribosomal L35 was downregulated by 6.89- and 1.6-fold at T24 and T48, respectively. The ribosomal S4-related gene was downregulated by 5.17- and 1.5-fold at T24 and T48, respectively. The gene encoding the dephospho-coenzyme kinase (CoAK) was downregulated by 7.15- and 1.4-fold at T24 and T48, respectively. The three genes were all highly downregulated in the transcriptome analysis of gfp-transfected *L. pneumophila*-infected *A. castellanii* at T48 (Table 4.4.5). Although the three genes were all highly downregulated when *A. castellanii* was infected with *L. pneumophila* at T24, the infected *A. castellanii* at T48 showed less downregulation of the three genes. The decreased viability of infected *A. castellanii* at T48 could have affected the RNA quality during RT-qPCR verification.

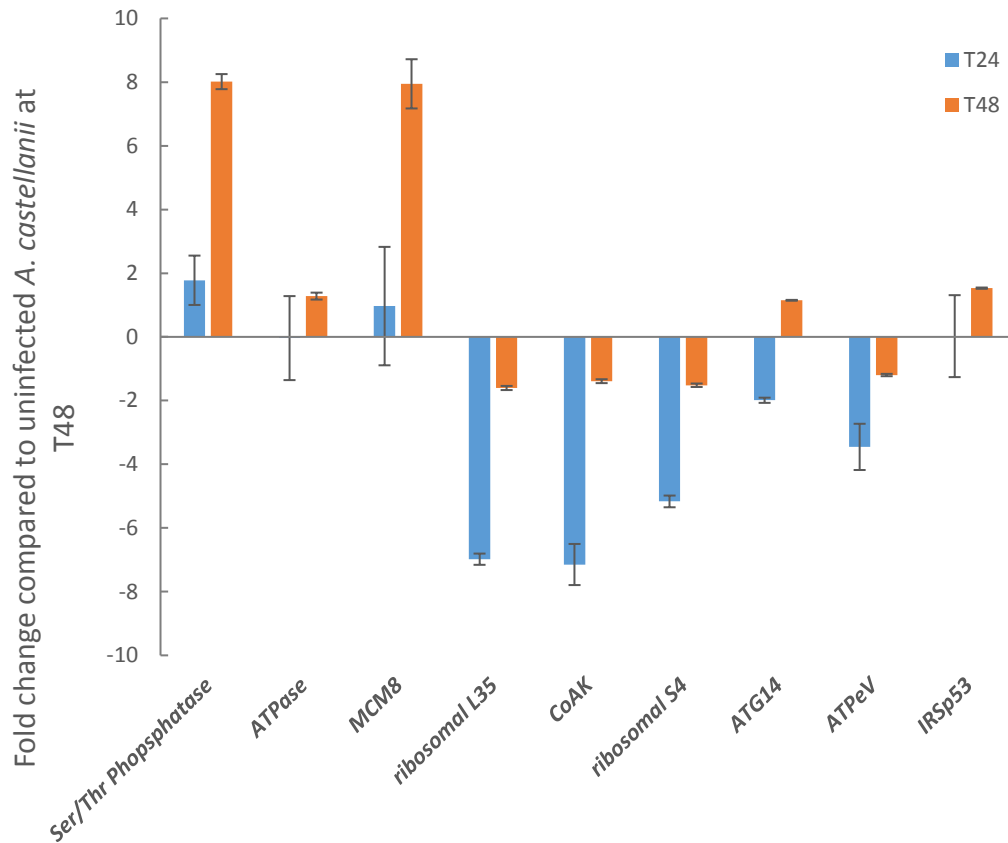


Figure 4.4.6 Two-step RT-qPCR verification of *A. castellanii* genes expression. FACS-enriched *gfp*-transfected *L. pneumophila*-infected *A. castellanii* at T24 and T48, and *A. castellanii* without challenging *L. pneumophila* at T48 were respectively collected for RNA extraction. Total RNA was reverse transcribed to cDNA, and cDNA were used for quantitative PCR and normalized to the housekeeping *18S rRNA* gene. The expression levels of genes were calculated based on a comparison with the uninfected *A. castellanii* at T48. The data were expressed as the fold change ($2^{-\Delta\Delta C_t}$). Wilcoxon-signed tests were used to compare the fold changes between infected *A. castellanii* at T24 and T48.

4.4.7 *L. pneumophila* and mutant strains grown in L-cysteine–limited and supplied BYE broths

L. pneumophila pvcA and *pvcB* were both highly upregulated when *L. pneumophila* was grown in *A. castellanii*, and both *pvcA* and *pvcB* are allocated in the amino acid metabolism, including the L-cysteine anabolism in KEGG allocation. The functional roles of *L. pneumophila pvcAB* have yet to be revealed. This study generated *pvcA*-knockout and *pvcB*-knockout *L. pneumophila* strains to determine whether *pvcA*-or *pvcB*-knockout affects *L. pneumophila* growth under L-cysteine-limited conditions. *L. pneumophila*, *pvcA*-knockout, and *pvcB*-knockout *L. pneumophila* were grown in two different BYE broths, supplemented with L-cysteine and without L-cysteine.

When the wild-type *L. pneumophila*, *pvcA*-knockout, and *pvcB*-knockout *L. pneumophila* were grown in BYE broth supplemented with L-cysteine, no obvious difference was seen in the bacterial growth between the wild-type and mutant *L. pneumophila* strains (Figure 4.4.7, upper panel). When cultured in L-cysteine–sufficient medium, wild-type *L. pneumophila* showed 434% and 488% greater growth at T12 than *pvcA*-knockout ($p=0.00001$) and *pvcB*-knockout ($p=0.0001$) *L. pneumophila*, respectively. However, no significant difference was seen between wild-type *L. pneumophila* with either *pvcA*-knockout or *pvcB*-knockout *L. pneumophila* between T24 and T72. The wild-type *L. pneumophila* showed 3740% growth during the 72-h culture in the supplied BYE broth, and *pvcA*-knockout and *pvcB*-knockout *L. pneumophila* showed 3404% and 3500% growth, respectively, from T0 to T72 in the supplied BYE broth.

When the *L. pneumophila* and mutant strains were grown in L-cysteine-limited BYE broth (Figure 4.4.7, lower panel) from T0 to T72, the wild-type *L. pneumophila* showed 1133% growth; however, *pvcA*-knockout and *pvcB*-knockout *L. pneumophila* showed 678% and 654% growth, respectively. When grown in L-cysteine-limited medium, the wild-type *L. pneumophila* showed 46.28% and 44.22% higher growth at T24 than the *pvcA*-knockout ($p=0.034$) and *pvcB*-knockout ($p=0.007$) strains, respectively. The wild-type *L. pneumophila* also showed 96.48% and 122.11% higher growth at T36 than the *pvcA*-knockout ($p=0.01$) and *pvcB*-knockout ($p=0.002$) strains, respectively. The wild-type *L. pneumophila* showed 349% and 322.75% higher growth at T60 than the *pvcA*-knockout ($p=0.0003$) and *pvcB*-knockout ($p=0.001$) *L. pneumophila*, respectively. The wild-type *L. pneumophila* showed greater growth in the L-cysteine-limited condition than either the *pvcA*-knockout and *pvcB*-knockout strains from T0 to T72, and the gap between the wild-type *L. pneumophila* and the two mutant strains continued to increase from T0 to T72.

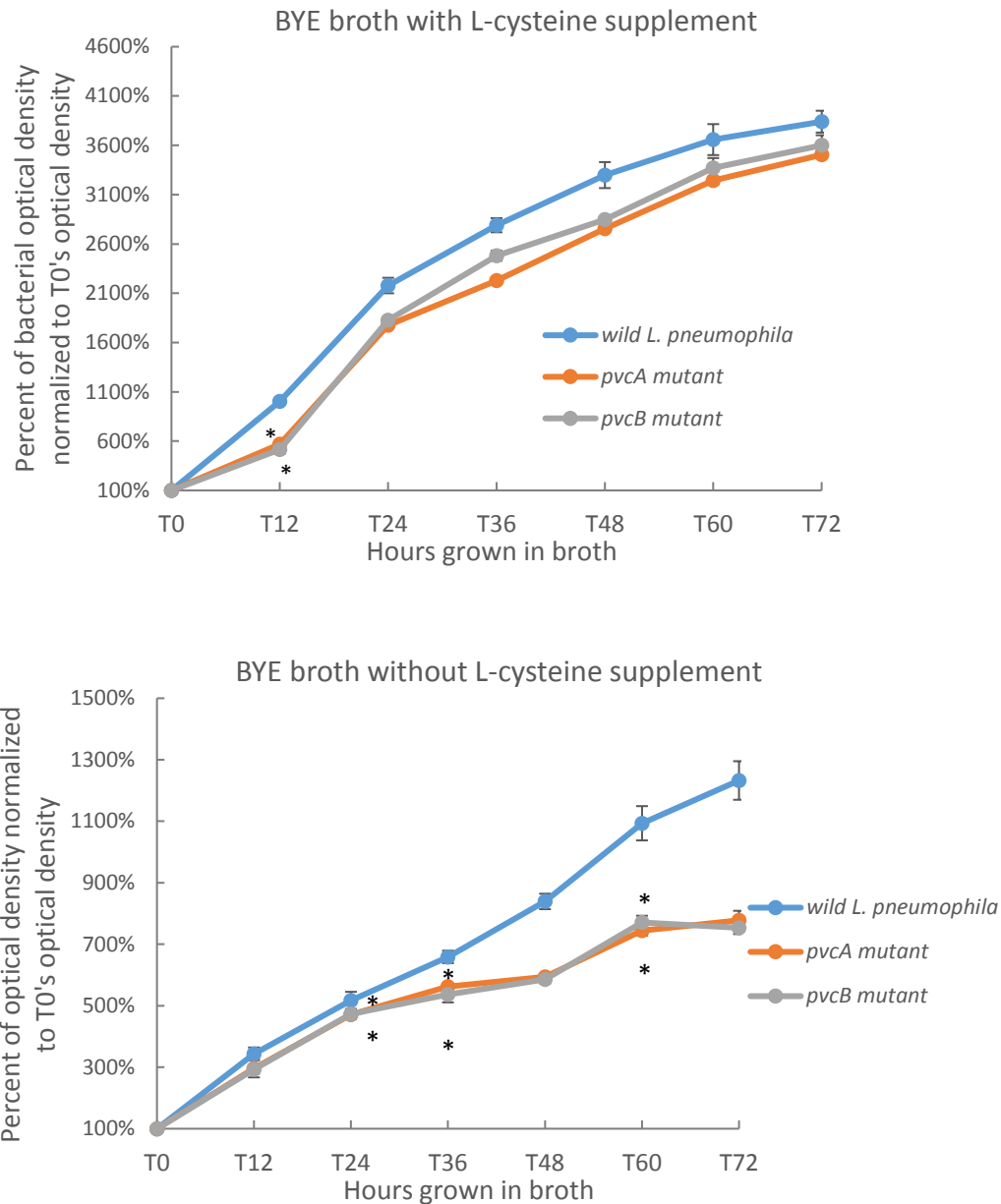


Figure 4.4.7 *L. pneumophila* and mutant strains grown in BYE broths. Upper and lower panels show three different *L. pneumophila* strains grown in BYE broth with L-cysteine (upper panel) and without L-cysteine supplement (lower panel). The optical density at each time point was normalized to T0's optical density, and the data are expressed as percentages. A paired *t*-test was used to compare the wild-type *L. pneumophila* with either *pvcA*-knockout or *pvcB*-knockout *L. pneumophila*, and a *p* value of less than 0.05 indicates a significant difference (*).

4.4.8 Intracellular growth of *pvcA*-knockout and *pvcB*-knockout *L. pneumophila* strains

4.4.8.1 *pvcA*-knockout and *pvcB*-knockout *L. pneumophila* grown in *A. castellanii* and THP-1

When *L. pneumophila* and the mutant strains were grown in *A. castellanii* (Figure 4.4.8.1), the wild-type *L. pneumophila*, *pvcA*-knockout, and *pvcB*-knockout *L. pneumophila* showed 4135%, 4279%, and 2490% growth, respectively, during the 48 h after infection. All three *L. pneumophila* strains had growth from T0 to T48 in *A. castellanii*. No significant difference was seen in the growth between the wild-type *L. pneumophila* with either the *pvcA*-knockout or the *pvcB*-knockout *L. pneumophila* between T12 and T48. The results show that the knockout of neither *L. pneumophila pvcA* nor *pvcB* had a visible negative effect on the intracellular growth of *L. pneumophila* in *A. castellanii*.

When *L. pneumophila* and the mutant strains were grown in THP-1 (Figure 4.4.8.2), both wild-type and *pvcA*-knockout *L. pneumophila* showed 296% growth during the 48 h after infection. However, the *pvcB*-knockout *L. pneumophila* showed 522% growth between T0 and T48. The wild-type *L. pneumophila* showed 237% and 241% higher growth at T24 and T36, respectively, than *pvcA*-knockout *L. pneumophila*, but neither difference was statistically significant (T24, $p=0.25$; T36, $p=0.304$). Although *pvcB*-knockout *L. pneumophila* showed 30% greater growth at T24 than the wild-type strain, the difference was not statistically significant ($p=0.836$). The wild-type *L.*

pneumophila showed 44% higher growth than the *pvcB*-knockout strain at T36, but the difference was not statistically significant ($p=0.852$). Most interestingly, the *pvcB*-knockout *L. pneumophila* showed 226% higher ($p=0.022$) growth than the wild-type *L. pneumophila* at T48, possibly because the growth rate of wild-type *L. pneumophila* peaked at T36 (603%), whereas that of *pvcB*-knockout *L. pneumophila* peaked at T48 (622%). The results show that *pvcA*-knockout *L. pneumophila* displayed lower growth rates at T24 and T36 than wild-type *L. pneumophila* in THP-1; the knockout of *pvcB* showed no negative effect on the intracellular growth of *L. pneumophila* in THP-1.

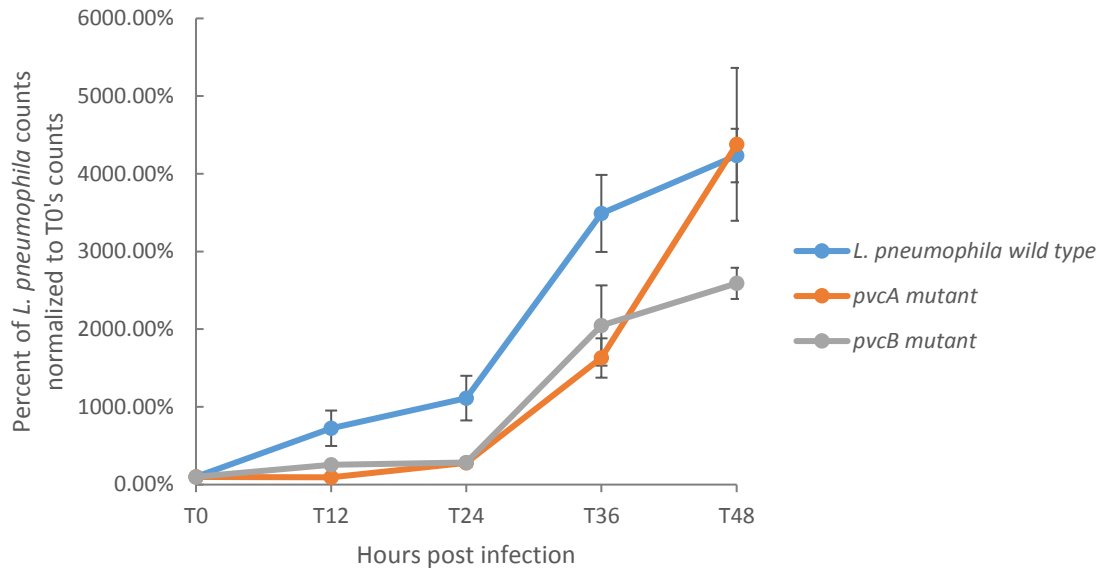


Figure 4.4.8.1 Intracellular growth of wild-type, *pvcA*-knockout, and *pvcB*-knockout *L. pneumophila* in *A. castellanii*. The three bacteria grown on α BCYE agar plates were challenged into *A. castellanii* at an MOI of 10. After co-culture, the *L. pneumophila* strains grown in *A. castellanii* were respectively released and counted with a standard plate count method every 12 h from 0 to 48 h after infection. The data are expressed as the percentage of the bacterial count at each time point normalized to T0's counts. A paired *t*-test was used to compare the data of wild-type *L. pneumophila* with either *pvcA*-knockout or *pvcB*-knockout *L. pneumophila* from T12 to T48, and a *p* value of greater than 0.05 indicates a lack of a significant difference.

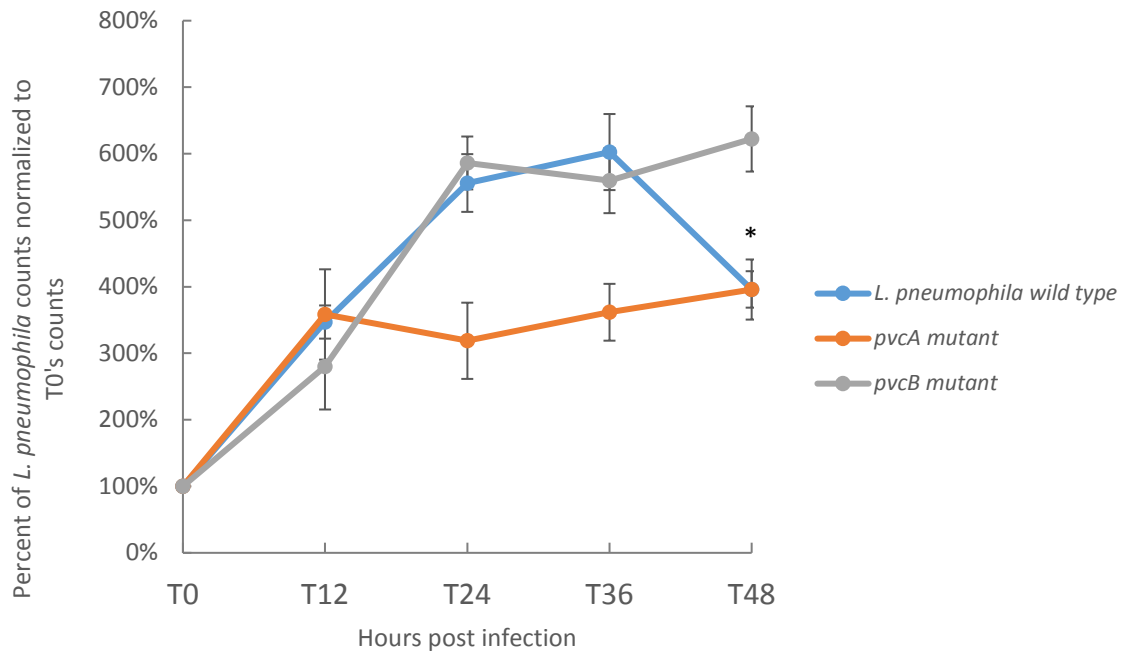


Figure 4.4.8.2 Intracellular growth of wild-type, *pvcA*-knockout, and *pvcB*-knockout *L. pneumophila* in THP-1. The three bacteria grown on α BCYE agar plates were challenged into THP-1 at an MOI of 10. After co-culture, *L. pneumophila* strains grown in THP-1 were released and counted using a standard plate counting method every 12 h from 0 to 48 h after infection. The data are expressed as the percentage of the bacterial count at each time point normalized to T0's counts. A paired *t*-test was used to compare the data of wild-type *L. pneumophila* with either *pvcA*-knockout or *pvcB*-knockout *L. pneumophila* from T12 to T48; a *p* value of less than 0.05 indicates a significant (*) difference.

4.4.8.2 *pvcA*-knockout and *pvcB*-knockout *L. pneumophila* released from *A. castellanii* showed lower replication in THP-1

Wild-type, *pvcA*-knockout, and *pvcB*-knockout *L. pneumophila* were co-cultured with *A. castellanii* and then released from *A. castellanii* at T48 (transmissive phase) via hypotonic lysis (described in Section 3.4.1). The released bacteria were further used to infect THP-1.

From the intracellular growth assay (Figure 4.4.8.3), the growth rate of the wild-type *L. pneumophila* continued to increase between T12 (585.5%) and T36 (765.3%), and the growth rate then declined by T48 (667%). *pvcA*-knockout *L. pneumophila* (*pvcA* mutant) had the most growth at T12 (493.6%); it then decreased to 459.9% at T24 and to 194.1% at T36 and then increased to 401.28% at T48. *pvcB*-knockout *L. pneumophila* (*pvcB* mutant) also had the most growth at T12 (434.4%), and the growth rate remained around 370% between T24 and T48. The wild-type *L. pneumophila* showed 190.7% and 517.2% higher growth at T24 ($p=0.007$) and T36 ($p=0.005$), respectively, than the *pvcA*-knockout *L. pneumophila*. The wild-type *L. pneumophila* also showed 285.4%, 403.9%, and 286.1% higher growth at T24 ($p=0.0001$), T36 ($p=0.002$), and T48 ($p=0.006$), respectively, than the *pvcB*-knockout *L. pneumophila*. The greater degree of significance shown in Figure 4.4.8.3 than in Figure 4.4.8.2 could be a result of the greater number of bacterial counts collected in this study for statistical analysis. As a result, the knockout of either *pvcA* or *pvcB* in *L. pneumophila* had a negative effect on the bacteria released from *Acanthamoeba* to further infect THP-1.

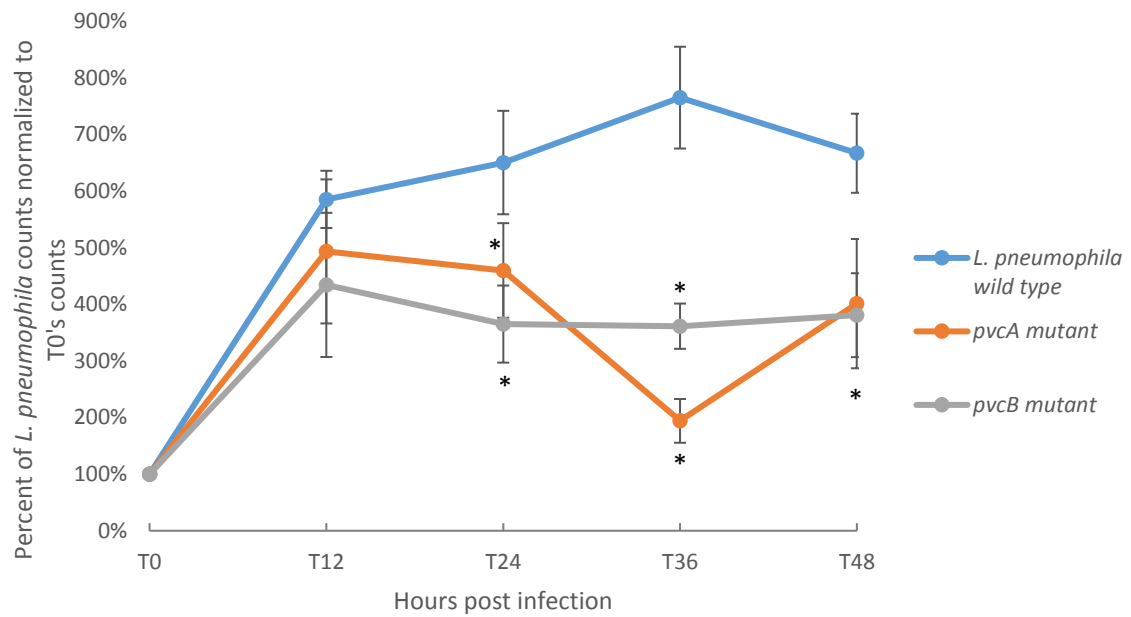


Figure 4.4.8.3 *L. pneumophila* strains released from *A. castellanii* grown in THP-1. Wild-type *L. pneumophila*, *pvcA*, and *pvcB* mutated strains were co-cultured with *A. castellanii* and released at T48. The released bacteria were respectively co-cultured with THP-1 at an MOI of 1. After co-culture, the *L. pneumophila* strains grown in THP-1 were counted every 12 h from 0 to 48 h after infection. The data are expressed as the percentage of the bacterial count at each time point normalized to T0's counts. A paired *t*-test was used to compare the data of the wild-type *L. pneumophila* with either *pvcA*-knockout or *pvcB*-knockout *L. pneumophila* from T12 to T48, and a p value of less than 0.05 indicates a significant (*) difference.

5. Discussion

5.1 Intracellular growth of *L. pneumophila* and virulence gene expression

This study investigated the intracellular growth of *L. pneumophila* in two different hosts—*A. castellanii* and human monocyte THP-1—and the association with *L. pneumophila* virulence gene expression. The successful pathogenesis of *L. pneumophila* depends upon its intracellular replication in hosts. A comparison of the intracellular growth of *L. pneumophila* in different hosts could reveal the differences in permissiveness, and a study of the virulence gene expression patterns can further uncover the underlying mechanisms. This exploration contributes to a more integrated view of the interaction of *L. pneumophila* with various host cells.

Intracellular-grown *L. pneumophila* experienced various growth phases and finally differentiated into a mature intracellular form that could be more transmissible at the end of the growth cycle (Garduno et al. 2002), and virulent traits were expressed at this stage (Bruggemann et al. 2006). *L. pneumophila* intracellular replications were reported to contribute to our understanding of growth dynamics inside various hosts (Molofsky and Swanson 2004).

5.1.1 *A. castellanii* showed greater support for *L. pneumophila* intracellular replication than THP-1

Our results indicate that *A. castellanii* showed greater support for the intracellular replication of *L. pneumophila* than THP-1, which could explain why *L. pneumophila* is ubiquitous in environmental water. Although THP-1 has a pattern recognition receptor, THP-1 internalized less *L. pneumophila* than *A. castellanii* at the initial time point. The video microscopic visualization of gfp-transfected *L. pneumophila*-infected macrophages revealed that internalized gfp-transfected *L. pneumophila* disappeared in some macrophages during the 48-h infection. The low growth of *L. pneumophila* in macrophages might have been caused by the macrophage defense system rather than an inability to internalize *L. pneumophila*.

Studies of the intracellular growth of *L. pneumophila* have been performed by various research groups (Table 5.1). Our findings regarding the intracellular growth of *Legionella* species in *Acanthamoeba* and THP-1 cells were similar to those reported by Weissenmayer et al. (2013) and Roland et al. (2013), respectively, but differed from those reported by Dey (Dey et al. 2009) and Lebeau (Lebeau et al. 2004), respectively. Dey et al. (2009) reported the exponential replication of *Legionella* in *Acanthamoeba* only after 24 h, whereas Lebeau et al. (2004) observed *Legionella* duplication for up to 72 h after infection. The discrepancies in these findings might have been the result of differences in the experimental operations.

Previous studies reported that monocyte-derived macrophages supported a higher level of *L. pneumophila* replication (Alli et al. 2000, Horwitz and Silverstein 1980) than *Acanthamoeba* (Holden et al. 1984), but other studies showed that *Acanthamoeba* supported greater and quicker replication of *L. pneumophila*. Rolando et al. (2013) indicated that *L. pneumophila* grown in *A. castellanii* showed more than 100-fold replication between T0 and T50, whereas *L. pneumophila* in THP-1 replicated only 10-fold over a 50-h period (Rolando et al. 2013), which is similar to our findings.

The underlying reasons for the variations in the results regarding the intracellular growth of *L. pneumophila* could be caused by the different MOIs, a counting method bias, and differences in the cell lysis method used before the cells were spread onto the plate (Dietersdorfer et al. 2016). Researchers have also indicated that the co-culture conditions, including the temperature and the co-culture medium, could affect the results obtained (Buse and Ashbolt 2011, Dey et al. 2009).

Table 5.1 Summary of *Legionella* growth in different hosts reported by different research groups. Standard plate counting techniques were used to measure the bacterial CFU per mL in co-cultures. Information including host cells, the initial concentration of host cells, and MOIs is shown. All data are presented as bacterial CFU per mL at various times after infection.

***Acanthamoeba* host**

***A. castellanii* (10^5 /mL), MOI=0.5 (Holden et al. 1984)**

Time points (h)	T1	T24	T48	T72
Total <i>Legionella</i>	5×10^4	3×10^5	1×10^6	2×10^7

***A. castellanii* ($\sim 10^5$ /mL), MOI=2 (Lebeau et al. 2004)**

Time points (h)	T0	T24	T48	T72
Intracellular <i>Legionella</i>	6×10^4	2×10^5	6×10^6	4×10^7

***A. polyphaga* (10^5 /mL), MOI=10 (Abu-Zant et al. 2006)**

Time points (h)	T2	T24	T48	T72
Intracellular <i>Legionella</i>	5×10^4	10^7	5×10^8	10^8

***A. castellanii* ($\sim 10^5$ /mL), MOI=50 (Dey et al. 2009)**

Time points (h)	T0	T24	T48	T72	T96
Intracellular <i>Legionella</i>	5×10^6	5×10^6	4×10^7	10^8	8×10^7

***A. castellanii* (10^6 /mL), MOI=100 (Weissenmayer et al. 2011)**

Time points (h)	T0	T8	T12	T14
Intracellular <i>Legionella</i>	8×10^6	8×10^6	3×10^7	10^8

Table 5.1 Continued***A. castellanii* (10⁵/mL), MOI=0.1 (Rolando et al. 2013)**

Time points (h)	T0	T50	T100	T150
Intracellular <i>Legionella</i>	10 ⁻⁵	10 ⁻³	10 ⁻¹	1

Human cell host**Human Blood Monocyte (5×10⁶/mL), MOI=5 (Horwitz and Silverstein 1980)**

Time points (h)	T0	T24	T48	T72
Total <i>Legionella</i>	10 ³	10 ⁵	5×10 ⁵	10 ⁵

U937 macrophage (10⁵/mL), MOI=0.5 (Alli et al. 2000)

Time points (h)	T0	T20	T40	T50
Intracellular <i>Legionella</i>	5×10 ⁴	5×10 ⁷	10 ⁹	4×10 ⁹

Human monocyte derived macrophage (10⁵/mL), MOI=10 (Abu-Zant et al. 2006)

Time points (h)	T2	T24	T48	T72
Intracellular <i>Legionella</i>	10 ⁵	5×10 ⁶	10 ⁶	8×10 ⁵

THP-1 (10⁵/mL), MOI=10 (Rolando et al. 2013)

Time points (h)	T0	T20	T40	T60
Intracellular <i>Legionella</i>	10 ⁻²	10 ⁻²	10 ⁻¹	10 ⁻¹

5.1.2 *L. pneumophila* virulence genes involved in host cell death showed differences in expression in *A. castellanii* and THP-1

5.1.2.1 *L. pneumophila* virulence gene expression associated with THP-1 CASP genes expression patterns

This study compares the expression pattern of *L. pneumophila* genes involved in the manipulation of host cell death. When *L. pneumophila* was grown in THP-1 cells, the expression of the pyroptotic protein *flaA* was downregulated over time. In contrast, the expression of *sdhA*, which stabilized the LCV and inhibits pyroptosis, increased steadily after infection with *L. pneumophila*. The expression profiles of *flaA* and *sdhA*, together with the reduced expression of *CASP* genes in *L. pneumophila*-infected THP-1 cells, indicated that the cell death pathways were inhibited after infection. Although this inhibition of host death favored the intracellular multiplication of *L. pneumophila*, it might have also hindered the egress of *L. pneumophila* and decreased the overall number of intracellular *L. pneumophila* in THP-1 cells.

In a transcriptome study, Faucher et al. demonstrated the upregulation of *sidF* in *Legionella*-infected THP-1 macrophages (Faucher et al. 2011). *Legionella sidF* is involved in phosphoinositide metabolism and remodeling and is therefore essential to LCV maintenance (Hsu et al. 2012). In our study, we observed downregulation of less than 2-fold in *sidF* expression at all time points. We similarly observed changes of less than 2-fold in *vipD* expression levels. The involvement of both *sidF* and *vipD* in apoptosis suggests that pyroptosis, which involves pore formation and thus facilitates

the release of intracellular agents, plays a greater role in THP-1 monocytes during *Legionella* infection. Despite the small changes in *vipD* and *sidF* expression, however, we observed downregulation of 8.6-fold in *CASP-3* expression at 48 h after infection that might have been caused by a decrease in the total number of viable THP-1 cells. Accordingly, this decrease might have also induced only slight upregulation of *CASP-1* at 48 h after infection.

In infected THP-1 cells, the downregulation of *flaA* occurred gradually, although significant changes in gene expression were observed at the late time point (48 h) rather than at earlier time points. The downregulation of *flaA* could have been due to the low number of intracellular *Legionella* and the slow consumption of nutrients that failed to induce *flaA* expression. *sdhA* was upregulated gradually over the time points studied, and the expression levels were significantly higher at 24 to 48 h after infection. *sdhA* played an indirect role in inhibiting cell death by maintaining the integrity of LCV, and an increased level of *sdhA* ensured protection of the *Legionella* replication niche.

In uninfected THP-1 cells, upregulation of 16.3-fold was observed in *CASP-1* expression at 48 h, with no corresponding remarkable reduction in the number of viable cells. Accordingly, we did not identify a clear relationship between the pattern of cell death and the *CASP-1* expression, possibly due to the decreased number of viable cells, particularly at 48 h, because this would have affected the RNA yields and quantified gene expression levels. Previous reports did not describe the expression pattern of *flaA*, *vipD*, *sdhA*, and *sidF* during *L. pneumophila* infection in *A. castellanii*.

In this study, we found that the expression patterns of these four genes differed somewhat from those in monocytes.

5.1.2.2 *L. pneumophila* grown in *A. castellanii* presented different virulence gene expression patterns than that grown in THP-1

The growth of *L. pneumophila* in *A. castellanii* led to the upregulation of *flaA* and *vipD* and the downregulation of *sdhA* at later time points. Bruggemann et al. (2006) demonstrated upregulation of *flaA* (lpg1340) from 4 to 11 h after infection during intracellular growth in *Acanthamoeba* (Bruggemann et al. 2006). The activation of *flaA* is known to promote cell death (Ren et al. 2006). Our findings show that the expression of *flaA* were highly induced during 24-48 h after infection during the intracellular growth phase of *L. pneumophila* in *A. castellanii*. The activated *L. pneumophila flaA* could be one trigger for cell death in *Acanthamoeba*, and there is an exponential increase of the proportion of dead cell from 24 h to 48 h after *L. pneumophila* infection. This increase in host cell death after replication facilitated the egress of *Legionella* and the further infection of new host cells.

Although we observed a sharp increase in *flaA* expression during the first infection cycle, this expression decreased and then rebounded to a lower peak during the second cycle. This decrease in *flaA* corresponded to the invasion of new hosts and the multiplication of *L. pneumophila* and might have been attributable to the increased

frequency of encystation. Furthermore, the second infection cycle was slower than the first, which led to a subdued *flaA* response. Nevertheless, in infected *A. castellanii*, significant changes in *flaA* expression were observed at an early time point (24 h), corresponding to the time point at which the intracellular *Legionella* had multiplied to the point of release. Therefore, the *Legionella* genes responsible for the control of host cell death were better adapted to *Legionella* replication within *A. castellanii* than the THP-1 cells. Accordingly, *Legionella* species were better adapted to *Acanthamoeba* than to macrophages.

Although *vipD* expression was downregulated during the first infection cycle, the expression levels exhibited an increasing from T12 to T48. Although the slow activation response is not fully understood, *vipD* may play a less important role than *flaA* in the regulation of *Legionella* growth within an *Acanthamoeba* host. In the second infection cycle, no obvious increase was observed in the intracellular *L. pneumophila* count, despite upregulated levels of *vipD*. During the second cycle, the proportion of *Acanthamoeba* cysts increased, and lysosomal proteases might have degraded cytosolic proteins and organelles within these cysts (Leitsch et al. 2010). Notably, because *vipD* is an inhibitor of lysosome fusion, its upregulation might have reduced the fusion of lysosomes with LCVs during encystation. The expression levels of *sdhA* varied slightly from 12 to 36 h, followed by a decrease at 48 h. *sdhA* is involved in the stabilization of LCV and protection from cell death. Accordingly, its downregulation destabilizes vacuoles, leading to cell death and the release of *L. pneumophila* from the host.

We observed an initial downregulation of *MCASP-1* expression in *Legionella*-infected *A. castellanii*, followed by increased expression over the course of infection. In a previous study, bacteria-infected amoebae grown at lower temperatures exhibited upregulated expression of *MCASP-1* at 48 h compared with their uninfected counterparts (Ohno et al. 2008). The protozoan metacaspase has been shown to activate encystment (Saheb et al. 2013, Trzyna et al. 2008). Over the course of infection, we observed cysts in both uninfected and *L. pneumophila*-infected *A. castellanii* at various time points, but it should be noted that more cysts were observed in the latter group at 24 h and thereafter.

5.1.2.3 Limitations of gene expression study

We note that our study of *Legionella* gene expression is subject to several limitations. First, the number of viable host cells decreased at later time points. Although no host cell exhaustion was observed at late time points, a decrease in the number of viable host cells could affect the *Legionella* replication cycle, which might consequently affect gene expression. The second limitation concerns the growth of *A. castellanii* in PYG media at later time points. Although amoebas can grow in PYG medium, our study used an incubation temperature of 37°C, which was not optimal for amoeba multiplication. However, we note that *Legionella* could not grow in PYG medium, which lacked a growth supplement. Third, the *Legionella* burden (i.e., the number of intracellular bacteria) differed between the monocyte THP-1 cells and the *A. castellanii*. To overcome this discrepancy, we normalized the expression of the four target genes to that of the reference gene *gyrB*, thus minimizing the effects of variations in the bacterial burden on the quantification of gene expression. Fourth, the

accumulation of metabolic waste in the culture environment could have interfered with host viability; to minimize the background interference, uninfected cell controls were set up in the study.

5.2 Host cell death after infection by *L. pneumophila*

It has been widely recognized that bacteria can manipulate host cell death when grown in host cells during different phases (Ashida et al. 2011). Two different types of cell death—apoptosis and pyroptosis—were observed in the *L. pneumophila*-infected hosts (Speir et al. 2014). Both caspase-3-associated apoptosis and caspase-1-associated pyroptosis have been reported in *L. pneumophila*-infected macrophages (Miao et al. 2011, Zhu et al. 2013). However, it remains unknown whether apoptosis or pyroptosis were predominant in facilitating the release of *L. pneumophila* in THP-1 cells. In this study, the production of active caspase-1 and caspase-3 proteins in THP-1 cells was investigated during *L. pneumophila* infection.

5.2.1 Cell death responses of THP-1 after infection by *L. pneumophila*

Our results show that the *L. pneumophila*-infected THP-1 had a significantly higher percentage of cells that produced active caspase-1 than the uninfected THP-1 only during the late stage (T48) of infection. However, the microscopic visualization of cells positive for caspase-1 staining in *L. pneumophila*-infected THP-1 revealed less intensive green fluorescence than the caspase-1-positive cells in the uninfected group.

The gene expression study of *CASP-1* also indicated that uninfected THP-1 showed greater upregulation of *CASP-1* than infected THP-1 at every time point. Although *L. pneumophila*-infected THP-1 had a higher percentage of caspase-1-positive cells than uninfected THP-1 during the late stage, the production of caspase-1 in infected THP-1 was lower than that in the uninfected THP-1. The percentage of caspase-1-positive cells in the infected group was significantly lower than that in the uninfected group at T24. According to the intracellular growth curve, a 0.4-log increase in *L. pneumophila* occurred from T24 to T36; it is possible that the *L. pneumophila* was ready to duplicate at T24 and suppressed cell death in THP-1. These findings also concurred with the downregulation of *flaA* and the upregulation of *sdhA* in *L. pneumophila*. *L. pneumophila flA* was found to trigger caspase-1-associated pyroptosis to clear bacterial infection (Miao et al. 2010), and *sdhA* could prevent *L. pneumophila* in LCV from exposure to the macrophage proinflammatory response (Creasey and Isberg 2012). Although *flaA* was repressed when *L. pneumophila* was grown in THP-1, *L. pneumophila* had many other effectors, such as *legK1*, which was also found to be able to trigger the NF κ B signaling pathway to further promote the release and pyroptosis of inflammatory cytokines (Ge et al. 2009, Gomes et al. 2015). This could explain the higher percentage of caspase-1-positive cells in *L. pneumophila*-infected THP-1 during the late stage.

This study showed that the percentages of infected and uninfected THP-1 cells that produced active caspase-3 were very low (less than 1.5%) at all time points compared with those that produced caspase-1. This finding generally complies with the gene expression patterns, in which the *CASP-3* gene in the infected group was not activated at most time points studied but was only slightly upregulated at T36. *CASP-3* gene

expression in the uninfected group was only slightly upregulated at most time points, except at T24, at which the gene was upregulated by 4.35-fold. This study of the production of active caspase-3 protein suggested that *L. pneumophila* infection could not trigger the activation of caspase-3. Although the activation of caspase-3 was reported in *L. pneumophila*-infected U937 macrophages (Molmeret et al. 2004), it was considered necessary to halt lysosomal degradation during LCV formation. Most importantly, Molmeret et al. (2004) showed that *L. pneumophila* had more than 1-log replication grown in U937 macrophages during the 24 h after infection. This study showed less than 1-log replication of THP-1 in *L. pneumophila* during the 48 h after infection, which might have been one reason why *L. pneumophila* was unable to trigger caspase-3 activation. The intracellular activation of caspase-3 might have depended on the bacterial dose.

Although no significant difference was seen in the percentage of caspase-3-positive cells between the infected and uninfected groups, the difference in the percentage of active caspase-1-positive cells between the *L. pneumophila*-infected and uninfected THP-1 was also small (less than 2%) at all time points, which also suggested the weak impact of triggering caspase-1 activation in *L. pneumophila*-infected THP-1. From the gene expression study and PI staining of gfp-transfected *L. pneumophila*-infected THP-1, *L. pneumophila* showed the ability to inhibit THP-1 cell death. However, *L. pneumophila* was unable to replicate greatly in THP-1. As a result, the effect of *L. pneumophila* on THP-1 cell death also presented at a less discernible level.

This was the first combination study to compare the production of active caspase-1 and caspase-3 in both *L. pneumophila*-infected and uninfected THP-1 at various time points after infection. The results show that both *L. pneumophila*-infected and uninfected THP-1 had higher percentages of active caspase-1-producing cells than active caspase-3-producing cells at all time points, suggesting less involvement of caspase-3-induced apoptosis in THP-1 death. The increased production of active caspase-1 in uninfected THP-1 might have resulted from the culturing of THP-1 in a nutrient-limited co-culture medium, which could have triggered the autophagy pathway, and the highly activated autophagy could have further triggered the active caspase-1-mediated pyroptosis (Byrne et al. 2013, Labbe and Saleh 2008). The results of this study are also supported by the results of a recent report by Speir's group, who demonstrated that *L. pneumophila* infection in macrophages could not directly trigger apoptosis but that *L. pneumophila* could trigger pyroptosis, which could then further activate the apoptotic pathway (Speir et al. 2017).

5.2.2 Cell death responses in *A. castellanii* after *L. pneumophila* infection

PI staining was used to assess the extent of cell death in *A. castellanii* after *L. pneumophila* infection. In this study, it was observed that *L. pneumophila*-infected *A. castellanii* had significantly higher percentages of PI-permeable cells than uninfected *A. castellanii* from T12 to T48. The intracellular growth of *L. pneumophila* in *A. castellanii* also showed high duplication levels during the first 24 h of infection, and the rapid intracellular replication of *L. pneumophila* could trigger *A. castellanii* cell death to release *L. pneumophila* once intracellular replication is complete.

In contrast, a mild gap (~1%) was seen in the PI-permeable cells between *L. pneumophila*-infected and uninfected THP-1 from T0 to T36; the only exception was that the *L. pneumophila*-infected THP-1 had significantly (1.7%) more PI-permeable cells than the uninfected THP-1 at T48. The low gap in the cell death rate between *L. pneumophila*-infected and uninfected THP-1 also reflected the low impact of *L. pneumophila* infection on THP-1 cell death, which could be due to its low growth level in THP-1.

L. pneumophila flaA and *vipD*, which have been reported to induce cell death (Speir et al. 2014), were both downregulated in *L. pneumophila*-infected THP-1; however, both were upregulated in *L. pneumophila*-infected *A. castellanii*. Our gene expression study suggests that *L. pneumophila* infection could have triggered *A. castellanii* cell death but inhibited THP-1 cell death. This finding was further supported by the use of *gfp*-transfected *L. pneumophila* to infect THP-1 and *A. castellanii* at T48 before staining with PI. The results show that THP-1 cells with *gfp* (indicating the presence of *L. pneumophila*) could not be stained with PI, whereas PI-permeable THP-1 cells had no *gfp*, which suggests that *L. pneumophila* infection could prevent THP-1 death. In contrast, *A. castellanii* had both *gfp*-positive and PI-positive cells, which suggests that *L. pneumophila* infection could directly trigger *A. castellanii* cell death. This study showed that the intracellular-grown *L. pneumophila* activated *A. castellanii* cell death, which could further facilitate the lytic release of *L. pneumophila*. However, the nonlytic release of *L. pneumophila* from *A. castellanii* was also seen in this study. The upregulated gene encoding metacaspase and the increased cysts in *L. pneumophila*-infected *A. castellanii* during the later hours, and the *gfp*-transfected *L. pneumophila*-infected *A. castellanii* at T48 after staining with PI, also showed that the cells carried

only intensive green fluorescence without red fluorescence, which suggested the existence of nonlytic release. All evidence shows that both lytic and nonlytic release can be used by *L. pneumophila* to escape from *A. castellanii*.

5.2.3 Difference between THP-1 and *A. castellanii* cell death

Interestingly, differences in cell morphology were seen between cell death in the *L. pneumophila*-infected THP-1 and that in the infected *A. castellanii* cells. The dead *L. pneumophila*-infected *A. castellanii* cells showed cell shrinkage and fragmentation with a reduced cellular volume, which resembles apoptosis. Apoptosis was reported as programmed cell death with nuclear condensation and cell shrinkage (Ziegler and Groscurth 2004), but it is possible that *L. pneumophila* infection induced apoptosis-like programmed cell death in *A. castellanii*.

In contrast, it has been reported that both necrosis and pyroptosis result in abnormal cell morphology, such as cell swelling and dilated cell volume (Miao et al. 2011), both of which may facilitate the release of cytokines for further inflammatory response (Bergsbaken et al. 2009). The dead cells in both *L. pneumophila*-infected and uninfected THP-1 cells had a larger cell volume than viable cells, which resembles necrosis and pyroptosis. This may explain why both *L. pneumophila*-infected and uninfected THP-1 cells showed increased production of caspase-1

between T0 and T48. It is possible that nutrient deprivation in the co-culture medium induced sufficient autophagy in THP-1 and further triggered active caspase-1 and pyroptosis in both *L. pneumophila*-infected and uninfected THP-1 cells. Meanwhile, *L. pneumophila* struggled to prevent THP-1 cell death for intracellular replication. The very low counts of *L. pneumophila* grown in THP-1 cells indicate that *L. pneumophila* was not successful in this battle.

5.3 Dual transcriptome analysis of FACS-enriched gfp-transfected *L. pneumophila*-infected *A. castellanii*

L. pneumophila has a wide range of hosts, from environmental amoeba to human macrophages (Al-Quadani et al. 2012). It has been widely reported that *L. pneumophila* released from amoeba are more transmissible to humans (Cirillo et al. 1999); however, human-to-human *L. pneumophila* transmission has not been reported (Cunha et al. 2016). *L. pneumophila* could be more adaptive to environmental amoeba hosts, which has a selective effect on *L. pneumophila* virulence expression that ultimately enhances the pathogen's invasiveness in human cells (Escoll et al. 2013). However, the underlying mechanisms are poorly understood.

Transcriptome analysis of *L. pneumophila* grown in host cells can provide a comprehensive picture for bacteria and host interaction. Previous researchers have

also used *L. pneumophila* co-culture with various host cells, including *Acanthamoeba* and macrophages, to reveal the bacterial transcriptome profile (Bruggemann et al. 2006, Faucher et al. 2011). This study was the first to use FACS-enriched gfp-transfected *L. pneumophila*–infected *A. castellanii* for dual transcriptome analysis based on Illumina NGS reads.

5.3.1 *L. pneumophila* protein synthesis, amino acid metabolism, and flagellar assembly were activated when grown in *A. castellanii*

From DEG allocation of gfp-transfected *L. pneumophila* grown in *A. castellanii* compared with extracellular-grown gfp-transfected *L. pneumophila*, ribosomal biosynthesis, flagellar assembly, and amino acid metabolism were the three most significantly enriched pathways. Genes related to ribosomal biosynthesis, amino acid metabolism, and flagellum biosynthesis were also highly upregulated in *L. pneumophila* grown in *A. castellanii*, suggesting activation of *L. pneumophila* protein translation, metabolism, and flagellar assembly when grown in *A. castellanii* during the late phase. This finding agrees with the previous transcriptome profiles of *L. pneumophila* grown in *A. castellanii* (Bruggemann et al. 2006, Weissenmayer et al. 2011) regarding the upregulated flagellar assembly and amino acid metabolism. Bruggemann et al. (2006) reported the enriched pathway of flagellar assembly, metabolism, and glycolysis. Weissenmayer et al. (2011) had findings similar to those reported by Bruggemann et al. (2006); however, neither transcriptome profile of intracellular *L. pneumophila* showed upregulation of ribosomal biosynthesis. The

difference could be that their results were generated based on a comparison of *L. pneumophila* between the transmissive phase and the replicative phase in *A. castellanii* co-culture. Our transcriptome profiles were generated based on a comparison of *L. pneumophila* grown in *A. castellanii* during the transmissive phase with extracellular *L. pneumophila* during the stationary phase, which aimed to reveal the differences between intracellular *L. pneumophila* and extracellular *L. pneumophila*. Upregulation of ribosomal biosynthesis was shown in our transcriptome profiles, possibly because intracellular *L. pneumophila* translated higher dosages of effector proteins than extracellular *L. pneumophila*.

In addition to amino acid metabolism and ribosomal and flagellar biosynthesis, *L. pneumophila* glycolysis was significantly enriched in this transcriptome profile, which suggests that significant sources of carbon and energy were produced by intracellular *L. pneumophila* (Price et al. 2014). *L. pneumophila* has been reported to use the Entner-Dondoroff pathway for glycolysis of exogenous glucose, and the *L. pneumophila* genes *edd-glk-eda-ywtG* form an operon involved in glucose metabolism (Harada et al. 2010). All four genes were also upregulated in this transcriptome profile. The finding is supported by Eisenreich and Heuner's theory that *L. pneumophila* grown in *Acanthamoeba* became flagellated and metabolically dormant in the transmissive phase as compared with the exponential phase (Eisenreich and Heuner 2016). Our study further proves that *L. pneumophila* grown in *A. castellanii* became highly flagellated and metabolically active in the transmissive phase compared with the extracellular stationary phase. The release of *L. pneumophila* from *A. castellanii* has been reported to be more resistant and virulent

(Cirillo et al. 1994a, Molofsky and Swanson 2004), possibly because the *L. pneumophila* in *A. castellanii* are highly flagellated and metabolically active.

This study revealed the activation of the amino acid metabolism in *L. pneumophila* grown in *A. castellanii*, and the *L. pneumophila pvc* genes involved in amino acid metabolism were also highly upregulated. Compared with the *L. pneumophila* transcriptome profiles reported by Faucher et al., *pvcA* and *pvcB* were both upregulated when *L. pneumophila* was grown in macrophages; however, bacterial genes related to glucose metabolism were not differentially expressed (Faucher et al. 2011). This finding suggests that *pvc* genes involving the bacterial amino acid metabolism were activated in macrophages but that *L. pneumophila* could not activate glycolysis when grown in macrophages. However, *pvcA* and *pvcB* were not upregulated in the transcriptome data of Bruggemann et al. (2006) when comparing *L. pneumophila* grown in *A. castellanii* in the transmissive phase and in the replicative phase. The transcriptomic raw data of Weissenmayer et al. (2011) did not show upregulated *pvc* genes when the *L. pneumophila* grown in *A. castellanii* co-culture were compared with the extracellular-grown *L. pneumophila* during the post-exponential growth phase. The difference could be that this transcriptome study was generated based on FACS-enriched *L. pneumophila*-infected *A. castellanii*; a more concentrated target population yielded different results.

5.3.2 *A. castellanii* protein synthesis and amino acid metabolism were repressed when infected with *L. pneumophila*

No study of the transcriptomes of *L. pneumophila*-infected *A. castellanii* has been published. Our study explores the transcriptional response of the *A. castellanii* host against *L. pneumophila* infection. This transcriptomic profile revealed that the *L. pneumophila*-infected *A. castellanii* had downregulated pathways related to protein translation and amino acid metabolism as compared with uninfected *A. castellanii*. The comparison between *A. castellanii* cyst and trophozoite transcriptomes showed inhibited ribosomal activity and amino acid metabolism in the cyst, which was a suppressed state of *A. castellanii* (Moon et al. 2011b). An isotope-labeled amino acid metabolism study showed that *A. castellanii* amino acids were used mainly for intracellular *L. pneumophila* metabolism (Schunder et al. 2014). As a result, the suppression of the amino acid metabolism of *A. castellanii* could have been caused by *L. pneumophila*, which consumed amino acids from the *A. castellanii* host to support the intracellular growth of *L. pneumophila*.

The microarray analysis of the amoeba *Dictyostelium* host's transcriptional response to *L. pneumophila* infection showed that the genes involved in ribosomal proteins and the tricarboxylic acid cycle for energy production were also downregulated at 48 h after infection as compared with uninfected *Dictyostelium* (Farbrother et al. 2006), which agrees with our findings regarding the *A. castellanii* host's response to *L. pneumophila* infection. The transcriptomic profiles of *Dictyostelium* and *A. castellanii* also differed after infection with *L. pneumophila*. This study also showed the

significantly but not most enriched pathway of cytoskeleton rearrangement in *L. pneumophila*-infected *A. castellanii*; however, the *Dictyostelium* genes related to cytoskeletal activity showed no change 48 h after infection with *L. pneumophila* (Farbrother et al. 2006). Amoeba cytoskeletal activity is related to bacterial uptake and delivery (Miki et al. 2000, Rivero 2008), and the enriched cytoskeleton rearrangement reflected its involvement in *L. pneumophila* delivery during the late phase when grown in *A. castellanii*. The *A. castellanii* genes involved in the tricarboxylic acid cycle were downregulated, which suggests that *L. pneumophila*-infected *A. castellanii* could have entered a suppressed state with reduced consumption of carbon and energy sources.

A previous transcriptome analysis of macrophages infected with *L. pneumophila* revealed upregulated inflammatory signaling and downregulated translation, proteolysis, and DNA damage repair (Price and Abu Kwaik 2014). The inflammatory pathway of *L. pneumophila*-infected *A. castellanii* differs from that of macrophages, but they share a similar response to *L. pneumophila* infection, including inhibited protein translation and amino acid catabolism. This study showed that genes that encode MCM8 and transposase involved in DNA damage repair were highly upregulated in *L. pneumophila*-infected *A. castellanii* as compared with uninfected *A. castellanii*. It is possible that *L. pneumophila* infection activated the *A. castellanii* pathway related to DNA damage repair for cell cycle arrest that further triggered apoptosis (Branzei and Foiani 2008), or that *L. pneumophila* caused a modification of the *A. castellanii* genome that triggered DNA damage repair.

5.3.3 Verification of both *L. pneumophila* and *A. castellanii* gene expression in FACS-enriched gfp-transfected *L. pneumophila*-infected *A. castellanii*

This study used two-step RT-qPCR to verify the gene expression of both *L. pneumophila* and *A. castellanii* in FACS-enriched gfp-transfected *L. pneumophila*-infected *A. castellanii*. *L. pneumophila pvc* genes were upregulated at both T24 and T48 when grown in *A. castellanii* but only at T48 in the extracellular-grown *L. pneumophila*. The intracellular *L. pneumophila* showed higher upregulation of *pvc* genes at T24 than at T48, indicating that the *pvc* genes could be more involved in the early stage of intracellular growth. Both *fliA* and *flaA* were highly upregulated in intracellular *L. pneumophila* at both T24 and T48, indicating the activation of flagellar assembly (Appelt and Heuner 2017) in *L. pneumophila* grown in *A. castellanii* at the end of each round of intracellular replication.

L. pneumophila legK1, *legK3*, and *sidI* involved in the activation of the NFκB pathway for the delay of cell death (Haenssler and Isberg 2011) were all downregulated when grown in *A. castellanii* in the late phase. The most downregulated *L. pneumophila* gene *tnpA*, which encoded transposase related to bacterial homologous recombination for DNA damage repair (De Palmenaer et al. 2008), was also highly downregulated in RT-qPCR verification at both T24 and T48 in *L. pneumophila* grown in *A. castellanii*. Although *L. pneumophila tnpA* is less studied, it has been shown that the removal of *L. pneumophila tnpA* can enhance the stability of the knockout of other genes in *L. pneumophila* (Wiater et al. 1994). This finding suggests that the inhibition of *L. pneumophila tnpA* by *A. castellanii* may be

due to maintenance of the modification of the *L. pneumophila* genome. Overall, the RT-qPCR verification results agree with those in the transcriptome profile.

The DEG annotation of gfp-transfected *L. pneumophila*-infected *A. castellanii* transcriptome analysis revealed that the most upregulated *A. castellanii* genes encoded Ser/Thr phosphatase, Genes encoding ATPase and MCM8, were all upregulated in RT-qPCR verification of infected *A. castellanii* at T48 as compared with uninfected *A. castellanii*. Genes encoding Ser/Thr phosphatase and MCM8 protein were especially highly upregulated in infected *A. castellanii* at T48. The DEG-encoded Ser/Thr phosphatase was aligned to cell differentiation in KEGG pathway analysis, indicating that *L. pneumophila* triggered *A. castellanii* differentiation in the late phase. *L. pneumophila* could also trigger infected *A. castellanii* DNA repair pathway for cell cycle arrest-mediated apoptosis (Branzei and Foiani 2008) in the late phase by activating MCM8.

The transcriptomic profile of gfp-transfected *L. pneumophila*-infected *A. castellanii* revealed that the host genes encoded ribosomal proteins related to translation and dephospho-coenzyme kinase (CoAK) involved in amino acid metabolism were mostly downregulated. The RT-qPCR verification revealed that the highly downregulated genes encoding ribosomal L35, CoAK, and ribosomal S4 in *L. pneumophila*-infected *A. castellanii* at T24; however, the three genes were only mildly downregulated at T48. *A. castellanii* infected with *L. pneumophila* at T48 showed a decrease in viable cells that may have further affected the RNA quality and led to the above results. The *A. castellanii* gene encoding IRSp53 involved in actin rearrangement was only upregulated at T48 in *L. pneumophila*-infected *A. castellanii*, indicating that the actin

rearrangement could be involved in bacterial delivery in the late phase (Miki et al. 2000). The *A. castellanii* gene encoding ATPeV that facilitates lysosomal channel formation was downregulated at both T24 and T48 in *L. pneumophila*-infected *A. castellanii*, indicating the inhibition of the lysosomal pathway when *L. pneumophila* is grown in *A. castellanii*. *L. pneumophila*-infected *A. castellanii* gene encoded ATG12 (autophagy-related protein) was mildly downregulated at T24, but was mildly upregulated at T48 as compared with uninfected *A. castellanii*. This pattern was similar to the expression of the *Dictyostelium* gene encoded ATG8, which was mildly downregulated at T24 and showed no change at T48 when infected with *L. pneumophila* (Farbrother et al. 2006). Furthermore, *A. castellanii* autophagy-related proteins were reported to be involved in *A. castellanii* encystment (Moon et al. 2011a), and *L. pneumophila* grown in *A. castellanii* could trigger host encystment in the late stage by activating the host genes that encode autophagy-related proteins. Because the remaining RNA sample of FACS-enriched *L. pneumophila*-infected *A. castellanii* is insufficient for investigating more genes, the enriched RNAs need to be collected more in future to verify more genes expression that revealed by dual transcriptome profiling.

5.3.4 Growth assay of *pvcA*-knockout and *pvcB*-knockout *L. pneumophila* in different conditions

Both *pvcA* and *pvcB* were highly upregulated in the intracellular *L. pneumophila*. This study generated *pvcA*-knockout and *pvcB*-knockout *L. pneumophila*, both of which showed lower growth in L-cysteine–limited BYE broth than wild-type *L.*

pneumophila. KEGG analysis of the *L. pneumophila* transcriptome revealed that *pvcA* and *pvcB* were related to amino acid metabolism, including L-cysteine metabolism.

The *pvcA*-knockout and *pvcB*-knockout *L. pneumophila* also showed an effect on bacterial replication when grown in an L-cysteine–limited environment, perhaps due to the decrease in L-cysteine assimilation when *pvcAB* is lacking. No study has yet revealed the functional role of *L. pneumophila pvcAB*. It has been shown that knockout of *Legionella pvcAB* affected the biofilm-forming ability of *L. pneumophila* in an iron-overloaded environment (Hindre et al. 2008). Our study showed that the activation of *pvc* genes co-occurred with the upregulation of flagellum activity, and *L. pneumophila pvc* activation might have been associated with the *L. pneumophila* flagellum activity that was reported to positively regulate *L. pneumophila* biofilm formation (Schulz et al. 2012).

The intracellular growth assays of *pvcA*-knockout and *pvcB*-knockout *L. pneumophila* revealed that the two mutant strains showed no significant difference from the wild-type *L. pneumophila* regarding intracellular growth in both *A. castellanii* and THP-1. The results agree with those of a previous study of *L. pneumophila* in which the *pvcAB* knockout also showed no impact on the intracellular growth of *L. pneumophila*

in macrophages and *A. castellanii* (Allard et al. 2006). We can still observe the difference between *pvcA*-knockout and *pvcB*-knockout *L. pneumophila* when grown in two different hosts. When grown in *A. castellanii*, *L. pneumophila* without *pvcA* had higher growth at T48 compared to *pvcB*-knockout strain. This could imply that *L. pneumophila* without *pvcB* was more affected for growth at late stage. However, *pvcB*-knockout *L. pneumophila* had higher replication in THP-1 compared to *pvcA*-knockout *L. pneumophila*. This indicated that *pvcA* could be more important than *pvcB* in support of *L. pneumophila* intracellular growth in THP-1.

However, the *L. pneumophila* strains released from *A. castellanii* that further infected THP-1 showed differences in growth between wild-type *L. pneumophila* and *pvcA*-knockout and *pvcB*-knockout *L. pneumophila*. Both *pvcA*-knockout and *pvcB*-knockout *L. pneumophila* presented significantly less growth than the wild-type *L. pneumophila* released from *A. castellanii* and grown in THP-1. Later the three *L. pneumophila* strains grown in BYE broth need to respectively compare with the bacteria released from *A. castellanii* to infect THP-1, which will provide a more integrated view.

During the past 40 years of exploration of *L. pneumophila*, researchers have attempted to determine how environmental host cells facilitate the evolution of this pathogen. Intracellular *L. pneumophila* has shown differentiation from the replicative form to a mature infection form (Garduño 2008). *L. pneumophila* in the mature infection form was reported to be metabolically dominant (Eisenreich and Heuner 2016), which could regulate the virulence of this pathogen (Oliva et al. 2018). *L. pneumophila*

released from *A. castellanii* possessed activated *pvc* genes that could play a regulative role in *L. pneumophila* virulence, which is crucial for its further infection of human cells.

5.3.5 Advantages and limitations of this dual transcriptome study

This study took the very first action of using FACS-enriched *L. pneumophila*-infected *A. castellanii* for RNA sequencing and performed dual transcriptome analysis, including both *L. pneumophila* and the host cell *A. castellanii*. First, the use of FACS to collect *A. castellanii* infected with gfp-transfected *L. pneumophila* could reduce the interference of extracellular bacteria in the co-culture. Second, the simultaneous transcriptional profiling of both pathogen and host provided a more integrated picture of the interaction between the pathogen and the host (Dillon et al. 2015).

This study also had limitations. First, FACS was a high-voltage facilitated designation that might have damaged the FACS-enriched *A. castellanii* cells. Second, gfp-transfected *L. pneumophila* showed lower replication in both extracellular and intracellular growth during the late phase, which could have reduced the quantity of RNA for sequencing. Third, it was difficult to efficiently remove both prokaryotic and eukaryotic ribosomal RNA during library preparation for dual transcriptional profiling (Avraham et al. 2016). These challenges must be overcome to improve the accuracy of dual transcriptome analysis.

5.4 Conclusions

This study demonstrated that *L. pneumophila* was more adaptive to its environmental host *A. castellanii* than to human THP-1. One underlying reason could be that *A. castellanii* lacks an antimicrobial inflammatory response, such as pyroptosis. *L. pneumophila* showed greater replication in *A. castellanii* and induced more cell death in the infected *A. castellanii* via activation of the bacterial *flaA* and *vipD* effector proteins. Environmental *A. castellanii* can activate intracellular *L. pneumophila pvc* gene expression, which may play a regulative role in *L. pneumophila* virulence. This is important for further pathogenesis in macrophages.

In summary, we demonstrated that the expression patterns of *L. pneumophila* genes involved in host cell death differed between THP-1 macrophages and *A. castellanii* hosts. Notably, in THP-1 cells, the genes involved in cell death were downregulated, whereas those involved in the suppression of cell death were upregulated, and the expression of the cell death-related genes *CASP-1* and *-3* was lower in *L. pneumophila*-infected vs. uninfected THP-1 cells. However, the opposite expression pattern was observed in *A. castellanii* with regard to *L. pneumophila* genes, and increased expression of the *A. castellanii MCASP-1* gene from T12 to T48 was also observed in the *L. pneumophila*-infected group. Both *L. pneumophila* and *A. castellanii* are natural biofilm inhabitants, and our results demonstrate that the expression pattern of *flaA*, the *Legionella* gene responsible for inducing host death, is better adapted to the *Legionella* replication cycle within *A. castellanii* than to that

within the THP-1 macrophages. Therefore, *Legionella* is better adapted to *A. castellanii* and more readily induces cell death therein.

L. pneumophila-infected THP-1 showed only very small differences from uninfected THP-1 in producing active caspase-1 and caspase-3. The percentages of dead cells in *L. pneumophila*-infected THP-1 and uninfected THP-1 showed a very mild gap. In contrast, *L. pneumophila*-infected *A. castellanii* had a higher proportion of dead cells than uninfected *A. castellanii*. Overall, *L. pneumophila* showed lower replication in THP-1, and *L. pneumophila* infection also showed little effect on THP-1 cell death. In contrast, *L. pneumophila* showed greater higher replication in *A. castellanii*, and bacterial infection triggered more cell death in the infected *A. castellanii*.

The simultaneous transcriptional profiling of *L. pneumophila*-infected *A. castellanii* showed that intracellular-grown *L. pneumophila* activated ribosomal biosynthesis for protein synthesis and amino acid metabolism for carbon and energy assimilation. In contrast, *L. pneumophila*-infected *A. castellanii* showed inhibited ribosomal activity and amino acid metabolism. *L. pneumophila* grown in *A. castellanii* may have used most of the amino acid resources to support bacterial growth; however, the *L. pneumophila*-infected *A. castellanii* were in a suppressed state with low consumption of carbon and energy.

L. pneumophila pvc genes that encode enzymes involved in amino acid metabolism were highly upregulated, which co-occurred with the involvement of upregulated *L. pneumophila fliA* and *fliA* in flagellar assembly when grown in *A. castellanii*. Both

pvcA-knockout and *pvcB*-knockout *L. pneumophila* released from *A. castellanii* showed lower replication in THP-1 than the wild-type *L. pneumophila*. *L. pneumophila pvc* genes were activated in *A. castellanii*, which could play a regulative role in *L. pneumophila* virulence that can further affect intracellular growth in human cells.

5.5 Suggestions for future works

This study used FACS-enriched *gfp*-transfected *L. pneumophila*-infected *A. castellanii* for transcriptional profiling and revealed highly upregulated *pvc* genes. *L. pneumophila pvc* genes encoded enzymes involved in amino acid metabolism in our DEGs allocation analysis; however, their functional roles in *L. pneumophila* grown in a host cell remain unknown. Although we proved that *L. pneumophila pvc* genes could regulate the pathogen virulence when grown in *A. castellanii* and further affect its pathogenesis in macrophages, the exact regulative role of *pvc* genes requires further exploration. Our DEG analysis of *L. pneumophila* grown in *A. castellanii* revealed the co-occurrence of upregulated *pvc* genes and flagellum-related genes, and a further study could investigate whether an association exists between the activation of *pvc* genes and the activation of flagellar assembly. Whether *pvc* genes that encode protein are Dot/Icm-associated effectors could be investigated via β -lactamase fusion translocation assay (Faucher et al. 2011). More biochemical and cellular studies should be performed to examine *pvc* gene cluster-encoded enzyme functions in *L. pneumophila*.

This study revealed that *L. pneumophila* showed lower replication in THP-1 and that *L. pneumophila* also showed little effect in inducing THP-1 cell death; however, *L. pneumophila* showed high replication in *A. castellanii* and triggered significant cell death in infected *A. castellanii*. A further study could use different MOIs to infect THP-1 and *A. castellanii* with *L. pneumophila* to investigate whether *L. pneumophila*-infected host cell death is dependent on the bacterial dose. A further study could also compare the transcriptome of *L. pneumophila*-infected THP-1 and *L. pneumophila*-infected *A. castellanii* during the transmissive phase to obtain a more integrated and comprehensive view of the manner in which the two hosts differentially manipulate and affect the virulence of *L. pneumophila*.

As gfp-transfected *L. pneumophila* showed lower growth compared to wild-type *L. pneumophila* in both extracellular and intracellular growth. It is unknown whether the expressing of green fluorescence protein increase the metabolic burden for growth. Whether the low copy of plasmid pBC(gfp)Pmip caused the low growth of *L. pneumophila* under the supplement of chloramphenicol. As a result, it would be better to compare the growth between *L. pneumophila* with plasmid pBC(gfp)Pmip and *L. pneumophila* with the plasmid pBC-Pmip that without the fragment for expressing green fluorescence protein in future study. It has also introduced that the modification of pBC(gfp)Pmip on its promoter could increase copy numbers of the plasmid in *L. pneumophila* (Chen et al. 2006). Later it would be valuable to use the modified pBC(gfp)Pmip to transfect *L. pneumophila* and see if the bacterial number in both

extracellular and intracellular growth increase, which will greatly enhance the efficiency for collecting sufficient FACS-enriched *A. castellanii* infected with gfp-transfected *L. pneumophila*.

Appendices

Appendix 1 Culture media, buffers and reagents

α BCYE growth supplement:

ACES (N-(2-Acetamido)-2-aminoethanesulfonic acid)	10g
KOH	2g
L-cysteine	0.4g
Ferric pyrophosphate	0.25g
α -ketoglutarate	1g

Dissolved in 200-mL distilled water, filter through 0.2 μ m membrane filter (filter sterilize); and then added into 800-mL CYE agar base (autoclave sterilized, and kept at 50°C) to a final 1-litre BCYE medium.

GVPC selective supplement (for 1-litre BCYE medium) (Oxoid):

Glycine (Ammonia free)	3g
Vancomycin hydrochloride	1mg
Polymyxin B sulphate	80,000 IU
Cycloheximide	80 mg

Dissolved in 10-mL sterilized distilled water, and then added into 1-litre BCYE medium.

BYE broth:

ACES 5g

Yeast extract 5g

Added with 400-mL distilled water, adjust pH to 6.9, autoclave; and then added with following supplements:

2.5g Bovine Serum Albumin (BSA) dissolved in 50mL distilled water, filter sterilize;

0.2g L-cysteine and 0.125g Ferric pyrophosphate dissolved in 50mL distilled water, filter sterilized;

Added into cooled 400-mL autoclaved medium to a final 500-mL BYE broth.

10% Glycerol solution (v/v) for electroporation:

10mL Glycerol (Sigma, >99%)

90mL Deionized water

Mix, and filter sterilize.

PYG broth:

Propeose Peptone (Peptone Water, Oxoid) 18.48g

Yeast Extract 0.92g

Dissolved in 878-mL distilled water, adjust pH to 6.5, autoclave; and then added with following supplements:

MgSO₄ (0.4M, 9.9g in 100mL distilled water) 9.2mL

CaCl₂ (0.05M, 0.7g in 100mL distilled water) 7.4mL

Sodium Citrate·2H₂O (0.1M, 2.9g in 100mL distilled water) 31.4mL

FeNH₄(SO₄)₂·12H₂O (0.005M, 0.2g in 100mL distilled water) 9.2mL

Na₂HPO₄·12H₂O (0.25M, 8.95g in 100mL distilled water) 9.2mL

KH₂PO₄ (0.25M, 3.4g in 100mL distilled water) 9.2mL

Glucose (2M, 36g in 100mL distilled water) 46.22mL

Filter sterilize all the above 7 supplements together through 0.2μM membrane filter, and then added into the autoclaved 878-mL medium to a final 1-L PYG medium.

PAS buffer:

NaCl 0.12g

MgSO₄·7H₂O 0.004g

CaCl₂·2H₂O 0.004g

Na₂HPO₄ 0.142g

KH₂PO₄ 0.136g

Dissolved in 1-litre distilled water, adjust pH to 6.5, and then filter sterilize.

20% Glycerol for bacterial freezer store:

20mL Glycerol (Sigma, >99%)

80mL BYE broth

Mix, and filter sterilize

BYE broth with/without L-cysteine supplement:

ACES 5g

Yeast extract 5g

Added with 400-mL distilled water, adjust pH to 6.9, autoclave; and then added with following supplements:

ACES (N-(2-Acetamido)-2-aminoethanesulfonic acid) 5g

KOH 1g

L-cysteine 0.2g/0g

Ferric pyrophosphate 0.125g

α -ketoglutarate 0.5g

the above supplements dissolved in distilled water and filter sterilized, and subsequently added into cooled 400-mL autoclaved medium to a final 500-mL BYE broth.

Appendix 2 Sources of materials, reagents and equipment

Reagents and supplements

CYE agar base	Oxoid, Basingstoke, UK
α BCYE growth supplement	Oxoid, Basingstoke, UK
GVPC selective supplement	Oxoid, Basingstoke, UK
ACES (BioUltra, 99.5%)	Sigma-Aldrich, St. Louis, US
L-Cysteine hydrochloride	Sigma-Aldrich, St. Louis, US
Yeast Extract	Oxoid, Basingstoke, UK
Iron(III) pyrophosphate (Ferric pyrophosphate)	Sigma-Aldrich, St. Louis, US
Bovine Serum Albumin (A2058, for cell culture)	Sigma-Aldrich, St. Louis, US
Peptone Water	Oxoid, Basingstoke, UK
RPMI 1640 medium	Gibco, Fisher Scientific, Pittsburg, US
Fetal Bovine Serum (FBS)	Gibco, Fisher Scientific, Pittsburg, US
Penicillin–Streptomycin (5,000 U/mL)	Gibco, Fisher Scientific, Pittsburg, US
PBS (Phosphate-buffered saline, 10 \times , pH 7.4)	Gibco, Fisher Scientific, Pittsburg, US

Trizol Reagent	Invitrogen, Thermo Fisher Scientific, Waltham, US
Chloroform (C2432)	Sigma-Aldrich, St. Louis, US
Gentamicin sulfate salt	Sigma-Aldrich, St. Louis, US
Chloramphenicol succinate sodium salt	Sigma-Aldrich, St. Louis, US
Lysozyme chloride (L2827)	Sigma-Aldrich, St. Louis, US
Faststart Universal SYBR Green Mastermix	Roche, Basel, Switzerland
TaqMan Universal Mastermix	Applied Biosystems, Foster City, US
Ethanol (absolute, $\geq 99.8\%$)	Sigma-Aldrich, St. Louis, US
Glycerol (G5516)	Sigma-Aldrich, St. Louis, US
Matrix for MALDI-TOF Mass Spectrometry	Bruker, Billerica, US
CS&T Beads	BD, New Jersey, US
Accudrop Beads	BD, New Jersey, US
Propidium Iodide	Abcam, San Francisco, USA
PrimeTime Gene Expression Mastermix	Integrated DNA Technologies, Coralville, USA

Consumables and Kits

Syringe with needle (1-mL, 5-mL)	Terumo, Tokyo, Japan
Centrifuge tube (1-mL, 5-mL)	SPL LifeSciences, Pocheon, South Korea
Culture plate (6-well, 48-well, 96-well)	Corning, New York, US
PureLink RNA mini Kit	Invitrogen, Thermo Fisher Scientific, Waltham, US
DNaseI (Amplification Grade, AMPD1-Kit)	Sigma-Aldrich, St. Louis, US
RevertAid First Strand Kit	Fermentas, Thermo Fisher Scientific, Waltham, US
QIAprep plasmid Miniprep kit	Qiagen, Hilden, Germany
96-well PCR plate	Eppendorf, Hamburg, Germany
Gene Pulser Electroporation Cuvettes	Bio-Rad, Hercules, California, USA
FastDigest KpnI	Fermentas, Thermo Fisher Scientific, Waltham, US
Caspase 1 (active) Staining Kit	Abcam, San Francisco, USA
Caspase 3 (active) Red Staining Kit	Abcam, San Francisco, USA

Equipment

NanoDrop 2000 spectrophotometer	Thermo Fisher Scientific
ABI7500 real-time system	Applied Biosystems
Veriti 96-well thermal cyclers	Applied Biosystems
DTX800 Multimode Microplate Reader	Beckman Coulter
Gene Pulser Electroporation apparatus	Bio-Rad
UV Box	Chromato-Vue
MALDI-TOF Mass Spectrometry	Bruker
FACS™ AriaIII	Becton-Dickinson
Eclipse Ti Inverted Microscope	Nikon
Qubit 3.0 fluorometer	Invitrogen
LightCycler 480	Roche

References

- Abdel-Nour, M., Duncan, C., Low, D.E. and Guyard, C.** (2013) Biofilms: The Stronghold of *Legionella pneumophila*. *International Journal of Molecular Sciences* 14(11), 21660-21675.
- Abu-Zant, A., Asare, R., Graham, J.E. and Kwaik, Y.A.** (2006) Role for RpoS but not RelA of *Legionella pneumophila* in modulation of phagosome biogenesis and adaptation to the phagosomal microenvironment. *Infection and Immunity* 74(5), 3021-3026.
- Abu Khweek, A., Davila, N.S.F., Caution, K., Akhter, A., Abdulrahman, B.A., Tazi, M., Hassan, H., Novotny, L.A., Bakaletz, L.O. and Amer, A.O.** (2013) Biofilm-derived *Legionella pneumophila* evades the innate immune response in macrophages. *Frontiers in Cellular and Infection Microbiology* 3.
- Al-Bana, B.H., Haddad, M.T. and Garduno, R.A.** (2014) Stationary phase and mature infectious forms of *Legionella pneumophila* produce distinct viable but non-culturable cells. *Environmental Microbiology* 16(2), 382-395.
- Al-Khodor, S., Price, C.T., Habyarimana, F., Kalia, A. and Abu Kwaik, Y.** (2008) A Dot/Icm-translocated ankyrin protein of *Legionella pneumophila* is required for intracellular proliferation within human macrophages and protozoa. *Molecular Microbiology* 70(4), 908-923.
- Al-Quadani, T., Price, C.T. and Abu Kwaik, Y.** (2012) Exploitation of evolutionarily conserved amoeba and mammalian processes by *Legionella*. *Trends in Microbiology* 20(6), 299-306.
- Allard, K.A., Viswanathan, V.K. and Cianciotto, N.P.** (2006) lbtA and lbtB are required for production of the *Legionella pneumophila* siderophore legiobactin. *Journal of Bacteriology* 188(4), 1351-1363.
- Allgood, S.C., Duenas, B.P.R., Noll, R.R., Pike, C., Lein, S. and Neunuebel, M.R.** (2017) *Legionella* Effector AnkX Disrupts Host Cell Endocytic Recycling in a Phosphocholination-Dependent Manner. *Frontiers in Cellular and Infection Microbiology* 7.
- Alli, O.A.T., Gao, L.Y., Pedersen, L.L., Zink, S., Radulic, M., Doric, M. and Abu Kwaik, Y.** (2000) Temporal pore formation-mediated egress from macrophages and alveolar epithelial cells by *Legionella pneumophila*. *Infection and Immunity* 68(11), 6431-6440.
- Amor, J.C., Swails, J., Zhu, X.J., Roy, C.R., Nagai, H., Ingmundson, A., Cheng, X.D. and Kahn, R.A.** (2005) The structure of RalF, an ADP-ribosylation factor guanine nucleotide exchange factor from *Legionella pneumophila*, reveals the presence of a cap over the active site. *Journal of Biological Chemistry* 280(2), 1392-1400.
- Appelt, S. and Heuner, K.** (2017) The Flagellar Regulon of *Legionella*-A Review. *Frontiers in Cellular and Infection Microbiology* 7.
- Ashida, H., Mimuro, H., Ogawa, M., Kobayashi, T., Sanada, T., Kim, M. and Sasakawa, C.** (2011) Host-pathogen interactions Cell death and infection: A double-edged sword for host and pathogen survival. *Journal of Cell Biology* 195(6), 931-942.

- Avraham, R., Haseley, N., Fan, A., Bloom-Ackermann, Z., Livny, J. and Hung, D.T.** (2016) A highly multiplexed and sensitive RNA-seq protocol for simultaneous analysis of host and pathogen transcriptomes. *Nature Protocols* 11(8), 1477-1491.
- Bachman, M.A. and Swanson, M.S.** (2004) Genetic evidence that *Legionella pneumophila* RpoS modulates expression of the transmission phenotype in both the exponential phase and the stationary phase. *Infection and Immunity* 72(5), 2468-2476.
- Banga, S., Gao, P., Shen, X.H., Fiscus, V., Zong, W.X., Chen, L.L. and Luo, Z.Q.** (2007) *Legionella pneumophila* inhibits macrophage apoptosis by targeting pro-death members of the Bcl2 protein family. *Proceedings of the National Academy of Sciences of the United States of America* 104(12), 5121-5126.
- Belyi, Y., Niggeweg, R., Opitz, B., Vogelsgesang, M., Hippenstiel, S., Wilm, M. and Aktories, K.** (2006) *Legionella pneumophila* glucosyltransferase inhibits host elongation factor 1A. *Proceedings of the National Academy of Sciences of the United States of America* 103(45), 16953-16958.
- Belyi, Y., Tabakova, I., Stahl, M. and Aktories, K.** (2008) Lgt: a family of cytotoxic Glucosyltransferases produced by *Legionella pneumophila*. *Journal of Bacteriology* 190(8), 3026-3035.
- Benjamini, Y. and Yekutieli, D.** (2001) The control of the false discovery rate in multiple testing under dependency. *Annals of Statistics* 29(4), 1165-1188.
- Bergsbaken, T., Fink, S.L. and Cookson, B.T.** (2009) Pyroptosis: host cell death and inflammation. *Nature Reviews Microbiology* 7(2), 99-109.
- Berk, S.G., Ting, R.S., Turner, G.W. and Ashburn, R.J.** (1998) Production of respirable vesicles containing live *Legionella pneumophila* cells by two *Acanthamoeba* spp. *Applied and Environmental Microbiology* 64(1), 279-286.
- Best, A., and Kwaik, Y.A.** (2018) Evolution of the Arsenal of *Legionella pneumophila* Effectors to Modulate Protist Hosts. *MBio*, 9(5).
- Bitar, D.M., Molmeret, M. and Abu Kwaik, Y.** (2004) Molecular and cell biology of *Legionella pneumophila*. *International Journal of Medical Microbiology* 293(7-8), 519-527.
- Branzei, D. and Foiani, M.** (2008) Regulation of DNA repair throughout the cell cycle. *Nature Reviews Molecular Cell Biology* 9(4), 297-308.
- Broz, P., von Moltke, J., Jones, J.W., Vance, R.E. and Monack, D.M.** (2010) Differential Requirement for Caspase-1 Autoproteolysis in Pathogen-Induced Cell Death and Cytokine Processing. *Cell Host & Microbe* 8(6), 471-483.
- Bruggemann, H., Hagman, A., Jules, M., Sismeiro, O., Dillies, M.A., Gouyette, C., Kunst, F., Steinert, M., Heuner, K., Coppee, J.Y. and Buchrieser, C.** (2006) Virulence strategies for infecting phagocytes deduced from the in vivo transcriptional program of *Legionella pneumophila*. *Cellular Microbiology* 8(8), 1228-1240.
- Buse, H.Y. and Ashbolt, N.J.** (2011) Differential growth of *Legionella pneumophila* strains within a range of amoebae at various temperatures associated with in-premise plumbing. *Letters in Applied Microbiology* 53(2), 217-224.

- Byrne, B. and Swanson, M.S.** (1998) Expression of *Legionella pneumophila* virulence traits in response to growth conditions. *Infection and Immunity* 66(7), 3029-3034.
- Byrne, B.G., Dubuisson, J.F., Joshi, A.D., Persson, J.J. and Swanson, M.S.** (2013) Inflammasome Components Coordinate Autophagy and Pyroptosis as Macrophage Responses to Infection. *Mbio* 4(1).
- Case, C.L., Kohler, L.J., Lima, J.B., Strowig, T., de Zoete, M.R., Flavell, R.A., Zamboni, D.S. and Roy, C.R.** (2013) Caspase-11 stimulates rapid flagellin-independent pyroptosis in response to *Legionella pneumophila*. *Proceedings of the National Academy of Sciences of the United States of America* 110(5), 1851-1856.
- Cazalet, C., Rusniok, C., Bruggemann, H., Zidane, N., Magnier, A., Ma, L., Tichit, M., Jarraud, S., Bouchier, C., Vandenesch, F., Kunst, F., Etienne, J., Glaser, P. and Buchrieser, C.** (2004) Evidence in the *Legionella pneumophila* genome for exploitation of host cell functions and high genome plasticity. *Nature Genetics* 36(11), 1165-1173.
- Chan-Yeung, M. and Yu, W.C.** (2003) Outbreak of severe acute respiratory syndrome in Hong kong special administrative region: case report. *British Medical Journal* 326(7394), 850.
- Chen, D.Q., Zheng, X.C. and Lu, Y.J.** (2006) Identification and characterization of novel ColE1-type, high-copy number plasmid mutants in *Legionella pneumophila*. *Plasmid* 56(3), 167-178.
- Chen, J., de Felipe, K.S., Clarke, M., Lu, H., Anderson, O.R., Segal, G. and Shuman, H.A.** (2004) *Legionella* effectors that promote nonlytic release from protozoa. *Science* 303(5662), 1358-1361.
- Chen, J., Reyes, M., Clarke, M. and Shuman, H.A.** (2007) Host cell-dependent secretion and translocation of the LepA and LepB effectors of *Legionella pneumophila*. *Cellular Microbiology* 9(7), 1660-1671.
- Chen, N.T., Chen, M.J., Guo, C.Y., Chen, K.T. and Su, H.J.** (2014) Precipitation Increases the Occurrence of Sporadic Legionnaires' Disease in Taiwan. *PLoS One* 9(12).
- Choy, A., Dancourt, J., Mugo, B., O'Connor, T.J., Isberg, R.R., Melia, T.J. and Roy, C.R.** (2012) The *Legionella* Effector RavZ Inhibits Host Autophagy Through Irreversible Atg8 Deconjugation. *Science* 338(6110), 1072-1076.
- Cianciotto, N.P.** (2001) Pathogenicity of *Legionella pneumophila*. *International Journal of Medical Microbiology* 291(5), 331-343.
- Cianciotto, N.P.** (2007) Iron acquisition by *Legionella pneumophila*. *Biometals* 20(3-4), 323-331.
- Cianciotto, N.P. and Fields, B.S.** (1992) *Legionella pneumophila* Mip gene Potentiates Intracellular Infection of Protozoa and Human Macrophages. *Proceedings of the National Academy of Sciences of the United States of America* 89(11), 5188-5191.
- Cianciotto, N.P., Long, R., Eisenstein, B.I. and Engelberg, N.C.** (1988) Site-Specific Mutagenesis in *Legionella-Pneumophila* by Allelic Exchange Using Counterselectable Cole1 Vectors. *Fems Microbiology Letters* 56(2), 203-207.

- Cirillo, J.D., Cirillo, S.L.G., Yan, L., Bermudez, L.E., Falkow, S. and Tompkins, L.S.** (1999) Intracellular growth in *Acanthamoeba castellanii* affects monocyte entry mechanisms and enhances virulence of *Legionella pneumophila*. *Infection and Immunity* 67(9), 4427-4434.
- Cirillo, J.D., Falkow, S. and Tompkins, L.S.** (1994) Growth of *Legionella pneumophila* in *Acanthamoeba castellanii* enhances invasion. *Infect Immun* 62(8), 3254-3261.
- Cirillo, S.L.G., Bermudez, L.E., El-Etr, S.H., Duhamel, G.E. and Cirillo, J.D.** (2001) *Legionella pneumophila* entry gene *rtxA* is involved in virulence. *Infection and Immunity* 69(1), 508-517.
- Cirillo, S.L.G., Yan, L., Littman, M., Samrakandi, M.M. and Cirillo, J.D.** (2002) Role of the *Legionella pneumophila* *rtxA* gene in amoebae. *Microbiology-Sgm* 148, 1667-1677.
- Coers, J., Kagan, J.C., Matthews, M., Nagai, H., Zuckman, D.M. and Roy, C.R.** (2000) Identification of Icm protein complexes that play distinct roles in the biogenesis of an organelle permissive for *Legionella pneumophila* intracellular growth. *Molecular Microbiology* 38(4), 719-736.
- Conover, G.M., Derre, I., Vogel, J.P. and Isberg, R.R.** (2003) The *Legionella pneumophila* LidA protein: a translocated substrate of the Dot/Icm system associated with maintenance of bacterial integrity. *Molecular Microbiology* 48(2), 305-321.
- Copenhaver, A.M., Casson, C.N., Nguyen, H.T., Fung, T.C., Duda, M.M., Roy, C.R. and Shin, S.** (2014) Alveolar Macrophages and Neutrophils Are the Primary Reservoirs for *Legionella pneumophila* and Mediate Cytosolic Surveillance of Type IV Secretion. *Infection and Immunity* 82(10), 4325-4336.
- Creasey, E.A. and Isberg, R.R.** (2012) The protein SdhA maintains the integrity of the *Legionella*-containing vacuole. *Proceedings of the National Academy of Sciences of the United States of America* 109(9), 3481-3486.
- Cunha, B.A., Burillo, A. and Bouza, E.** (2016) Legionnaires' disease. *Lancet* 387(10016), 376-385.
- Daigneault, M., Preston, J.A., Marriott, H.M., Whyte, M.K.B. and Dockrell, D.H.** (2010) The Identification of Markers of Macrophage Differentiation in PMA-Stimulated THP-1 Cells and Monocyte-Derived Macrophages. *PLoS One* 5(1).
- De Palmenaer, D., Siguier, P. and Mahillon, J.** (2008) IS4 family goes genomic. *Bmc Evolutionary Biology* 8.
- Declerck, P.** (2010) Biofilms: the environmental playground of *Legionella pneumophila*. *Environmental Microbiology* 12(3), 557-566.
- Delafont, V., Brouke, A., Bouchon, D., Moulin, L. and Hechard, Y.** (2013) Microbiome of free-living amoebae isolated from drinking water. *Water Research* 47(19), 6958-6965.
- Demirjian, A., Lucas, C.E., Garrison, L.E., Kozak-Muiznieks, N.A., States, S., Brown, E.W., Wortham, J.M., Beaudoin, A., Casey, M.L., Marriott, C., Ludwig, A.M., Sonel, A.F., Muder, R.R. and Hicks, L.A.** (2015) The Importance of Clinical Surveillance in Detecting Legionnaires' Disease Outbreaks: A Large Outbreak in a Hospital With a *Legionella* Disinfection System-Pennsylvania, 2011-2012. *Clinical Infectious Diseases* 60(11), 1596-1602.

- Derre, I. and Isberg, R.R.** (2004) Legionella pneumophila replication vacuole formation involves rapid recruitment of proteins of the early secretory system. *Infection and Immunity* 72(5), 3048-3053.
- Dey, R., Bodennec, J., Mameri, M.O. and Pernin, P.** (2009) Free-living freshwater amoebae differ in their susceptibility to the pathogenic bacterium Legionella pneumophila. *Fems Microbiology Letters* 290(1), 10-17.
- Diederren, B.M.** (2008) Legionella spp. and Legionnaires' disease. *J Infect* 56(1), 1-12.
- Dietersdorfer, E., Cervero-Arago, S., Sommer, R., Kirschner, A.K. and Walochnik, J.** (2016) Optimized methods for Legionella pneumophila release from its Acanthamoeba hosts. *Bmc Microbiology* 16.
- Dillon, L.A.L., Suresh, R., Okrah, K., Bravo, H.C., Mosser, D.M. and El-Sayed, N.M.** (2015) Simultaneous transcriptional profiling of Leishmania major and its murine lemacrophage host cell reveals insights into host-pathogen interactions. *Bmc Genomics* 16.
- Dobrowsky, P.H., Khan, S., Cloete, T.E. and Khan, W.** (2016) Molecular detection of Acanthamoeba spp., Naegleria fowleri and Vermamoeba (Hartmannella) vermiformis as vectors for Legionella spp. in untreated and solar pasteurized harvested rainwater. *Parasites & Vectors* 9.
- Doleans, A., Aurell, H., Reyrolle, M., Lina, G., Freney, J., Vandenesch, F., Etienne, J. and Jarraud, S.** (2004) Clinical and environmental distributions of Legionella strains in France are different. *Journal of Clinical Microbiology* 42(1), 458-460.
- Dreskin, S.C., Thomas, G.W., Dale, S.N. and Heasley, L.E.** (2001) Isoforms of jun kinase are differentially expressed and activated in human monocyte/macrophage (THP-1) cells. *Journal of Immunology* 166(9), 5646-5653.
- Dumenil, G., Montminy, T.P., Tang, M. and Isberg, R.R.** (2004) IcmR-regulated membrane insertion and efflux by the Legionella pneumophila IcmQ protein. *Journal of Biological Chemistry* 279(6), 4686-4695.
- Ehrhardt, H.M. and Rehm, H.J.** (1985) Phenol Degradation by Microorganisms Adsorbed on Activated Carbon. *Applied Microbiology and Biotechnology* 21(1-2), 32-36.
- Eisenreich, W. and Heuner, K.** (2016) The life stage-specific pathometabolism of Legionella pneumophila. *Febs Letters* 590(21), 3868-3886.
- Ensminger, A.W.** (2016) Legionella pneumophila, armed to the hilt: justifying the largest arsenal of effectors in the bacterial world. *Current Opinion in Microbiology* 29, 74-80.
- Ensminger, A.W. and Isberg, R.R.** (2009) Legionella pneumophila Dot/Icm translocated substrates: a sum of parts. *Current Opinion in Microbiology* 12(1), 67-73.
- Escoll, P., Rolando, M., Gomez-Valero, L. and Buchrieser, C.** (2013) From amoeba to macrophages: exploring the molecular mechanisms of Legionella pneumophila infection in both hosts. *Curr Top Microbiol Immunol* 376, 1-34.
- Falkinham, J.O., Hilborn, E.D., Arduino, M.J., Pruden, A. and Edwards, M.A.** (2015) Epidemiology and Ecology of Opportunistic Premise Plumbing Pathogens: Legionella pneumophila, Mycobacterium avium, and Pseudomonas aeruginosa. *Environmental Health Perspectives* 123(8), 749-758.

- Farbrother, P., Wagner, C., Na, J.B., Tunggal, B., Morio, T., Urushihara, H., Tanaka, Y., Schleicher, M., Steinert, M. and Eichinger, L.** (2006) Dictyostelium transcriptional host cell response upon infection with Legionella. *Cellular Microbiology* 8(3), 438-456.
- Faucher, S.P., Mueller, C.A. and Shuman, H.A.** (2011) Legionella pneumophila transcriptome during intracellular multiplication in human macrophages. *Frontiers in Microbiology* 2.
- Feeley, J.C., Gibson, R.J., Gorman, G.W., Langford, N.C., Rasheed, J.K., Mackel, D.C. and Baine, W.B.** (1979) Charcoal-Yeast Extract Agar - Primary Isolation Medium for Legionella-Pneumophila. *Journal of Clinical Microbiology* 10(4), 437-441.
- Fields, B.S.** (1996) The molecular ecology of legionellae. *Trends in Microbiology* 4(7), 286-290.
- Fields, B.S., Benson, R.F. and Besser, R.E.** (2002) Legionella and Legionnaires' disease: 25 years of investigation. *Clin Microbiol Rev* 15(3), 506-526.
- Fischer, G., Bang, H., Ludwig, B., Mann, K. and Hacker, J.** (1992) Mip Protein of Legionella-Pneumophila Exhibits Peptidyl-Prolyl-Cis Trans Isomerase (Pplase) Activity. *Molecular Microbiology* 6(10), 1375-1383.
- Fitzhenry, R., Weiss, D., Cimini, D., Balter, S., Boyd, C., Alleyne, L., Stewart, R., McIntosh, N., Econome, A., Lin, Y., Rubinstein, I., Passaretti, T., Kidney, A., Lapierre, P., Kass, D. and Varma, J.K.** (2017) Legionnaires' Disease Outbreaks and Cooling Towers, New York City, New York, USA. *Emerging Infectious Diseases* 23(11), 1769-1776.
- Gacouin, A., Le Tulzo, Y., Lavoue, S., Camus, C., Hoff, J., Bassen, R., Arvieux, C., Heurtin, C. and Thomas, R.** (2002) Severe pneumonia due to Legionella pneumophila: prognostic factors, impact of delayed appropriate antimicrobial therapy. *Intensive Care Medicine* 28(6), 686-691.
- Gao, L.Y. and Abu Kwaik, Y.** (1999a) Activation of caspase 3 during Legionella pneumophila-induced apoptosis. *Infection and Immunity* 67(9), 4886-4894.
- Gao, L.Y. and Abu Kwaik, Y.** (1999b) Apoptosis in macrophages and alveolar epithelial cells during early stages of infection by Legionella pneumophila and its role in cytopathogenicity. *Infection and Immunity* 67(2), 862-870.
- Gao, L.Y., Harb, O.S. and Abu Kwaik, Y.** (1997) Utilization of similar mechanisms by Legionella pneumophila to parasitize two evolutionarily distant host cells, mammalian macrophages and protozoa. *Infection and Immunity* 65(11), 4738-4746.
- Gao, L.Y. and Kwaik, Y.A.** (2000) The mechanism of killing and exiting the protozoan host Acanthamoeba polyphaga by Legionella pneumophila. *Environ Microbiol* 2(1), 79-90.
- Garcia-Fulgueiras, A., Navarro, C., Fenoll, D., Garcia, J., Gonzalez-Diego, P., Jimenez-Bunuales, T., Rodriguez, M., Lopez, R., Pacheco, F., Ruiz, J., Segovia, M., Baladron, B. and Pelaz, C.** (2003) Legionnaires' disease outbreak in Murcia, Spain. *Emerging Infectious Diseases* 9(8), 915-921.

Garcia, M.T., Jones, S., Pelaz, C., Millar, R.D. and Abu Kwaik, Y. (2007) *Acanthamoeba polyphaga* resuscitates viable non-culturable *Legionella pneumophila* after disinfection. *Environmental Microbiology* 9(5), 1267-1277.

Garduño, R.A. (2008) *Legionella pneumophila*, pp. 65-84, Springer.

Garduno, R.A., Garduno, E., Hiltz, M. and Hoffman, P.S. (2002) Intracellular growth of *Legionella pneumophila* gives rise to a differentiated form dissimilar to stationary-phase forms. *Infection and Immunity* 70(11), 6273-6283.

Garrison, L.E., Kunz, J.M., Cooley, L.A., Moore, M.R., Lucas, C., Schrag, S., Sarisky, J. and Whitney, C.G. (2016) Vital Signs: Deficiencies in Environmental Control Identified in Outbreaks of Legionnaires' Disease-North America, 2000-2014 (Reprinted from vol 65, pg 576-584, 2016). *American Journal of Transplantation* 16(10), 3049-3058.

Gaspar, A.H. and Machner, M.P. (2014) VipD is a Rab5-activated phospholipase A1 that protects *Legionella pneumophila* from endosomal fusion. *Proc Natl Acad Sci U S A* 111(12), 4560-4565.

Ge, J.N., Gong, Y.N., Xu, Y. and Shao, F. (2012) Preventing bacterial DNA release and absent in melanoma 2 inflammasome activation by a *Legionella* effector functioning in membrane trafficking. *Proceedings of the National Academy of Sciences of the United States of America* 109(16), 6193-6198.

Ge, J.N. and Shao, F. (2011) Manipulation of host vesicular trafficking and innate immune defence by *Legionella* Dot/Icm effectors. *Cellular Microbiology* 13(12), 1870-1880.

Ge, J.N., Xu, H., Li, T., Zhou, Y., Zhang, Z.B., Li, S., Liu, L.P. and Shao, F. (2009) A *Legionella* type IV effector activates the NF-kappa B pathway by phosphorylating the I kappa B family of inhibitors. *Proceedings of the National Academy of Sciences of the United States of America* 106(33), 13725-13730.

Geissmann, F., Manz, M.G., Jung, S., Sieweke, M.H., Merad, M. and Ley, K. (2010) Development of Monocytes, Macrophages, and Dendritic Cells. *Science* 327(5966), 656-661.

Giao, M.S., Azevedo, N.F., Wilks, S.A., Vieira, M.J. and Keevil, C.W. (2011) Interaction of *legionella pneumophila* and *helicobacter pylori* with bacterial species isolated from drinking water biofilms. *Bmc Microbiology* 11.

Gomes, A., Capela, J.P., Ribeiro, D., Freitas, M., Silva, A.M.S., Pinto, D.C.G.A., Santos, C.M.M., Cavaleiro, J.A.S., Lima, J.L.F.C. and Fernandes, E. (2015) Inhibition of NF-kB Activation and Cytokines Production in THP-1 Monocytes by 2-Styrylchromones. *Medicinal Chemistry* 11(6), 560-566.

Guerrieri, E., Bondi, M., Sabia, C., de Niederhausern, S., Borella, P. and Messi, P. (2008) Effect of bacterial interference on biofilm development by *Legionella pneumophila*. *Curr Microbiol* 57(6), 532-536.

Haenssler, E. and Isberg, R.R. (2011) Control of host cell phosphorylation by *Legionella pneumophila*. *Frontiers in Microbiology* 2.

Hagele, S., Hacker, J. and Brand, B.C. (1998) *Legionella pneumophila* kills human phagocytes but not protozoan host cells by inducing apoptotic cell death. *Fems Microbiology Letters* 169(1), 51-58.

- Hammer, B.K. and Swanson, M.S.** (1999) Co-ordination of *Legionella pneumophila* virulence with entry into stationary phase by ppGpp. *Molecular Microbiology* 33(4), 721-731.
- Hammer, B.K., Tateda, E.S. and Swanson, M.S.** (2002) A two-component regulator induces the transmission phenotype of stationary-phase *Legionella pneumophila*. *Molecular Microbiology* 44(1), 107-118.
- Hampton, L.M., Garrison, L., Kattan, J., Brown, E., Kozak-Muiznieks, N.A., Lucas, C., Fields, B., Fitzpatrick, N., Sopian, L., Martin-Escobar, T., Waterman, S., Hicks, L.A., Alpuche-Aranda, C. and Lopez-Gatell, H.** (2016) Legionnaires' Disease Outbreak at a Resort in Cozumel, Mexico. *Open Forum Infectious Diseases* 3(3).
- Harada, E., Iida, K.I., Shiota, S., Nakayama, H. and Yoshida, S.I.** (2010) Glucose Metabolism in *Legionella pneumophila*: Dependence on the Entner-Doudoroff Pathway and Connection with Intracellular Bacterial Growth. *Journal of Bacteriology* 192(11), 2892-2899.
- Hayashi, T., Nakamichi, M., Naitou, H., Ohashi, N., Imai, Y. and Miyake, M.** (2010) Proteomic Analysis of Growth Phase-Dependent Expression of *Legionella pneumophila* Proteins Which Involves Regulation of Bacterial Virulence Traits. *PLoS One* 5(7).
- Helbig, J.H., Kurtz, J.B., Pastoris, M.C., Pelaz, C. and Luck, P.C.** (1997) Antigenic lipopolysaccharide components of *Legionella pneumophila* recognized by monoclonal antibodies: Possibilities and limitations for division of the species into serogroups. *Journal of Clinical Microbiology* 35(11), 2841-2845.
- Hervet, E., Charpentier, X., Vianney, A., Lazzaroni, J.C., Gilbert, C., Atlan, D. and Doublet, P.** (2011) Protein Kinase LegK2 Is a Type IV Secretion System Effector Involved in Endoplasmic Reticulum Recruitment and Intracellular Replication of *Legionella pneumophila*. *Infection and Immunity* 79(5), 1936-1950.
- Heuner, K., Dietrich, C., Skriwan, C., Steinert, M. and Hacker, J.** (2002) Influence of the alternative sigma(28) factor on virulence and flagellum expression of *Legionella pneumophila*. *Infection and Immunity* 70(3), 1604-1608.
- Heuner, K., Hacker, J. and Brand, B.C.** (1997) The alternative sigma factor sigma(28) of *Legionella pneumophila* restores flagellation and motility to an *Escherichia coli* fliA mutant. *Journal of Bacteriology* 179(1), 17-23.
- Hilbi, H., Hoffmann, C. and Harrison, C.F.** (2011) *Legionella* spp. outdoors: colonization, communication and persistence. *Environ Microbiol Rep* 3(3), 286-296.
- Hilbi, H., Jarraud, S., Hartland, E. and Buchrieser, C.** (2010) Update on Legionnaires' disease: pathogenesis, epidemiology, detection and control. *Mol Microbiol* 76(1), 1-11.
- Hilbi, H., Segal, G. and Shuman, H.A.** (2001) Icm/Dot-dependent upregulation of phagocytosis by *Legionella pneumophila*. *Mol Microbiol* 42(3), 603-617.
- Hilbi, H., Weber, S.S., Ragaz, C., Nyfeler, Y. and Urwyler, S.** (2007) Environmental predators as models for bacterial pathogenesis. *Environmental Microbiology* 9(3), 563-575.
- Hindre, T., Bruggemann, H., Buchrieser, C. and Hechard, Y.** (2008) Transcriptional profiling of *Legionella pneumophila* biofilm cells and the influence of iron on biofilm formation. *Microbiology-Sgm* 154, 30-41.

- Holden, E.P., Winkler, H.H., Wood, D.O. and Leinbach, E.D.** (1984) Intracellular Growth of Legionella-Pneumophila within Acanthamoeba-Castellanii Neff. *Infection and Immunity* 45(1), 18-24.
- Horwitz, M.A. and Silverstein, S.C.** (1980) Legionnaires-Disease Bacterium (Legionella-Pneumophila) Multiplies Intracellularly in Human-Monocytes. *Journal of Clinical Investigation* 66(3), 441-450.
- Hsu, F.S., Zhu, W.H., Brennan, L., Tao, L.L., Luo, Z.Q. and Mao, Y.X.** (2012) Structural basis for substrate recognition by a unique Legionella phosphoinositide phosphatase. *Proceedings of the National Academy of Sciences of the United States of America* 109(34), 13567-13572.
- Hubber, A. and Roy, C.R.** (2010) Modulation of Host Cell Function by Legionella pneumophila Type IV Effectors. *Annual Review of Cell and Developmental Biology*, Vol 26 26, 261-283.
- Isaac, D.T. and Isberg, R.** (2014) Master manipulators: an update on Legionella pneumophila Icm/Dot translocated substrates and their host targets. *Future Microbiology* 9(3), 343-359.
- Isaac, D.T., Laguna, R.K., Valtz, N. and Isberg, R.R.** (2015) MavN is a Legionella pneumophila vacuole-associated protein required for efficient iron acquisition during intracellular growth. *Proceedings of the National Academy of Sciences of the United States of America* 112(37), E5208-E5217.
- Isberg, R.R., O'Connor, T.J. and Heidtman, M.** (2009) The Legionella pneumophila replication vacuole: making a cosy niche inside host cells. *Nature Reviews Microbiology* 7(1), 12-24.
- Joseph, C.A.** (2004) Legionnaires' disease in Europe 2000-2002. *Epidemiology and Infection* 132(3), 417-424.
- Jules, M. and Buchrieser, C.** (2007) Legionella pneumophila adaptation to intracellular life and the host response: clues from genomics and transcriptomics. *FEBS Lett* 581(15), 2829-2838.
- Kagan, J.C., Stein, M.P., Pypaert, M. and Roy, C.R.** (2004) Legionella subvert the functions of Rab1 and Sec22b to create a replicative organelle. *Journal of Experimental Medicine* 199(9), 1201-1211.
- Khan, N.A.** (2006) Acanthamoeba: biology and increasing importance in human health. *FEMS Microbiol Rev* 30(4), 564-595.
- Khodr, A., Kay, E., Gomez-Valero, L., Ginevra, C., Doublet, P., Buchrieser, C. and Jarraud, S.** (2016) Molecular epidemiology, phylogeny and evolution of Legionella. *Infection Genetics and Evolution* 43, 108-122.
- Khunkitti, W., Lloyd, D., Furr, J.R. and Russell, A.D.** (1998) Acanthamoeba castellanii: Growth, encystment, excystment and biocide susceptibility. *Journal of Infection* 36(1), 43-48.
- Kohler, R., Bubert, A., Goebel, W., Steinert, M., Hacker, J. and Bubert, B.** (2000) Expression and use of the green fluorescent protein as a reporter system in Legionella pneumophila. *Molecular and General Genetics* 262(6), 1060-1069.

Kroemer, G., Galluzzi, L., Vandenabeele, P., Abrams, J., Alnemri, E.S., Baehrecke, E.H., Blagosklonny, M.V., El-Deiry, W.S., Golstein, P., Green, D.R., Hengartner, M., Knight, R.A., Kumar, S., Lipton, S.A., Malorni, W., Nunez, G., Peter, M.E., Tschopp, J., Yuan, J., Piacentini, M., Zhivotovsky, B. and Melino, G. (2009) Classification of cell death: recommendations of the Nomenclature Committee on Cell Death 2009. *Cell Death and Differentiation* 16(1), 3-11.

Kruse, E.B., Wehner, A. and Wisplinghoff, H. (2016) Prevalence and distribution of *Legionella* spp in potable water systems in Germany, risk factors associated with contamination, and effectiveness of thermal disinfection. *American Journal of Infection Control* 44(4), 470-474.

Labbe, K. and Saleh, M. (2008) Cell death in the host response to infection. *Cell Death and Differentiation* 15(9), 1339-1349.

Laguna, R.K., Creasey, E.A., Li, Z., Valtz, N. and Isberg, R.R. (2006) A *Legionella pneumophila*-translocated substrate that is required for growth within macrophages and protection from host cell death. *Proceedings of the National Academy of Sciences of the United States of America* 103(49), 18745-18750.

Lam, M.C., Ang, L.W., Tan, A.L., James, L. and Goh, K.T. (2011) Epidemiology and Control of Legionellosis, Singapore. *Emerging Infectious Diseases* 17(7), 1209-1215.

Lamkanfi, M. and Dixit, V.M. (2010) Manipulation of Host Cell Death Pathways during Microbial Infections. *Cell Host & Microbe* 8(1), 44-54.

Lamkanfi, M., Kanneganti, T.D., Franchi, L. and Nunez, G. (2007) Caspase-1 inflammasomes in infection and inflammation. *Journal of Leukocyte Biology* 82(2), 220-225.

Lau, H.Y. and Ashbolt, N.J. (2009) The role of biofilms and protozoa in *Legionella* pathogenesis: implications for drinking water. *Journal of Applied Microbiology* 107(2), 368-378.

Lebeau, I., Lammertyn, E., De Buck, E., Maes, L., Geukens, N., Van Mellaert, L. and Anne, J. (2004) Novel transcriptional regulators of *Legionella pneumophila* that affect replication in *Acanthamoeba castellanii*. *Archives of Microbiology* 181(5), 362-370.

Leitsch, D., Kohler, M., Marchetti-Deschmann, M., Deutsch, A., Allmaier, G., Duchene, M. and Walochnik, J. (2010) Major Role for Cysteine Proteases during the Early Phase of *Acanthamoeba castellanii* Encystment. *Eukaryotic Cell* 9(4), 611-618.

Liu, M.Y., Conover, G.M. and Isberg, R.R. (2008) *Legionella pneumophila* EnhC is required for efficient replication in tumour necrosis factor alpha-stimulated macrophages. *Cellular Microbiology* 10(9), 1906-1923.

Liu, M.Y., Haenssler, E., Uehara, T., Losick, V.P., Park, J.T. and Isberg, R.R. (2012a) The *Legionella pneumophila* EnhC Protein Interferes with Immunostimulatory Muramyl Peptide Production to Evade Innate Immunity. *Cell Host & Microbe* 12(2), 166-176.

Liu, R.Y., Yu, Z.S., Guo, H.G., Liu, M.M., Zhang, H.X. and Yang, M. (2012b) Pyrosequencing analysis of eukaryotic and bacterial communities in faucet biofilms. *Science of the Total Environment* 435, 124-131.

Lorenzo-Morales, J., Khan, N.A. and Walochnik, J. (2015) An update on *Acanthamoeba keratitis*: diagnosis, pathogenesis and treatment. *Parasite* 22.

- Lu, H. and Clarke, M.** (2005) Dynamic properties of Legionella-containing phagosomes in Dictyostelium amoebae. *Cellular Microbiology* 7(7), 995-1007.
- Luo, Z.Q. and Isberg, R.R.** (2004) Multiple substrates of the Legionella pneumophila Dot/Icm system identified by interbacterial protein transfer. *Proc Natl Acad Sci U S A* 101(3), 841-846.
- Machner, M.P. and Isberg, R.R.** (2006) Targeting of host rab GTPase function by the intravacuolar pathogen Legionella pneumophila. *Developmental Cell* 11(1), 47-56.
- Magnet, A., Peralta, R.H.S., Gomes, T.S., Izquierdo, F., Fernandez-Vadillo, C., Galvan, A.L., Pozuelo, M.J., Pelaz, C., Fenoy, S. and Del Aguila, C.** (2015) Vectorial role of Acanthamoeba in Legionella propagation in water for human use. *Science of the Total Environment* 505, 889-895.
- Manske, C. and Hilbi, H.** (2014) Metabolism of the vacuolar pathogen Legionella and implications for virulence. *Frontiers in Cellular and Infection Microbiology* 4.
- Marciano-Cabral, F. and Cabral, G.** (2003) Acanthamoeba spp. as agents of disease in humans. *Clinical Microbiology Reviews* 16(2), 273-307.
- Mengue, L., Regnacq, M., Aucher, W., Portier, E., Hechard, Y. and Samba-Louaka, A.** (2016) Legionella pneumophila prevents proliferation of its natural host Acanthamoeba castellanii. *Sci Rep* 6, 36448.
- Mentasti, M., Fry, N.K., Afshar, B., Palepou-Foxley, C., Naik, F.C. and Harrison, T.G.** (2012) Application of Legionella pneumophila-specific quantitative real-time PCR combined with direct amplification and sequence-based typing in the diagnosis and epidemiological investigation of Legionnaires' disease. *European Journal of Clinical Microbiology & Infectious Diseases* 31(8), 2017-2028.
- Miao, E.A., Leaf, I.A., Treuting, P.M., Mao, D.P., Dors, M., Sarkar, A., Warren, S.E., Wewers, M.D. and Aderem, A.** (2010) Caspase-1-induced pyroptosis is an innate immune effector mechanism against intracellular bacteria. *Nature Immunology* 11(12), 1136-1194.
- Miao, E.A., Rajan, J.V. and Aderem, A.** (2011) Caspase-1-induced pyroptotic cell death. *Immunological Reviews* 243, 206-214.
- Miki, H., Yamaguchi, H., Suetsugu, S. and Takenawa, T.** (2000) IRSp53 is an essential intermediate between Rac and WAVE in the regulation of membrane ruffling. *Nature* 408(6813), 732-735.
- Molmeret, M., Alli, O.A.T., Zink, S., Flieger, A., Cianciotto, N.P. and Abu Kwaik, Y.** (2002) icmT is essential for pore formation-mediated egress of Legionella pneumophila from mammalian and protozoan cells. *Infection and Immunity* 70(1), 69-78.
- Molmeret, M., Jones, S., Santic, M., Habyarimana, F., Esteban, M.T.G. and Abu Kwaik, Y.** (2010) Temporal and spatial trigger of post-exponential virulence-associated regulatory cascades by Legionella pneumophila after bacterial escape into the host cell cytosol. *Environmental Microbiology* 12(3), 704-715.
- Molmeret, M. and Kwaik, Y.A.** (2002) How does Legionella pneumophila exit the host cell? *Trends in Microbiology* 10(6), 258-260.

- Molmeret, M., Zink, S.D., Han, L.H., Abu-Zant, A., Asari, R., Bitar, D.M. and Abu Kwaik, Y.** (2004) Activation of caspase-3 by the Dot/Icm virulence system is essential for arrested biogenesis of the Legionella-containing phagosome. *Cellular Microbiology* 6(1), 33-48.
- Molofsky, A.B., Shetron-Rama, L.M. and Swanson, M.S.** (2005) Components of the Legionella pneumophila flagellar regulon contribute to multiple virulence traits, including lysosome avoidance and macrophage death. *Infection and Immunity* 73(9), 5720-5734.
- Molofsky, A.B. and Swanson, M.S.** (2003) Legionella pneumophila CsrA is a pivotal repressor of transmission traits and activator of replication. *Molecular Microbiology* 50(2), 445-461.
- Molofsky, A.B. and Swanson, M.S.** (2004) Differentiate to thrive: lessons from the Legionella pneumophila life cycle. *Mol Microbiol* 53(1), 29-40.
- Moon, E.K., Chung, D.I., Hong, Y. and Kong, H.H.** (2011a) Atg3-Mediated Lipidation of Atg8 Is Involved in Encystation of Acanthamoeba. *Korean Journal of Parasitology* 49(2), 103-108.
- Moon, E.K., Xuan, Y.H., Chung, D.I., Hong, Y. and Kong, H.H.** (2011b) Microarray Analysis of Differentially Expressed Genes between Cysts and Trophozoites of Acanthamoeba castellanii. *Korean Journal of Parasitology* 49(4), 341-347.
- Mortazavi, A., Williams, B.A., Mccue, K., Schaeffer, L. and Wold, B.** (2008) Mapping and quantifying mammalian transcriptomes by RNA-Seq. *Nature Methods* 5(7), 621-628.
- Murata, T., Delprato, A., Ingmundson, A., Toomre, D.K., Lambright, D.G. and Roy, C.R.** (2006) The Legionella pneumophila effector protein DrrA is a Rab1 guanine nucleotide-exchange factor. *Nature Cell Biology* 8(9), 971-976.
- Nagai, H., Kagan, J.C., Zhu, X.J., Kahn, R.A. and Roy, C.R.** (2002) A bacterial guanine nucleotide exchange factor activates ARF on Legionella phagosomes. *Science* 295(5555), 679-682.
- Nagai, H. and Kubori, T.** (2011) Type IVB secretion systems of Legionella and other Gram-negative bacteria. *Frontiers in Microbiology* 2.
- Nakao, M., Bono, H., Kawashima, S., Kamiya, T., Sato, K., Goto, S. and Kanehisa, M.** (1999) Genome-scale Gene Expression Analysis and Pathway Reconstruction in KEGG. *Genome Inform Ser Workshop Genome Inform* 10, 94-103.
- Neunuebel, M.R., Chen, Y., Gaspar, A.H., Backlund, P.S., Yergey, A. and Machner, M.P.** (2011) De-AMPylation of the Small GTPase Rab1 by the Pathogen Legionella pneumophila. *Science* 333(6041), 453-456.
- Newton, H.J., Ang, D.K., van Driel, I.R. and Hartland, E.L.** (2010) Molecular pathogenesis of infections caused by Legionella pneumophila. *Clin Microbiol Rev* 23(2), 274-298.
- Nogueira, C.V., Lindsten, T., Jamieson, A.M., Case, C.L., Shin, S., Thompson, C.B. and Roy, C.R.** (2009) Rapid Pathogen-Induced Apoptosis: A Mechanism Used by Dendritic Cells to Limit Intracellular Replication of Legionella pneumophila. *Plos Pathogens* 5(6).

- Ogata, H., Goto, S., Sato, K., Fujibuchi, W., Bono, H. and Kanehisa, M.** (1999) KEGG: Kyoto Encyclopedia of Genes and Genomes. *Nucleic Acids Res* 27(1), 29-34.
- Ohno, A., Kato, N., Sakamoto, R., Kimura, S. and Yamaguchi, K.** (2008) Temperature-dependent parasitic relationship between *Legionella pneumophila* and a free-living amoeba (*Acanthamoeba castellanii*). *Applied and Environmental Microbiology* 74(14), 4585-4588.
- Oliva, G., Sahr, T. and Buchrieser, C.** (2018) The Life Cycle of *L. pneumophila*: Cellular Differentiation Is Linked to Virulence and Metabolism. *Frontiers in Cellular and Infection Microbiology* 8.
- Phin, N., Parry-Ford, F., Harrison, T., Stagg, H.R., Zhang, N., Kumar, K., Lortholary, O., Zumla, A. and Abubakar, I.** (2014) Epidemiology and clinical management of Legionnaires' disease. *Lancet Infect Dis* 14(10), 1011-1021.
- Pierre, D.M., Baron, J., Yu, V.L. and Stout, J.E.** (2017) Diagnostic testing for Legionnaires' disease. *Annals of Clinical Microbiology and Antimicrobials* 16.
- Pine, L., George, J.R., Reeves, M.W. and Harrell, W.K.** (1979) Development of a Chemically Defined Liquid-Medium for Growth of *Legionella-Pneumophila*. *Journal of Clinical Microbiology* 9(5), 615-626.
- Portier, E., Zheng, H., Sahr, T., Burnside, D.M., Mallama, C., Buchrieser, C., Cianciotto, N.P. and Hechard, Y.** (2015) *IroT/mavN*, a new iron-regulated gene involved in *Legionella pneumophila* virulence against amoebae and macrophages. *Environ Microbiol* 17(4), 1338-1350.
- Price, C.T. and Abu Kwaik, Y.** (2014) The transcriptome of *Legionella pneumophila*-infected human monocyte-derived macrophages. *PLoS One* 9(12), e114914.
- Price, C.T.D., Richards, A.M., Von Dwingelo, J.E., Samara, H.A. and Abu Kwaik, Y.** (2014) Amoeba host-*Legionella* synchronization of amino acid auxotrophy and its role in bacterial adaptation and pathogenic evolution. *Environmental Microbiology* 16(2), 350-358.
- Qin, Z.Y.** (2012) The use of THP-1 cells as a model for mimicking the function and regulation of monocytes and macrophages in the vasculature. *Atherosclerosis* 221(1), 2-11.
- Ren, T., Zamboni, D.S., Roy, C.R., Dietrich, W.F. and Vance, R.E.** (2006) Flagellin-deficient *Legionella* mutants evade caspase-1- and Naip5-mediated macrophage immunity. *Plos Pathogens* 2(3), 175-183.
- Richards, A.M., Von Dwingelo, J.E., Price, C.T. and Abu Kwaik, Y.** (2013) Cellular microbiology and molecular ecology of *Legionella*-amoeba interaction. *Virulence* 4(4), 307-314.
- Ridley, A.J.** (2006) Rho GTPases and actin dynamics in membrane protrusions and vesicle trafficking. *Trends in Cell Biology* 16(10), 522-529.
- Rivero, F.** (2008) Endocytosis and the actin cytoskeleton in *Dictyostelium discoideum*. *International Review of Cell and Molecular Biology*, Vol 267 267, 343-397.
- Robertson, P., Abdelhady, H. and Garduno, R.A.** (2014) The many forms of a pleomorphic bacterial pathogen-the developmental network of *Legionella pneumophila*. *Frontiers in Microbiology* 5.

- Robey, M. and Cianciotto, N.P.** (2002) *Legionella pneumophila* feoAB promotes ferrous iron uptake and intracellular infection. *Infection and Immunity* 70(10), 5659-5669.
- Roig, J., Carreres, A. and Domingo, C.** (1993) Treatment of Legionnaires-Disease - Current Recommendations. *Drugs* 46(1), 63-79.
- Roig, J. and Rei, J.** (2003) Legionnaires' disease: a rational approach to therapy. *Journal of Antimicrobial Chemotherapy* 51(5), 1119-1129.
- Rolando, M. and Buchrieser, C.** (2014) *Legionella pneumophila* type IV effectors hijack the transcription and translation machinery of the host cell. *Trends in Cell Biology* 24(12), 771-778.
- Rolando, M., Sanulli, S., Rusniok, C., Gomez-Valero, L., Bertholet, C., Sahr, T., Margueron, R. and Buchrieser, C.** (2013) *Legionella pneumophila* Effector RomA Uniquely Modifies Host Chromatin to Repress Gene Expression and Promote Intracellular Bacterial Replication. *Cell Host & Microbe* 13(4), 395-405.
- Sabria, A., Pedro-Botet, M.L., Gomez, J., Roig, J., Vilaseca, B., Sopena, N., Banos, V. and Grp, L.D.T.** (2005) Fluoroquinolones vs macrolides in the treatment of Legionnaires disease. *Chest* 128(3), 1401-1405.
- Saheb, E., Trzyna, W. and Bush, J.** (2013) An *Acanthamoeba castellanii* metacaspase associates with the contractile vacuole and functions in osmoregulation. *Experimental Parasitology* 133(3), 314-326.
- Scheid, P.** (2014) Relevance of free-living amoebae as hosts for phylogenetically diverse microorganisms. *Parasitology Research* 113(7), 2407-2414.
- Schulz, T., Albert-Weissenberger, C., Akamine, M. and Heuner, K.** (2008) Virulence-associated genes of the flagellar regulon of *Legionella pneumophila*. *International Journal of Medical Microbiology* 298, 65-65.
- Schulz, T., Rydzewski, K., Schunder, E., Holland, G., Bannert, N. and Heuner, K.** (2012) FliA expression analysis and influence of the regulatory proteins RpoN, FleQ and FliA on virulence and in vivo fitness in *Legionella pneumophila*. *Archives of Microbiology* 194(12), 977-989.
- Schunder, E., Gillmaier, N., Kutzner, E., Herrmann, V., Lautner, M., Heuner, K. and Eisenreich, W.** (2014) Amino Acid Uptake and Metabolism of *Legionella pneumophila* Hosted by *Acanthamoeba castellanii*. *Journal of Biological Chemistry* 289(30), 21040-21054.
- Segal, G., Russo, J.J. and Shuman, H.A.** (1999) Relationships between a new type IV secretion system and the icm/dot virulence system of *Legionella pneumophila*. *Mol Microbiol* 34(4), 799-809.
- Seshadri, R., Paulsen, I.T., Eisen, J.A., Read, T.D., Nelson, K.E., Nelson, W.C., Ward, N.L., Tettelin, H., Davidsen, T.M., Beanan, M.J., Deboy, R.T., Daugherty, S.C., Brinkac, L.M., Madupu, R., Dodson, R.J., Khouri, H.M., Lee, K.H., Carty, H.A., Scanlan, D., Heinzen, R.A., Thompson, H.A., Samuel, J.E., Fraser, C.M. and Heidelberg, J.F.** (2003) Complete genome sequence of the Q-fever pathogen *Coxiella burnetii*. *Proceedings of the National Academy of Sciences of the United States of America* 100(9), 5455-5460.

- Sexton, J.A., Miller, J.L., Yoneda, A., Kehl-Fie, T.E. and Vogel, J.P.** (2004) Legionella pneumophila DotU and IcmF are required for stability of the Dot/Icm complex. *Infection and Immunity* 72(10), 5983-5992.
- Shanmuganathan, V. and Khan, N.A.** (2009) Presence of Acanthamoeba spp. in water purification plants in southern England. *Asian Pacific Journal of Tropical Medicine* 2(6), 40-42.
- Shen, X.H., Banga, S., Liu, Y.C., Xu, L., Gao, P., Shamovsky, I., Nudler, E. and Luo, Z.Q.** (2009) Targeting eEF1A by a Legionella pneumophila effector leads to inhibition of protein synthesis and induction of host stress response. *Cellular Microbiology* 11(6), 911-926.
- Shin, S. and Roy, C.R.** (2008) Host cell processes that influence the intracellular survival of Legionella pneumophila. *Cellular Microbiology* 10(6), 1209-1220.
- Shinoda, Y., Sakai, Y., Uenishi, H., Uchihashi, Y., Hiraishi, A., Yukawa, H., Yurimoto, H. and Kato, N.** (2004) Aerobic and anaerobic toluene degradation by a newly isolated denitrifying bacterium, Thauera sp strain DNT-1. *Applied and Environmental Microbiology* 70(3), 1385-1392.
- Shoff, M.E., Rogerson, A., Kessler, K., Schatz, S. and Seal, D.V.** (2008) Prevalence of Acanthamoeba and other naked amoebae in South Florida domestic water. *Journal of Water and Health* 6(1), 99-104.
- Siddiqui, R. and Khan, N.A.** (2012) Biology and pathogenesis of Acanthamoeba. *Parasites & Vectors* 5.
- Silveira, T.N. and Zamboni, D.S.** (2010) Pore Formation Triggered by Legionella spp. Is an Nlrc4 Inflammasome-Dependent Host Cell Response That Precedes Pyroptosis. *Infection and Immunity* 78(3), 1403-1413.
- Speir, M., Vince, J.E. and Naderer, T.** (2014) Programmed cell death in Legionella infection. *Future Microbiology* 9(1), 107-118.
- Speir, M., Vogrin, A., Seidi, A., Abraham, G., Hunot, S., Han, Q., Dorn, G.W., Masters, S.L., Flavell, R.A., Vince, J.E. and Naderer, T.** (2017) Legionella pneumophila Strain 130b Evades Macrophage Cell Death Independent of the Effector SidF in the Absence of Flagellin. *Frontiers in Cellular and Infection Microbiology* 7.
- Springer, J.E., Azbill, R.D. and Knapp, P.E.** (1999) Activation of the caspase-3 apoptotic cascade in traumatic spinal cord injury. *Nature Medicine* 5(8), 943-946.
- Stewart, C.R., Muthye, V. and Cianciotto, N.P.** (2012) Legionella pneumophila Persists within Biofilms Formed by Klebsiella pneumoniae, Flavobacterium sp., and Pseudomonas fluorescens under Dynamic Flow Conditions. *PLoS One* 7(11).
- Trabelsi, H., Dendana, F., Sellami, A., Sellami, H., Cheikhrouhou, F., Neji, S., Makni, F. and Ayadi, A.** (2012) Pathogenic free-living amoebae: Epidemiology and clinical review. *Pathologie Biologie* 60(6), 399-405.
- Trzyna, W.C., Legras, X.D. and Cordingley, J.S.** (2008) A type-1 metacaspase from Acanthamoeba castellanii. *Microbiol Res* 163(4), 414-423.

- Valster, R.M., Wullings, B.A. and van der Kooij, D.** (2010) Detection of Protozoan Hosts for *Legionella pneumophila* in Engineered Water Systems by Using a Biofilm Batch Test. *Applied and Environmental Microbiology* 76(21), 7144-7153.
- van Schaik, E.J., Chen, C., Mertens, K., Weber, M.M. and Samuel, J.E.** (2013) Molecular pathogenesis of the obligate intracellular bacterium *Coxiella burnetii*. *Nature Reviews Microbiology* 11(8), 561-573.
- Vincent, C.D., Friedman, J.R., Jeong, K.C., Buford, E.C., Miller, J.L. and Vogel, J.P.** (2006) Identification of the core transmembrane complex of the *Legionella* Dot/Icm type IV secretion system. *Molecular Microbiology* 62(5), 1278-1291.
- Wang, J., Li, X., Chen, A. and Lu, Y.** (2014) *Legionella pneumophila* eukaryotic-like effector LegK3 inhibits growth of *Saccharomyces cerevisiae* and modulates its vesicle trafficking pathway. *Weisheng wuxue bao = Acta microbiologica Sinica* 54(4), 417-423.
- Wang, S.Y., Mak, K.L., Chen, L.Y., Chou, M.P. and Ho, C.K.** (1992) Heterogeneity of Human Blood Monocyte - 2 Subpopulations with Different Sizes, Phenotypes and Functions. *Immunology* 77(2), 298-303.
- Weiss, D., Boyd, C., Rakeman, J.L., Greene, S.K., Fitzhenry, R., McProud, T., Musser, K., Huang, L., Kornblum, J., Nazarian, E.J., Fine, A.D., Braunstein, S.L., Kass, D., Landman, K., Lapiere, P., Hughes, S., Tran, A., Taylor, J., Baker, D., Jones, L., Kornstein, L., Liu, B.N., Perez, R., Lucero, D.E., Peterson, E., Benowitz, I., Lee, K.F., Ngai, S., Stripling, M., Varma, J.K. and Inve, S.B.L.D.** (2017) A Large Community Outbreak of Legionnaires' Disease Associated With a Cooling Tower in New York City, 2015. *Public Health Reports* 132(2), 241-250.
- Weissenmayer, B.A., Prendergast, J.G.D., Lohan, A.J. and Loftus, B.J.** (2011) Sequencing Illustrates the Transcriptional Response of *Legionella pneumophila* during Infection and Identifies Seventy Novel Small Non-Coding RNAs. *PLoS One* 6(3).
- Wen, H.T., Miao, E.A. and Ting, J.P.Y.** (2013) Mechanisms of NOD-like Receptor-Associated Inflammasome Activation. *Immunity* 39(3), 432-441.
- Westermann, A. J., Barquist, L., and Vogel, J.** (2017). Resolving host–pathogen interactions by dual RNA-seq. *PLoS pathogens*, 13(2).
- Wiater, L.A., Sadosky, A.B. and Shuman, H.A.** (1994) Mutagenesis of *Legionella pneumophila* Using Tn903 Diilacz - Identification of a Growth-Phase-Regulated Pigmentation Gene. *Molecular Microbiology* 11(4), 641-653.
- Wieland, H., Ullrich, S., Lang, F. and Neumeister, B.** (2005) Intracellular multiplication of *Legionella pneumophila* depends on host cell amino acid transporter SLC1A5. *Molecular Microbiology* 55(5), 1528-1537.
- Xiong, L., Yamasaki, S.J., Chen, H.S., Shi, L. and Mo, Z.Y.** (2017) Intracellular Growth and Morphological Characteristics of *Legionella pneumophila* during Invasion and Proliferation in Different Cells. *Biological & Pharmaceutical Bulletin* 40(7), 1035-1042.
- Xu, L. and Luo, Z.Q.** (2013) Cell biology of infection by *Legionella pneumophila*. *Microbes and Infection* 15(2), 157-167.

Xu, L., Shen, X.H., Bryan, A., Banga, S., Swanson, M.S. and Luo, Z.Q. (2010) Inhibition of Host Vacuolar H⁺-ATPase Activity by a Legionella pneumophila Effector. *Plos Pathogens* 6(3).

Yu, V.L., Plouffe, J.F., Pastoris, M.C., Stout, J.E., Schousboe, M., Widmer, A., Summersgill, J., File, T., Heath, C.M., Paterson, D.L. and Cheresky, A. (2002) Distribution of Legionella species and serogroups isolated by culture in patients with sporadic community-acquired legionellosis: An international collaborative survey. *Journal of Infectious Diseases* 186(1), 127-128.

Zhou, D., Chen, L.M., Hernandez, L., Shears, S.B. and Galan, J.E. (2001) A Salmonella inositol polyphosphatase acts in conjunction with other bacterial effectors to promote host cell actin cytoskeleton rearrangements and bacterial internalization. *Mol Microbiol* 39(2), 248-259.

Zhan, X.Y., Hu, C.H., and Zhu, Q.Y. (2015) Legionella pathogenesis and virulence factors. *Annals of Clinical and Laboratory Research* 3(2):15.

Zhu, W.H., Hammad, L.A., Hsu, F.S., Mao, Y.X. and Luo, Z.Q. (2013) Induction of caspase 3 activation by multiple Legionella pneumophila Dot/Icm substrates. *Cellular Microbiology* 15(11), 1783-1795.

Ziegler, U. and Groscurth, P. (2004) Morphological features of cell death. *News in Physiological Sciences* 19, 124-128.

Zink, S.D., Pedersen, L., Cianciotto, N.P. and Abu Kwaik, Y. (2002) The Dot/Icm type IV secretion system of Legionella pneumophila is essential for the induction of apoptosis in human macrophages. *Infection and Immunity* 70(3), 1657-1663.